

https://dspace.org/

Analysis and design of simple antenna geometries for broadband high frequency communications.

Fourie, Andries Petrus Cronje.

1991

https://hdl.handle.net/10539/24683

Downloaded from a DSpace repository. https://dspace.org/

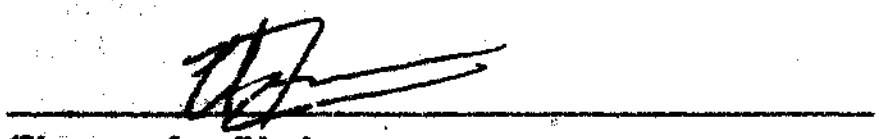
ANALYSIS AND DESIGN OF SIMPLE ANTENNA GEOMETRIES FOR BROADBAND HIGH FREQUENCY COMMUNICATIONS

Andries Petrus Cronje Fourie

A thesis submitted to the Faculty of Engineering, University of the Witwatersrand, Johannesburg, in fulfilment of the requirements for the degree of Doctor of Philosophy.

Johannesburg, 1991.

I declare that this thesis is my own, unaided work. It is being submitted for the Degree of Doctor of Philosophy in the University of the Witwatersrand, Johannesburg. It has not been submitted before for any degree or examination in any other University.



(Signature of candidate)

27th day of November 1991

ABSTRACT

The general argument of the thesis is that the design of broadband antennas demands a thorough understanding of the factors influencing the current distribution on antenna wires. Specifically, current distribution concepts are used to improve the evaluation and design of small broadband antennas for the high frequency (HF) 2 to 30 MHz range. The current distribution on an antenna governs its input impedance, radiation efficiency and radiation patterns.

The efficiency and impedance performance of known antennas were obtained using the Numerical Electromagnetics Code, NEC2, method of moments program. Factors influencing the current distribution on these antennas were identified. Staggered loads were used on a novel antenna to achieve a better current distribution than that on existing antennas. NEC2 and measured results for the staggered loads antenna (SLA) indicate superior performance to known antennas of similar geometry. The SLA efficiency is higher than 40 percent and the voltage standing wave ratio, VSWR, is less than 2.5 over the 3 to 30 MHz band.

The long computational time of NEC2 analysis frustrates the natural iterative design process. The complex algorithm also makes it difficult for the engineer to relate antenna performance to design parameters. Two design tools, in which complex theory was minimized by using current distribution principles, were developed and tested to overcome the difficulties with NEC2. Theory was developed to analyze two dipoles inter-connected by a transmission line (DTD theory). A free space current distribution was assumed to exist on the dipoles which allowed the use of conventional transmission line and circuit theory for their analysis. An antenna consisting of two dipoles and a transmission line was optimized using the DTD theory. The performance of the unique DTD antenna is considerably better than that of an optimized traditional fan dipole. The efficiency is higher than 50 percent with the VSWR lower than 2.5 over a 2 to 30 MHz band. The DTD theory obtains results more than a thousand times faster than NEC2 using a PC AT compatible computer. The second analytical technique exploits the similarity between the current distribution on dipole antennas to that on transmission lines. Existing theory based on this analogy assumes lossless transmission line theory and uniform line parameters. A new non-uniform, lossy transmission line mathematical model of loaded dipole antennas was formulated. The lossy line theory was tested by analyzing a number of loaded dipole antennas. Comparison to NEC2 results are presented to demonstrate the accuracy of this method. Analysis using the Lossy Line theory is about a hundred times faster than using NEC2 on a PC AT computer.

NEC2 generated radiation patterns are presented for all the antennas studied to enable an assessment of their performance in an HF environment. Specific examples of HF antennas are presented but the findings are applicable to other frequencies and scaled antennas.

In memory of my grandmother
Hyla Lavina Fourie
1903 - 1975

ACKNOWLEDGEMENTS

I wish to acknowledge most gratefully the following:

My wife Nel-Marié without whose support and encouragement the work would not have been such a pleasure.

Prof. H E Hanrahan, my supervisor, for his advice, guidance and patience during the research.

Dr. Brian Austin, my erstwhile supervisor, who taught me by example the value of thorough research.

The assistance of Mr. Dave Larsen of SALBU (Pty) Ltd who sponsored the research.

Mr. Louis Botha of the Aerotek division of the Council for Scientific and Industrial Research, CSIR for providing access to their computing facilities and the NEC2 program.

My colleagues Alan Clark and Ofer Givati who were the first users of my theory and provided valuable suggestions.

My sister Yiana Fourie, who prepared some of the graphical material for the thesis most competently.

Table of Contents

1 INTRODUCTION 1
1.1 Thesis Statement and Approach 1
1.2 Justification for Study 3
1.3 Thesis Layout 5

2 REVIEW OF DEFINITIONS, METHODS OF ANALYSIS AND HF BROADBAND ANTENNAS 8
2.1 Review of HF Communications 8
2.2 Ionospheric Propagation and Simple Antenna Radiation Patterns 11
2.2.1 Ionospheric properties in relation to short distance HF communications 11
2.2.2 Radiation patterns of unloaded and loaded dipoles in free space 14
2.2.3 Radiation patterns of horizontal loaded and unloaded dipoles at different heights above a perfect earth 16
2.2.4 Radiation patterns of dipoles mounted in an inverted-v configuration 20
2.2.5 Influence of different ground models on loaded antenna radiation pattern 21
2.2.6 Problems with representing radiation patterns using two dimensional cuts. 23
2.2.7 Conclusion on radiation pattern characteristics of simple dipole antennas 24
2.3 Antenna Bandwidth - Definition, Terminology and Implications 25
2.4 The Power Radiated Ratio (PRR) 28
2.5 Different Methods of Obtaining Broadband Performance 29
2.6 Method of Moments 33
2.6.1 The Numerical Electromagnetic Code version 2, NEC2 34
2.6.2 Modelling Techniques 35
Ground Effects 36
Effects of wire length 41
Wire junctions 43
Modelling two or more wires by single wire with equivalent radius 46
The value of measured results to validate numerical models 46
2.7 Summary 47

3 ACHIEVING BROADBAND PERFORMANCE BY CONTROLLING WIRE CURRENT DISTRIBUTION 49
3.1 Known Simple Broadband HF Antennas and their Performance 49
3.1.1 The Treharne antenna 49
3.1.2 The Guertler and Collyer antenna 55
3.1.3 The Harris antenna 58
3.1.4 The resistively loaded fan dipole 61
3.2 The Fourie and Austin Staggered Loads Antenna (SLA) 65
3.2.1 The design method 66
3.2.2 Computed and measured performance of Staggered Load Antenna 71
3.3 Summary 75

4 TWO SIMPLE DESIGN AIDS FOR LOADED DIPOLES AND MULTI-WIRE ANTENNAS 78
4.1 The Dipole-Transmission line-Dipole Method (DTD) 79
4.1.1 DTD Theory 80
4.1.2 Design method to obtain novel antenna 81
4.1.3 Results for DTD antenna 83
4.2 The Lossy Transmission Line method 87
4.2.1 Various Methods of Analyzing Loaded Dipole Antennas 88
4.2.2 Review of Schelkunoff's Theory 89
4.2.3 Development of the Lossy Transmission Line Method 93
4.2.4 Results of Lossy Line method 98
Unloaded dipoles 99
The Altshuler dipole 100
The Guertler and Collyer antenna 103
The multi-load dipole of Clark and Givati 105
4.3 Summary of Performance of Simple HF Broadband Antennas 107
4.4 Summary 111

5 RADIATION PATTERNS OF SIMPLE BROADBAND HF ANTENNAS 113
5.1 Radiation pattern generation, evaluation and presentation 113
5.2 Radiation patterns of all the antennas evaluated. 114
5.2.1 Treharne antenna 114
5.2.2 Guertler and Harris antennas 118
5.2.3 Fan dipole antenna 121
5.2.4 Staggered load antenna (SLA) 124
5.2.5 Multi-load antenna 128
5.2.6 Dipole-Transmission line-Dipole (DTD) antenna. 131
5.3 Conclusion on radiation pattern performance 134

6 CONCLUSION 136
6.1 Summary of Findings and Conclusions 136
6.2 Novel Aspects Arising from this Research 138

Appendix A THEORY OF THE METHOD OF MOMENTS 139

Appendix B ERROR IN TREHARNE PAPER 146

Appendix C EXPERIMENTAL METHODS 147

Appendix D TABULATED RESULTS OF TREHARNE ANTENNA 149

Appendix E TABULATED RESULTS FOR THE GUERTLER DIPOLE 151

Appendix F TABULATED RESULTS FOR THE HARRIS ANTENNA 152

Appendix G TABULATED RESULTS FOR THE RESISTIVELY LOADED FAN DIPOLE 153

Appendix H TABULATED RESULTS FOR THE STAGGERED LOADS ANTENNA 155

Appendix I DESCRIPTION AND USE MANUAL FOR THE PROGRAM SIMULATION AND ANALYSIS OF LOADED DIPOLE ANTENNAS (SALDA) 158

Appendix J TABULATED RESULTS FOR DTD 175

Appendix K TABULATED RESULTS FOR UNLOADED DIPOLE WITH THICKNESS FACTOR OF 15 177

Appendix L TABULATED RESULTS FOR ALTSHULER DIPOLE 181

Appendix M TABULATED RESULTS FOR GUERTLER AND COLLYER ANTENNA 183

Appendix N TABULATED RESULTS FOR MULTI-LOAD ANTENNA 185

REFERENCES 188

Table of Figures

Fig 2.1 The azimuth plane radiation pattern of a free space horizontal dipole at low frequencies 15
Fig 2.2 The azimuth plane radiation pattern of a free space horizontal dipole at high frequencies 15
Fig 2.3 The azimuth plane radiation pattern of a free space horizontal loaded dipole at low frequencies 15
Fig 2.4 The azimuth plane radiation pattern of a free space horizontal loaded dipole at high frequencies 15
Fig 2.5 The elevation plane radiation pattern of horizontal dipole at 12 m height at low frequencies 16
Fig 2.6 The elevation plane radiation pattern of horizontal dipole at 12 m height at high frequencies 16
Fig 2.7 The azimuth plane radiation pattern of horizontal dipole at 12 m height at low frequencies 17
Fig 2.8 The azimuth plane radiation pattern of horizontal dipole at 12 m height at high frequencies 17
Fig 2.9 The elevation plane radiation pattern of horizontal dipole at 24 m height at low frequencies 17
Fig 2.10 The elevation plane radiation pattern of horizontal dipole at 24 m height at high frequencies 17
Fig 2.11 The azimuth plane radiation pattern of horizontal dipole at 24 m height at low frequencies 18
Fig 2.12 The azimuth plane radiation pattern of horizontal dipole at 24 m height at high frequencies 18
Fig 2.13 The elevation plane radiation pattern of horizontal loaded dipole at 12 m height at low frequencies 19
Fig 2.14 The elevation plane radiation pattern of horizontal loaded dipole at 12 m height at high frequencies 19
Fig 2.15 The azimuth plane radiation pattern of horizontal loaded dipole at 12 m height at low frequencies 19
Fig 2.16 The azimuth plane radiation pattern of horizontal loaded dipole at 12 m height at high frequencies 19
Fig 2.17 The elevation plane radiation pattern of horizontal loaded dipole at 24 m height at low frequencies 20
Fig 2.18 The elevation plane radiation pattern of horizontal loaded dipole at 24 m height at high frequencies 20
Fig 2.19 The azimuth plane radiation pattern of horizontal loaded dipole at 24 m height at low frequencies 20
Fig 2.20 The azimuth plane radiation pattern of horizontal loaded dipole at 24 m height at high frequencies 20
Fig 2.21 The elevation plane radiation pattern of inverted-v loaded dipole on perfect ground at low frequencies 21
Fig 2.22 The elevation plane radiation pattern of inverted-v loaded dipole on perfect ground at high frequencies 21
Fig 2.23 The azimuth plane radiation pattern of inverted-v loaded dipole above perfect ground at low frequencies 21

Fig 2.24 The azimuth plane radiation pattern of inverted-v loaded dipole above perfect ground at high frequencies 21
Fig 2.25 The elevation plane radiation pattern of inverted-v loaded dipole above a real Fresnel earth at low frequencies 22
Fig 2.26 The elevation plane radiation pattern of loaded inverted-v loaded dipole above a real Fresnel earth at high frequencies 22
Fig 2.27 The azimuth plane radiation pattern of loaded inverted-v loaded dipole above a real Fresnel earth at low frequencies 22
Fig 2.28 The azimuth plane radiation pattern of loaded inverted-v loaded dipole above a real Fresnel earth at low frequencies 22
Fig 2.29 The azimuth plane radiation pattern of inverted-v loaded dipole 12 m above real Sommerfeld earth 23
Fig 2.30 The elevation plane radiation pattern of inverted-v loaded dipole 12 m above real Sommerfeld earth 23
Fig 2.31 The azimuth plane radiation pattern of inverted-v loaded dipole 12 m above real Fresnel earth 23
Fig 2.32 The elevation plane radiation pattern of inverted-v loaded dipole 12 m above real Fresnel earth 23
Fig 2.33 The azimuth plane radiation pattern cuts of loaded dipole 12 m above a perfect earth at 30 MHz 24
Fig 2.34 The azimuth plane radiation pattern cuts of loaded dipole at 12 m above a perfect earth 30 MHz 24
Fig 2.35 The consequences of the Chu-Harrington limits 27
Fig 2.36 The log-periodic dipole array 30
Fig 2.37 A practical HF monopole antenna 31
Fig 2.38 Altshuler's resistively loaded monopole 33
Fig 2.39 The Guertler and Collyer antenna 36
Fig 2.40 The impedance of the Guertler and Collyer antenna. 38
Fig 2.41 The effect of ground types on structure efficiency 39
Fig 2.42 Structure and upper half space efficiencies 41
Fig 2.43 Simplified Guertler and Collyer monopole 42
Fig 2.44 The geometry to investigate the wirelength concept 42
Fig 2.45 Graph of resonant length versus angle 43
Fig 2.46 The two wire transmission line 44
Fig 2.47 The impedance error versus wire spacing 44
Fig 2.48 The two wire junction criterion 45
Fig 3.1 The Treharne antenna 50
Fig 3.2 The modified Treharne geometry 52
Fig 3.3 The VSWR of the Treharne antenna 53
Fig 3.4 The efficiency of the Treharne antenna 54
Fig 3.5 The PRR of the Treharne antenna 55
Fig 3.6 The Guertler and Collyer antenna 6
Fig 3.7 The VSWR of the Guertler and Collyer antenna 57
Fig 3.8 The efficiency of the Guertler and Collyer antenna 57
Fig 3.9 The PRR of the Guertler and Collyer antenna 58
Fig 3.10 The Harris antenna 59
Fig 3.11 The VSWR of the Harris antenna 59
Fig 3.12 The efficiency of the Harris antenna 60
Fig 3.13 The PRR of the Harris antenna 60
Fig 3.14 The resistively loaded fan dipole 61

Fig 3.15 The VSWR of the resistively loaded fan dipole 64
Fig 3.16 The efficiency of the resistively loaded fan dipole 64
Fig 3.17 The PRR of the resistively loaded fan dipole 65
Fig 3.18 The impedance of the Guertler and Collyer antenna 67
Fig 3.19 Critical lengths on the Guertler and Collyer dipole 68
Fig 3.20 The staggered loads antenna, SLA 71
Fig 3.21 The SLA configuration for measurements 72
Fig 3.22 The VSWR of the SLA 73
Fig 3.23 The efficiency of the SLA 73
Fig 3.24 The PRR of the SLA 74
Fig 4.1 Schematic diagram of the DTD geometry 80
Fig 4.2 Practical method to implement the 500 Ohm line 83
Fig 4.3 The input resistance of the DTD 84
Fig 4.4 The input reactance of the DTD 85
Fig 4.5 The VSWR of the DTD 85
Fig 4.6 The efficiency of the DTD 86
Fig 4.7 The PRR of the DTD 87
Fig 4.8 Biconical dipole with transmission line equivalent 90
Fig 4.9 Schematic of a loaded biconical antenna 92
Fig 4.10 Non-uniform, lossy line model of a dipole antenna 94
Fig 4.11 The R(koh) values for different thickness dipoles 96
Fig 4.12 The length adjustment for different dipoles 97
Fig 4.13 Resistance of a dipole with thickness factor of 15 99
Fig 4.14 The reactance of a dipole of thickness factor of 15 100
Fig 4.15 Altshuler type antenna used for tests 101
Fig 4.16 Resistance of Altshuler type antenna 101
Fig 4.17 Reactance of Altshuler type antenna 102
Fig 4.18 Efficiency of the Altshuler type antenna 102
Fig 4.19 The resistance of the Guertler and Collyer antenna 103
Fig 4.20 The reactance of the Guertler and Collyer antenna 104
Fig 4.21 The efficiency of the Guertler and Collyer dipole 104
Fig 4.22 The multi-load antenna 105
Fig 4.23 The VSWR of the multi-load antenna 106
Fig 4.24 The efficiency of the multi-load antenna 106
Fig 4.25 The VSWR comparison between various antennas 107
Fig 4.26 The efficiency comparison between various antennas 108
Fig 2.27 The PRR performance of various antennas 108
Fig 4.28 VSWR comparison between two fan dipoles 109
Fig 4.29 Efficiency comparison of two fan dipoles 110
Fig 4.30 The PRR comparison between two fan dipoles 110
Fig 5.1 Treharne antenna : Perpendicular elevation plane radiation pattern cut at low frequencies. 115
Fig 5.2 Treharne antenna : Longitudinal elevation plane radiation pattern cut at low frequencies. 115
Fig 5.3 Treharne antenna : Azimuth plane radiation pattern cut at low frequencies. .. 116
Fig 5.4 Treharne antenna : Perpendicular elevation plane radiation pattern cut at high frequencies. 116
Fig 5.5 Treharne antenna : Longitudinal elevation plane radiation pattern cut at high frequencies. 117

Fig 5.6 Treharne antenna : Azimuth plane radiation pattern cut at high frequencies. 117
Fig 5.7 Guertler antenna : Perpendicular elevation plane radiation pattern cut at low frequencies. 118
Fig 5.8 Guertler antenna : Longitudinal elevation plane radiation pattern cut at low frequencies. 119
Fig 5.9 Guertler antenna : Azimuth plane radiation pattern cut at low frequencies. ... 119
Fig 5.10 Guertler antenna : Perpendicular elevation plane radiation pattern cut at high frequencies. 120
Fig 5.11 Guertler antenna : Longitudinal elevation plane radiation pattern cut at high frequencies. 120
Fig 5.12 Guertler antenna : Azimuth plane radiation pattern cut at high frequencies. 121
Fig 5.13 Fan dipole : Perpendicular elevation plane radiation pattern cut at low frequencies. 121
Fig 5.14 Fan dipole : Longitudinal elevation plane radiation pattern cut at low frequencies. 122
Fig 5.15 Fan dipole : Azimuth plane radiation pattern cut at low frequencies. 122
Fig 5.16 Fan dipole : Perpendicular elevation plane radiation pattern cut at high frequencies. 123
Fig 5.17 Fan dipole : Longitudinal elevation plane radiation pattern cut at high frequencies. 123
Fig 5.18 Fan dipole : Azimuth plane radiation pattern cut at high frequencies. 124
Fig 5.19 Staggered loads antenna (SLA) : Perpendicular elevation plane. 125
Fig 5.20 Staggered loads antenna (SLA) : Longitudinal elevation plane. 125
Fig 5.21 Staggered loads antenna (SLA) : Azimuth plane radiation pattern. 126
Fig 5.22 Staggered loads antenna (SLA) : Perpendicular elevation plane. 126
Fig 5.23 Staggered loads antenna (SLA) : Longitudinal elevation plane. 127
Fig 5.24 Staggered loads antenna (SLA) : Azimuth plane radiation pattern. 127
Fig 5.25 Multi-load antenna : Perpendicular elevation plane radiation pattern cut at low frequencies. 128
Fig 5.26 Multi-load antenna : Longitudinal elevation plane radiation pattern cut at low frequencies. 128
Fig 5.27 Multi-load antenna : Azimuth plane radiation pattern cut at low frequencies. 129
Fig 5.28 Multi-load antenna : Perpendicular elevation plane radiation pattern cut at high frequencies. 130
Fig 5.29 Multi-load antenna : Longitudinal elevation plane radiation pattern cut at high frequencies. 130
Fig 5.30 Multi-load antenna : Azimuth plane radiation pattern cut at high frequencies. 131
Fig 5.31 DTD antenna : Perpendicular elevation plane radiation pattern cut at low frequencies. 131
Fig 5.32 DTD antenna : Longitudinal elevation plane radiation pattern cut at low frequencies. 132
Fig 5.33 DTD antenna : Azimuth plane radiation pattern cut at low frequencies. 132
Fig 5.34 DTD antenna : Perpendicular elevation plane radiation pattern cut at high frequencies. 133
Fig 5.35 DTD antenna : Longitudinal elevation plane radiation pattern cut at high frequencies. 134

Fig 5.36 DTD antenna : Azimuth plane radiation pattern cut at high frequencies. 134
Fig A1 General radiating body 139
Fig A2 Cylindrical wire 141
Fig A3 Delta gap source model 144
Fig A4 The current source discontinuity source model 145

Table of Tables

Table 2.1 Frequency requirement for short wave HF links 12
Table 3.1 Parameters used in the Treharne antenna 50
Table 4.1 Critical lengths on the Guerler and Collyer dipole 66
Table 4.2 Critical lengths on the SLA 68

List of symbols

C	Euler's constant
C'	capacitance per unit length
E^s, E^i	scattered and incident electric field
I	current
J	current density
L'	inductance per unit length
L_n	length of nth element in LPDA, nth inductor in antenna
MUF	maximum usable frequency
N	total number of segments
P_i, P_r, P_t	forward, reflected and transmitted power
PRR	power radiated ratio
Q	quality factor
R'	series resistance per unit length
R_n	distance to nth element in LPDA
VSWR	voltage standing wave ratio
V_r, V_f	reflected and forward voltage on transmission lines
W	weighting function
Z'	impedance per unit length
Z_{ant}, Z_{in}, Z_i	antenna input impedance
Z_L	load impedance
Z_o	characteristic impedance
Z_{av}	average characteristic impedance
Z_t	terminating load impedance
Y'	admittance per unit length
a	radius
f	frequency
f_n	nth break frequency
f_c	critical frequency
i, k	generalized segment number
k_g	Guertler and Collyer's constant
k_w	Wood's constant
l, l_n	distances on antennas (defined)
m,n,k	positive integers
η	radiation efficiency, free space characteristic impedance

ω	radian frequency
μ_0	permeability of free space
μ	permeability of material
ε_0	permittivity of free space
ε	permittivity of material
η_u	upper half space efficiency
η_s	structure efficiency
η_g	ground efficiency
Δ	segment length
λ	free space wavelength
ϕ	angle, azimuth angle, ionospheric incidence angle
β	phase shift factor
γ	propagation factor
θ	angle, elevation angle
ρ_v	voltage reflection coefficient
τ	LPDA scale factor
α	LPDA generating angle
σ	LPDA spacing factor, conductivity
Ω	thickness factor

1 INTRODUCTION

1.1 Thesis Statement and Approach

The overall contention of the thesis is that manipulation of the current distribution on the wires of broadband antennas is the essence of their behaviour and hence design. Designers of these structures should therefore endeavour to manipulate the current distribution to their advantage using various techniques. Suitable methods of manipulating the current distribution on the antenna wires are considered, new antennas are designed using this knowledge and simplified theories to predict the current distribution are developed. The input impedance and radiation efficiency are presented versus frequency later in the thesis rather than the actual current distribution. The current distribution governs both these parameters (and in fact all other antenna parameters) where the input impedance is a function of the current at the feed point and the efficiency is a function of the current through resistive components. The approach is hence rather to relate both input impedance and efficiency to the current distribution in order to illustrate how this primary parameter influences practical antenna behaviour.

Antenna bandwidth in the thesis refers to the constancy of input impedance with frequency. Power lost in resistors, incorporated to reduce antenna input impedance variations, causes reduced radiation efficiency. The variation in radiation efficiency with frequency is therefore of considerable concern as will be shown later. Antenna radiation patterns are also of considerable importance in order to determine the overall value of an antenna. An investigation presented later showed that the radiation patterns of simple antennas present quite a suitable compromise for omnidirectional, short distance HF communications. Radiation pattern control over the HF band is shown to be unrealistic using such simple geometries. Input impedance constancy, accompanied by maximum radiation efficiency, is hence emphasized, since maximum benefit is obtained by optimizing these parameters. Radiation patterns of antenna considered are examined towards the end of the document again to validate this approach and allow a full assessment of antenna value.

Many broadband High Frequency (HF) antennas have been designed in the past with the emphasis usually on impedance constancy which is easy to measure. Their performance was often not fully quantified due to the lack of available methods. Modern computational techniques were used during this study to determine the full performance of popular existing antennas. The previously unknown radiation efficiency in combination with the input impedance present a more complete picture of broadband antenna behaviour.

The method of moments (Harrington, 1961) was used to compute the performance of existing antennas as mentioned above. Two problems were encountered when attempting to use this method to design new antennas:

- the mechanisms which cause a particular current distribution are often hidden from the user when using the method of moments
- the method of moments is computationally intensive and the time between presenting a problem and obtaining results frustrates the natural iterative design process.

Suitable mechanisms to achieve broadband performance were identified by analyzing the detailed results produced by computer simulation. These mechanisms may be used in a qualitative manner to design improved antennas (Fourie and Austin, 1987). Furthermore the knowledge gained from analyzing the performance of specific classes of antennas was afterwards used to develop simplified design theory. The simplifications were made possible by ignoring aspects which result in small performance variations and only implementing the essential theory governing the dominant characteristics. Improved HF broadband antennas were then designed to demonstrate the suitability of the techniques developed.

The general philosophy outlined above was investigated using the approach which is summarized below:

- An investigation to obtain the antenna performance requirement for short distance HF communications.
- An investigation into the problems associated with simple broadband antennas and techniques to increase their bandwidth.
- An examination of computational issues involved in simulation of the antennas of interest.
- The evaluation of a number of existing simple broadband HF antennas using the method of moments antenna analysis program, NEC2.
- The development and evaluation of a simple theory for the design of centre loaded multi-wire antennas.
- The development of a method exploiting the analogy between transmission lines and dipole antennas as well as verification of its performance.
- Design of improved broadband HF antennas using the simplified theory.

- Experimental verification of the performance of novel antennas and comparison to existent versions.
- Finally the directive properties of various antennas investigated are presented to allow a full assessment of performance.

A specific contention is that well designed simple broadband HF antennas provide a suitable tactical and electrical compromise. Another argument presented here is that simplified theory is more suitable for the design of specific loaded antennas rather than the more general method of moments programs. The statements above tie up with the overall contention that the design of simple broadband antennas essentially involves clever manipulation of the antenna current distribution.

1.2 Justification for Study

The findings presented in the thesis are shown to be applicable to the HF range from 2 to 30 MHz. The methods are also believed to be of use at other frequencies and by implementing scaled geometries. Practical examples used to test the theory are chosen from known HF antennas. Novel designs and verification of the theory pertain specifically to the HF band. The HF field also provides traditional examples of the state of the art, and users of HF communications demand improved simple broadband antennas to suit modern applications.

Broadband antennas employing simple structures with minimized profiles and mass are of primary interest. This interest stems from a renewed interest in the HF band for long distance communications despite the favour enjoyed by satellite and other relay based systems in recent years. The popularity of relay based systems is due to the higher frequencies commonly used which ensure low power levels, high bandwidth, small antennas and high fidelity. Relay systems have two severe disadvantages:

- large initial capital outlay is required to establish the infrastructure (lines, relay stations or satellites) which is often not within the capabilities of small users or developing countries.
- these systems are very vulnerable during times of war - even satellites will be threatened when developments such as the Strategic Defence Initiative (SDI) come to fruition.

The second disadvantage is clearly of considerable concern to the military since modern warfare relies exceedingly on radio communications for command and control.

The disadvantages of the relay stations stated above give a few reasons why HF communications is regaining popularity. Broadband antennas are of particular interest for HF communications since:

- ionospheric variations dictate different optimum frequencies at various times and
- modern trends in HF communications are towards frequency agile operation due to the improved resistance to interference and security for tactical communications (Dawson and Darnell, 1985 ; Rogers and Turner, 1985 ; Townsend , 1985 and many others)
- real time channel evaluation (RTCE) techniques are increasingly used to optimize use of ionospheric conditions (McGregor et al, 1985) and ideally require antennas capable of operation at any suitable frequency.

Ionospheric variations require relatively slow frequency changes (of the order of hours) while frequency agile communications may demand many changes of frequency per second. From an antenna design point the only feasible methods of accommodating such frequency changes are:

- the use of fast automatic antenna tuning units (ATU's) or
- the use of antennas with an inherently large impedance bandwidth.

Automatic ATU's involve considerable electronic complexity and hence decreased reliability. ATU's also consume relatively large amounts of DC current with resultant heating of these units (Royce, 1985 and Wilson, 1985). Broadband antennas on the other hand employ only passive components which is an attractive feature. The main disadvantage of broadband antennas, especially when they are electrically small and simple, is lower radiation efficiency. Modern frequency agile systems require much less radiated power for acceptable communication. Broadband antennas therefore present an acceptable solution as compared to a technological tour de force in ATU development (Wilson, op cit).

Most of the well known broadband antennas suitable for tactical application were designed well before the advent of the modern computational techniques for antenna analysis. Design methods were therefore largely empirical with mainly intuitive analytical techniques to provide qualitative estimates of performance.

The impedance bandwidth of an antenna is usually defined in terms of the voltage standing wave ratio, VSWR on the feedline to the structure. Measurement of VSWR is relatively simple. Most simple broadband antennas employ some form of resistive loading in order to broaden the impedance bandwidth of the antenna. Resistive loading results in ohmic losses

and hence a reduction in the radiation efficiency. The empirical determination of antenna radiation efficiency at HF is usually very difficult if not impossible. Early designers therefore realized that efficiency was sacrificed for bandwidth but had no way of quantifying this loss and therefore frequently ignored this parameter. Efficiency is a key parameter in defining the performance of simple broadband antennas and impedance bandwidth has to be viewed in conjunction with efficiency to assess the value of an antenna.

A convenient method to determine the efficiency of wire antennas is provided by modern computational techniques. For wire antennas of moderate size in terms of wavelength the method of moments solves Maxwell's equations to yield the complete current distribution. The antenna impedance and efficiency are derived from the current distribution which determine the performance of a structure. Traditional designs may therefore be investigated using computational techniques and their performance determined. Such evaluation is important in providing insight into the important mechanisms governing the behaviour of these antennas. Once these principles have been grasped the way is clearly open to improve traditional designs as well as to develop new antennas with desirable properties.

The method of moments based computer program, the Numerical Electromagnetics Code (version 2), NEC2, provides a rigorous method of assessing antenna performance. Analysis using NEC2 is time consuming due to the computational complexity of the method of moments. Antenna design is by nature iterative and requires numerous evaluations of variations of a generic structure. It is therefore desirable to develop faster methods to do rapid analysis of specific structures. It is advantageous if such techniques reveal the mechanisms of operation to the user by virtue of the mathematical model or simplification of the structure. Fast methods need not be general and absolute accuracy is of lesser concern. Faithful reproduction of trends to aid optimization is of more importance. Once a suitable antenna has been designed using such a rough technique its performance can be more accurately determined using the method of moment or by measurement. The final part of this research programme is therefore concerned with the development of convenient methods for the design of specific antennas.

1.3 Thesis Layout

The thesis layout is briefly outlined to conclude this chapter.

- The second chapter provides background to this study. An overview of HF communications, with emphasis on the requirement for broadband antennas, establishes the relevance of the research. An outline of the definitions and limitations imposed on broadband antennas follows. The typical radiation patterns of loaded and unloaded

dipoles in various configurations and environments are examined and related to their suitability for short distance omnidirectional HF communications. General methods of increasing antenna bandwidth, which were found in the literature, are critically examined. The literature survey reveals that broadband performance using simple antennas necessitates the use of resistive loading. The resultant decrease in radiation efficiency is difficult to measure and it is apparent that a numerical solution method is imperative. The method of moments, which is a well known computational technique for antenna analysis, is reviewed at the end of this chapter. Special emphasis is placed on the modelling techniques applicable to simple broadband antennas.

- In the third chapter traditional broadband antennas are examined to indicate the part played by manipulation of the current distribution on their performance. The analysis of various existing antennas is done for the first time using modern computational techniques which provide the complete performance. Once the methods for manipulating the current distribution are understood, a novel antenna benefiting from these findings is developed and the improvement in its performance is illustrated. Antenna input characteristics over the frequency band are considered, since these parameters are of main interests. The directive properties of the antennas studied in this chapter are presented in chapter 5, together with those of other antennas considered during the research.

- The fourth chapter deals with the development of simple techniques to analyze the performance of two general types of antennas. These methods capitalise on the essential mechanisms governing the current distribution and hence impedance and efficiency bandwidth of antennas. The intrinsic properties of the antenna are used in the mathematical models. The argument is that the engineer can relate the antenna performance to these simple models which aids in the design process. The validity of computed results is demonstrated by comparisons to NEC2 and measured results. The improved performance of antennas obtained using the simplified methods is shown to indicate the design benefits.

- The fifth chapter presents the radiation pattern results of antennas considered in chapters 3 and 4. The background study on radiation patterns in chapter 2 indicated that the directive properties of simple antennas are difficult to manipulate without increasing the complexity of geometries. In addition it was noted that the radiation patterns of typical simple broadband antennas are suitable albeit not ideal for short range tactical HF communications. A design approach which emphasized input impedance and radiation efficiency was hence persued. The radiation patterns of all antennas evaluated are hence

presented in this chapter to demonstrate the validity of this design approach. A brief assessment of the suitability of the antenna patterns produced for short range, tactical, HF communications is also performed.

- In the concluding chapter the findings of this study are summarized. Two improved HF broadband antenna designs and new theory to aid in the design of multi-wire and loaded dipole antennas are highlighted to show the contribution of the thesis to the field of antenna design.

2 REVIEW OF DEFINITIONS, METHODS OF ANALYSIS AND HF BROADBAND ANTENNAS

The second chapter provides background concerning the general field of HF communications. A few terms which are important to this study are clarified and theoretical limitations to antenna bandwidth are considered. The reasons for concentrating on simple broadband antennas are outlined and known antennas conforming to these requirements are examined. A brief discussion of a technique for analyzing wire antennas, the method of moments, is provided. The Numerical Electromagnetics Code (NEC2), which implements the method of moments, is briefly reviewed. Modelling aspects which were found to be important for simulating the performance of the simple broadband antennas are emphasized.

2.1 Review of HF Communications

The main advantage of high frequency (HF) radio networks is the ability to communicate over the horizon. Most popular latter-day radio links resort to artificial satellites or other types of relay stations for long-range transmission. Relay based systems are popular due to such factors as better noise performance, lower transmitter powers and increased signal bandwidth. In this realm the very high frequencies (VHF) and beyond are typically employed. The HF spectrum is however widely used in situations where relay stations are not available, too costly or in some cases not preferred. Recent developments, in the military arena specifically, indicate a renewed interest in this stalwart of long distance communications.

The controversial SDI or "Star Wars" project under way in the USA has indicated the vulnerability of satellites to military intervention (Watterson, 1979). Further interest was sparked by reports on the invaluable role played by HF communications in the Falkland war (Raggett, 1983). Recent progress in broadband, frequency agile (FA) HF systems indicates a number of advantages inherent in this method namely: improved resistance to interference and inherent security for tactical communications (Dawson and Darnell, 1985 ; Rogers and Turner, 1985 ; Townsend, 1985). Other users of HF are found in vast rural areas where telecommunication networks are hardly developed, roads are poor and where relay stations are uneconomical. Harris (1982) reported the successful use of HF by Radio Botswana for collecting local news from distant outposts. Treharne (1983a) suggested considerable application of HF communications in the Australian outback. It is significant that NATO planners have budgeted 100 million pounds on HF communications projects recently (Noonan, 1981). HF is thus still of particular interest to the military and other users who rely on it for various reasons. This interest is likely to increase in the foreseeable future.

HF propagation owes its long distance capability to the reflective properties of the ionosphere. The ionosphere enables radio waves at certain frequencies to travel between two positions on earth via one or more 'hops' from the ionosphere. The frequency band at which the ionosphere acts as a reflector is a strong function of the ionospheric conditions at the time of transmission. The ionospheric conditions, which are governed by many variables including the time of day, the time of year and solar activity can only be statistically predicted. The ionosphere is therefore pivotal in HF communications and dictates the design and application of such systems. The antenna as a component of the total system must thus be designed with due regard to the propagating medium as well as the transceiver electronics (Austin, 1985). Ionospheric propagation in relation to antenna characteristics is considered in more detail in section 2.2.

The antenna interfaces the transmitter and receiver circuitry to free space and is therefore a vital component in any radio link. HF free space wavelengths of 10 m to 100 m necessitate radiators of comparable size which result in physically large structures. Operational requirements on the other hand often require that antennas be simple and as small as possible. Conventional HF antennas are thus limited to geometries such as horizontal, vertical or inclined wires. In military and other applications masts of about ten metres high are commonly used to facilitate erection and reduce the visibility of the structure (Theron, 1983). Antennas conforming to the restrictions above have been designed for operation at a single frequency (resonant antenna), a number of discrete frequencies (multi-band antenna) or a continuous range of frequencies (broadband antenna). Normally such tactical antennas are used for short distance (typically up 1000 km) communications in arbitrary directions. The radiation patterns required for such application are discussed in the next section in more detail.

The ionospheric variations mentioned before require the use of different frequencies for operating a continuous HF link. The problem can be addressed by any of the antenna types mentioned above. The merit of a solution must be considered in conjunction with the application envisaged and the combination finally dictates a suitable choice. The usefulness of the three possibilities therefore should be considered in more detail.

An antenna tuning unit (ATU) is a circuit which matches the input impedance presented by the antenna to the feedline characteristic impedance. The ATU therefore allows simple resonant antennas to be used at different frequencies. The disadvantage of this attractive solution is the slow speed of manual tuning or the added electronic complexity involved when tuning automatically. In addition the system efficiency is degraded by the efficiency of the tuning unit which is always less than one hundred percent due to component losses. Another alterna-

tive is a multi-band antenna which yields high efficiencies at its design frequencies. Austin (1986) has shown that careful frequency management permits the use of a multi-band geo y under the day-night variations of the ionosphere. Multi-band antennas only operate on a limited number of frequencies which render them unsuitable for use in frequency agile and RTCE systems where continuous frequency selection is required. Ideally broadband antennas, which provide a good impedance match to the transceiver over a large frequency band, should be used.

A fundamental trade-off exists between efficiency and size in broadband antennas (Hansen, 1981). The result is that efficiency is sacrificed to minimize size. The difficulty of measuring efficiency at HF further complicates matters. All of the antennas described above could be used for point-to-point narrow band communication links. The growing interest in frequency agile radio however demands a re-evaluation of suitable antenna systems.

The antennas used in experimental and commercial FA systems are usually resonant structures combined with an automatic ATU (Wilson, 1985). New FA systems will require much less power for acceptable communications. Less efficient broadband antennas will hence be a more acceptable solution as compared to a "technological tour de force" in ATU development (Wilson, op. cit.). At the United States Naval Research Laboratories, where a broadband approach to Inter Task Force HF communications has been adopted, this same conclusion was reached (Royce, 1985). The literature confirms that less efficient broadband antennas are therefore an elegant complement to FA communications.

Broadband behaviour of HF antennas, particularly in tactical applications, mainly concerns the constancy of the input impedance with frequency. The radiation pattern variations are of lesser consequence as a result of the general non-directional nature of these structures. Directivity is further reduced by their relative proximity to the real earth (Austin, 1986). The typical radiation patterns of loaded and unloaded dipole antennas are considered in more detail in section 2.2 to shed more light on this parameter. The radiation efficiency is more important, because simple broadband geometries invariably incorporate resistive loads which lead to lower efficiencies. The problem that faces the engineer is the analytical determination of these parameters. Typical antennas of interest can be modelled as single wire geometries combined with loads to broaden the impedance bandwidth. Once the current distribution on any structure has been determined, input impedance and efficiency can easily be obtained (Ramsdale, 1978). Unfortunately the complexity of the analysis often belies the simplicity of

the geometry (Schelkunoff, 1952). The matter is further complicated by the difficulty of measuring the radiation efficiency of structures at HF. Efficiency is of paramount importance in loaded antennas and analytical solutions must be reliable.

2.2 Ionospheric Propagation and Simple Antenna Radiation Patterns

The effect of antenna directivity, which was mentioned in passing before, is considered in more detail in this section. The section starts off with a brief look at the ionosphere since the propagation medium obviously plays a predominant role in assessing the suitability of antenna directional characteristics. This enables a definition of the requirements on antenna radiation patterns at different frequencies. The patterns of simple loaded and unloaded dipole antennas in various environments and configurations are then examined to assess the general suitability of horizontal dipole geometries for short distance HF communications.

2.2.1 Ionospheric properties in relation to short distance HF communications

A brief discussion of some key aspects of ionospheric propagation is provided as derived from Braun (1982). This discussion will be limited to aspects necessary in order to relate to the antenna characteristics presented later.

The ionosphere consists of several conducting layers in the higher atmosphere, where the lower air density and pressure allows solar radiation to ionize the gas molecules. The ionized gas molecules recombine and the relation between ion formation and recombination determines the characteristics of the layers. Recombination rates are lower at higher altitudes due to the lower pressure and increase with a decrease in altitude. It follows that lower altitude layers are present during day time and that only the high altitude layers exist at night time due to the higher amount of ionized gas and the lower recombination rates. The nature of the ionosphere is hence mainly determined by solar activity - the most notable effect clearly being due to day-night variation. Seasonal and longer variations in solar activity also take place which complicate prediction of ionospheric characteristics.

The three layers normally distinguished are the D-layer, the E-layer and the F-layers. These layers are briefly characterized as follows:

- The D-layer occurs at an altitude between 60 to 90 km above the earth. This layer is typically only present during day-time hours and ion concentrations are usually too low to reflect HF frequencies. HF frequencies penetrate this layer and are attenuated, with the attenuation decreasing with increasing frequency.

- The E-layer occurs at an altitude of 110 km and is generally only present during daytime. The E-layer does reflect lower HF frequencies in some cases.
- The F-layer is the most important for HF communications. Its high altitude permits long communication ranges and the low recombination rate ensures its presence during night time. The layer may be subdivided into the F1 and F2 layers. The F1-layer is located 170 to 220 km above the earth and as a rule disappears during night hours. The F2-layer is located 225 to 450 km above the earth and is normally present during night hours where it permits propagation, albeit at lower frequencies. Most HF link planning assumes reflection from the F2-layer.

The highest frequency at which reflection occurs for vertical incidence on the ionosphere is known as the critical frequency, f_c, and depends on the amount of ionization of the ionosphere and hence on the time of day and sun state. Reflection occurs for higher frequencies when the angle of incidence to the ionosphere is decreased. The maximum usable frequency (MUF) for a specific angle of incidence between the wave and the ionosphere, ϕ, is given by:

$$MUF = f_c \sec\phi \qquad -(2.1)$$

The angle of incidence is once again dependent on the communication distance, d, and the virtual altitude at which reflection occurs, h. The equation relating these parameters using a flat earth approximation is:

$$\sec\phi = \sqrt{1+\left(\frac{d}{2h}\right)^2} \qquad -(2.2)$$

The equations above serve to illustrate that the MUF increases with increasing communication distance. It should also be clear that the required antenna beam take-off angle decreases with increase in communication distance. Tactical antennas are generally applied for short distance HF communications which is considered to encompass the range 0 to 1000 km. The minimum distance requirement clearly requires near vertical incidence or take-off angles close to 90°. The required take-off angle for the maximum distance of 1000 km depends on the virtual height of reflection. The virtual height of the F2-layer varies between 225 and 450 km with a typical value around 320 km. This corresponds to take-off angles between 21° and 38° with a value of 32° corresponding to a height of 320 km for a 1000 km path. Ideally the antenna radiation pattern should hence ensure coverage of take-off angles ranging from 21° to 90° in the extreme, and more typically between 30° and 90°. This characteristic should ideally be maintained in all azimuth directions for true omnidirectional short range communications.

Another aspect which is of interest in the evaluation of antenna radiation patterns with regard to ionospheric communications is the frequency requirement. The frequency range depends on the communication range, solar activity (typically quantified using the sun spot number, SSN), the season and time of day. Table 2.1 below was generated using the method described by Braun (1982). The following should be noted:

- Frequency maps for Southern Africa region were used, but the general conclusions would apply to HF communications in most temperate zones.
- Only F2-layer propagation at a constant virtual height of 320 km is considered, since this is the dominant mode normally employed.
- Two extreme daily variations (00h00 and 12h00 local times) are considered.
- January and July values are provided to indicate the effect of seasonal changes
- Sun Spot Numbers (SSN) of 0, 100 and 150 are considered to take long term changes in solar activity into account.
- Distances of 0 km and 1000 km are taken into account.

The following interesting points are apparent from this table:

- High take-off angles (corresponding to 0 km distance) are mostly required for frequencies not exceeding 10 MHz.
- The low take-off angles (corresponding to 1000 km distance) are mainly required for frequencies higher than 5 MHz.
- Short range HF communications primarily uses frequencies below 15 MHz. The only exception to this may occur when the virtual height of the F2-layer is much lower or during very rare solar cycles when the SSN is higher than 150. It should be noted that SSN in excess of 150 occurred for only approximately 2% of the time between the years 1830 to 1980. SSN's in excess of 100 occurred for about 18% of the time during the same period. These statistics viewed in conjunction with the data presented in Table 2.1 hence indicate the importance of the lower frequency ranges. Even the frequencies between 10 MHz and 15 MHz are not often required.

Table 2.1 Frequency requirement for short distance HF communications.

MUF in MHz (0 km)	MUF in MHz (1000 km)	SSN	Local time	Month
3.0	4.0	0	00h00	Jan
2.5	3.6	0	00h00	Jul
6.0	9.0	0	12h00	Jan
5.5	7.5	0	12h00	Jul
4.0	5.2	100	00h00	Jan
3.0	4.0	100	00h00	Jul
10.0	13.0	100	12h00	Jan
8.5	11.5	100	12h00	Jul
4.5	6.0	150	00h00	Jan
3.25	4.2	150	00h00	Jul
11.5	15.0	150	12h00	Jan
10.0	14.0	150	12h00	Jul

2.2.2 Radiation patterns of unloaded and loaded dipoles in free space

The simple HF broadband antennas considered in this research are mainly resistively loaded dipoles or combinations of resonant dipoles. The patterns of such antennas in various environments and configurations will hence provide an indication of expected behaviour.

Many of the antennas studied later attempt to establish a travelling wave current distribution in order to extend antenna impedance bandwidth. The Altshuler antenna (Altshuler, 1961) was taken as representative of such antenna types. This antenna, which is discussed in detail in section 2.5, was scaled to the HF frequency range and studied in a dipole configuration. The radiation patterns of antennas are represented throughout in terms of directive gain, which excludes the effect of power lost. This approach allows evaluation of antennas purely in terms of their directive properties. Other parameters which effect the communication performance of broadband antennas, such as mismatch loss and radiation efficiency, are studied in considerable detail in other chapters.

The radiation patterns of a free space unloaded dipole and Altshuler dipole (Altshuler, 1961), both of 75 m length (half wave at lowest frequency of 2 MHz) are shown in figs 2.1 and 2.2 for both antennas in free space. The antennas are both parallel to the y-axis and azimuth radiation patterns (variations in ϕ) at representative frequencies are shown. The elevation plane pattern (variations in θ) at azimuth angle perpendicular to the dipole ($\phi = 0°$) is omnidirectional in the absence of a ground and is not shown. Elevation plane patterns in line with the dipole ($\phi = 90°$) will be exactly the same as the azimuth plane radiation plane and will likewise not be shown.

The radiation patterns of the free space dipole (figs 2.1 and 2.2) show a single lobe at low frequency with an expected increase in lobes at the higher frequencies. The patterns of the resistively loaded antenna (figs 2.3 and 2.4) are similar, except for a more constant pattern with changes in frequency. Note for instance the similarity between the 2 MHz and 5 MHz pattern in fig 2.3 and the similar lobes in the 20 and 30 MHz patterns shown in fig 2.4.

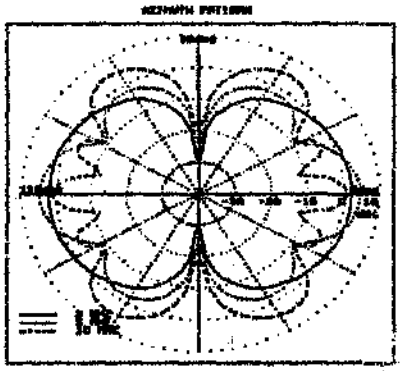


Fig 2.1 The low frequency azimuth radiation pattern of a free space dipole

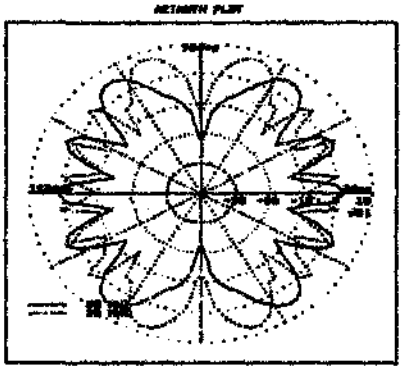


Fig 2.2 The high frequency azimuth radiation pattern of a free space dipole

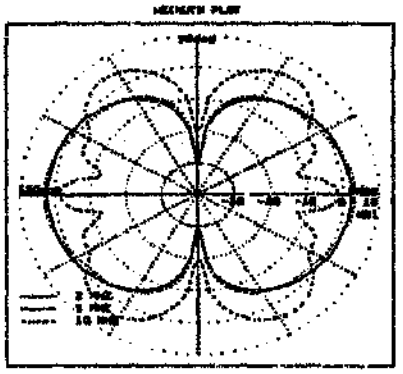


Fig 2.3 The low frequency azimuth radiation pattern of a free space resistively loaded dipole

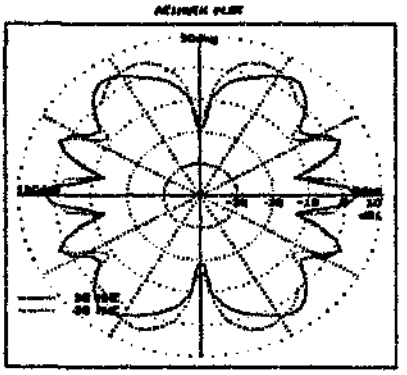


Fig 2.4 The high frequency azimuth radiation pattern of a free space loaded dipole

2.2.3 Radiation patterns of horizontal loaded and unloaded dipoles at different heights above a perfect earth

The antenna pattern when mounted above the ground is of more interest however and figs 2.5 to 2.8 show both elevation plane as well as azimuth plane patterns for an unloaded dipole at a height of 12 m above a perfect earth. The elevation plane patterns are taken perpendicular to the dipole which remains parallel to the y-axis (i. e. variation of θ with ϕ constant at 0°). Representation of the azimuth plane patterns are problematic since the perfect earth plane causes no radiation at ground level ($\theta = 90°$). All azimuth radiation plane patterns for antennas above a earth plane were hence plotted with elevation angle constant at 60° which is equivalent to a take-off angle of 30°.

The low frequency elevation plane radiation patterns in fig 2.5 indicate the antenna to be quite suitable for short range HF communications. Radiation is concentrated in the take off angles between 30° to the zenith with no pattern nulls in these directions. The elevation plane patterns at higher frequencies (fig 2.6) show an increase in pattern lobes with nulls occurring in the required range of take-off angles. Table 2.1 however, indicates that frequencies above 15 MHz will very seldom be required for short range communications. The low frequency azimuth plane radiation patterns showed in fig 2.7 are more problematic, since the antenna is only omnidirectional at the lowest frequencies. Lobes start to occur at 5 MHz and the number of lobes (and nulls) increases with increase in frequency. This tendency is continued at higher frequencies as indicated in fig 2.8. Ideally a more omnidirectional azimuth pattern is required, especially for the main frequency range of interest (2 - 15 MHz).

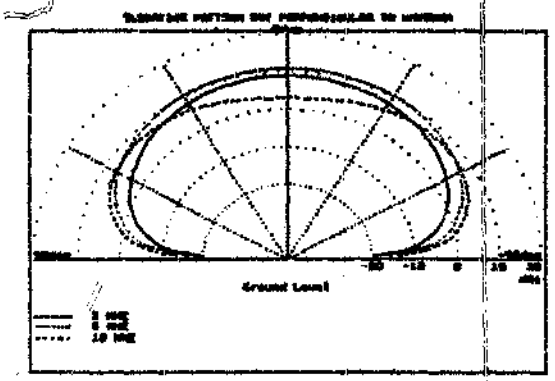


Fig 2.5 Perpendicular elevation plane radiation patterns of a horizontal dipole 12 m above a perfect earth.

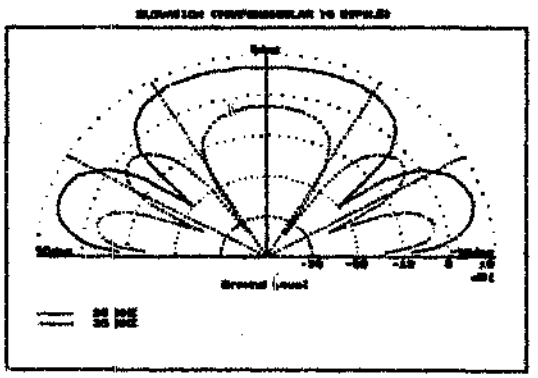


Fig 2.6 Perpendicular elevation plane radiation patterns of a horizontal dipole 12 m above a perfect earth.

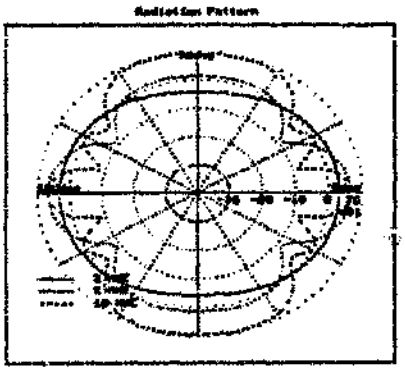


Fig 2.7 Azimuth radiation patterns of a horizontal dipole 12 m above a perfect earth

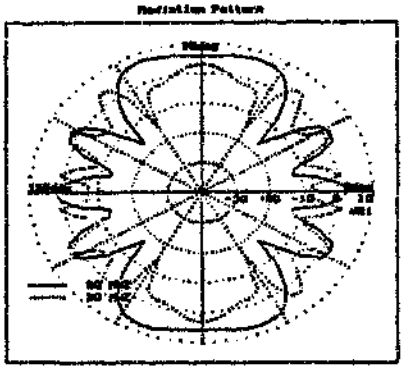


Fig 2.8 Azimuth radiation patterns of a horizontal dipole 12 m above a perfect earth

The effect of raising the antenna height to 24 m for the same antenna is illustrated in figs 2.9 to 2.12. The elevation plane patterns (figs 2.9 and 2.10) show an increase in lobes and pattern nulls which start to occur at 10 MHz. The azimuth patterns (figs 2.11 and 2.12) are very similar to the ones for a 12 m antenna height.

The increase in nulls when increasing antenna height is explained by image theory. The antenna and its image form an array with spacing equal to twice the antenna height and 180° phase shift in excitation. As the array electrical separation increases due to an increase in frequency, the pattern naturally becomes more multi-lobed. Lowering the antenna, on the other hand, will result in better pattern behaviour, but with detrimental effect on input parameters due to coupling between antenna and the ground plane. The ground losses when the antenna is mounted over a lossy ground also increase. The 12 m mast antenna height therefore represents a suitable compromise for short distance HF communications.

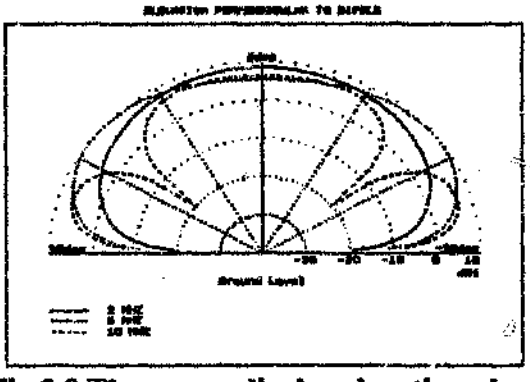


Fig 2.9 The perpendicular elevation plane radiation patterns of a horizontal dipole 24 m above a perfect earth.

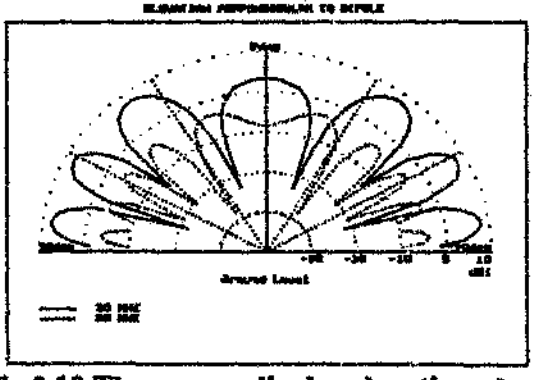


Fig 2.10 The perpendicular elevation plane radiation patterns of a horizontal dipole 24 m above a perfect earth.

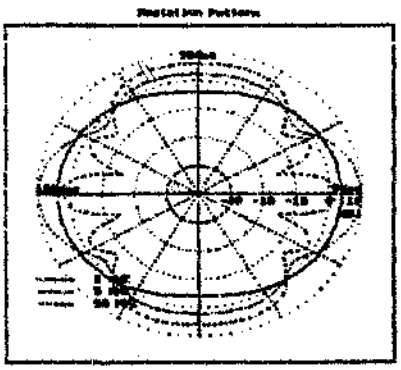


Fig 2.11 The azimuth plane radiation patterns of a horizontal dipole 24 m above a perfect earth.

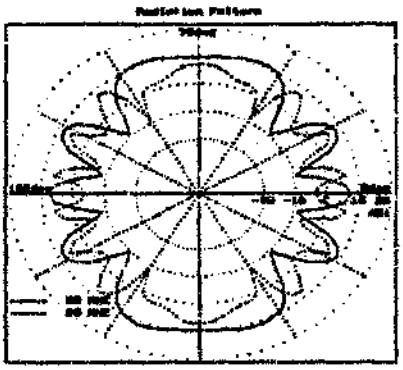


Fig 2.12 The azimuth plane radiation patterns of a horizontal dipole 24 m above a perfect earth.

The performance of the Altshuler type dipole, also in horizontal configuration above a perfect earth, should be compared to that of the unloaded dipole. Image theory mentioned before suggests that the elevation patterns perpendicular to the dipole axis will be the same shape as that of an unloaded dipole. The absolute values may differ however due to differences in the azimuth radiation characteristics. The radiation patterns for an Altshuler type dipole at 12 m height are given in figs 2.13 to 2.16.

The elevation plane radiation patterns have exactly the same shape as that of the unloaded dipole when figs 2.13 and 2.14 are compared to figs 2.5 and 2.6. The only difference between the two sets of patterns is in absolute values which implies that the normalized patterns would be identical. The azimuth plane radiation patterns at low frequency (fig 2.15) are in general more omnidirectional than that of the unloaded dipole. The high frequency azimuth radiation patterns (fig 2.16) show more lobes than the low frequency case but the nulls are generally not as deep or frequent as in the case of the unloaded dipole (fig 2.8).

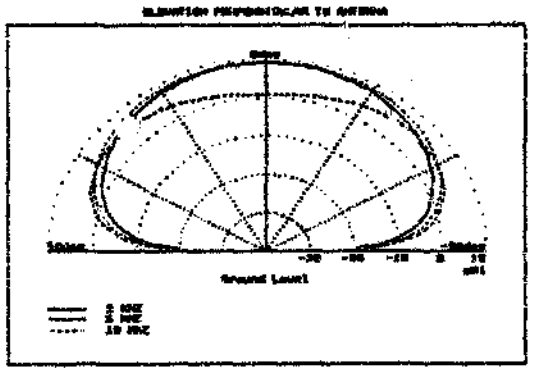


Fig 2.13 The elevation plane radiation patterns of a horizontal Altshuler type dipole 12 m above a perfect earth.

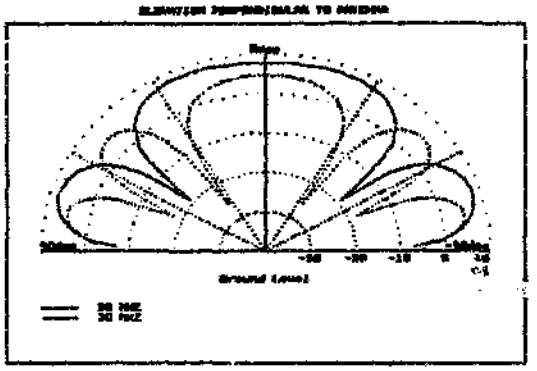


Fig 2.14 The elevation plane radiation patterns of a horizontal Altshuler type dipole 12 m above a perfect earth.

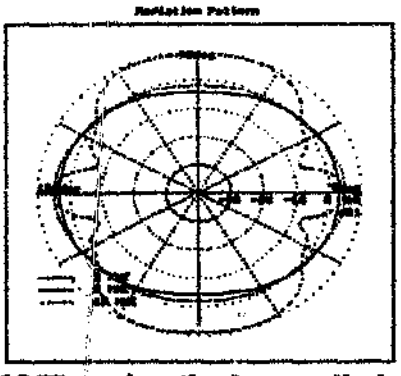


Fig 2.15 The azimuth plane radiation patterns of a horizontal Altshuler type dipole 12 m above a perfect earth.

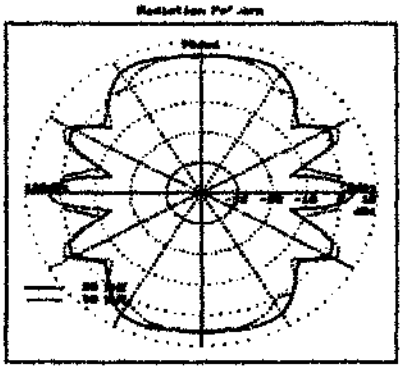


Fig 2.16 The azimuth plane radiation patterns of a horizontal Altshuler type dipole 12 m above a perfect earth.

Figs 2.17 to 2.20 show the same sets of radiation patterns for the Altshuler type antenna at a height of 24 m. The same changes in elevation plane patterns (figs 2.17 and 2.18) as in the case of the unloaded dipole are observed when increasing the antenna height. Once again the azimuth radiation patterns (figs 2.19 and 2.20) are not much altered from those observed at lower mounting height. The comments regarding optimum antenna height given before apply to this antenna. The important factor to note is that the elevation radiation pattern, which is the important parameter relating to HF communications, is mainly affected by antenna height above ground. This parameter is hence difficult to manipulate during design without increasing the antenna complexity. The general elevation plane performance of loaded and unloaded dipoles is however generally acceptable for short range HF communications. This study hence strengthens the argument that radiation pattern can be largely ignored during design optimization due to constraints imposed by the simplicity of the geometry.

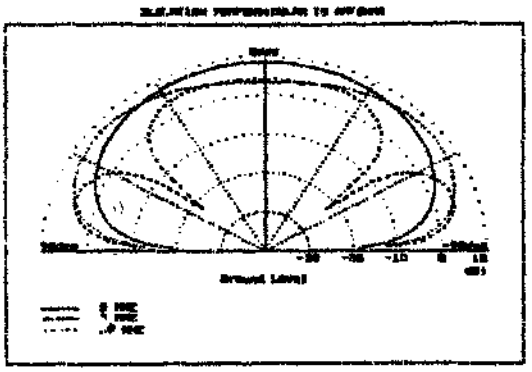


Fig 2.17 The elevation plane radiation patterns of a horizontal Altshuler type dipole 24 m above a perfect earth.

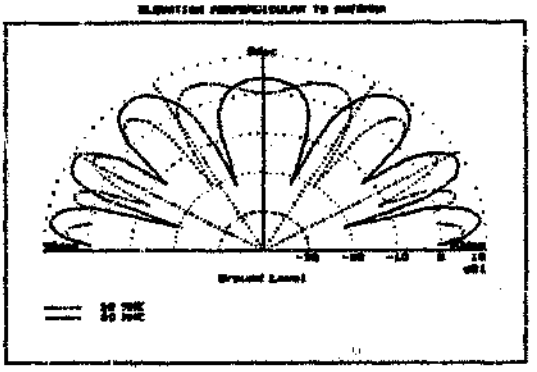


Fig 2.18 The elevation plane radiation patterns of a horizontal Altshuler type dipole 24 m above a perfect earth.

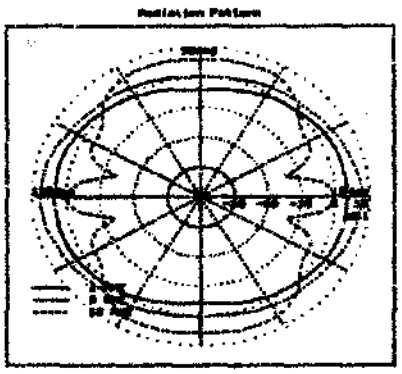


Fig 2.19 The azimuth plane radiation patterns of a horizontal Altshuler type dipole 24 m above a perfect earth.

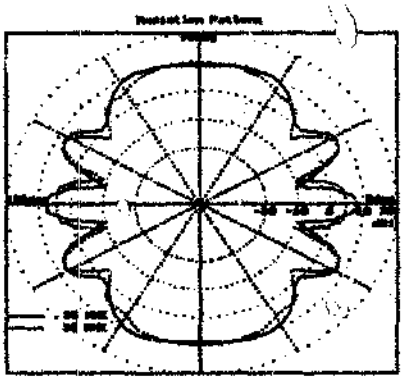


Fig 2.20 The azimuth plane radiation patterns of a horizontal Altshuler type dipole 24 m above a perfect earth.

2.2.4 Radiation patterns of dipoles mounted in an inverted-v configuration

A configuration which is often employed in practice is the so-called inverted-v antenna mounting. This allows the antenna to be mounted on a single mast with the feed point at the top of the mast and the antenna wires sloping towards the ground. The Altshuler type antenna was modelled in this configuration on a 12 m centre mast with the wires sloping to a final height of 2 m. The radiation patterns for this configuration are shown in figs 2.21 to 2.24.

The low frequency elevation plane patterns (fig 2.21) once again consist of single lobes, suitable for the required application and the higher frequency patterns (fig 2.22) having multiple lobes which are similar to those of the horizontal dipole. The azimuth plane radiation patterns (figs 2.23 and 2.24) are similar to those for the horizontal dipole with the main difference being the lower radiation broadside to the antenna at 10 MHz.

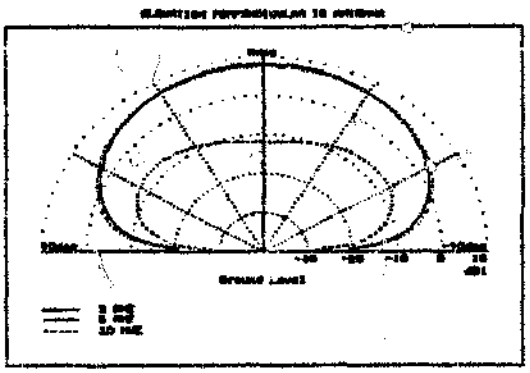


Fig 2.21 The elevation plane radiation patterns of an inverted-v Altshuler type dipole with 12 m mast height above a perfect earth.

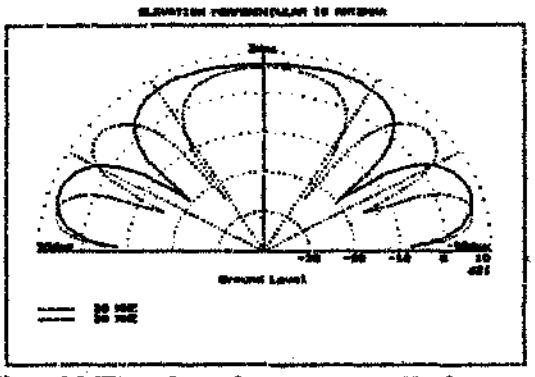


Fig 2.22 The elevation plane radiation patterns of an inverted-v Altshuler type dipole with 12 m mast height above a perfect earth.

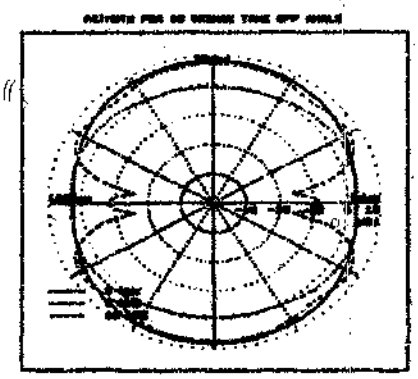


Fig 2.23 The azimuth plane radiation patterns of an inverted-v Altshuler type dipole with 12 m mast height above a perfect earth.

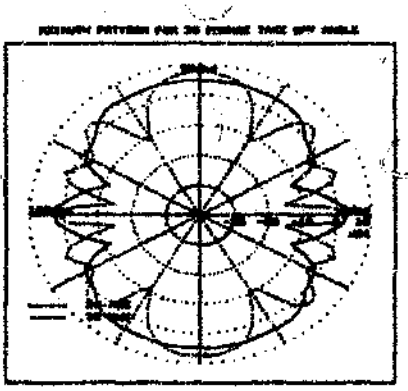


Fig 2.24 The azimuth plane radiation patterns of an inverted-v Altshuler type dipole with 12 m mast height above a perfect earth.

2.2.5 Influence of different ground models on loaded antenna radiation pattern

The patterns for the same inverted-v antenna on a 12 m mast were also obtained when the antenna is mounted above a real (lossy) earth (figs 2.25 to 2.28). The patterns were generated using the Fresnel reflection coefficient option in NEC2 and average ground parameters of $\sigma = 0.01$ mS and $\varepsilon_r = 20$ were specified. The radiation patterns above the real earth are in general very similar to those above the perfect earth considered before. The most notable difference is the reduction in the depth of the nulls in the high frequency elevation plane patterns (fig 2.25).

There is some doubt as to the validity of the Fresnel reflection coefficient approximation at the low frequencies. The NEC2 manual states that the more rigorous Sommerfeld method should be used when structures are closer than 0.2 wavelengths above ground. This condition is violated below 5 MHz for an antenna height of 12 m. The two ground models can be compared by studying the patterns for 2 and 5 MHz shown in Figs 2.29 to 2.32. These figures indicate that the Fresnel reflection approximation is quite suitable in terms of radiation pattern representation.

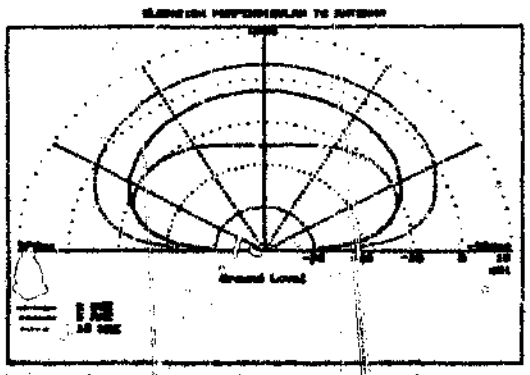


Fig 2.25 The elevation plane radiation patterns of an inverted-v Altshuler type dipole with 12 m mast height above a lossy (Fresnel) earth.

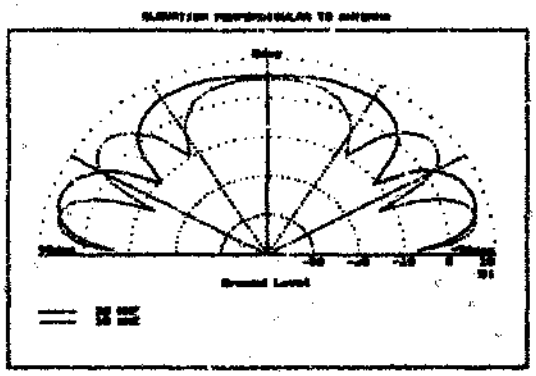


Fig 2.26 The elevation plane radiation patterns of an inverted-v Altshuler type dipole with 12 m mast height above a lossy (Fresnel) earth.

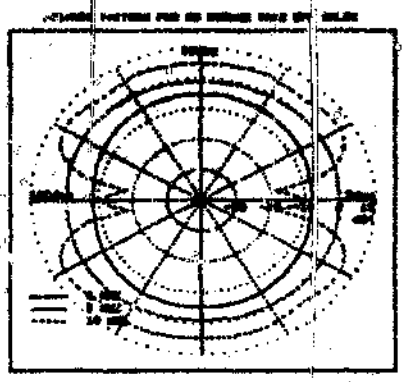


Fig 2.27 The azimuth plane radiation patterns of an inverted-v Altshuler type dipole with 12 m mast height above a lossy (Fresnel) earth.

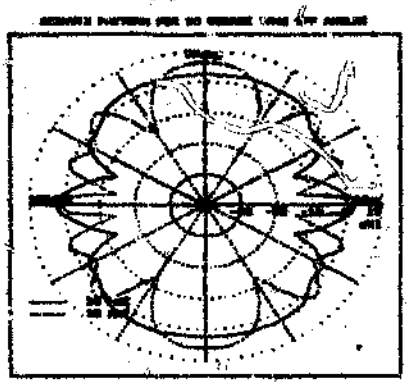


Fig 2.28 The azimuth plane radiation patterns of an inverted-v Altshuler type dipole with 12 m mast height above a lossy (Fresnel) earth.

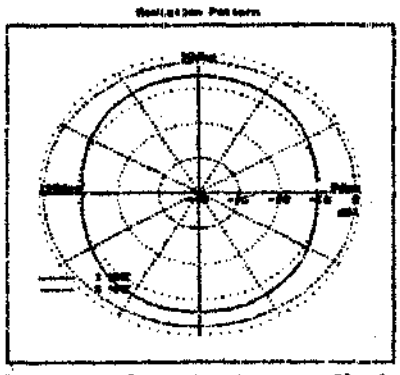


Fig 2.29 The azimuth plane radiation patterns of an inverted-v Altshuler type dipole on 12 m mast above a lossy (Sommerfeld) earth.

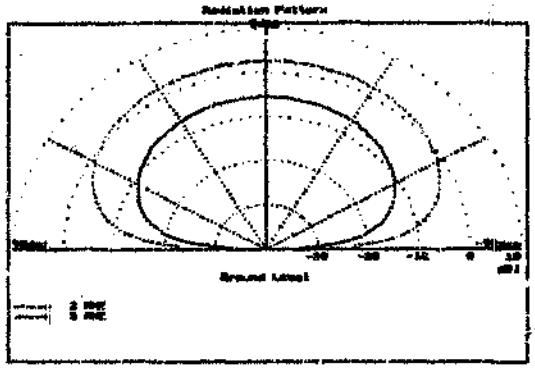


Fig 2.30 The elevation plane radiation patterns of an inverted-v Altshuler type dipole on a 12 m mast above a lossy (Sommerfeld) earth.

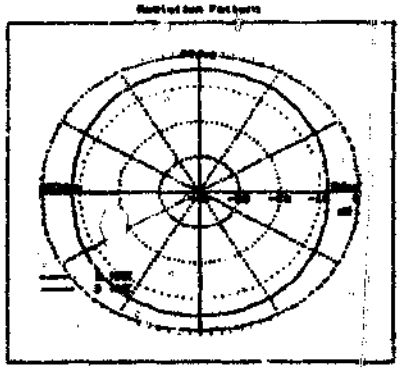


Fig 2.31 The azimuth plane radiation patterns of an inverted-v Altshuler type dipole on 12 m mast above a lossy (Fresnel) earth.

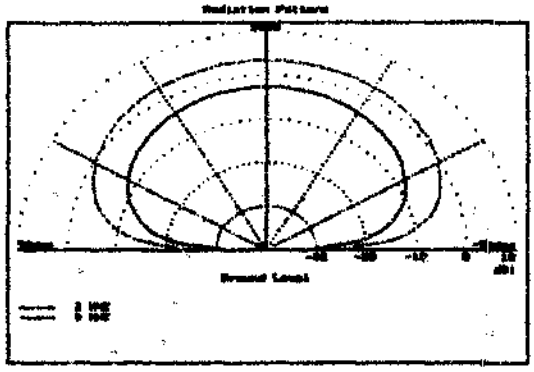


Fig 2.32 The elevation plane radiation patterns of an inverted-v Altshuler type dipole on a 12 m mast above a lossy (Fresnel) earth.

2.2.6 Problems with representing radiation patterns using two dimensional cuts.

Antenna radiation patterns are inherently three dimensional and hence some information is lost in a two dimensional representation. Radiation patterns consisting of a single main beam are less problematic since these are normally adequately represented using two perpendicular cuts through the beam axis. The problem of representing the patterns of non-directional antennas such as the ones studied is more severe. The method used in chapter 5 employs the same elevation and azimuth cuts as used in this section with an additional elevation plane cut orthogonal to the cut perpendicular to the dipole axis. This is probably the most complete picture which can be represented without overwhelming the reader with data. There is a possibil-

ity that the chosen method of representing patterns may lead to some incorrect conclusions. This is best illustrated by considering figs 2.33 and 2.34. A number of azimuth cuts are shown for the Altshuler type antenna in an inverted-v configuration 12 m above a perfect ground plane at 30 MHz. The problem with evaluating the omnidirectional nature of this antenna using a single cut is clearly illustrated. Nulls at specific elevation angles do not necessarily occur at other angles. Care should hence be taken when evaluating the directional characteristics of these antennas. The representation of 2.33 and 2.34 would give a more comprehensive picture, but since this will have to be repeated for all the frequencies the reader is likely to emerge more confused than enlightened. Normally the three cuts mentioned before present a reasonable indication of antenna performance and are sufficient for a qualitative analysis. This is certainly true at the lower frequencies.

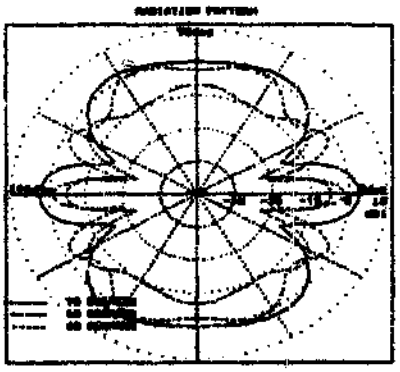


Fig 2.33 Azimuth radiation patterns at different elevation angles for an Altshuler type inverted-v antenna at 30 MHz

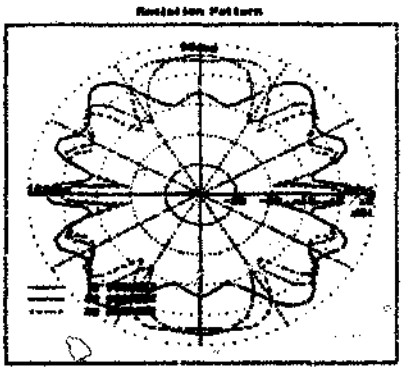


Fig 2.34 Azimuth radiation patterns at different elevation angles for an Altshuler type inverted-v antenna at 30 MHz

2.2.7 Conclusion on radiation pattern characteristics of simple dipole antennas

The following conclusions can be drawn from the investigation presented in this section:

- Short range HF communications requires elevation plane illumination between take-off angles of 30° and 90°.
- Frequencies between 2.5 and 15 MHz are most important for communication over a 0 - 1000 km link.
- The radiation patterns of travelling wave antennas mounted in a inverted-v configuration on a 12 m mast present a suitable compromise to the stated requirement.
- The Fresnel ground reflection approximation is suitable for modelling real ground effects on radiation patterns.

- The patterns of simple dipole antennas have characteristics which are difficult to alter without resorting to more complex geometries.
- One should exercise care when evaluating the two dimensional radiation pattern cuts, since the patterns are inherently three dimensional. This is not normally a problem at low frequencies, but may result in incorrect conclusions at higher frequencies.

2.3 Antenna Bandwidth - Definition, Terminology and Implications

Bandwidth of antennas is rather nebulously defined by Stutzman and Thiele (1981: p 260) as the upper and lower frequencies for which satisfactory performance is obtained. Usually such "satisfactory performance" refers to either the pattern or impedance constancy of a structure with changes in frequency. Subsequent research findings suggest that it may be prudent to add efficiency performance to this list when relatively small broadband antennas are studied. In the case of HF antennas the bandwidth of interest is naturally 2 or 3 - 30 MHz (Maslin, 1987), and Treharne (1983b) aptly named geometries with this bandwidth "whole-band" rather than broadband.

The typical non-directional low gain nature of tactical antennas indicates their pattern constancy to be of lesser importance (Austin, 1986) when optimizing simple broadband HF antennas. The radiation patterns ultimately play a very important part in HF communications as shown in detail in the previous section. The radiation patterns of typical dipole antennas above a real earth was shown to be a suitable compromise for short range HF communications. The studies presented in section 2.2 also suggest that this parameter cannot be altered significantly without resorting to more complex geometries. Very often input characteristics can be more successfully modified and adapted while maintaining a simple geometry. The antenna designer is hence forced to disregard radiation pattern and rather maximize radiated power (Gnabs, 1966 ; Guertler and Collyer, 1973 ; Harris, 1982 ; Treharne, 1983 and Wilson, 1985). Radiation patterns should thus be ignored when designing and optimizing simple HF broadband antennas. The patterns of the antennas studied in the following chapters will however be examined in Chapter 5 again to verify this approach as well as to allow a complete assessment of the antennas which were studied and evaluated.

The more commonly encountered measure of broadband performance in this class of antennas is the impedance bandwidth commonly expressed in terms of the voltage standing wave ratio, VSWR, on the feedline. The expression for VSWR in terms of the voltage reflection coefficient, ρ_v, is:

$$VSWR = \frac{1+|\rho_v|}{1-|\rho_v|} \qquad -(2.3)$$

where

$$\rho_v = \frac{Z_i - Z_o}{Z_i + Z_o} \qquad -(2.4)$$

and Z_i is the antenna input impedance and Z_o is the characteristic impedance of the feedline.

Clearly the optimum value of VSWR is unity, since this corresponds to the matched case, that is when $Z_i = Z_o$. The impedance bandwidth of an antenna will be defined as the frequency range for which the VSWR is less than some predefined value. The sensitivity of the transmitter electronics generally indicates that a maximum VSWR of 2:1 is tolerable before output power is reduced or damage results. This value will therefore be considered as a yardstick for evaluating impedance bandwidth. Topics that need to be addressed are the practical and theoretical limitations in achieving such performance using broadband antennas.

The structural limits are usually determined by the specific application. Tactical deployment is of primary concern in this investigation and Theron (1983) provided a few guide lines:

- Mast height should be minimized.
- Mast and antenna should be easy to erect.
- Antenna profile should be minimized, implying the use of thin wire construction.

As is often the case in engineering, the laws of nature oppose these ideals. The Chu-Harrington limits (Hansen, 1981), which are reproduced in fig 2.35, illustrate the fundamental limitations. The Chu-Harrington limits apply to broadband HF antennas at the lower frequencies where the antenna length is in the order of half a wavelength and illustrates the general dilemma facing the designer of such antennas.

Impedance bandwidth is related to the quality or Q factor of the antenna. The Q factor is the ratio of the stored energy in an antenna (or circuit) to the dissipated (due to radiation or ohmic losses) energy present. Stored energy must be minimized and hence the Q reduced for broadband antennas (Treharne, 1983b). Fig 2.35 shows that radiation efficiency must be sacrificed if the effective length is reduced in low Q or broadband structures. The values in Chu-Harrington limits were obtained by assuming that all possible wave modes are excited in a sphere enclosing the radiating structure. Dipole antennas do not excite all wave modes so they will never achieve the limiting (ideal) case. The Chu-Harrington limits serve to highlight the effect of size on radiation efficiency.

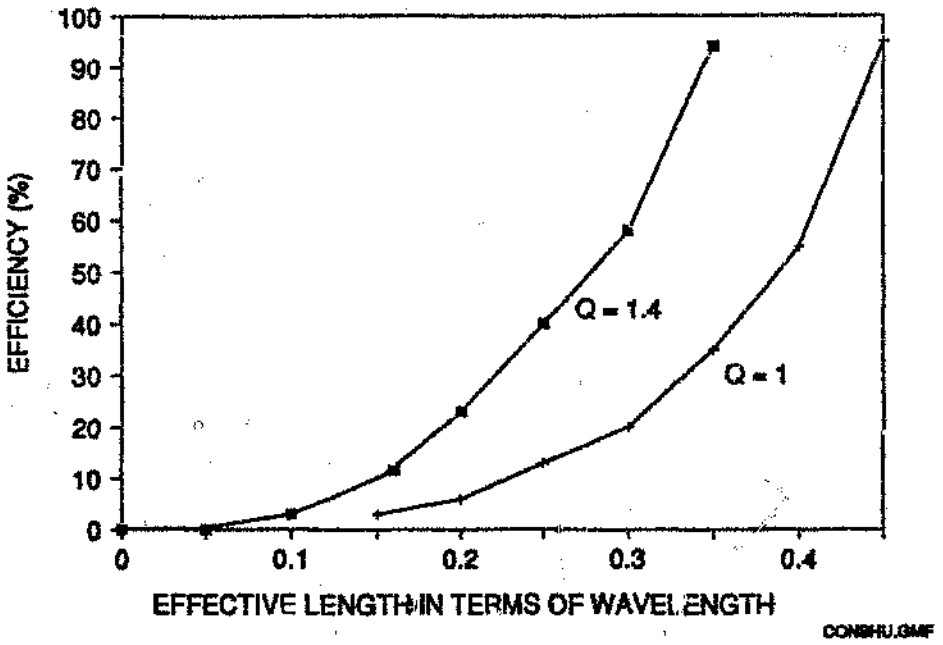


Fig 2.35 Consequences of the Chu-Harrington limits (after Treharne, 1983b)

Efficiency is hence an important parameter in the design and evaluation of simple broadband antennas. Efficiency is often degraded as a result of the reduction in dimensions brought about to satisfy practical constraints. The fact that radiation efficiency of HF antennas is particularly difficult to measure compounds the problem (Smith, 1977). Efficiency can practically only be determined by summing the power radiated over a full hemisphere. Radiated power has to be measured in the antenna far field and at HF the typical wavelengths this requires the use of an aircraft to do so. VSWR performance viewed in isolation is misleading and therefore an indication of efficiency is necessary.

Evaluation of efficiency in later chapters considers only the losses due to resistive components in the antenna structure. Losses due to finite wire conductivity are normally neglected. Fitzgerrel (1965) showed that a typical half wave dipole constructed of 2 mm radius copper wire has an efficiency of 99.3 % at 10 MHz for instance. Losses due to wire conductivity are hence much less than those due to resistive components and neglecting these will cause negligible errors. The efficiency of input transformers are similarly ignored since these have been shown (Sevick, 1976) to have efficiencies exceeding 99% over the HF band.

The last parameter which may be of importance in defining antenna bandwidth is the polarization of the antenna. Fortunately polarization plays a negligible part in sky wave propagation and may generally be chosen for convenience of antenna design (Maslin, 1987 : 105).

2.4 The Power Radiated Ratio (PRR)

As explained before, neither the VSWR, nor the efficiency provide complete figures of merit in isolation. A more worthwhile measure of broadband performance should incorporate both of these parameters. A ratio, named the Power Radiated Ratio (PRR), is defined for the purpose of this study to be:

PRR = power radiated/power radiated by a matched, lossless antenna.

= (forward power - ohmic losses - reflected power)/forward power

The PRR is the fraction of power radiated by a real antenna compared to the power radiated by an ideal antenna. The ideal antenna is assumed lossless and perfectly matched to the feedline. Both poor matching and any decrease in efficiency would thus reduce this ratio. An expression for this ratio is developed as follows:

$$P_t = P_f - P_r \qquad \text{-(2.5)}$$

where:

P_t is the power transferred to the antenna ;

P_f is the forward power to the antenna ;

P_r is the power reflected by the antenna.

$$\frac{P_t}{P_f} = 1 - \frac{P_r}{P_f} \qquad \text{-(2.6)}$$

$$\frac{P_t}{P_f} = 1 - \frac{|V_r|^2}{|V_f|^2} \qquad \text{-(2.7)}$$

where V_f is the incident voltage on the antenna and V_r is the voltage reflected by the antenna. If the voltage reflection coefficient, ρ_v, is now defined to be V_r/V_f equation (2.7) can be written as:

$$\frac{P_t}{P_f} = 1 - |\rho_v|^2 \qquad \text{-(2.8)}$$

But from 2.4:-

$$\rho_v = \frac{Z_i - Z_o}{Z_i + Z_o} \qquad \text{-(2.9)}$$

where Z_i is the input impedance of the antenna and Z_o is the characteristic impedance of the feedline.

Since efficiency,

$$\eta = \frac{P_{radiated}}{P_t} \qquad \text{-(2.10)}$$

The PRR is defined at the outset to be the product of the mismatch factor and the efficiency factor or mathematically:

$$\text{PRR} = \frac{P_t}{P_f} \times \frac{P_{radiated}}{P_t}$$

Replacing equations 2.8 and 2.10 gives :

$$\text{PRR} = \eta \cdot (1 - |\rho_v|^2) \qquad \text{-(2.11)}$$

The only values necessary for calculating this ratio are Z_i, the known Z_o and the efficiency, η. The PRR thus provides a composite picture of antenna bandwidth with both efficiency and impedance matching (VSWR) taken into account. In section 2.6 a rigorous numerical method to obtain these parameters will be discussed in detail. The PRR is clearly dominated by the efficiency for well matched antennas, but during an optimization phase the VSWR may be high and the PRR is the obvious parameter to maximize.

2.5 Different Methods of Obtaining Broadband Performance

Three different methods of achieving broadband performance were identified from the literature:

- Employing self scaling or angular structures
- Increasing antenna thickness
- Loading antenna with partially resistive loads

The first involves antennas that are naturally "self scaling". Self scaling structures can be specified in terms of angles rather than in linear dimensions (Balanis, 1982: p 414). Angular geometries will have to be infinite in extent to be completely frequency independent. Truncated structures however do achieve broadband performance over a limited frequency range. A well known antenna utilizing this principle is the log periodic dipole array, LPDA, (Isbell, 1960) illustrated in fig 2.36.

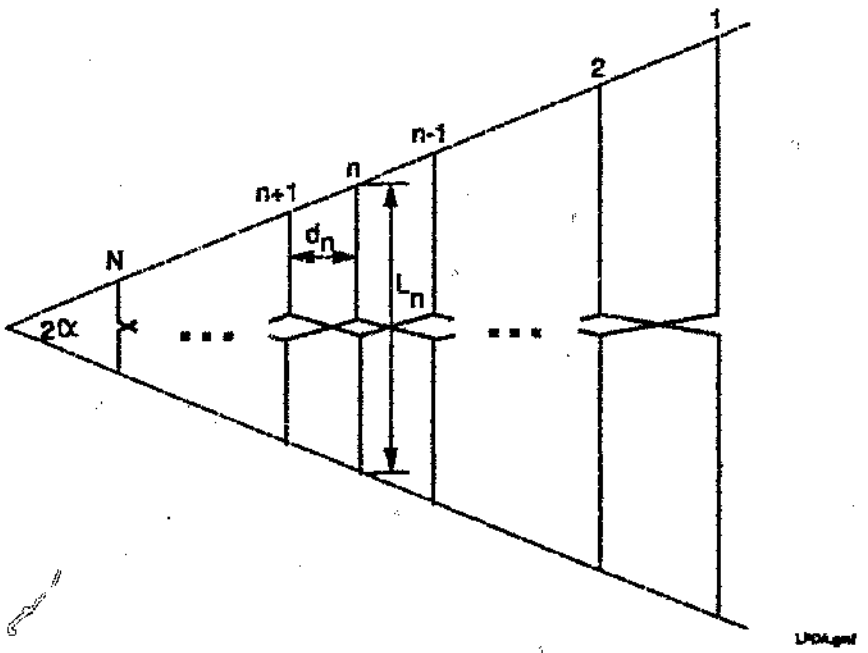


Fig 2.36 The log-periodic dipole array geometry (adapted from Stutzman and Thiele, 1981: p 295)

The LPDA is fed at the shortest dipole end. Very little power is absorbed by the dipoles which are shorter than their resonant lengths since these dipoles are capacitive and present a severe mismatch. Most of the power (and current) is concentrated about the antenna active region. The active region is made up of dipoles which are close to resonance at the specific frequency. Frequency changes merely shift the location of the active region on the LPDA and hence the term "self scaling".

The envelope of this structure as determined by the generating angle α is expressed in terms of the scale factor τ as:

$$\tau = \frac{L_{n+1}}{L_n} = \frac{d_{n+1}}{d_n} \qquad -(2.12)$$

and the spacing factor, σ, is defined by:

$$\sigma = \frac{d_n}{2L_n} \qquad -(2.13)$$

The longest element, L_1, is chosen to be approximately half a free space wavelength at the lowest frequency of operation. The shortest element L_N is similarly made about half a wavelength at the highest frequency of operation. Reliable curves for τ and σ in relation to other LPDA parameters were published by (Peixeiro, 1988). Peixeiro's design graphs together with the required frequency range facilitates the design of such a structure. It is instructive to obtain an indication of the size of a LPDA antenna use over the HF band ; the longest element would be at least 50 m with the total length of the structure being of the same order. Clearly this size is not very suitable for tactical applications!

A second well known method for achieving broadband behaviour uses electrically thick structures. It has been known for many years that thicker wires have a broader bandwidth when compared to thin ones (Ramsdale, 1978). Solid antennas of this type are not feasible at HF because of practical constraints . Thicker structures may be approximated by vestigial emulation using a number of thin wires spaced apart by much less than a wavelength. An electrically "thick" conical monopole is illustrated in fig 2.37

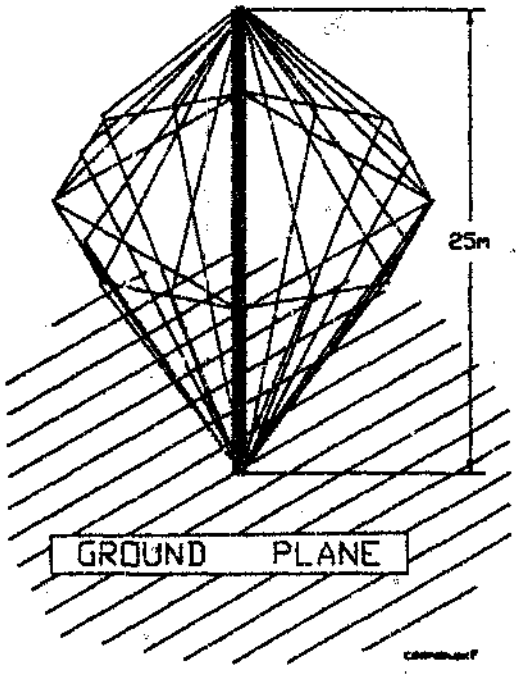


Fig 2.37 A practical wire HF conical monopole

The current distribution on thin dipoles is approximately sinusoidal (Balanis, 1982). The input current, which determines the antenna input impedance, therefore varies rapidly with changes in electrical length. The anti-resonant condition, which occurs when a dipole is about a wavelength long, causes a current minimum at the feed point. The current minimum is very

small (almost zero) for thin dipoles which gives rise to high impedance peaks. The ratio of maximum to minimum values of the current distribution on dipoles therefore determine the dipole impedance bandwidth. The current deviates from its sinusoidal nature as the antenna thickness increases. Mathematically the current may be represented by a sinusoidal term with an additional cosinusoidal term added to it. The amplitude of the cosinusoidal or quadrature term is a direct function of the wire thickness and increases with wire thickness (Balanis, 1982: 128 and Woolf, 1988: 54). The two sinusoids are out of phase by 90 degrees and adding them hence reduces the ratio between current distribution peaks and troughs. Thicker wires hence exhibit less impedance variation as a result of a more constant current distribution. The same argument clearly applies for monopoles since they may be similarly treated analytically using image theory.

Conical monopoles yield good broadband performance with relatively high efficiencies (Mason, 1963), but are unsuitable due to their size. The two general antenna types described above are large and complex to achieve broadband performance whereas the applications addressed here require just the opposite.

A third and more practical way to achieve broadband performance is to allow only travelling waves to flow on simple dipoles. Travelling waves in this instance refer to the current distribution on a structure and implies that no current is reflected from the antenna terminations. Travelling waves therefore result in little circulating or stored energy. The resultant low Q-value of the antenna implies a large bandwidth. The analogy to a transmission line terminated in a load equal to its characteristic impedance is evident. The input impedance of a matched transmission line is independent of frequency since only travelling waves exist on the line. Resistive loading seems to offer an easy solution to the problem of increasing antenna bandwidth. The problem is that all the power in this case is dissipated in the load since the radiation efficiency of a transmission line is zero. Real antenna geometries also do not lend themselves to a simple method of termination. These principles have been used with some measure of success with the pioneering work of Altshuler (1961) being of special significance.

An appropriate resistor is positioned one quarter of a wavelength away from the end of a thick antenna as shown in fig 2.38. The "open circuit" at the monopole tip is converted to a virtual earth point at the load by the well known quarter wave transmission line impedance transformer principle. The antenna is effectively terminated in its characteristic impedance in this way. This type of termination, in analogy to the matched transmission line, ensures that only travelling waves exist between the feedpoint and the load.

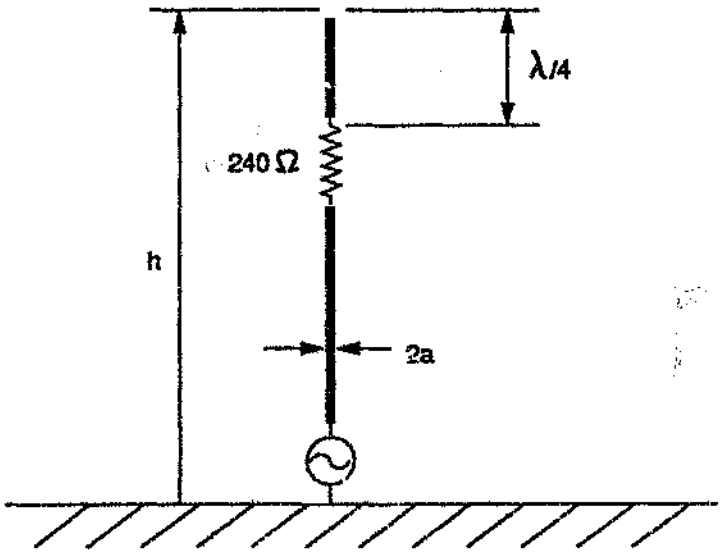


Fig 2.38 Altshuler's resistively loaded monopole

Frequency changes unfortunately alter the electrical length of the terminating section. The electrical thickness of the monopole increases the bandwidth which partially compensates for small changes in the terminating section electrical length. Altshuler measured the impedance of this antenna and showed that it was more or less constant over a 2:1 frequency band. He estimated the radiation efficiency to be 50 percent. Approximate theory (Maclean, 1973) yields radiation efficiency of 45 percent for the frequency where only travelling waves exist between feedpoint and load which supports Altshuler's estimate. The radiation efficiency over a larger frequency band remains uncertain and Maclean's theory does not allow for this to be calculated. A 10:1 or 15:1 bandwidth is required to cover the HF-band and this simplified antenna is not adequate. The increase in bandwidth while using the same dimensions will result in lower efficiencies in accordance with the Chu-Harrington limits mentioned before.

The broadband antennas mentioned above are either large and complex, or small and inefficient. A combination of electrically thick structures and some type of loading (sometimes of a log-periodic nature) provides a reasonable compromise in practice.

2.6 Method of Moments

The increasing availability of powerful computers in recent years led to the development of numerical methods to evaluate the performance of antennas. The most useful technique for analyzing HF geometries is the well known method of moments, described by Harrington

(1968) and others. This method involves a numerical solution to Maxwell's equations for connected wires where the electrical dimensions are not larger than a few wavelengths (Stutzman and Thiele, 1981: Ch. 7). The size limitation is a result of the computer time and the memory required to solve a problem, since both rise exponentially with an increase in dimensions. The structure is divided into a number of straight wires, which are then further subdivided into smaller segments. The method of moments primarily solves Maxwell's equations to yield the current on each segment. All other antenna parameters are easy to compute once the full current distribution and geometry of a radiating structure are known. The method of moments provides a useful alternative for evaluating antennas since it is difficult and expensive to measure efficiency at HF.

The computations performed while solving a method of moments problem bear no obvious relation to the actual antenna. The designer is hence removed from the electromagnetic mechanisms governing the behaviour of an antenna. This often leads to emphasis on results rather than observing the fundamental mechanisms involved in a given structure. Such physical insight is invaluable when a geometry is optimized or developed. It is true to say that computer hardware and software are not sophisticated enough to generate optimized designs in isolation. Design techniques are addressed again in later chapters and simple models of specific antennas are proposed. The operation of the algorithm to obtain solutions using these simple models is clear to the design engineer. An intimate understanding of the design process is therefore retained, allowing intelligent optimization of antennas. Engineering judgment and insight are always crucial in evaluating or developing antennas.

The Numerical Electromagnetics Code (version 2), NEC2 is reviewed in the subsequent section. A section on modelling techniques then highlights the problems encountered while modelling HF antennas. Appendix A provides background to the theory of the method of moments itself.

2.6.1 The Numerical Electromagnetic Code version 2, NEC2

A powerful method of moments program, NEC2, was used for the detailed evaluation of structures. The size of antennas that may be simulated is only limited by the computer used for execution. A special feature of NEC2 allows modelling of an imperfect earth which may be used to determine the effect of a real earth on antenna performance. Other special features of NEC2 are the modelling of solid surfaces, the option of specifying incident wave forms as sources, calculation of near fields and antenna interaction calculations. These features were

not used in this research and will not be commented upon any further. The main features of this code will be reviewed in broad outline. For full mathematical and programming details the manual by Burke and Poggio (1980) should be consulted.

NEC2 uses the Pocklington integral equation for currents on thin wires. Dirac delta functions are used as weighting functions with basis functions consisting of three terms. These terms are a constant, a sine and a cosine. Amplitudes for the bases are related such that their sum satisfies the boundary conditions for current and charge at the segment ends. The basis functions have been found to produce rapid solution convergence. An added advantage is that the fields from the sinusoidal currents are easily evaluated in closed form.

The NEC2 code has three options for ground planes:

- A perfect ground plane can be used.
- An imperfect ground may be modelled using the Fresnel plane-wave reflection coefficients when the antenna is at a height of approximately 0.2 wavelength or more above earth.
- For antennas less than 0.2 wavelength height the rigorous Sommerfeld method is used to determine the interaction between the antenna and a real earth (Burke and Poggio, 1980).

The first two types of ground planes approximately doubles the processing time. The Sommerfeld method however increases the processing time approximately fourfold.

NEC2 also allows two different voltage source models for transmitting antennas. These models are:

- An applied E-field source.
- A current slope discontinuity source (also known as the biconical transmission line source)

(Other types of excitation like plane waves and current sources are provided for, but these excitation methods are of little importance in this research)

2.6.2 Modelling Techniques

A very important part of antenna simulation is the conversion from the physical antenna and its surroundings into a mathematical representation. Naturally the mathematical model is not

exactly the same as the real antenna. The amount and type of deviation that would produce meaningful results are of prime concern. The process of converting the physical structure into a mathematical model is known in general as numerical modelling.

The first important consideration is the limitation due to either the mathematical approximations made in the theory or as result of numerical constraints. Most important is that the method of moments assumes all wires to be thin relative to the wavelength so that only axial currents are taken into account. As a consequence the following are usually important in any method of moments code:

- The ratio of wire radius to wavelength
- The ratio of segment length to radius
- The number of segments per wavelength

The limits on these parameters are usually code dependent and the documentation on the specific code gives an indication of acceptable values.

Ground Effects

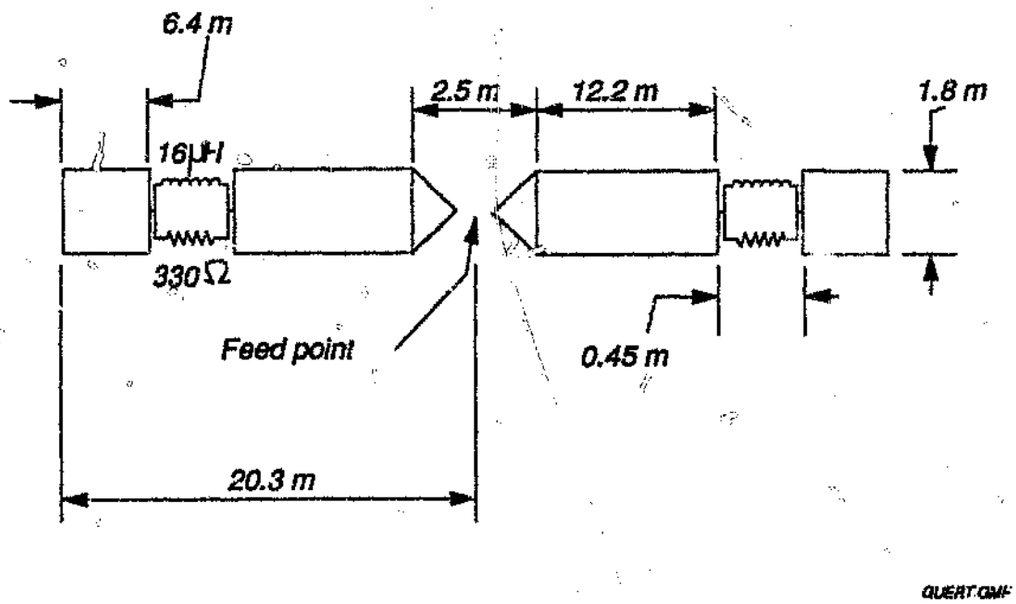


Fig 2.39 Geometry of the Guertler and Collyer dipole

The surroundings of the antenna can seldom be ignored when modelling structures at HF. The effect of different ground models on radiation pattern prediction was already considered in section 2.2. The effect of the earth, which is often electrically c e to the antenna at these

frequencies, on input characteristics is also important. NEC2 provides facilities for either modelling an antenna above a real, lossy earth or a perfect earth as was mentioned before. The Guertler and Collyer's dipole (encountered again in Chapter 3) was modelled in different environments to illustrate the effects of different ground planes on the broadband antenna behaviour. A schematic of the antenna is shown in fig 2.39. The antenna was modelled in three different environments:

- free space ,
- 10 m above a perfectly conducting earth,
- 10 m above a real earth (σ =0.01 S/m and ε_r = 10) using the Sommerfeld ground model.

These cases were investigated using the NEC2 code and impedance results are presented in fig 2.40:

The input impedance of the antenna is seen to be fairly independent of the type of earth. This is an important result, since the same antenna requires double the time to evaluate over perfect earth and four times as long if a real earth plane is included. These times obviously relate directly to the costs involved in the simulations.

The effect of these different environments on the structure radiation efficiencies is illustrated in fig 2.41.

Good correspondence exists between the real earth and perfect earth results except at low frequencies for this loaded antenna. The free space results also show reasonable correlation to the others at the higher frequencies because the height above earth, in wavelengths, increases with increase in frequency.

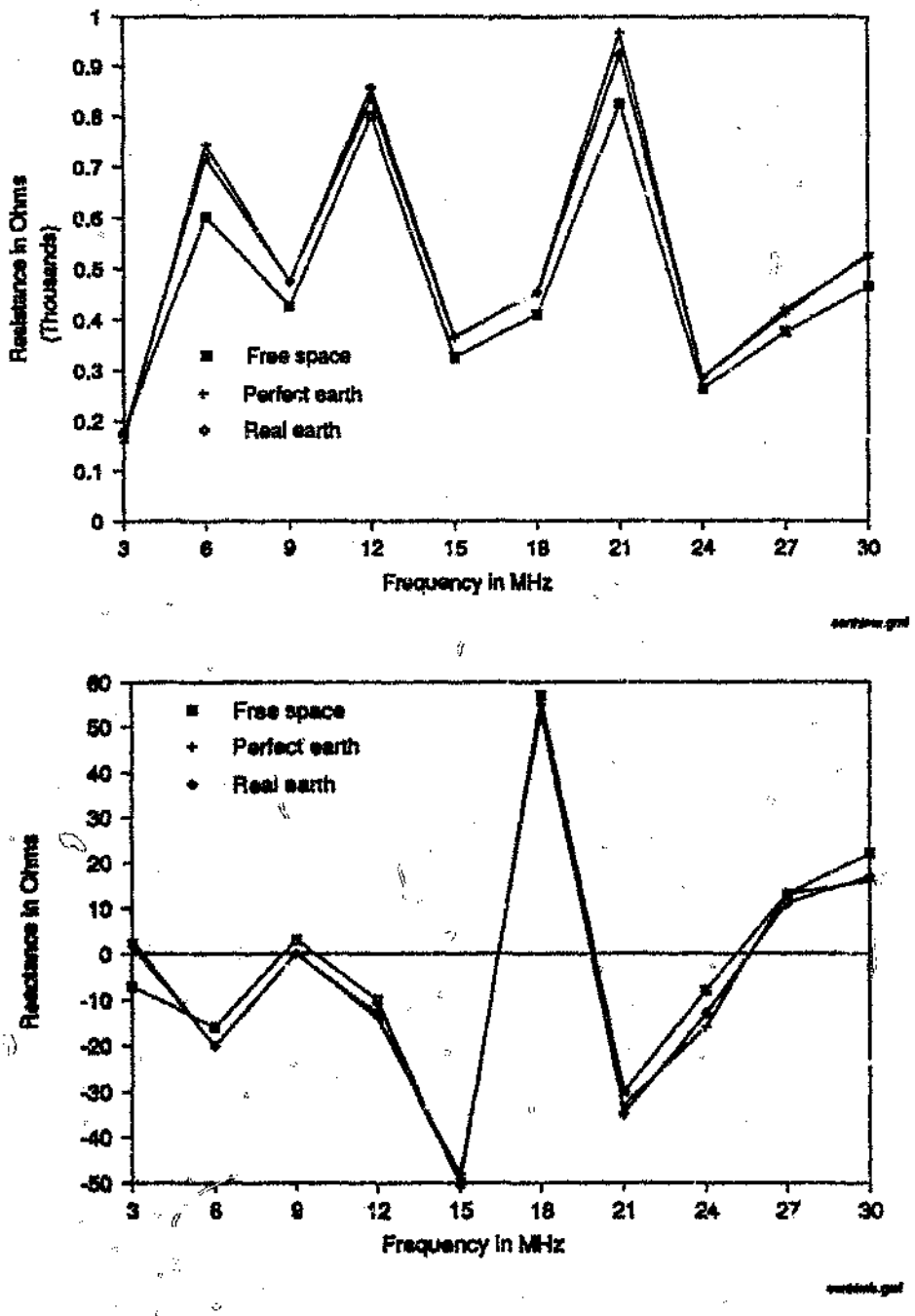


Fig 2.40 The effect of different earth conditions on the input impedance of the Guertler and Collyer dipole.

If the upper half space efficiency, η_u, is now considered to be:

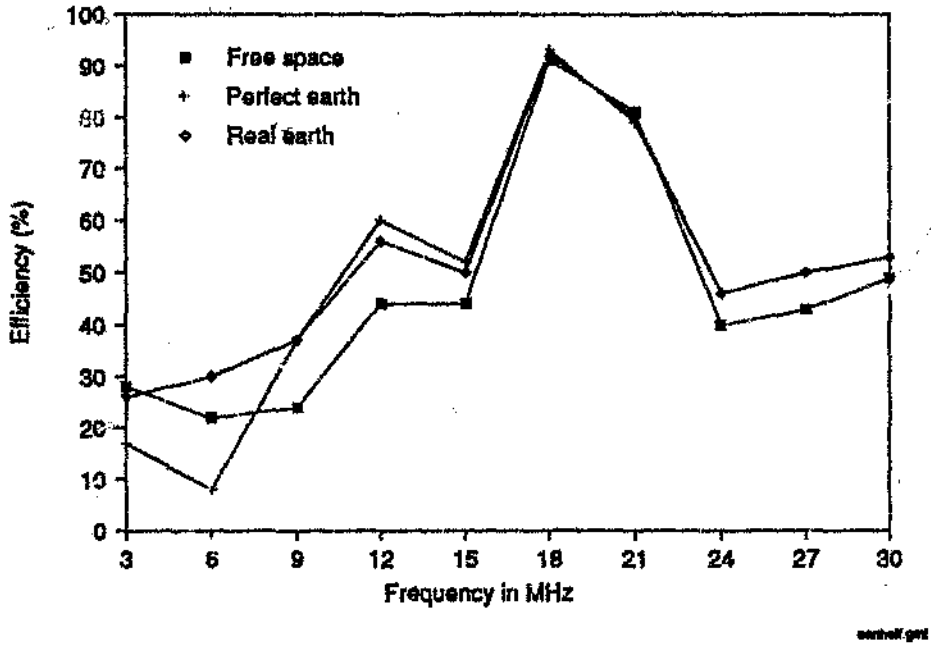


Fig 2.41 Influence of ground types on structure efficiency

$$\eta_u = \frac{\text{power radiated in upper half space}}{\text{input power}} \qquad \text{-(2.14)}$$

the following expression could be developed if:

P_{in} is the total power into the antenna,

P_r the total power radiated,

P_g the power lost in the lower half space (ground) and

P_s the power lost in the structure.

$$\eta_u = \frac{(P_{in} - P_g - P_s)}{P_{in}} \qquad \text{-(2.15)}$$

But since $P_s = P_{in} - P_r$

$$\eta_u = \frac{(P_r - P_g)}{P_{in}} \qquad \text{-(2.16)}$$

$$\eta_u = \frac{P_r(P_r - P_g)}{P_r P_{in}} \qquad \text{-(2.17)}$$

$$\eta_u = \frac{(P_{in} - P_s)(P_r - P_g)}{P_r P_{in}} \qquad \text{-(2.18)}$$

Equation 2.18 may simplified to a factor representing losses in the structure and a factor representing losses in the ground plane, therefore:

$$\eta_u = \eta_s \eta_g \qquad \text{-(2.19)}$$

where structure efficiency is:

$$\eta_s = \frac{(P_{in} - P_s)}{P_{in}} \qquad \text{-(2.20)}$$

and the modification due to ground losses is,

$$\eta_g = \frac{(P_r - P_g)}{P_r} \qquad \text{-(2.21)}$$

For perfectly conducting earth and free space η_g is equal to 1 and hence:

$$\eta_u = \eta_s$$

The upper half space efficiency is calculated using NEC2 by firstly integrating the power density in the upper half space numerically. The power radiated in the upper hemisphere is then compared to the input power to obtain the upper half space efficiency. The effect of the power lost into an imperfect earth is illustrated in fig 2.42 for the Guertler and Collyer dipole. The reduction in upper half space efficiency is evident for this lossy earth example.

Hansen (1972) demonstrated that power lost in a lossy earth becomes independent of height once the antenna is higher than approximately 0.2 wavelengths. This occurs at frequencies above 6 MHz for an antenna at 10 m above ground. For frequencies higher than 6 MHz this loss is also independent of the antenna used and is only dependent on the ground characteristics.

This is an important finding, since it enables comparison of antennas purely in terms of structure efficiency. The additional ground losses can be determined by using a graph such as fig 2.42 or (for different earth characteristics) the curves generated by Hansen. For system calculations the structure efficiency or PRR must therefore be multiplied by η_g.

Below 6 MHz the ground losses do become dependent on the structure and its height and the simplified solution does not apply. The loss at these frequencies must thus either be calculated using a program such as NEC2, or estimated by noting the trends as given by Hansen's (1972) work.

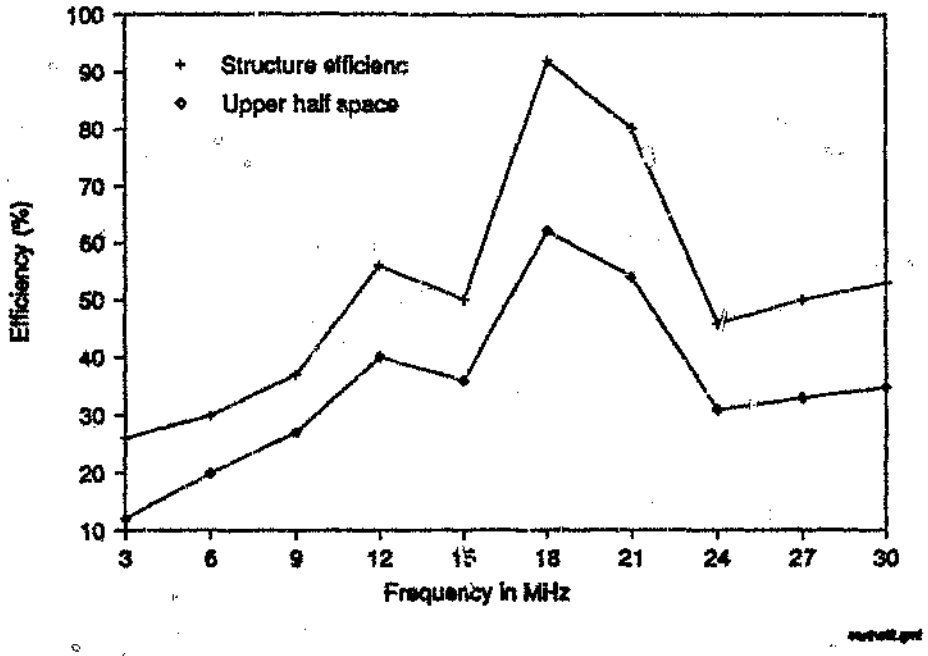


Fig 2.42 Structure efficiency and upper half space efficiency

Effects of wire length

The wire length was found to be an important parameter when simplifying a complex structure. Wire length in this context refers to the physical length of wire between discontinuities. Wire length needs to be retained if equivalent performance is to be achieved from a simplified structure. The wire length concept is explained using the Guertler and Collyer antenna once again (fig 2.39). This structure may be simplified to a single wire monopole with the same equivalent radius (Balanis, 1982: p 338) as the two wire dipole. (Fig 2.43)

The wire length phenomenon was mentioned by Kubina (1983) in relation to modelling curved aeroplane surfaces using straight wire segments. Kubina stated that the length measured along the contour of a curved surface should be reproduced in the straight wire model. Common sense indicates that if a wire is folded right back onto itself the wire length concept can no longer hold. A computational experiment was performed on a bent wire (Fig 2.44) to determine to what extent the wire length dominates wire behaviour.

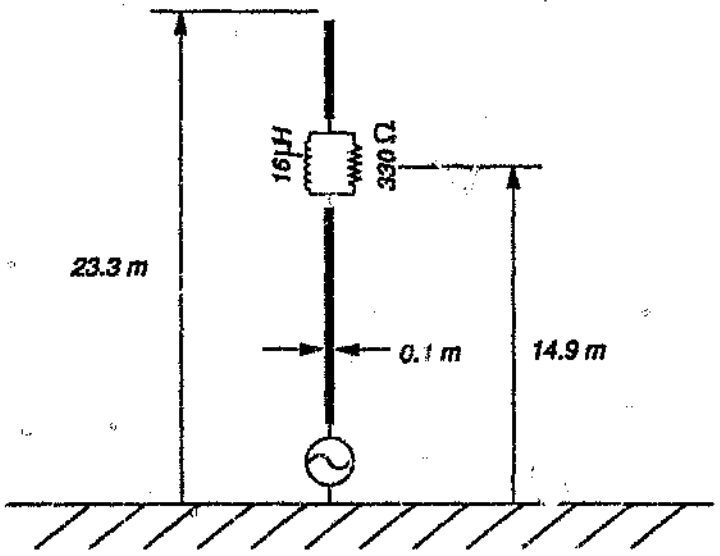


Fig 2.43 Simplified monopole version of the Guertler and Collyer dipole (Note that the distances between discontinuities on the monopole correspond to the distances on the real antenna as measured along the wire and not to straight line measurements).

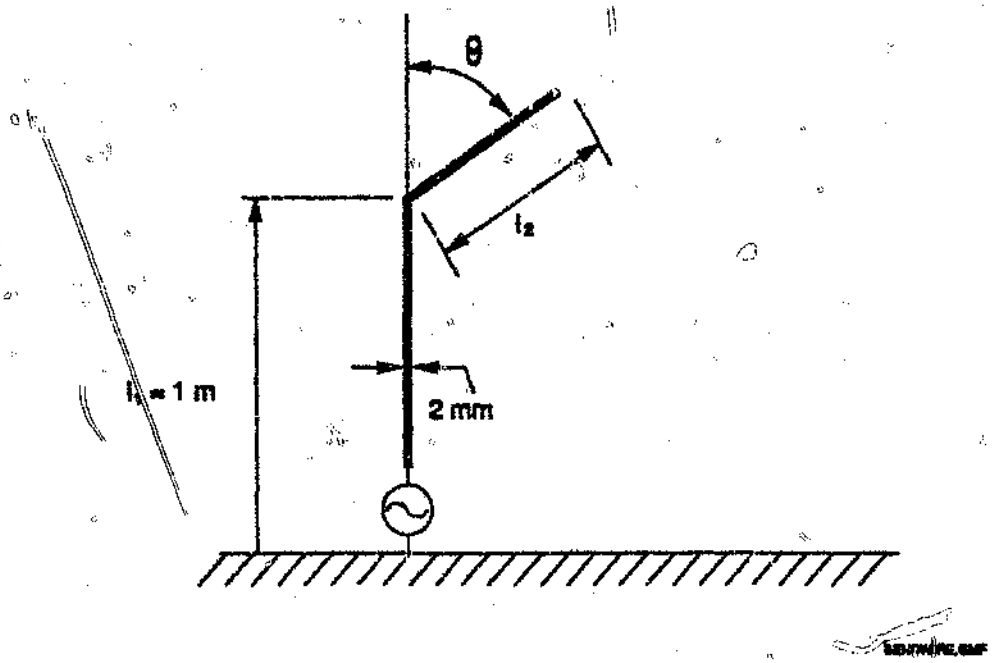


Fig 2.44 Geometry to investigate the validity of the wire length concept using NEC2

The resonant length of this antenna was found for different angles of θ and a number of l_2/l_1 ratios. The wire length concept outlined above holds if the resonant length corresponds to $l_1 + l_2$. For angles where the resonant length corresponds to l_1 the wire length concept fails completely. The resonant length versus the angle is plotted in Fig 2.45.

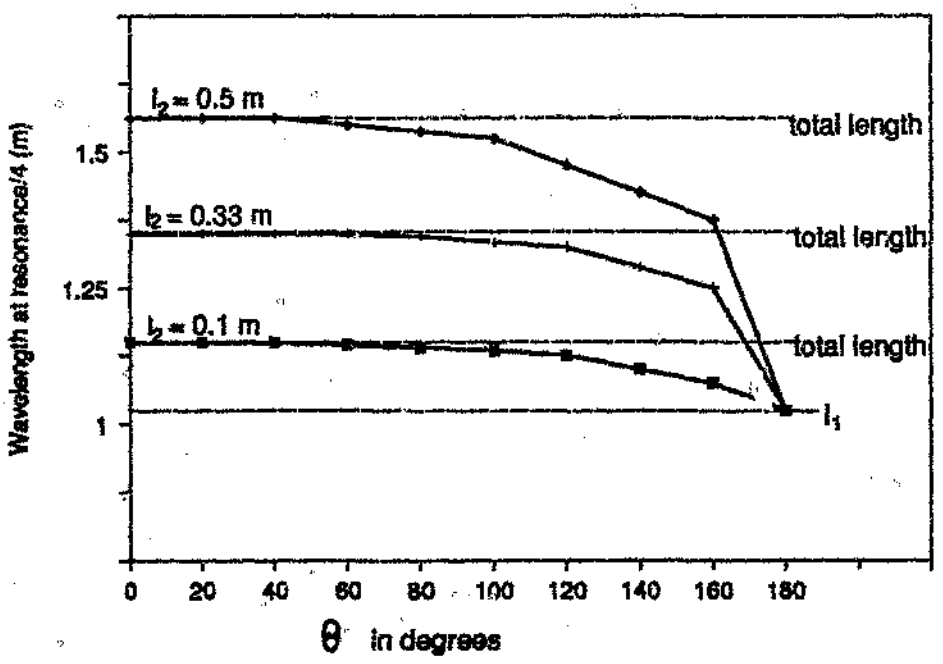


Fig 2.45 Graph of antenna resonant wavelength versus the angle with the vertical

The wire length concept remains fairly valid for angles of up to 90 degrees. The numerical experiment supports the validity of using the wire length between discontinuities. The wire length principle starts breaking down when the bend becomes very sharp as was expected.

Wire junctions

Problems were at encountered during this research when trying to model antennas which involve a transmission line section. A half wave transmission line (Fig 2.46) was simulated to establish the reasons for this problem.

The transmission line was modelled with 12 segments in each of the long wires and 4 segments each in the horizontal connecting wires. From transmission line theory the input impedance should equal the load resistance, R, for a half wave length line. When the spacing between wires, s, was more than 0.5 m the calculated input impedance was within 1 percent of the theoretical value. For values of s less than 0.45 m the calculated impedance was in error by a factor of a few hundred times (see fig 2.47).

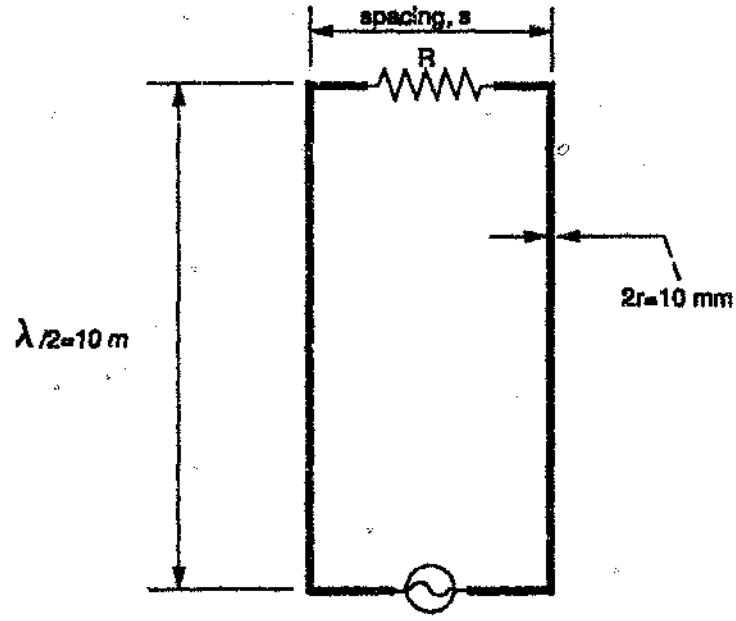


Fig 2.46 Two wire transmission line

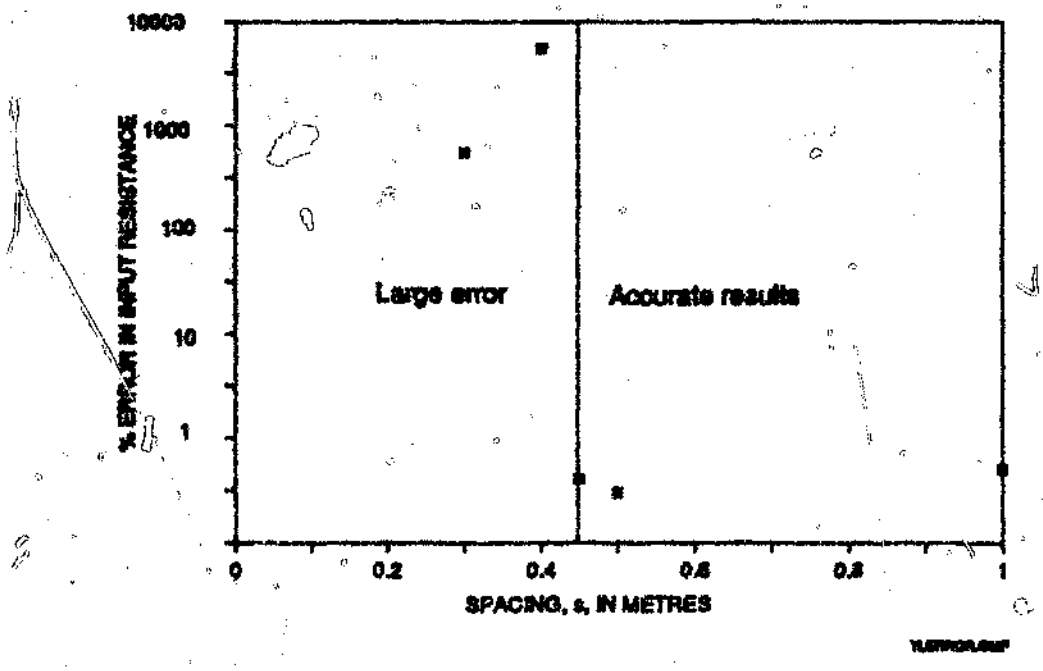


Fig 2.47 Graph of the error in the real part of the input impedance versus the line spacing, s

The problem was observed by Kubina (1983) and stated as follows: "The restriction on the relative length of segments that form a junction, requires that these lengths be comparable within a factor of five". The limitation is due to the numerical problem of maintaining current continuity across junctions. The constraint can be expressed mathematically with the aid of the fig 2.48.

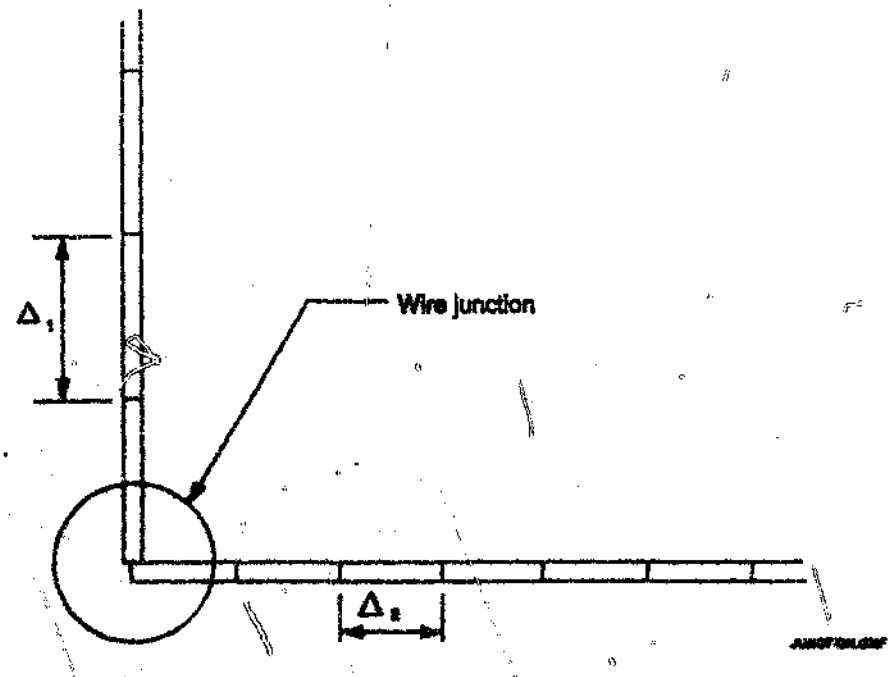


Fig 2.48 Two wire junction criterion

Numerical accuracy is ensured for two connecting segments of lengths Δ_1 and Δ_2 if:

$$5 > \frac{\Delta_1}{\Delta_2} > \frac{1}{5} \qquad \text{-(2.22)}$$

Applying the criterion to the transmission line problem of fig 2.46 and 2.47 showed that the answers became inaccurate when the ratio exceeded 6:1, hence confirming Kubina's rule of thumb.

An important implication of this limitation is that short sections of wire combined with very long ones require many segments to analyze. Simplifying the model to eliminate short pieces of wire sometimes provides an alternative method of circumventing this problem.

Modelling two or more wires by single wire with equivalent radius

Increasing the thickness of a dipole antenna naturally produces larger bandwidth. Broadband HF antennas must typically be in the order of half a wavelength long at the lowest frequency to obtain reasonable efficiency (Treharne, 1983b). A lower frequency of 2 or 3 MHz implies dipole lengths of 75 m and 50 m respectively. Electrically thick antennas of this length are not practical and other methods must be found to increase the apparent thickness. Antenna thickness is often quoted using the so called thickness factor, Ω, which is given by Woolf (1988) and others to be:

$$\Omega = 2 \cdot \ln\left(\frac{2h}{a}\right) \qquad -(2.23)$$

where h is the dipole half length and a the radius.

A thick antenna has Ω of 8 to 15 whereas a thin antenna has Ω of 20 or more. Achieving thick antennas at HF frequencies will therefore require the dipole diameter to be in the order of 0.2 m which is impractical. When two thin wires carry in phase current and the spacing between wires is much less than a wavelength they behave like a single thicker wire (Popovic, 1984). The equivalent radius, a_e of such a geometry is given by:

$$a_e = \sqrt{(a \cdot s)}$$

where a is the thin wire radius and s is the spacing between wires.

The technique is often utilised in HF antennas to achieve moderate thickness factors using thin wires. Clark and Fourie (1989) showed that NEC2 faithfully simulates this situation provided that care is exercised with the source model. Erratic results were produced when using the current slope discontinuity source model (source type 5 in NEC2 parlance) while the applied E-field source (Type 0) yielded convincing solutions.

The value of measured results to validate numerical models

The numerically determined input impedance of a structure is exceptionally prone to error. The input impedance is a sensitive parameter because the calculation uses the current on the feed segment only. Integrated quantities such as the efficiency, radiation pattern and gain are usually an order of magnitude more accurately determined with the method of moments (Kubina, 1983). Fortunately the input impedance is the easiest parameter to measure at HF. A large measure of confidence can be placed on the model employed if calculated and measured

input impedance shows agreement. Empirical results thus play an important part in ensuring the validity of the numerical model. Input impedance measurements were extensively used during this study to validate computer models.

2.7 Summary

Chapter 2 provided background information which was mostly obtained from the literature and related to this study. The first section reviewed the general field of HF communications. A renewed interest in HF communications for various applications is evident from many sources. The requirement for broadband antennas in modern HF communications systems was established. The practical requirements on broadband antennas in typical applications indicated the need for simple and small geometries.

The second section considered ionospheric propagation in more detail and related this to the required antenna radiation characteristics and frequency range. Short range HF communications (0 - 1000 km) was shown to require take-off angle coverage between 30° and near vertical. The most important frequency range for short range HF communications was shown to be 2.5 MHz to 15 MHz. The patterns of simple loaded and unloaded dipoles were then considered to assess their general suitability for this application. The radiation patterns obtained indicate that these antennas are not ideal, but a suitable compromise none the less. The elevation plane radiation patterns were also shown to be mainly affected by antenna height which is constant due to practical considerations. Azimuth radiation pattern characteristics for both unloaded and loaded dipoles in a number of configurations were very similar. It was quite clear that pattern constancy and control would require more complex geometries than those considered in this document.

A brief discussion on the definition of frequency bandwidth followed in the third section. Impedance bandwidth is of primary concern in simple HF antennas while pattern constancy is argued to be less important during design phases. The Chu-Harrington limits indicate the trade off between radiation efficiency and impedance bandwidth for small antennas. Efficiency is thus an essential parameter to consider when determining the value of a broadband antenna.

The Power Radiated Ratio, PRR, defined in the fourth section combines the losses incurred from reduced efficiency as well as impedance mismatches. The PRR variations with frequency therefore provide a unified picture of antenna bandwidth.

3 ACHIEVING BROADBAND PERFORMANCE BY CONTROLLING WIRE CURRENT DISTRIBUTION

In this chapter known antennas conforming to the structural requirements outlined in Chapter 2 are studied. Most of the popular simple HF broadband antennas were designed before the advent of modern computational techniques. Impedance performance is well documented but radiation efficiency is generally ignored. The difficulty of measuring efficiency at HF is the major reason for this neglect. NEC2 is used to evaluate antennas found in the literature. The antenna VSWR, efficiency and the RBR are calculated and critically examined. The outcome in terms of antenna lengths and load positions indicates the value and importance of careful manipulation of the current distribution. Suitable methods of controlling current distribution were identified. A novel geometry was designed by exploitation of the techniques uncovered during the previous phase. The improved performance of the new antenna illustrates the benefits of careful control of the current distribution. Measured results confirmed the computed performance of the new design.

The antenna radiation patterns are not considered in this chapter for the reasons mentioned before. The radiation patterns in terms of directive gain, which does not take reduction due to power losses into account, are presented in Chapter 5.

3.1 Known Simple Broadband HF Antennas and their Performance

3.1.1 The Treharne antenna

The Treharne geometry (Treharne, 1983b) is log-periodically loaded to obtain broadband performance. The characteristic impedance of a skeletal conical antenna above a ground plane is (Treharne, op cit):

$$Z_o = 138 \ln\left(\frac{7h}{w}\right) \qquad -(3.1)$$

The constant height-to-width ratio of the pseudo-conical structure (see Fig 3.1), results in a constant characteristic impedance of 377 Ohm. Treharne argued that this value of characteristic impedance is superior to others because it is equal to the that of free space. He contended that 377 Ohm provides a better match to the propagation medium.

The loads effectively shorten the antenna with increased frequency. The intention was to terminate the structure in its characteristic impedance over the HF spectrum. Successful termination will ensure a travelling wave current distribution and hence ensure impedance constancy.

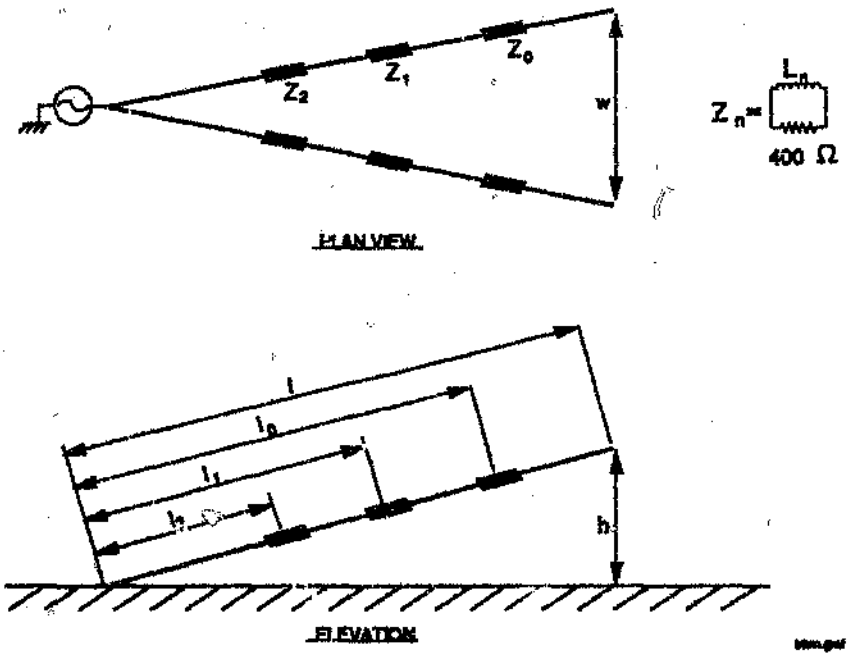


Fig 3.1 The Treharne Antenna

The first load is inserted at a position on the wire which is one third of the total length from the end. This process is repeated for subsequent loads, treating the remainder of the structure as the new full length.

The ultimate inductor (the one furthest removed from the feed point) was assigned the value of:

$$L_0 = 2k_e \cdot l \qquad (\mu H) \qquad \text{-(3.2)}$$

The constant, k_e, was chosen to be 1.3. The next inductors were found by the following equation:

$$L_n = 2k_n \cdot l\left(\frac{2}{3}\right)^n \qquad (\mu H) \qquad \text{-(3.3)}$$

The factor k_n is chosen to be 0.9.

The total antenna length is l.

The multiplication factor of 2 is due to the use of the two parallel wires requiring twice the inductance of a single wire version.

The operation of the antenna was explained as follows: a reactance has the same value as its parallel resistor (377 Ω) at its so-called "break" frequency. The break frequency, for a specific inductor is defined by:

$$f_n = \frac{400}{2\pi L_n} \quad \text{MHz} \qquad \text{-(3.4)}$$

with the parallel resistor value of 400 Ω used as convenient approximation to the previously stated ideal value of 377 Ω.

The parallel inductor reactance is smaller than the resistance below the break frequency and so allows currents to flow to the next section. The inductor presents a high reactance at frequencies well above this break frequency . The pseudo-conical antenna is effectively terminated in the parallel resistor with a value close to its characteristic impedance. The similarities to the principle used in Altshuler's structure should be evident.

Treharne stated that a 23 m long antenna with a 12 m mast produced a VSWR of less than 2:1 for frequencies from 2 - 30 MHz. He did not mention the efficiency performance of this antenna.

The antenna described by Treharne was modelled for NEC2 simulations in the inverted-v configuration as illustrated in Fig 3.2. The inverted-v configuration does not result in a constant "height-upon-width" ratio, the characteristic that was emphasized by Treharne. Later results proved that the current distribution is predominantly determined by the loads on the antenna. Only second order changes result as a consequence of ground interaction. Austin and Fourie (1986a) showed that the change in configuration does not degrade performance. The configuration suggested by Treharne, being dependent on a good ground, was less suitable from a practical point of view.

The number of segments per wire were varied as frequency was increased to minimize computer run time. The number of segments per wavelength was never less than ten to ensure compliance with that criterion in the NEC2 package.

The break frequencies are surprisingly low for this structure. The three break frequencies are 1.1, 2.3 and 3.55 MHz and these values seem to be very low if operation up to 30 MHz is desirable.

Treharne's equation to calculate these critical frequencies is incorrect (see Appendix B). The erroneous equation produced break frequencies of approximately double those mentioned above. The higher break frequencies are more easily reconcilable with the desired applica-

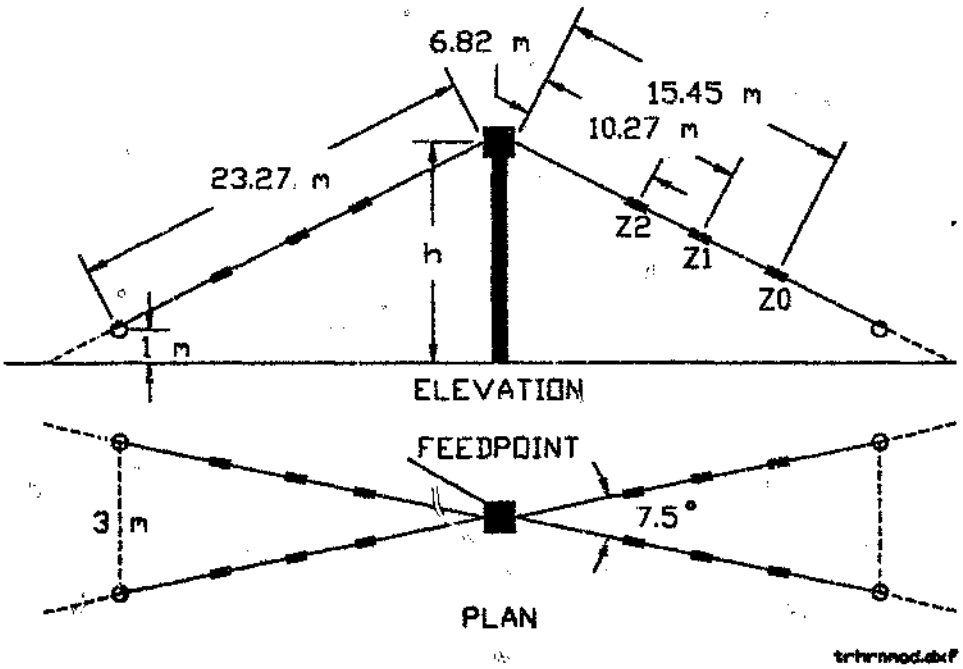


Fig 3.2 The Treharne antenna modelled for NEC2 simulation

tion. The inductor values found using Treharne's equations must hence be halved to yield the more acceptable break frequencies of 2.1, 4.6 and 7.1 MHz. The use of higher break frequencies in no way degraded the performance of the antenna. Austin and Fourie (1986a) showed that the antenna efficiency is worse when the higher inductor values are used. The critical parameters of the antenna are given in Table 3.1 with the symbols referred to indicated in Fig 3.1.

Table 3.1 Parameters used in the Treharne antenna

Parameter	Value
l (m)	23.27
l_0 (m)	15.45
l_1 (m)	10.27
l_2 (m)	6.82
R Ω	400
L_0 (μH)	20
L_1 (μH)	14
L_2 (μH)	9
f_0 (MHz)	2.1
f_1 (MHz)	4.6
f_2 (MHz)	7.1

The antenna performance in terms of VSWR and efficiency is indicated in figs 3.3 and 3.4 respectively. Measured impedance values at spot frequencies are shown to indicate the accuracy of the results obtained using NEC2. Appendix C outlines the experimental method while Appendix D shows the results in tabular form.

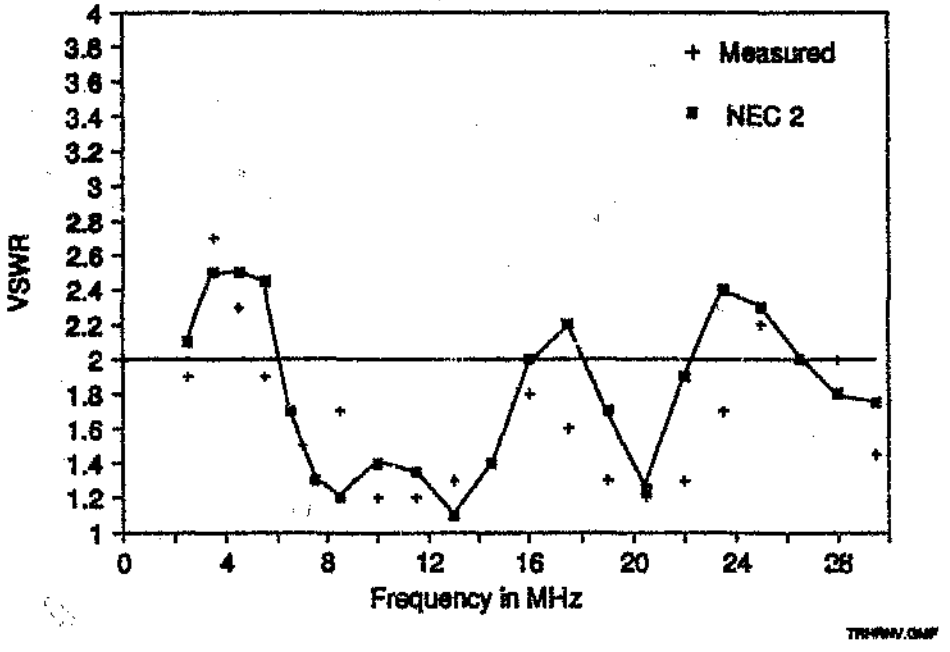


Fig 3.3 The VSWR performance of the Treharne antenna

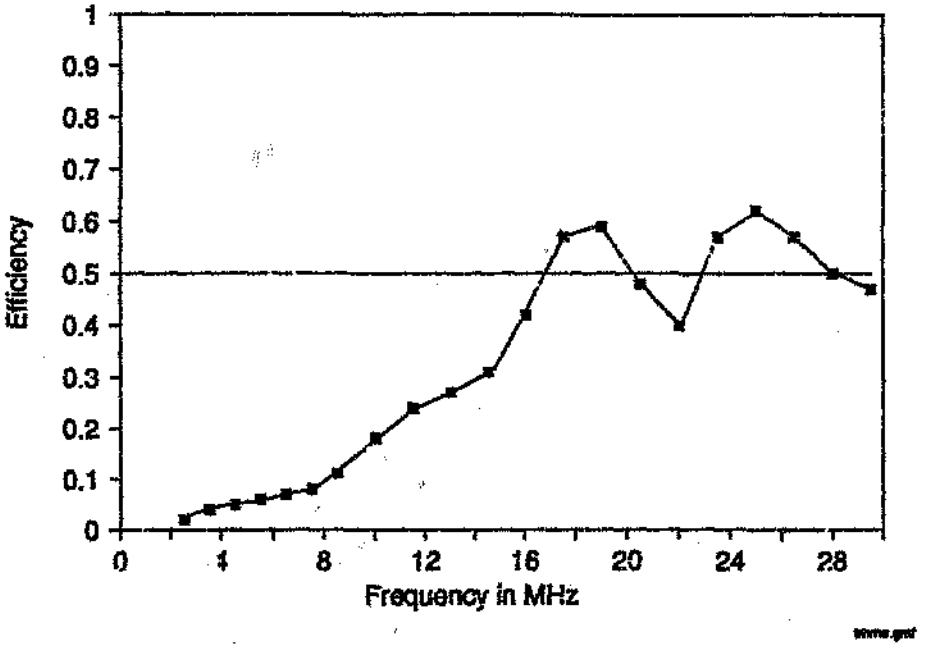


Fig 3.4 The efficiency of the Treharne antenna

The consequences of the Chu-Harrington limits are clearly reflected in the fig 3.4. The efficiency is very low when the antenna is short in terms of wavelength with gradual improvement as the frequency is increased. The VSWR performance over the HF band is acceptable but the efficiency at low frequencies renders it unsuitable for use in this range. The performance of the Treharne antenna indicates the importance of considering both VSWR and efficiency. The low efficiency is due to the large amount of resistive damping employed in the structure. A termination becomes predominantly resistive when the operating frequency exceeds the break frequency. The first break frequency is 2.1 MHz which effectively shortens the antenna before its designed lower frequency limit is reached. Other loads are below their break frequencies at the lower end of the spectrum but they too have a significant resistive component. The efficiency is hence further compromised by losses in loads below their break frequencies. The PRR shows the effect of both efficiency and the matching on the power radiated by this antenna (see Fig 3.5).

The PRR of this antenna is very similar to the efficiency curve, since the low efficiency is the major cause of power reduction. The antenna is successful in maintaining a travelling wave current distribution and hence impedance bandwidth. The severe resistive damping required to achieve an acceptable VSWR produced mediocre efficiency performance. The dipole described by Guertler and Collyer uses only one load per dipole arm. Further insight into the mechanisms at work in these structures will be provided by this antenna.

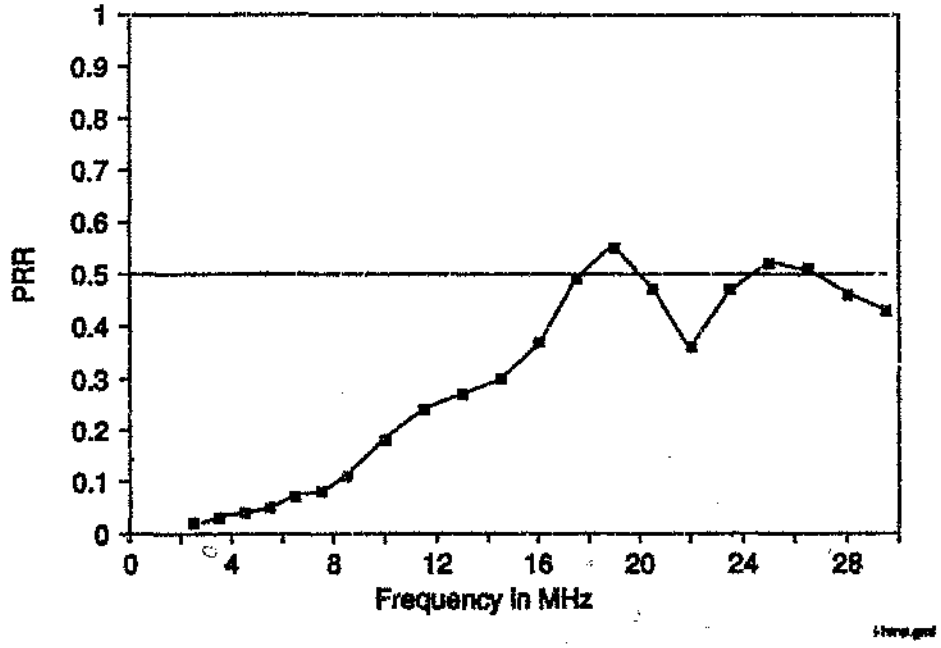


Fig 3.5 The PRR of Treharne's antenna

3.1.2 The Guertler and Collyer antenna

An antenna, known generally as the "Australian Dipole", was described by Guertler and Collyer (1973). The name is due to its popularity in Australia, where long distances and a sparse population often require the use of HF communications. Gnabs (1966) in fact first mentioned the antenna in Germany and he should be credited for this design. (Fig 2.5 is reproduced again as Fig 3.6 for clarity)

The principle of operation of this antenna is as follows:

The inductors have a low reactance at low frequencies. The resistors are effectively shunted to allow current to flow in the two end sections of the antenna. The inductors also add inductive loading to the antenna at low frequencies which make it effectively longer. At higher frequencies the reactance of the inductors increase and the antenna is terminated by the resistor. The principle is again similar to Altshuler's antenna discussed previously. The antenna employs a skeletal thin wire geometry to emulate a thicker structure which broadens the bandwidth. Guertler and Collyer measured the impedance of their antenna and found that it maintained a VSWR of less than 3:1 from 3 to 24 MHz. Gnabs estimated the efficiency to range from 20 to 60 percent.

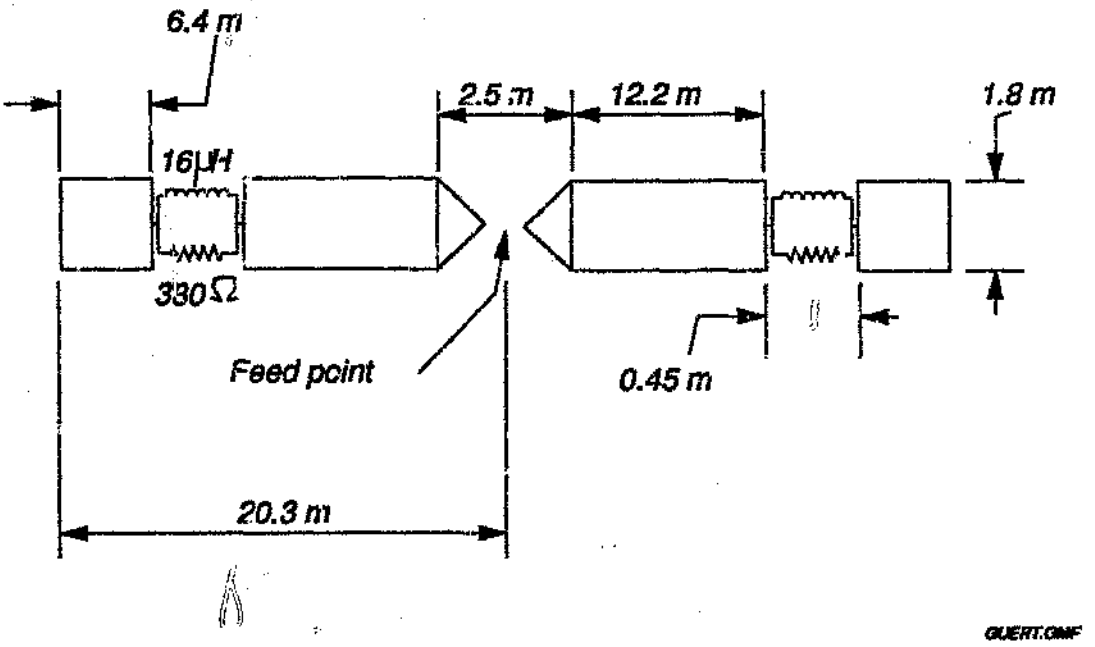


Fig 3.6 The Guertler and Collyer dipole

The antenna was modelled in free space. Care was taken not to violate any of the constraints in the NEC2 code and segments were gradually increased with frequency. More than ten segments per wavelength were used at all frequencies. The VSWR and efficiency of this antenna are illustrated in Figs 3.7 and 3.8 respectively with tabulated results in Appendix E. For comparison the VSWR measured by Guertler and Collyer (1973) is also shown.

The VSWR performance of this antenna is high in the areas around 13.5 and 19.5 MHz. The reason for these regions of bad matching will later become clear when the input impedance is considered in more detail. The efficiency of this antenna again confirms the Chu-Harrington limits qualitatively, since the efficiency is worse at low frequencies.

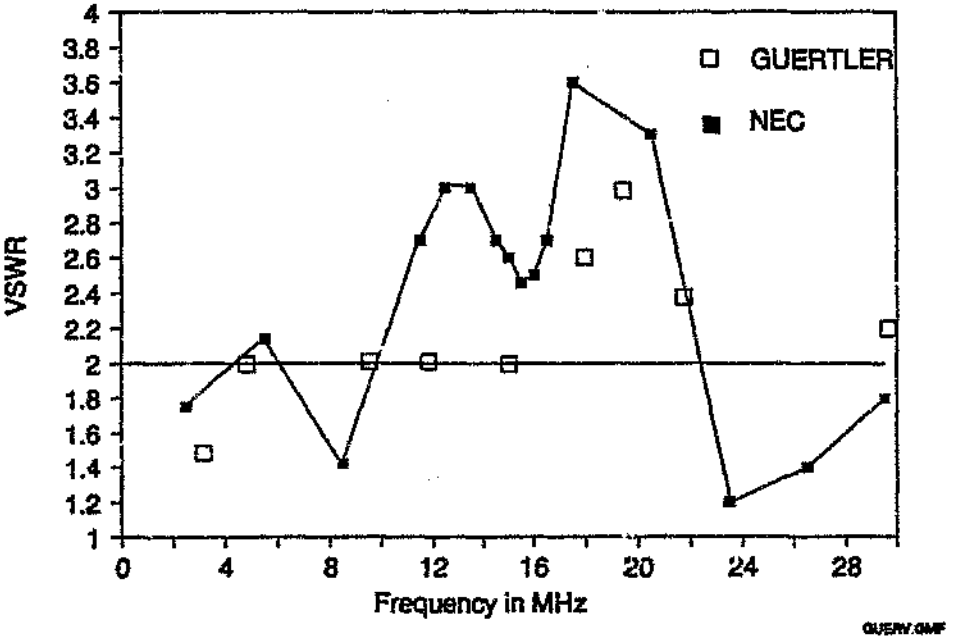


Fig 3.7 The VSWR performance of Guertler and Collyer's antenna

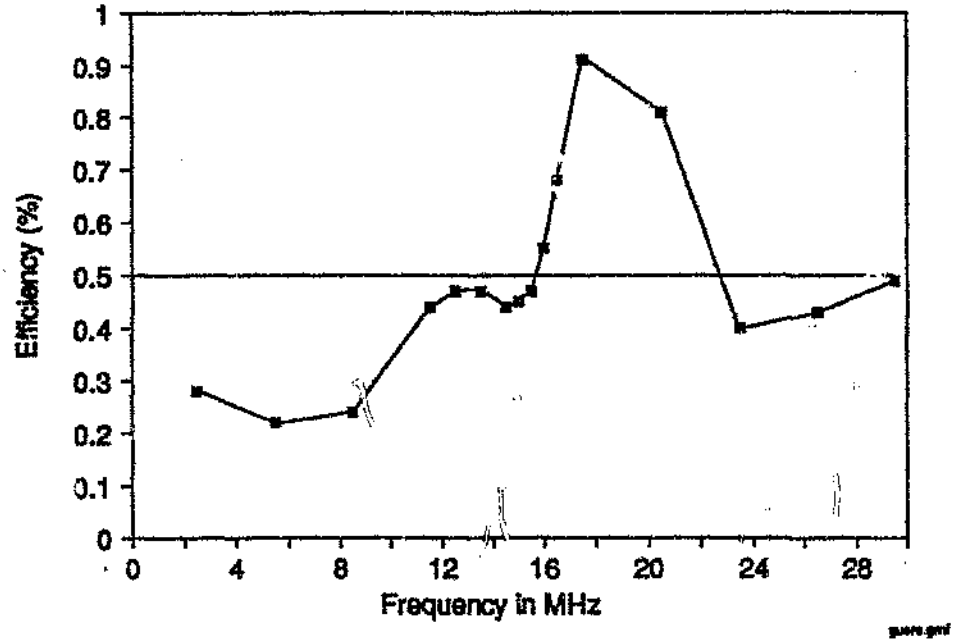


Fig 3.8 The efficiency of Guertler and Collyer's antenna

The efficiency is considerably higher than that of the Treharne antenna. The improved efficiency is due to the single load per arm and its position on the antenna. The larger number of variables controlling the current distribution on the Treharne antenna should seemingly

produce more acceptable results. The conclusion was that the load values and position for the Treharne antenna should be reconsidered in the light of the computer predicted efficiency. A redesign, taking efficiency in account, should yield an improved structure. The Treharne antenna was in fact successfully improved using the lossy line design technique described in 4.2. The PRR of the Guertler and Collyer antenna (fig 3.9) shows definite improvement on Treharne's version (fig 3.5).

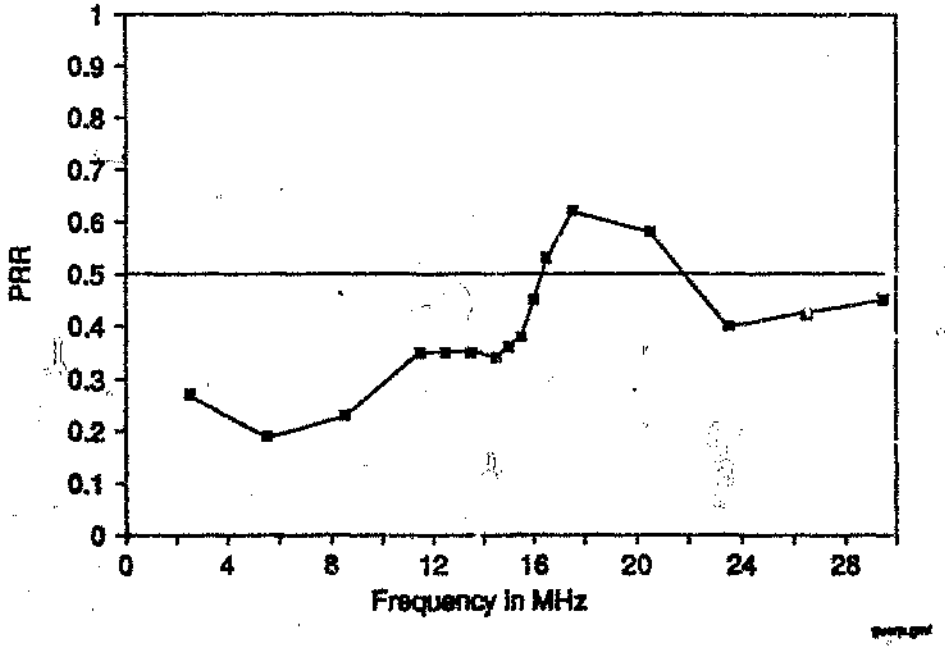


Fig 3.9 The PRR performance of the Guertler and Collyer antenna

A slight modification to the Guertler and Collyer geometry was suggested by Harris (1982). He claimed improvement on the Guertler and Collyer performance by adding a third wire in parallel with the other two.

3.1.3 The Harris antenna

The Guertler and Collyer antenna was subsequently modified by Harris (1982) by including a third parallel wire between the other two wires (see fig 3.10). Harris claimed that his modification improved the VSWR to 2.2 due to better emulation of a thick structure.

The structure was simulated in free space and the VSWR and efficiency are plotted in figures 3.11 and 3.12 with tabulated results in Appendix F.

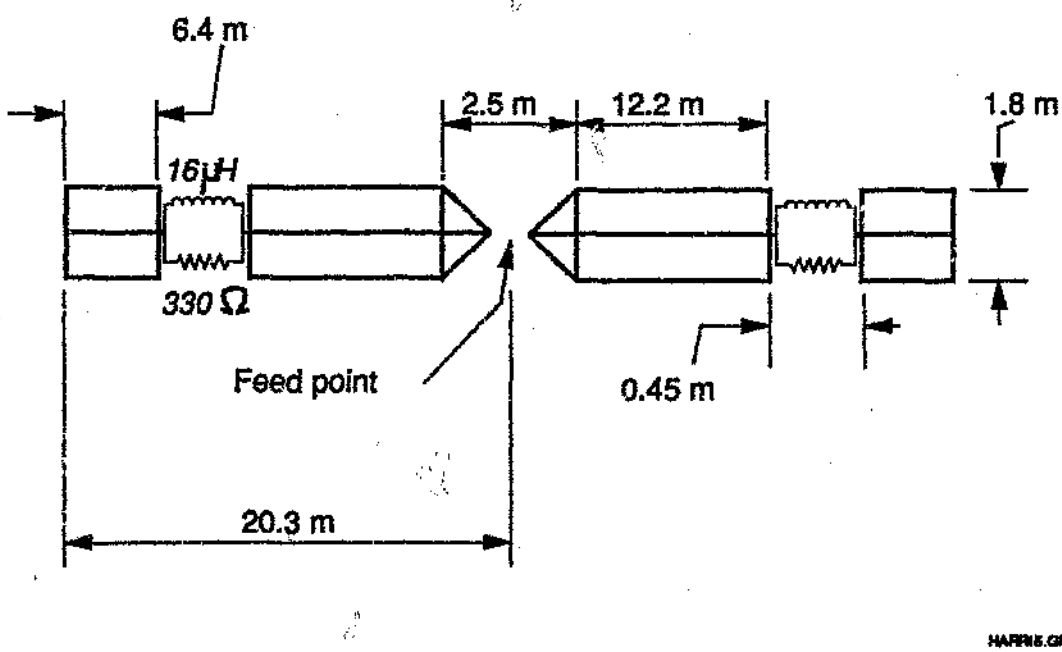


Fig 3.10 The Harris modified dipole

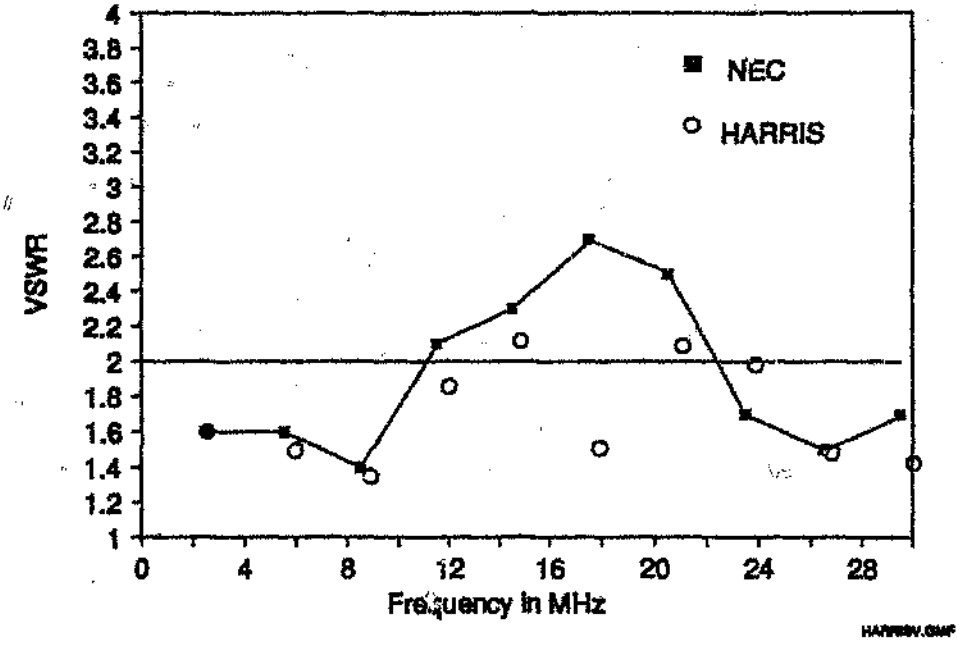


Fig 3.11 The VSWR performance of Harris's antenna

The improvement in VSWR on the Guertler and Collyer antenna is certainly apparent and confirms Harris's claims. The efficiency of this antenna (fig 3.12) also shows an improve-

ment on the original structure. Efficiency and VSWR are naturally traded off in simple broadband antennas. The fact that Harris succeeded in improving both indicates an inherently better design. The PRR shown in fig. 3.13 confirms this statement.

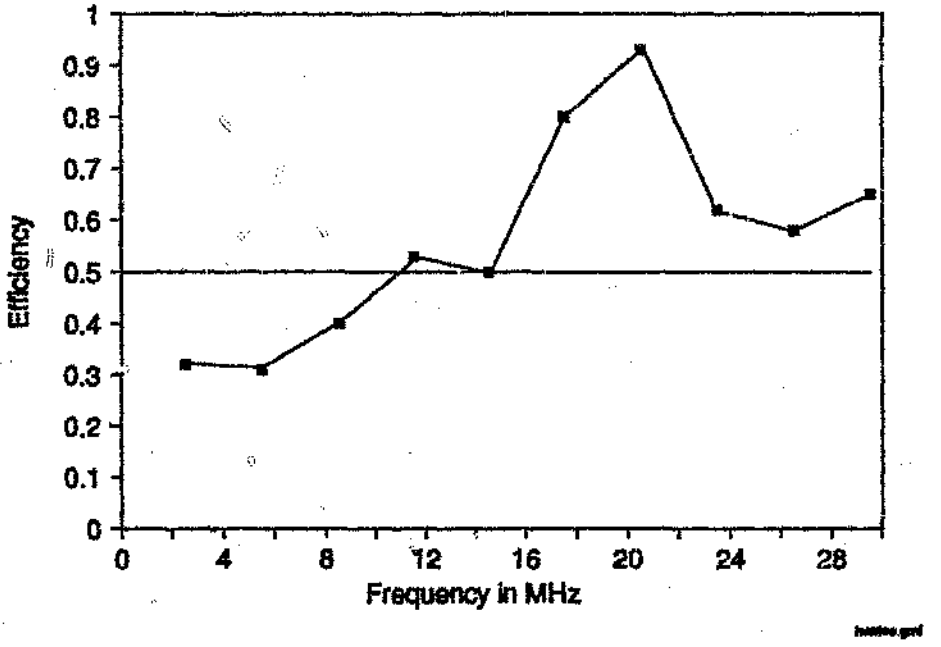


Fig 3.12 Efficiency of the antenna modified by Harris

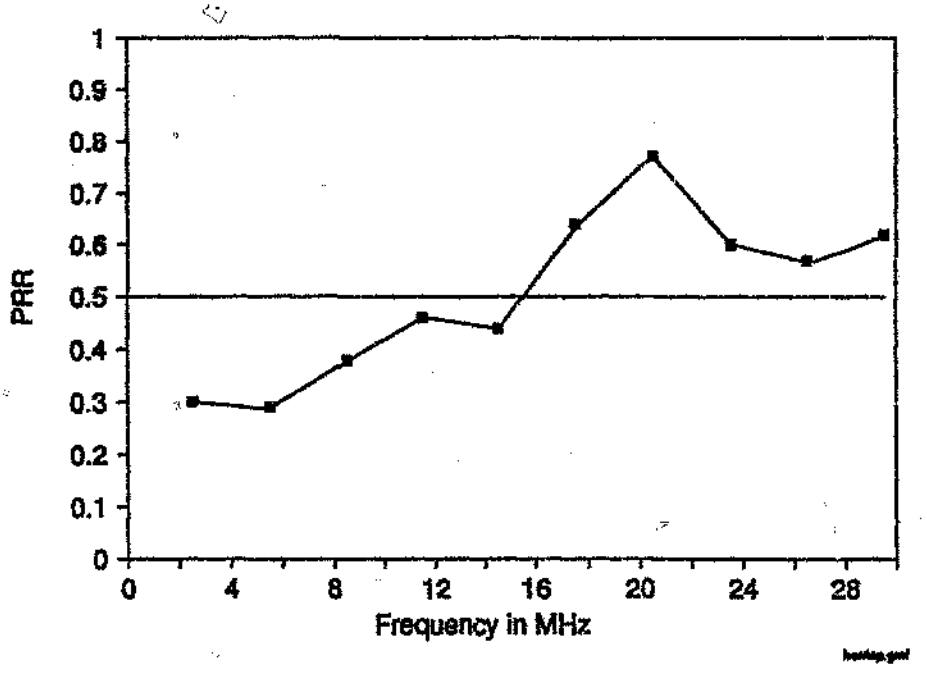


Fig 3.13 PRR of the antenna modified by Harris

Harris argued that the improvement was mainly due to the improved emulation of a thick structure. The explanation is valid but I believe that improvement was also due to the different length of the centre wire with respect to the outer wires. The centre wire provided a slightly longer wire length to the load. The problems associated with standing waves on the structure are hence alleviated by the different resonant lengths. The argument is developed further in section 3.2 where the effect of the wire length between the feedpoint and the load is investigated. Manipulation of the wire length is finally shown to yield a well behaved broadband antenna.

3.1.4 The resistively loaded fan dipole

A number of different length dipoles connected in parallel has long been known to yield multi-band performance (Austin, 1986). The frequencies where such an antenna exhibits satisfactory performance are determined by the lengths of the chosen dipoles. A fan dipole presents a bad mismatch to the transmitter at other frequencies. The introduction series resistors to the feed point of an antenna increases the minimum value of the input impedance. Similarly a resistor in parallel at the feedpoint limits the highest possible impedance. Lowering of the impedance peaks and raising the troughs implies that improved impedance constancy is achieved. The improved impedance bandwidth is at the cost of power dissipated in the feedpoint resistors which reduces the radiation efficiency. The fan dipole is illustrated in Fig 3.14 with the insert showing the feedpoint circuitry.

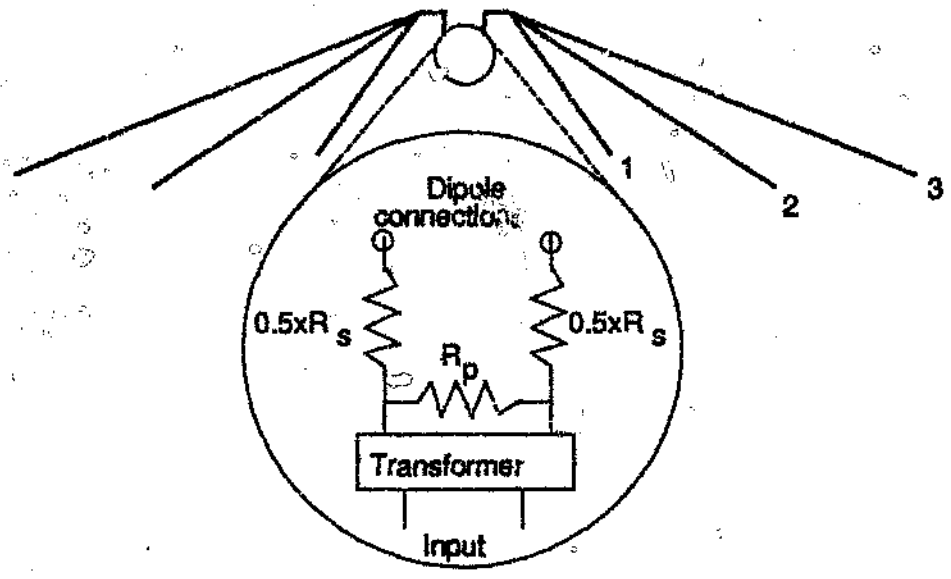


Fig 3.14 The resistively loaded fan dipole

Austin and Fourie (1986b,1988) developed a Smith Chart based technique to optimize this type of antenna design. A fan dipole was proposed with parameters as given below:

Parallel resistor, Rp - 1667 Ω
Series resistor, Rs - 2 x 72 = 144 Ω
Dipole 1 length - 21 m
Dipole 2 length - 30 m
Dipole 3 length - 50 m

The parallel resistor lowers the impedance peaks when the unloaded antenna input impedance is of the same order of magnitude as this resistor. Clearly the parallel resistor does not affect performance much when the antenna impedance is of a much lower value. At low impedance regions a similar role is played by the series resistor where it increases the minimum values. Conversely a small fraction of the input voltage is developed across the series resistor when antenna impedance is high which diminishes its effect on performance. The parallel resistor hence mainly influences the antenna behaviour at high impedance regions whereas the series resistor dominates at low impedance regions. The overall effect is a smaller ratio between impedance maxima and minima producing a more constant input impedance but at the same time reducing radiation efficiency.

The performance of this antenna was determined by obtaining the unloaded fan dipole impedances, Z'_{ant}, using NEC2. The effect of the resistors on the input impedance and efficiency was then found using circuit theory.

The input impedance of the resistively loaded antenna, Z_{ant}, is determined from normal circuit theory to be:

$$Z_{ant} = R_p \text{ in parallel with } (Z'_{ant} + R_s) \qquad \text{-(3.5)}$$

$$= \frac{R_p \cdot (Z'_{ant} + R_s)}{R_p + Z'_{ant} + R_s}$$

The efficiency of the feedpoint network is found by calculating the input power, the power dissipated in the resistor network and power radiated by the antenna.

Assuming a unity input voltage the current and power into the total circuit is:

$$|I_{in}| = \frac{1}{|Z_{ant}|} \qquad \text{-(3.6)}$$

$$P_{in} = \frac{1}{|Z_{ant}|^2} R_{ant}$$

Power lost into the parallel resistor is:

$$P_p = \frac{1}{R_p} \qquad \text{-(3.7)}$$

Power lost in the series resistor is:

$$P_s = |I_s|^2 R_s$$

where I_s is the current through the series resistor.

$$|I_s| = \frac{1}{|R_s + Z'_{ant}|}$$

hence:

$$P_s = \frac{R_s}{|Z'_{ant} + R_s|^2} \qquad \text{-(3.8)}$$

The resistor network loss, P_l is given is the sum of the two loss components:

$$P_l = P_p + P_s \qquad \text{-(3.9)}$$

The network efficiency is:

$$\eta = \frac{P_{in} - P_l}{P_{in}} \qquad \text{-(3.10)}$$

The VSWR, efficiency and PRR of the resistively loaded fan dipole are shown in figs. 3.15, 3.16 and 3.17. Tabulated results for this antenna appear in Appendix G.

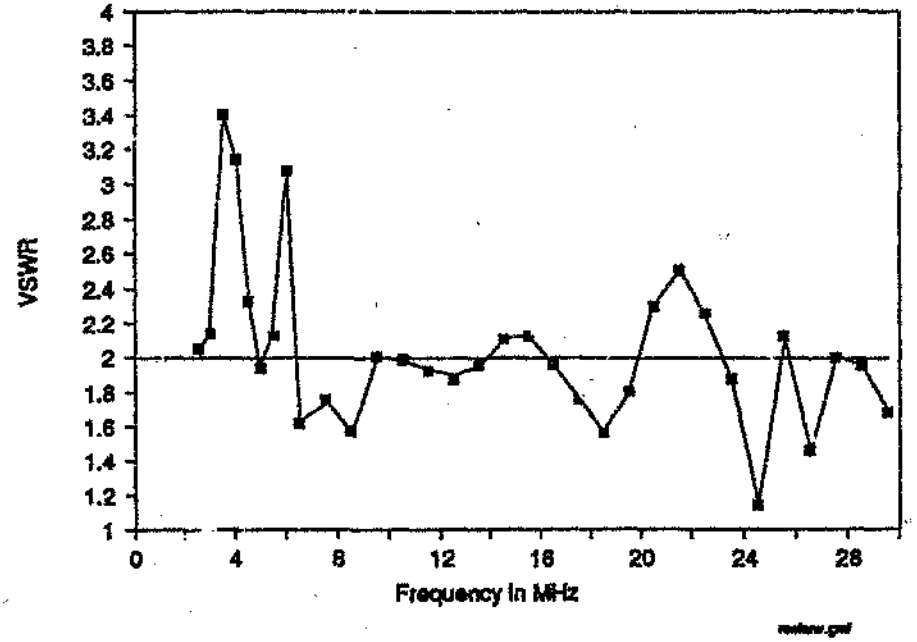


Fig 3.15 The VSWR of the resistively loaded fan dipole

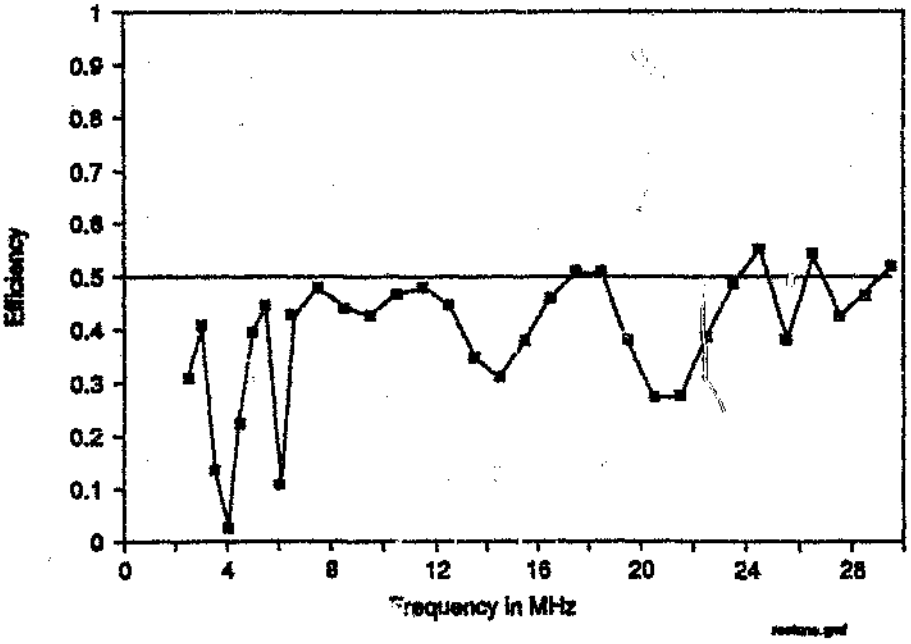


Fig 3.16 The efficiency of the resistively loaded fan dipole

The performance in the frequency range below 7 MHz is unsatisfactory. VSWR peaks at 3.4:1 and efficiency reaches a lower limit of 4 percent. Sharp fluctuations characterize the

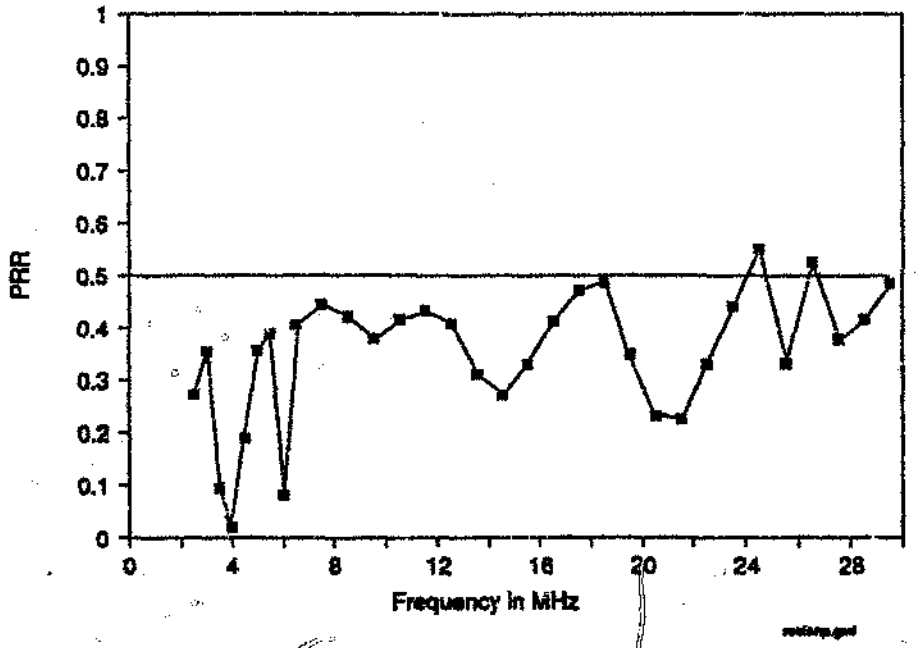


Fig 3.17 The PRR of the resistively loaded fan dipole

low frequency performance of the antenna. The PRR graph illustrates the variations in radiated power due the combined effect of efficiency and VSWR. The performance of the antenna above 7 MHz is more satisfactory.

The fluctuations in PRR are due to the behaviour of the dipoles used in this antenna. A dipole is inherently a high Q device and the impedance varies considerably with frequency. Normally this would result in a multi-band antenna with useful performance when one of the dipoles supports a resonant current distribution. Broadband impedance performance is obtained by using the parallel and series resistors to reduce impedance variations. Efficiency is hence traded off for VSWR improvement while not altering the shape of the current distribution on the dipoles. The current at the feed point is rather manipulated using the resistors to achieve impedance constancy.

The simplicity of the geometry makes it attractive for practical applications. An antenna with similar geometry to the resistively loaded dipole, but with increased complexity at the feed point, was later designed and is discussed in Chapter 4.

3.2 The Fourie and Austin Staggered Loads Antenna (SLA)

NEC2 analysis was used in the previous section to establish the performance of the antennas due to Treharne, Guertler & Collier, Harris, and the resistively loaded fan dipole of Austin and Fourie. The efficiency and VSWR behaviour of the antennas were determined and were

related to their current distributions. The computed input impedance provided valuable information regarding current standing waves on the antennas. The mechanisms affecting the current distribution were deduced by careful interpretation of the computed results. The new insights gained may be used to design an antenna with performance exceeding that of the others.

3.2.1 The design method

The following constraints were placed on the new design to ensure that it may be compared with the antenna versions discussed before:

- the total length of the antenna will be the same as that of Guertler and Collyer.
- the same load as in the Guertler and Collyer will be used
- only two wires per dipole arm will be used (unlike Harris' antenna where three wires were used)

The mechanisms that cause undesirable behaviour in the Guertler and Collyer version are first examined in more detail.

The Guertler and Collyer antenna is badly mismatched around 12 and 20 MHz. More light is shed on this problem by observing the input impedance around these frequencies (see Fig 3.18). The impedance at 12 and 21 MHz is high relative to the system impedance of 300 Ohm. The high resonant input impedance suggests behaviour resembling that of a normal dipole in so called "anti-resonance". Anti-resonance occurs in unloaded dipoles when the dipole is an integer number of wavelengths long.

The reason postulated for the impedance peaks was that some antenna dimension is an integer number wavelengths long at problematic frequencies. An anti-resonant portion would support a current standing wave with minima at the feed resulting in a high input impedance. The critical paths on the Guertler and Collyer antenna were identified to investigate this phenomenon (see Fig 3.19).

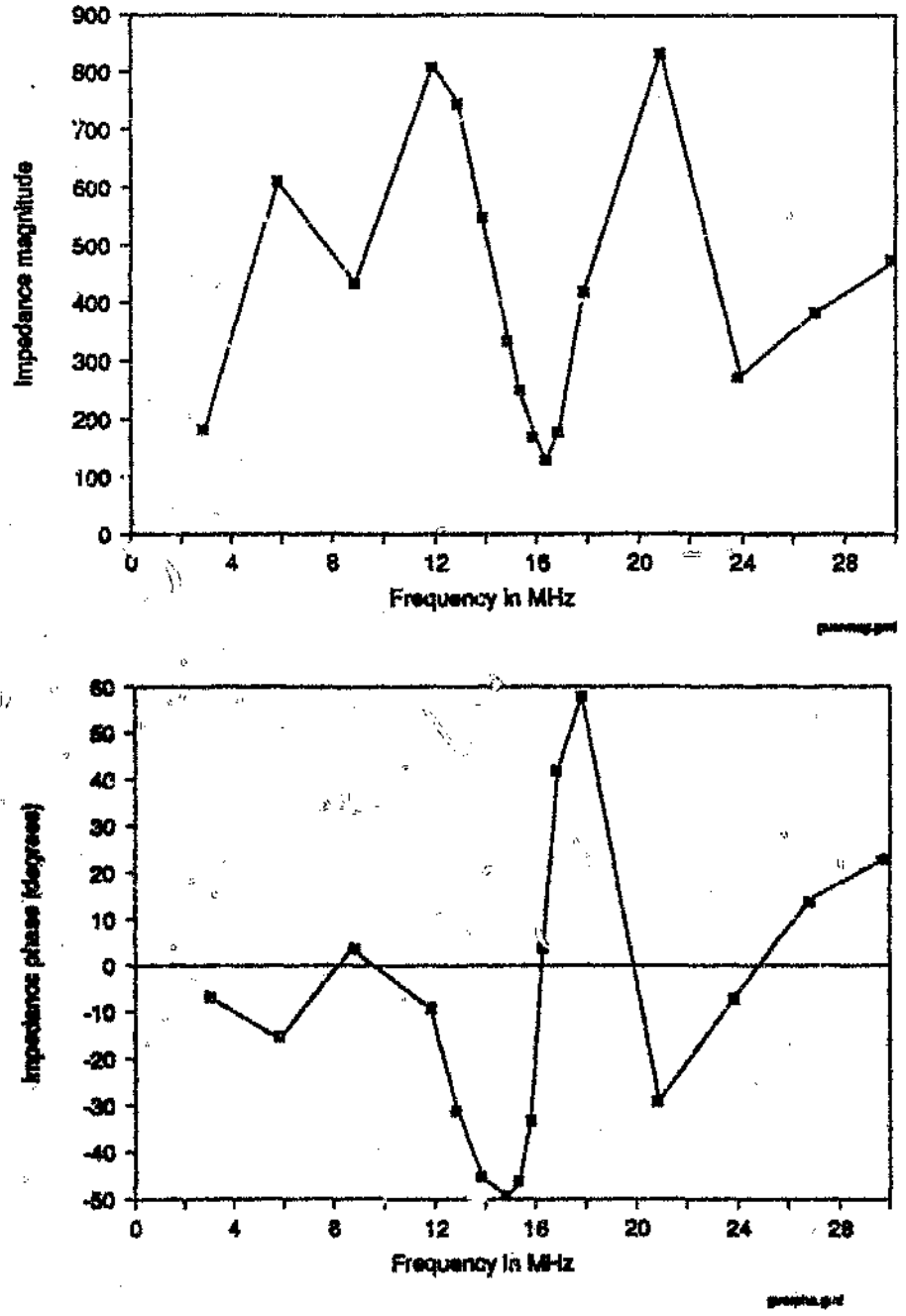


Fig 3.18 The input impedance of the Guertler and Collyer dipole.

The lengths are as measured along the wires and are not straight line measurements, due to the importance of wire length in antenna performance as shown in Chapter 2.

Critical paths identified were:

- The total wire length of the dipole arm, $h_t \approx 23.3$ m

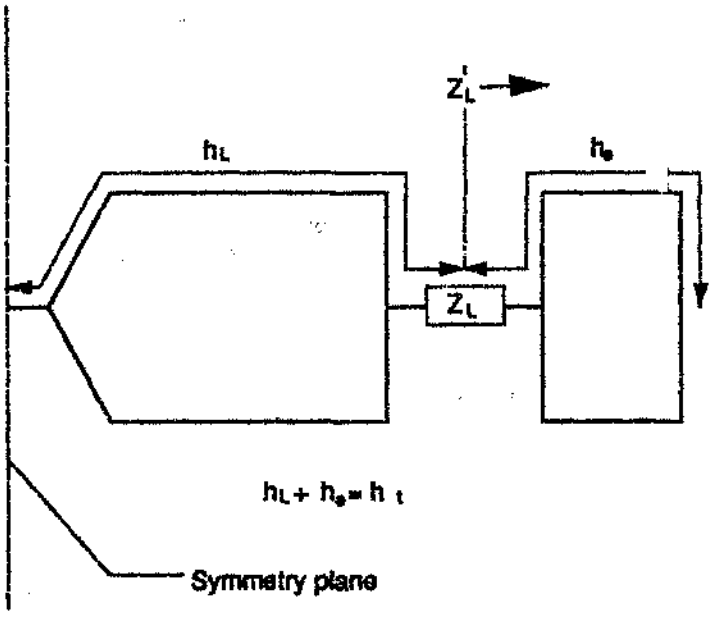


Fig 3.19 Critical lengths on the Guertler & Collyer antenna

- Wire length from feed to load, $h_L = 14.9$ m
- Wire length from load to antenna end, $h_s = 8.43$ m

The critical lengths in terms of wavelengths may be related to the impedance behaviour of the antenna with the aid of Table 4.1. The relationship between input impedance and dimensions is best explained using the transmission line analogy. The reactance of the inductor is more than double that of the parallel resistor at frequencies above 6 MHz. The antenna is hence terminated by the resistor and total length, h_t becomes unimportant and the lengths h_L and h_s determine the antenna's behaviour.

Table 3.1 The Critical Dimensions of the Guertler and Collyer Antenna in terms of Wavelength

Frequency (MHz)	h_L in terms of λ	h_e in terms of λ	h_t in terms of λ
3	0.15	0.1	1/4
6	0.3	0.2	1/2
9	0.5	1/4	0.7
12	0.6	0.3	0.9 ***
15	3/4	0.4	1.2
18	0.9	1/2	1.4
21	1	0.6	1.6 ***
24	1.2	0.7	1.9
27	1.3	3/4	2
30	3/2	0.8	2.3

The terminating impedance, Z'_L, as seen at point $h = h_L$, is clearly the load value, Z_L, in series with the impedance presented by the end section, h_e. As long as the end section, h_e, is a odd multiple of quarter wavelengths ($h_e = n\lambda/4$; n odd) the antenna is terminated by the load. For the terminated case $Z'_L = Z_L$, since the quarter wave end section converts the open circuit at the dipole ends to virtual short circuits. The antenna behaves in a pure travelling wave fashion if Z_L is equal to the dipole average characteristic impedance. Forcing travelling waves between the feed point and the load was the main intention in the Altshuler design and it is apt to call this the "Altshuler condition".

The value of Z'_L is larger than Z_L at frequencies where the end section is no longer an odd multiple of quarter wavelengths . The antenna is not ideally terminated and standing waves on the antenna section, h_L, govern the behaviour of the structure.

The distance h_L is approximately half a wavelength at 12 MHz and one wavelength at 21 MHz. Even multiples of quarter wavelengths, or mathematically speaking the cases where $h_L = n\lambda/2$ (n: integer,) produce anti-resonance. The input impedance associated with anti-resonance is approximately equal to Z'_L due to the half or full wave transmission line transformation. The behaviour of the Guertler and Collyer dipole at 12 and 20 MHz illustrates this condition. The high input impedances (approximately 800 + j0 Ohm) occur since Z'_L is large due to violation of the Altshuler condition outlined above.

The length h_L is also half a wavelength at 9 MHz but does not present a problem at this frequency since h_a is exactly a quarter wavelength and the Altshuler condition is satisfied. The qualitative method of analysis is confirmed by the low impedances observed at 15 and 24 MHz. The length h_L is an odd multiple of a quarter wavelength at these frequencies which transforms the high Z_L values to appreciably lower ones.

Two important mechanisms in the operation of loaded structures like the Guertler and Collyer were identified:

- The antenna is ideally terminated with an input impedance approximately equal to Z_L if the end section length, $h_a = n\lambda/4$ (n odd). The Altshuler condition is satisfied but cannot be maintained over a frequency range of more than 3:1 (Altshuler, 1961).
- When the Altshuler condition is not satisfied, Z'_L is larger than Z_L. A length $h_L = n\lambda/2$ (n integer) transforms the high Z'_L to the input as was shown for the Guertler and Collyer structure. The case where $h_L = n\lambda/4$ (n odd) on the other hand converts the high Z'_L to a lower value.

The design of an improved broadband antenna was facilitated by the judicious use of the principles above.

The regions of poor matching are only shifted about in frequency if the length h_L is varied with no overall improvement. The load was thus split into two parallel loads with approximately the same equivalent impedance as the Guertler and Collyer load viz. 32 μH in parallel with 600 Ohm (See Fig 3.20). The new antenna was called the Staggered Load Antenna, SLA, due to the unsymmetrical load configuration.

The lengths that must be optimized in this structure are h_L1 and h_L2. A simple program was written to give h_L1 and h_L2 in terms of wavelengths at 3 MHz intervals over the HF range. A combination of h_L1 and h_L2, where at least one length is approximately an odd multiple of a quarter wavelength, was found after a few iterations . This choice of lengths should produce an antenna with low input impedance regardless of whether the Altshuler condition is satisfied or not.

The most suitable combination found was $h_L1 = 13.5$ m and $h_L2 = 17$ m. The extent to which these values fulfil the requirement outlined above is indicated in Table 4.2.

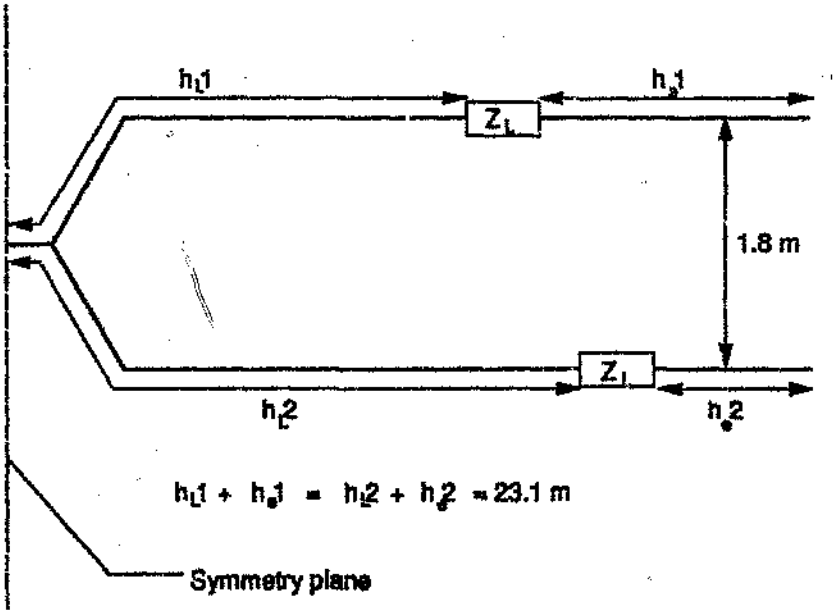


Fig 3.20 The Staggered Load Antenna (SLA) geometry

Table 3.2 Critical lengths on the Staggered Load Antenna (SLA) in terms of wavelength

Frequency (MHz)	h_L1 in terms of λ	h_L2 in terms of λ	h_s1 in terms of λ	h_s2 in terms of λ	h_t1 in terms of λ
3	0.14	0.2	0.1	0.06	1/4
6	1/4	0.3	0.2	0.13	0.34
9	0.4	1/2	0.3	0.2	0.7
12	1/2	0.7	0.4	1/4	0.9
15	0.7	0.85	1/2	0.3	1.2
18	0.8	1	0.6	0.4	1.4
21	1	1.2	0.7	0.44	1.6
24	1.1	1.36	3/4	1/2	1.9
27	5/4	3/2	0.9	0.6	2
30	1.35	1.7	1	0.63	2.33

3.2.2 Computed and measured performance of Staggered Load Antenna

The SLA was simulated on NEC2 in free space to established the validity of the design method described above . The input impedance of the antenna was also measured in the inverted-v configuration as shown in fig 3.21. Measurements were made with an acute angle,

ϕ, between adjacent wires, of 5° (approximating the model simulated with NEC2) as well as 90° degrees. Austin (1986) showed how the optimum system impedance may be found by choosing a normalisation factor which centres the input impedance values on a Smith Chart. System impedances, rounded to 500 Ω and 400 Ω for α of 5° and 90° respectively, were found using this technique. The VSWR was calculated from the measured input impedance using these values.

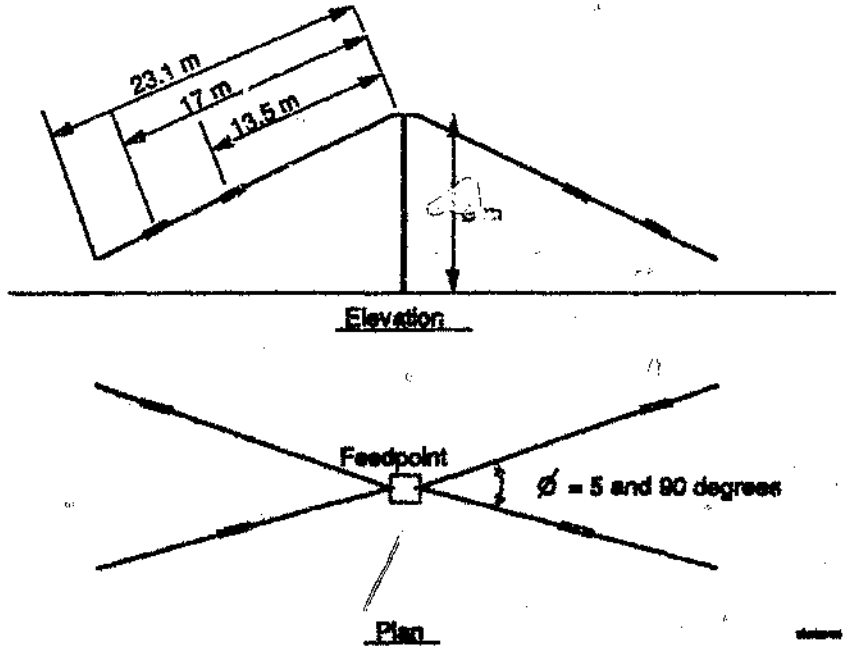


Fig 3.21 SLA configuration for measurement

The measured and NEC2 simulation results for efficiency, VSWR and PRR are available in Appendix H and are presented graphically in figs 3.22, 3.23 and 3.24. (Fourie and Austin, 1987).

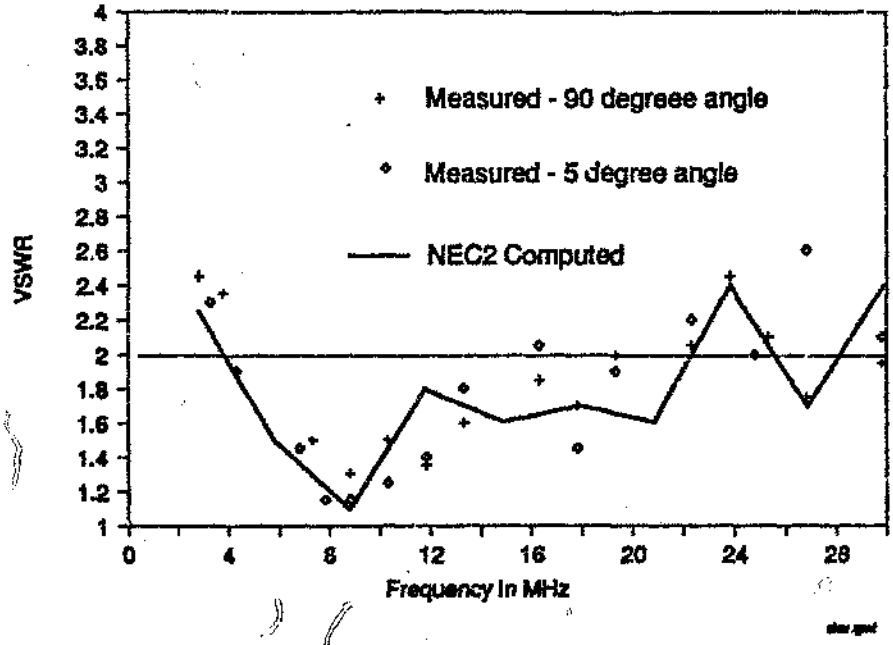


Fig 3.22 The VSWR performance of the SLA

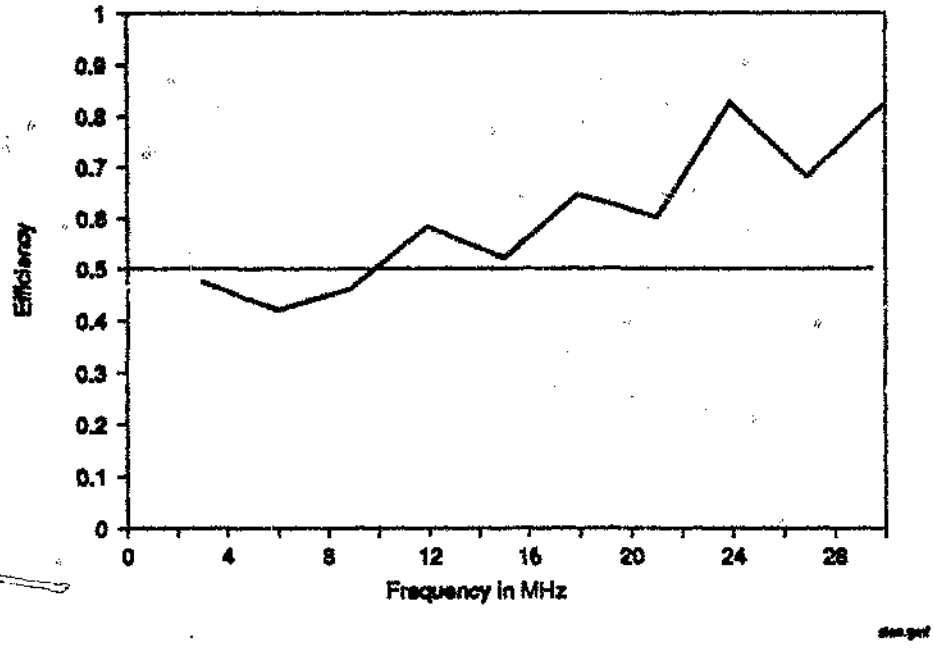


Fig 3.23 The efficiency of the SLA

The overall VSWR and efficiency performance of the new structure is clearly better than that the Guertler and Collyer antenna. The VSWR and efficiency form a fundamental trade off in broadband antennas of similar dimensions. The improvement in both efficiency and VSWR

by the SLA indicates an inherently better design. The correlation between the two sets of experimental results (with the structure in the two different inverted-v configurations above a real earth) and the free space straight dipole result from NEC2 indicates that the antenna is fairly insensitive to different configurations and ground characteristics. The PRR performance of the SLA is shown in fig 3.24.

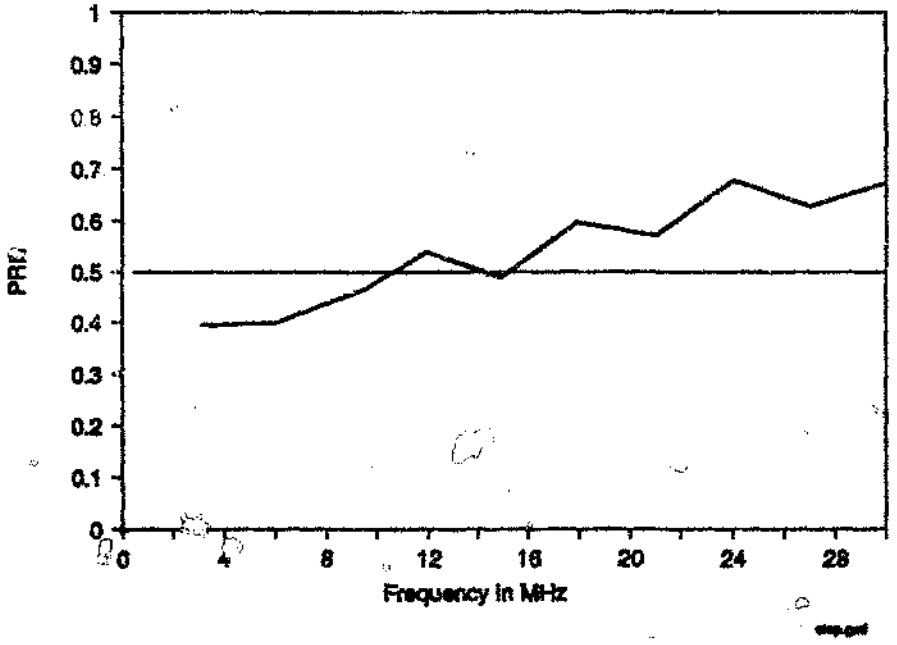


Fig 3.24 The PRR performance of the SLA

Two points are of practical significance:

- The efficiency variations of the new structure with frequency are much less than those of the other antennas. Less signal strength variations during wide band frequency agile communications are likely, which is an improvement.
- The inverted-v configuration is ideal in a tactical application, since only a single mast is required with the antenna wires replacing the normal guy ropes.

The SLA was only optimized with respect to the placement of the loads and not their value or number. The improvement obtained by recognizing the principles governing its behaviour and manipulating them for maximum benefit was significant. The qualitative analysis used assumed the current distribution on a loaded antenna to behave in a fashion analogous to a transmission line. The fact that this analogy can be used to great advantage is illustrated by the performance of the SLA. The transmission line analogy to a dipole antenna has been qualitatively used as a starting point for design by many researchers (Altshuler, 1961, Tre-

harne, 1983b, Guertler and Collyer, 1973 and many others). Altshuler is perhaps the most appropriate example. The pseudo-transmission line analysis may be useful if developed more rigorously to provide reasonable quantitative results. Attempts to do so have never really been successful for antennas that are both loaded and very long. The technique was pursued further and a method was developed that produced results of sufficient accuracy for design purposes. The next chapter concerns the further development of the transmission line analogy as well as the development of other simplified theory.

3.3 Summary

A number of known simple HF broadband antennas were evaluated using NEC2 in this chapter. The impedance or VSWR performance of most of the antennas were known from previous measurements. The efficiency, which is a difficult parameter to measure, was computed using NEC2 during this study. NEC2 computed VSWR and efficiency results were used determine the PRR which provides a composite index of input performance. The essential purpose of the investigation was to obtain insight into mechanisms affecting antenna performance. The antenna radiation patterns were not presented in this chapter, but are presented in Chapter 5 together with the patterns of antennas discussed in the next chapter, to allow for a full assessment of antenna performance.

The Treharne antenna performed well in terms of VSWR but low frequency efficiency performance was poor. Low efficiency performance was attributed to the proximity and values of the loads to the feed point. Current was assumed to be shunted past the resistors close to the feed point by their parallel inductors at low frequencies. The real part of the load complex impedance was not negligible below the break frequency as assumed in the design. The results indicate that most of the input power was lost in the load resistors. Spacing the loads further away from the feed point should improve the performance and an attempt to do so is detailed in the next chapter.

The Guertler and Collyer antenna employs only one load per dipole arm. The antenna is similar to the Altshuler dipole discussed in Chapter 2 except for the addition of a parallel inductor to the resistor. The parallel inductor was claimed to shunt current past the resistor at low frequencies in order to improve efficiency. The inductor becomes a high reactance as frequency increases and behaviour is dependent on the resistor only. Two thin parallel wires were used in this antenna to emulate a thicker structure. The Guertler and Collyer antenna performed better in terms of efficiency when compared to the Treharne antenna. A minimum

efficiency of 20 percent was achieved but the VSWR exceeded 2.5:1 at 12 and 20 MHz. Standing waves between load and feed point were postulated to be the cause of the VSWR peaks on the Guertler and Collyer dipole.

The Harris antenna is identical to the Guertler and Collyer version except for the addition of a third parallel wire. The designer of the antenna claimed the third wire improved the vestigial emulation of a thicker structure. This antenna performed slightly better than the Guertler and Collyer antenna in terms of both efficiency and VSWR. The physical length of a wire between discontinuities was shown to be an important antenna parameter in Chapter 2. The three wires on the Harris antenna were not equally long which may reduce the effect of standing waves on the impedance performance. The different wire lengths between feed and load may hence also contribute to the improved performance.

The last existing antenna investigated was the resistively loaded fan dipole. Broadband performance is obtained for this essentially multi-band structure by placing resistors in series and parallel with the antenna impedance. The resistors reduce impedance fluctuations and hence VSWR at the expense of efficiency. The unloaded antenna was simulated using NEC2 and circuit theory was used to calculate the performance with resistors. The VSWR and efficiency of the antenna fluctuated dramatically at frequencies below 7 MHz. The VSWR reached peaks of 3.4:1 while efficiency dropped as low as 4 percent. The inherent multi-band nature of the antenna was therefore only slightly altered by the feed point resistors. The antenna is usable for broadband performance in the sense of providing a VSWR characteristic which is acceptable to a modern transmitter with output protection. The PRR at discrete frequencies however will be very low. The theory to analyze and optimize a variant of this antenna is described in the next chapter.

The insights gained during the evaluation of the Guertler and Collyer antenna were used to develop a novel small HF broadband antenna. The dimensions of the new antenna were similar to the Guertler and Collyer version and the same total wire length was used. The Guertler and Collyer load was divided into two parallel loads which were placed at different distances from the feed point. The antenna was named the Staggered Loads Antenna, SLA, due to the offset load positions. Anti-resonant standing waves were shown to be the cause of VSWR peaks on the Guertler and Collyer antenna. The distances from the feed point to loads were therefore chosen to avoid standing waves on at least two of the four antenna wires. The VSWR and efficiency of the SLA were calculated with NEC2. An improvement in both

VSWR and efficiency in comparison to the antennas discussed before was apparent. The VSWR did not exceed 2.6:1 and the efficiency was better than 40 percent. Impedance measurements confirmed the validity of NEC2 results.

The complete performance of several well known simple broadband HF antennas was rigorously determined in this chapter. The impedance characteristics and radiation efficiency were related to the effectiveness of the various loading schemes in controlling the current distribution. A better understanding of the mechanisms and trade-offs in simple broadband antennas emerged and was reinforced by the design of an improved antenna using this knowledge qualitatively. The improvement in performance of the new antenna was confirmed by measured results

NEC2 was used as an evaluation tool during this phase of the research but the necessity to evaluate structures at many frequencies causes long run times on a personal computer. To evaluate one typical antenna required 10 to 30 hours of computer time. NEC2 also produces results based on the input of wires and loads while the relationship between input and output is not always intuitively obvious. Methods based on the actual mechanisms involved in specific geometries and which perhaps neglects some of the less important electromagnetic principles will provide a better design tool. Such methods should be faster in execution than NEC2 and the theory used to obtain results should be intuitively clear to the design engineer so that he may alter parameters in an intelligent fashion. This philosophy is pursued in chapter 4.

4 TWO SIMPLE DESIGN AIDS FOR LOADED DIPOLES AND MULTI-WIRE ANTENNAS

Chapter 4 is concerned with the development of simplified methods for the analysis of specific types of antennas. The need for such methods arise from the considerable time between submitting a specific geometry and obtaining results when using a method of moments program. Evaluating an antenna such as the Guertler and Collyer dipole from 3 to 30 MHz in 1 MHz increments, for instance, requires approximately 20 hours on an IBM AT personal computer. The relationship between NEC2 input and the performance obtained is not at all obvious since NEC2 solves Maxwell's equations in a very complicated manner to retain generality. NEC2 therefore tells the designer *how* the antenna performs but not *why* the antenna performs in a specific manner. These factors are of primary concern during the design phase of an antenna. The engineer usually has to perform numerous evaluations on seemingly promising structures while developing a new antenna. Computer solutions during this phase play an important role and it was argued that the following aspects should be embodied in these methods:

- Ideally they should be personal computer or work station orientated.
- Time span between submission of the problem and obtaining a solution should be short enough to retain interest and make the designer an important part of the loop.
- The methods must be readily understood and models should typically enlighten the designer about the physical mechanisms underlying the antenna operation.
- Absolute accuracy is not as important as the ability to reproduce trends and provide an indication of the merit of a solution. The method of moments may be used for evaluation of final versions.

The two techniques developed and evaluated in this chapter exploit prior knowledge of the general form of the current distribution on specific antennas. Design iteration time is reduced and antenna operation is apparent from the mathematical models employed. The requirements for a suitable design tool stated above are hence fulfilled. Examples of improved antennas obtained using the simple techniques illustrate their utility.

A program named Simulation and Analysis of Loaded Dipole Antennas, SALDA, was developed to implement the techniques emanating from this thesis and a user manual and description of this PASCAL program is provided in Appendix I. Diskettes containing the source code and executable code are in an envelope attached to the back page.

The methods discussed in this Chapter allow for the determination of antenna input impedance and efficiency. These parameters were argued to be most useful when optimizing antennas in Chapter 2. The radiation patterns of antenna examples considered in this chapter, obtained using NEC2, are shown in Chapter 5 to verify this approach and allow for complete assessment of the antennas.

4.1 The Dipole-Transmission line-Dipole Method (DTD)

The multi-wire dipole with resistive loading was reviewed in Chapter 3. The antenna was structurally the simplest of those described in the literature. The analysis and design of the antenna relied heavily on the method of moments to obtain the input impedance of the unloaded antenna. The determination of a suitable parallel and series resistor becomes a simple matter once the unloaded input impedance is known. The performance was not as good as that of some of the other structures which employed more elaborate loading techniques. The parallel and series resistors reduced the impedance variations (and hence VSWR) to a target value at the expense of efficiency. The result was large fluctuations in VSWR and efficiency, especially at the lower frequencies.

The method of moments obtains results by taking into account all possible interaction between the wire segments making up a structure. A simpler approach is to assume that the current distribution on the multi-wire antennas is very similar to that of the constituent dipoles in free space. This assumption implies minimal interaction which is true for wires of different length and orientation perpendicular to each other. Later comparison between the DTD method and NEC2 results indicates the validity of the assumption.

The optimization of the multi-wire antenna of Chapter 3 showed that even an optimum multi-wire antenna falls short of expectation. The behaviour is due to undesirable current distributions (and hence impedances) on the wires at certain frequencies. Interposing a transmission line between the two dipoles modifies the current distribution and it is postulated that this modification will influence the performance favourably. Introducing a transmission line into the analysis presents no analytical problem. The change in current distribution (or more familiarly termed the impedance transformation) due to a transmission line is theoretically easily calculable. This general arrangement was called the dipole-transmission line-dipole, abbreviated to DTD.

4.1.1 DTD Theory

The feed points of different length dipoles are connected in parallel to form a conventional "fan" dipole arrangement as discussed in Chapter 3. This concept is extended for the DTD structure by connecting the dipole feed points using a transmission line. Fig 4.1 shows this arrangement schematically.

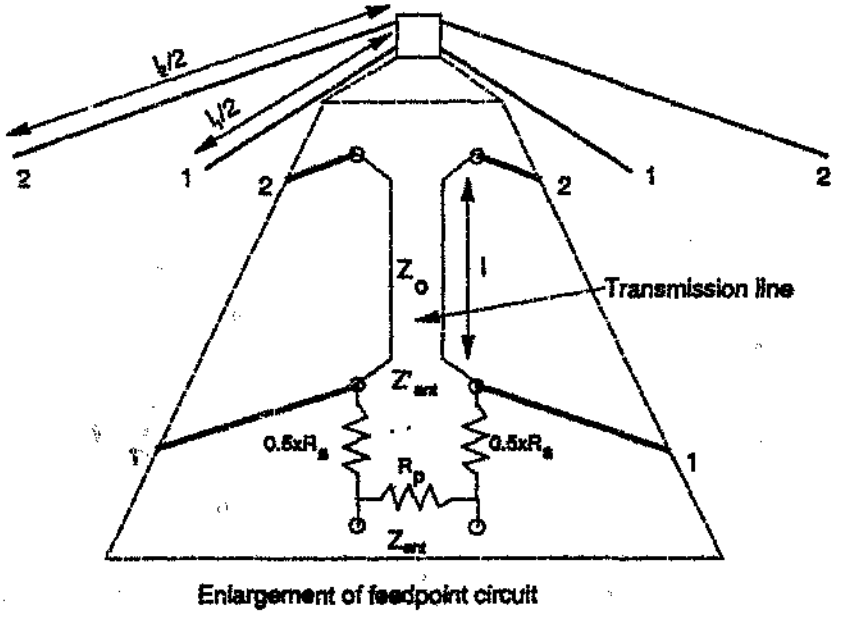


Fig 4.1 Schematic diagram of two dipoles connected with a transmission line

The mutual coupling between dipoles is minimized when they are perpendicular to each other and have different lengths. Results obtained using the theory below are later compared to NEC2 output, which takes coupling into account (Appendix A). The correlation between NEC2 and DTD results show only minor effects due to dipole interaction. Neglecting the coupling between the two dipoles is equivalent to saying that the current on the connected dipoles is the same as that on free space dipoles. The only important part of the dipole current distribution in the DTD theory is the feed point current. The feed point current defines the dipole input impedance and the efficiency of metal dipoles is very close to hundred percent. The free space input impedance of dipoles is available in published tables (King and Harrison, 1969) and these values were stored in a computer file. A first order solution to the antenna impedance was hence obtained by first converting the free space impedance of the second dipole, Z_2, to the feedpoint using the lossless transmission line equation for line length, *l*:

$$Z'_2 = Z_o \frac{Z_2 \cos(\beta l) + jZ_o \sin(\beta l)}{Z_o \cos(\beta l) + jZ_2 \sin(\beta l)} \qquad \text{-(4.1)}$$

where $\beta = 2\pi/\lambda$ is the spatial phase shift factor.

The input impedance of the unloaded antenna, Z'_{ant} is then Z'_2 in parallel with the free space input impedance of the first dipole, Z_1.

$$Z'_{ant} = \frac{Z_1 \cdot Z'_2}{Z_1 + Z'_2} \qquad \text{-(4.2)}$$

The analysis reduced to transmission line and circuit theory since the free space dipole impedances were available. The series and parallel resistors, R_s and R_p respectively, were then added at the feedpoint to reduce VSWR to a target value. Austin and Fourie (1988) showed how the parallel and series feed point resistors may be best selected. Large capacitive or inductive reactance however are only marginally affected by the parallel resistor and not at all by the series resistor.

The input impedance of the resistively loaded antenna, Z_{ant}, is easily determined from normal circuit theory to be:

$$Z_{ant} = R_p \text{ in parallel with } (Z'_{ant} + R_s) = \frac{R_p \cdot (Z'_{ant} + R_s)}{R_p + Z'_{ant} + R_s}$$

The efficiency of the feedpoint network was found by calculating the input power, the power dissipated in the resistor network and power radiated by the antenna using circuit theory presented in section 3.1.4. The only difference is that Z'_{ant} for this case is the input impedance of the unloaded DTD configuration rather than the normal unloaded fan dipole impedance used before.

4.1.2 Design method to obtain novel antenna

The impedance and efficiency of the DTD for one frequency are obtained by using one transmission line conversion and solving the circuit equations. This theory provided a very fast method to obtain the performance of a DTD over the full frequency band. For instance only 16 seconds is required to do a frequency sweep from 2 to 30 MHz at 1 MHz intervals using a PC AT personal computer running at 8 MHz. NEC2 on the same machine requires approximately 25 hours to do such a simulation.

The theory also suggests reasons for specific behaviour since the performance may be related back to the input impedance of the two dipoles and the length of transmission line. The DTD theory presented here therefore solves the two major problems mentioned at the beginning of this thesis. Absolute accuracy naturally suffered as result of the approximations but are sufficient for initial design optimization. Impedance values with average errors which are less than 25% of the system impedance are generally acceptable for most design purposes.

An exhaustive search of all possible parameters was performed to obtain an optimized version of the DTD for the 2 to 30 MHz band . The parameters of interest are l_1 and l_2 the lengths of dipole 1 and 2 respectively, the transmission line length, l, and the characteristic impedance of the line Z_o. A range of values are chosen for each parameter and all possible variations are analyzed and the average VSWR is recorded for each combination. The combination with the lowest average VSWR, and hence impedance variation, is then chosen. The structure found in this way is assumed lossless (two dipoles and a transmission line) and efficiency need not be considered at this stage. The ranges examined are given below:

l_1: 40m - 85m in 5m increments
l_2: 40m - 85m in 5m increments
l : 2m - 20 m in 3m increments
Z_o: 200Ω - 800Ω in 100Ω increments

The evaluation of all permutations of the parameters above called for almost 5000 full frequency iterations which was performed in one day using the DTD theory . The same number of simulations on NEC2 would have required approximately 10 years on a PC AT computer!

The design is fine tuned after the first optimization by applying smaller parameter variations about the optimum points.

The current distribution on the dipoles and the connecting transmission line are not changed by the feed point resistors. The resistors are thus omitted for optimization and afterwards incorporated to achieve a target VSWR. The optimum values found during this design cycle were:

l_1: 48m
l_2: 74m
l : 11m
Z_o: 500Ω

The values for Rp and Rs to achieve a VSWR of less than 2.5: 1 were as follows:

R_p: 1200 Ω

R_s: 90 Ω

The design produced a VSWR of less than 2.5:1 relative to a system impedance of 350Ω. The antenna therefore requires a 7:1 transformer before connection to a typical 50 Ω feed line. Such a transformer is easily obtained using a toroidal core with a tri-filar transmission line type transformer (Sevick, 1976). This transformer normally yields a 9:1 impedance transformation ratio but in this instance one winding is tapped to achieve the required impedance.

A practical problem is the implementation of the 500Ω transmission line. This problem is solved by using a 75Ω line with a 7:1 impedance transformer at either end of the line as shown in fig 4.2.

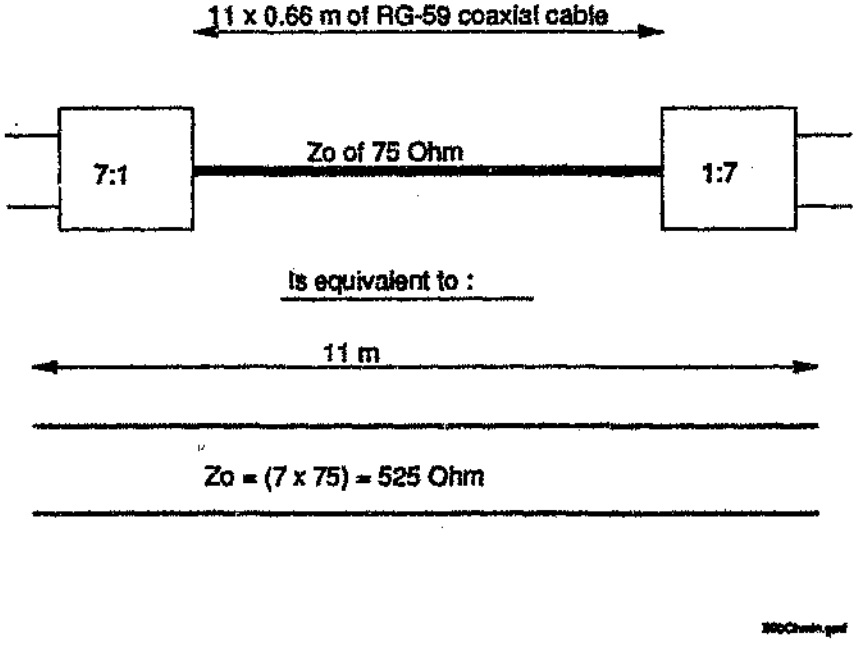


Fig 4.2 Practical method to obtain a 500Ω transmission line

The same transformers as discussed above are used for this implementation. The transmission line was coiled and fitted into a feed box of 25 cm x 20 cm x 12 cm.

4.1.3 Results for DTD antenna

The DTD antenna was analyzed using the fast DTD theory as well as the NEC2 program. Evaluations were only done up to 24 MHz using the DTD theory since the free space dipole impedances for frequencies above 24 MHz are not readily available. The VSWR was also

measured practically on a 12 m mast. The two dipole wires were perpendicular to each other in a drooping dipole configuration (wires sloping from the mast to the ground). All the results presented below are tabulated in Appendix J.

The first set of results shows the effect of the simplifications made in the DTD theory formulation. The input resistance and reactance of the DTD without the resistors is presented in comparison to NEC2 results in figs. 4.3 and 4.4. The antenna was modelled as two wires perpendicular to each other with 1 m vertical separation. The NEC2 transmission line feature (TL card in NEC2 card nomenclature) was used to connect the two central segments of each dipole. Segmentation was adjusted over the frequency band to ensure more than ten segments per wavelength throughout.

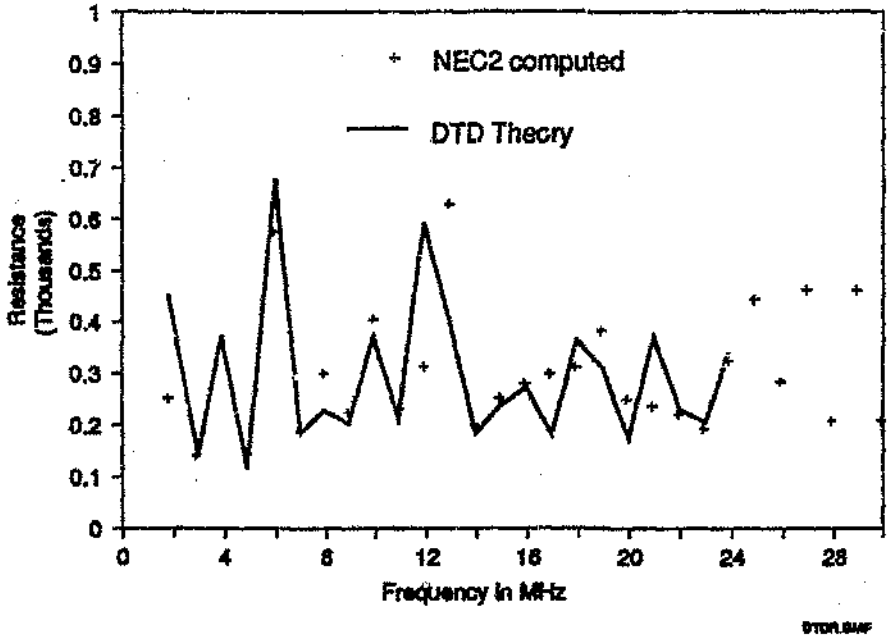


Fig 4.3 The resistance of an unloaded DTD obtained from the DTD theory as well as NEC2 simulation

The results indicate satisfactory correlation between NEC2 and the limited DTD theory. The effect of neglecting coupling between dipoles is not major as was argued in the previous section. The average error in the real part of the input impedance is 48Ω and 50Ω in the reactive part. This error is approximately 15 % when expressed relative to the system impedance of 350Ω and it is apparent that trends are reproduced faithfully.

Fig 4.5 shows the VSWR of the antenna as determined by the simple theory, NEC2 as well as measurement 12 m above a real earth.

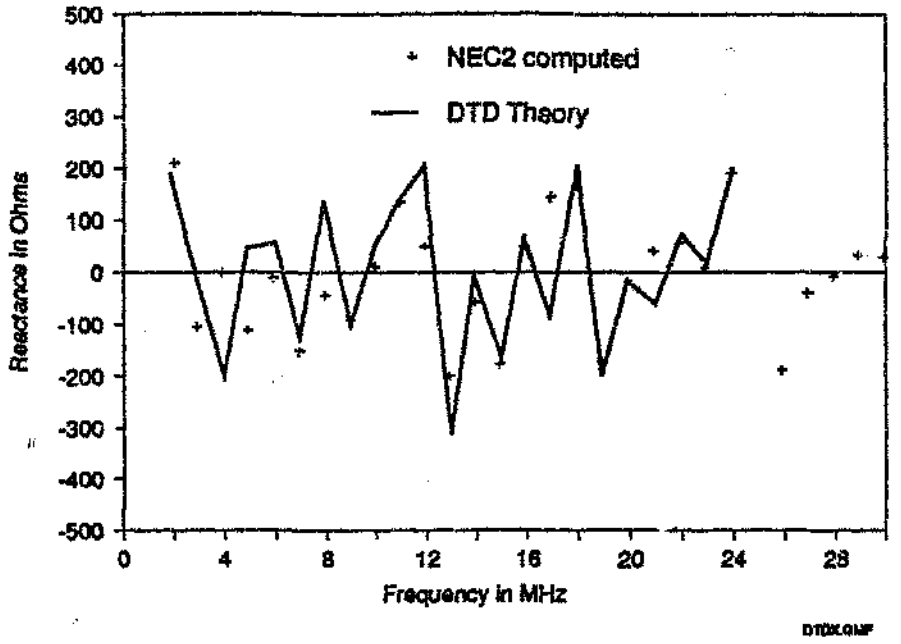


Fig 4.4 The reactance of an unloaded DTD obtained from the DTD theory as well as NEC2 simulation

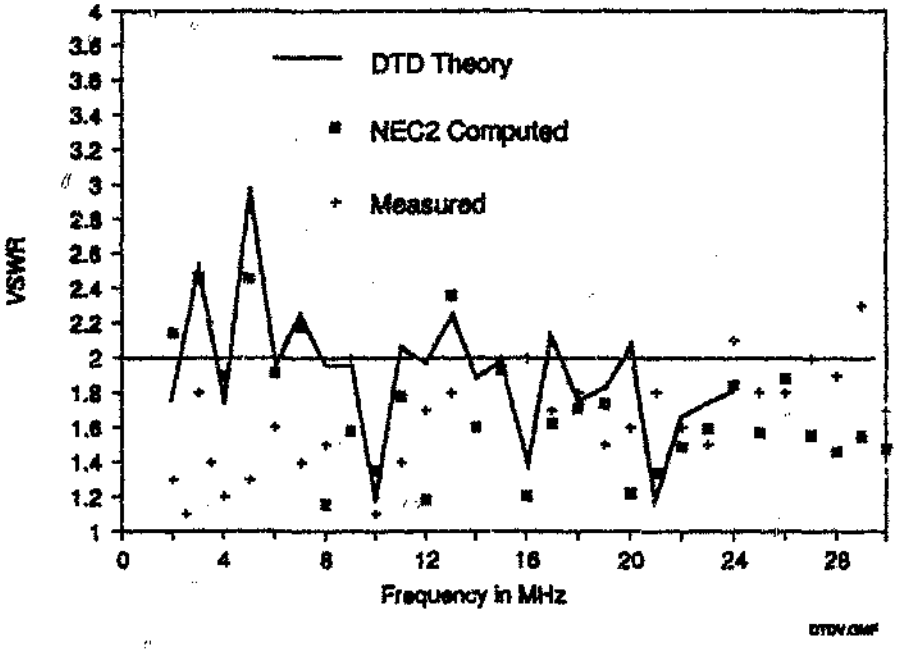


Fig 4.5 The VSWR of the DTD as determined by simplified theory, NEC2 as well as measured results.

The difference between the DTD theory and NEC2 results is on average less than 0.25 in absolute units. The measurements show similar values and trends as the theory but do not correlate well at low frequencies. The differences were due to the effects of a real earth which is electrically close at low frequencies and the wires which were not mutually perpendicular but rather sloped downwards from the 12m centre mast. The measured VSWR was overall better than that predicted by the theory.

Finally the efficiency performance of the antenna is shown in Fig 4.6. The efficiency was calculated from NEC2 impedances for the unloaded DTD using the equations in section 4.1.1.

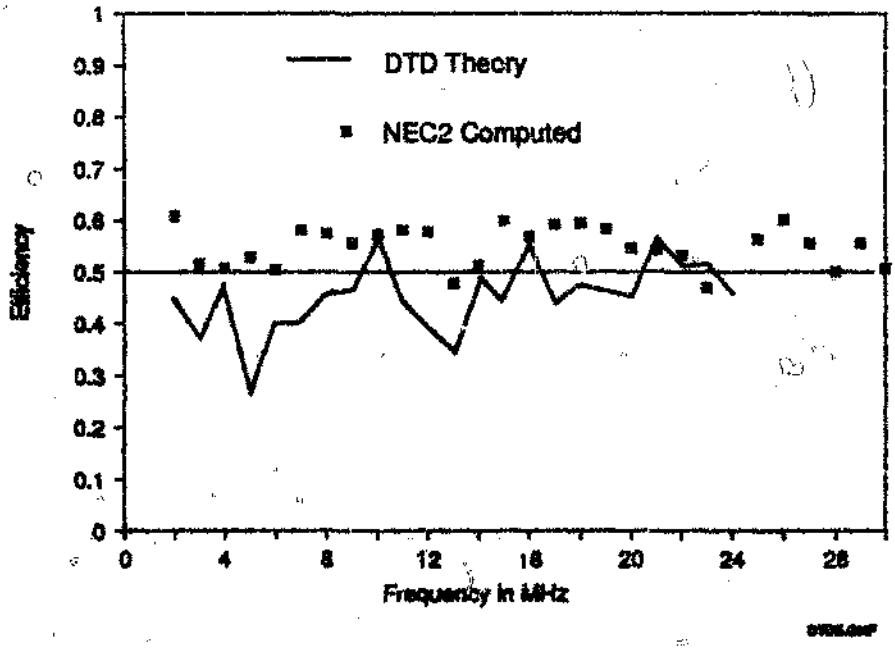


Fig 4.6 The efficiency of the DTD as calculated from NEC2 impedances

The average difference between the NEC2 and DTD theory values is 11% with the NEC values consistently better than those predicted by the DTD theory. The radiation efficiency of this antenna is virtually better than 50% over most of the 2 - 30 MHz range. The minimum efficiency of the DTD is higher than that of the Trideme, Guertler and Collyer, Harris and the optimized fan dipole antennas. The VSWR also remains below 2.5:1 over the full band of operation. The performance is better than the SLA antenna (Fourie and Austin, 1987) mentioned earlier. The PRR in fig 4.7 provides a composite illustration of the DTD broadband performance.

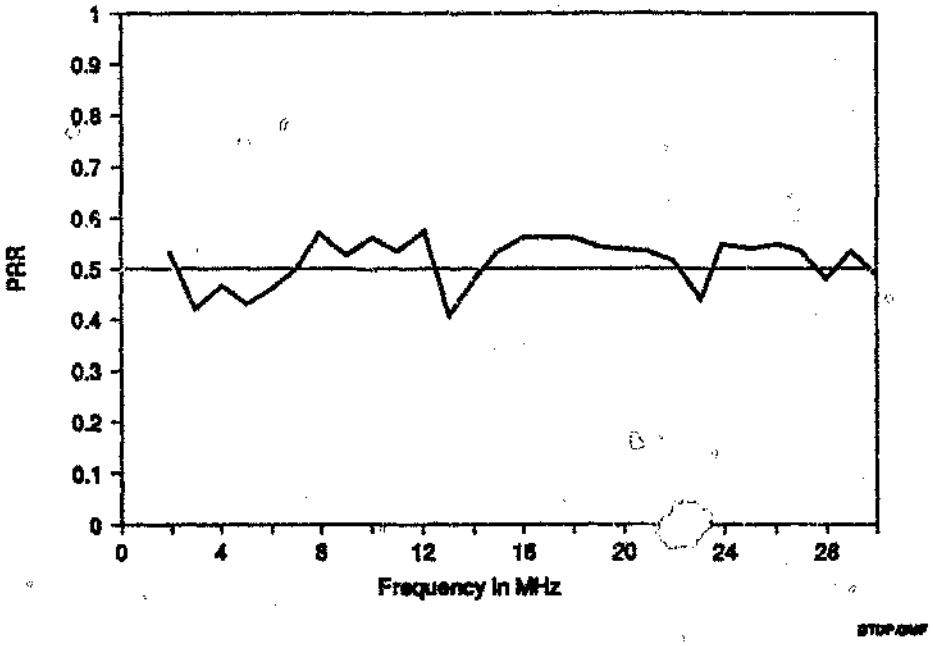


Fig 4.7 The PRR of the DTD as calculated from NEC2 impedances

4.2 The Lossy Transmission Line method

The current distribution on the single loaded dipoles examined in chapter 2 was shown to behave in a manner similar to current on a transmission line. Indeed much of the antenna literature refers to this analogy at some stage to illustrate the behaviour of dipole antennas (Schelkunoff, 1941, 1943 and 1952; Williams, 1966 ; Maclean, 1973 ; Hall and Maclean, 1971, Poggio and Mayes, 1971 and the pioneer of loaded wire antennas, Altshuler, 1961, relied on this analogy in proposing his resistively loaded monopole). Transmission line theory is usually never used beyond this point however. Obvious difficulties in applying transmission line theory to dipole antennas becomes apparent upon closer examination. The input impedance of an open circuited, quarter wave transmission line is clearly not 73 + j 42 Ω, which is the impedance of an equivalent half wave dipole. Such problems, combined with the considerable capabilities of the method of moments, have led most researchers to disregard transmission line methods. Transmission line methods solve some of the problems associated with the method of moments which were pointed out before, namely:

- Transmission line analytical techniques retain the very important physical mechanisms governing the current distribution. The method of moments on the other hand is essentially a "black box" process that produces numerical results. The cause of antenna

behaviour is not apparent from the mathematical model or from the output. The value of physical insight was demonstrated by the design of the SLA earlier and should not be underestimated.

- The computer time required to analyze an antenna using transmission line theory will be shown to be proportional to the antenna length. This time is in contrast to the method of moments codes where computer time is proportional to the second and third powers of the number of wire segments. Computer time is clearly significant, since it ultimately limits size of antennas and the number of design iterations. Long waiting times also frustrate the design process.

Novel methods of analyzing loaded dipoles using equivalent transmission lines were developed. Results obtained were compared to published and NEC2 results. An example of an improved broadband antenna designed using this technique is also briefly mentioned.

4.2.1 Various Methods of Analyzing Loaded Dipole Antennas

Nyquist and Chen (1968) developed theory to analyze loaded antennas which was applicable when travelling waves existed between feed and load. This theory was used to calculate the loads that are required to maintain travelling wave behaviour. The analysis in the previous chapter indicates however that travelling waves only exist at specific frequencies on most simple HF broadband antennas. This theory therefore does not lend itself to the analysis of loaded broadband antennas. Poggio and Mayes (1971) used transmission line theory in analyzing loaded dipoles by neglecting the effects of radiation and characteristic impedance variations. These simplifications again resulted in a theory which illustrates the principles involved, but which is too crude for generalized use. Altshuler (1961) employed transmission line theory to obtain approximate values for the resistive loads to be used in his monopole. He never attempted to use this theory to determine the behaviour of the antenna, however. Maclean (1973) used the biconical antenna theory developed by Schelkunoff (1941) to transform the load impedance of a travelling wave dipole to the feedpoint. He then added the transformed impedance to the resistance due to radiation, which he determined using the approximate current distribution on the antenna. This technique is again only applicable at the one frequency where a travelling wave exists between the feedpoint and the loads.

Most probably, the most important work in this regard was done by Schelkunoff (1941, 1943 and 1952). He developed the theory for biconical antennas which has many transmission line features. Schelkunoff (1941), in his historic article showed that an antenna could not be regarded as a simple, lossy, two wire transmission line. He concluded that (p 1188): "Thus from a theory in which antennas are regarded as multiple transmission lines, we have

obtained two restricted theories. In the first of these radiation appears as a terminal impedance and in the second it appears as a distributed series impedance. There is no inconsistency between these two views and both are valid provided they are suitably qualified." Fourie (1988) examined both approaches and found the one using distributed series resistance to be most promising. The lossy line model developed by Fourie (1988) was quite simplistic and produced poor results where a structure incorporated complex loads. The method has been further refined as outlined in this section.

Extensive use has been made of the theory developed by Schelkunoff with the addition of an incremental analysis, introduced here. This modification allows transmission line parameters to vary with distance from the feed point instead of using average values throughout as was done previously (Schelkunoff, 1952 ; Maclean, 1973). This approach is practical using the computer power available today. A lossy, non-uniform line theory were also developed during this research. This theory was developed by adapting a few of Schelkunoff's equations for line parameters and obtaining others by numerical experiments.

4.2.2 Review of Schelkunoff's Theory

The analogy between transmission lines and conical dipole antennas is shown in fig 4.8. Schelkunoff developed his theory by considering a lossless biconical transmission line and the effect of radiation are lumped together in the terminating impedance, Z_t. Z_t thus comprises real and imaginary components given by:

$$Z_t = R_t + jX_t \qquad -(4.3)$$

Schelkunoff (1952: p 45) defined the terminating impedance in terms of a transformed impedance a quarter wavelength away from the end, thus (using the quarter wave transformer equation):

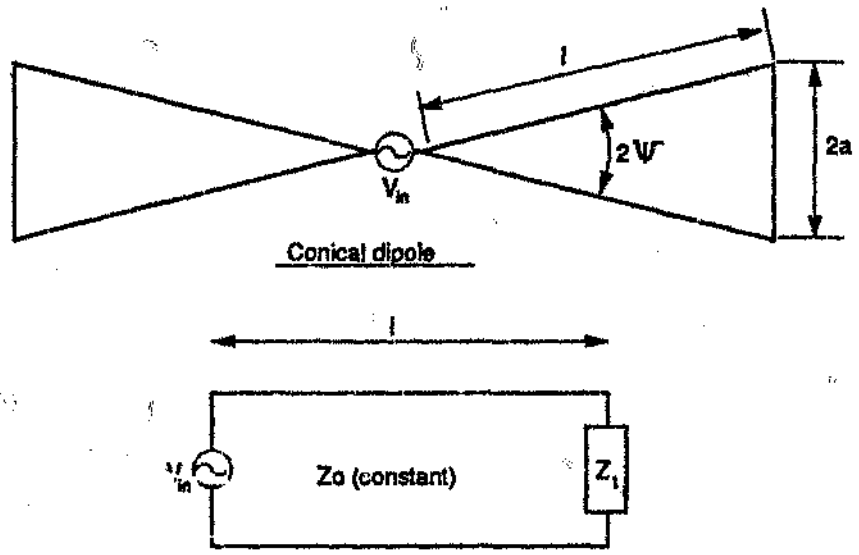


Fig 4.8 Biconical dipole antenna with transmission line equivalent

$$Z_i = \frac{Z_o^2}{Z_a} \qquad \text{-(4.4)}$$

where

$$Z_a = R_a + jX_a \qquad \text{-(4.5)}$$

with R_a and X_a defined by Sine and Cosine integrals as follows:

$$R_a = \frac{\eta}{2\pi} C_{in}(2\beta l) + \frac{\eta}{4\pi}[2C_{in}(2\beta l) - C_{in}(4\beta l)]\cos(2\beta l) +$$

$$\frac{\eta}{4\pi}[S_i(4\beta l) - 2S_i(2\beta l)]\sin(2\beta l)$$

$$X_a = \frac{\eta}{2\pi} S_i(2\beta l) - \frac{\eta}{4\pi}[C_{in}(2\beta l) - 2\ln 2]\sin(2\beta l)$$

$$-\frac{\eta}{4\pi} S_i(4\beta l)\cos(2\beta l)$$

and $\beta = 2\pi/\lambda$ is the spatial phase shift factor.

The conical dipole has constant characteristic impedance:

$$Z_o = \frac{\eta}{\pi}\ln(\cot\frac{\Psi}{2}) \approx 120 \cdot \ln\left(\frac{2l}{a}\right) \qquad \text{-(4.6)}$$

with

$\eta = 120\pi$ Ω (Characteristic impedance of free space)

Hence the input impedance of this idealized dipole is found using the well known lossless transmission line equation.

$$Z_i = Z_o \cdot \left[\frac{Z_t \cos(\beta l) + jZ_o \sin(\beta l)}{Z_o \cos(\beta l) + jZ_t \sin(\beta l)}\right] \qquad \text{-(4.7)}$$

Schelkunoff did not consider the inclusion of loads in this structure but this could be done by merely performing the transformation in steps. The principle is illustrated with the aid of fig 4.9. The procedure is performed in two steps in the case of a single load per arm:

- Z_t at l is first converted to Z'_t at l_1 using the transmission line equation. The loads are then added to Z'_t to form a new terminating impedance Z''_t as follows:

$$Z''_t = (2 \times Z_L) + Z'_t \qquad \text{-(4.8)}$$

- Z''_t is converted by the next transmission line transformation using l_1 to yield the input impedance.

Schelkunoff (1941,1953) also adapted the theory of conical dipoles to one for cylindrical dipoles by making the assumption that Z_o does not change too rapidly with position. An average value of the characteristic impedance, Z_{oa}, is used for this case.

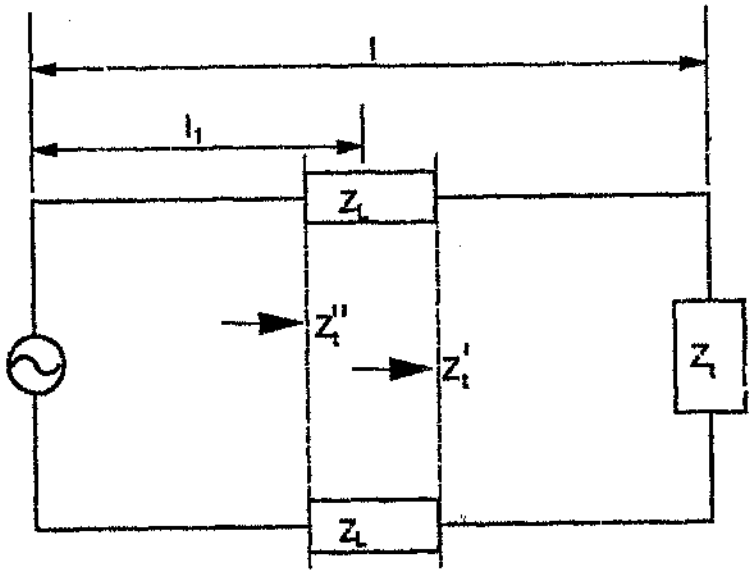


Fig 4.9 Modification to Schelkunoff's theory to include a single load in each conical dipole arm

$$Z_{aa} = 120 \cdot \left[\ln\left(2\frac{l}{a}\right) - 1 \right] \qquad \text{-(4.9)}$$

where the dipole half length is l and the radius is a.

A good approximation to the input impedance is given by:

$$Z_i = R_i + jX_i \qquad \text{-(4.10)}$$

where:

$$R_i = \frac{A}{B} \qquad \text{-(4.11)}$$

$$A = Z_{oa} G [Z_{aa} + N \sin(2\beta l) - M \cos(2\beta l)]$$

$$B = G^2 \cos^2(\beta l) + [(Z_{aa} + M)\sin(\beta l) + (F + N)\cos(\beta l)]^2$$

$$X_i = \frac{C}{D}$$

$$C = Z_{oa} [0.5 (G^2 + F^2 + M^2 - N^2 - Z_{aa} super 2) \sin(2\beta l) + MF - Z_{aa} N]$$

$$D = G^2 \cos^2(\beta l) + [(Z_{aa} + M)\sin(\beta l) + (F + N)\cos(\beta l)]^2$$

with:

$$G = 60[C + \ln(2\beta l) - C_i(2\beta l)] + 30[C + 2C_i(2\beta l) + C_i(4\beta l)]\cos(2\beta l)$$
$$+30[S_i(4\beta l) - 2S_i(2\beta l)]\sin(2\beta l)$$
$$F = 60S_i(2\beta l) + 30[C_i(4\beta l) - \ln L - C]\sin(2\beta l) - 30S_i(4\beta l)]\cos(2\beta l)$$
$$M = 60[\ln(2\beta l) - C_i(2\beta l) + C - 1 + \cos(2\beta l)]$$
$$N = 60[S_i(2\beta l) - \sin(2\beta l)]$$

and:

$$C = 0.5772 \qquad \text{(Euler's constant)}$$

The above equation for cylindrical dipoles is not as convenient as the one for the conical dipole, since the transmission line equation is "hidden" in the manipulation indicated above. Modifying it to accommodate loads is hence not easy.

4.2.3 Development of the Lossy Transmission Line Method

The loaded dipoles of interest in practical situations are usually cylindrical, or may be transformed to equivalent cylindrical configurations. Equivalent configurations already encountered are the two or three wire antennas of Guertler and Collyer (1973) and Harris (1982). More than one thin parallel wire are used to emulate a single wire dipole (Clark and Fourie, 1989) with a larger equivalent radius. The equivalent radius may therefore be used to model such antennas as loaded single wire dipoles.

Schelkunoff derived the theory for cylindrical antennas using the conical dipole as the starting point. This antenna is equivalent to a transmission line with constant characteristic impedance. The effect of radiation is clearly not accounted for when treating the antenna as a lossless transmission line. Schelkunoff lumped radiation effects together in a terminal impedance connected to the intuitively open circuited line. Schelkunoff used average parameter values to derive his cylindrical dipole theory, since the transmission line parameters for a cylindrical dipole are not constant. The approach presented here rather treats the cylindrical antenna as an incrementally conical antenna. The Z_o changes gradually with distance from the feed. This local $Z_o(h)$ was used for small increments along the wire over which it is assumed to be constant.

The radiation effects are lumped into the resistive part of the terminating impedance in the Schelkunoff model. This approach is suitable for the evaluation of unloaded dipoles but not for loaded ones. The loads may prevent current from reaching the wire ends and hence create

the impression that the antenna does not radiate. Fourie (1988) showed that a lossless incrementally conical line model produces less accurate results when compared to an unrefined lossy line model.

Schelkunoff indicated that a dipole may be viewed as multiple transmission lines with radiation accounted for by introducing line loss resistance. A novel method of doing so was developed by using a non-uniform, lossy transmission line model (Fig 4.10).

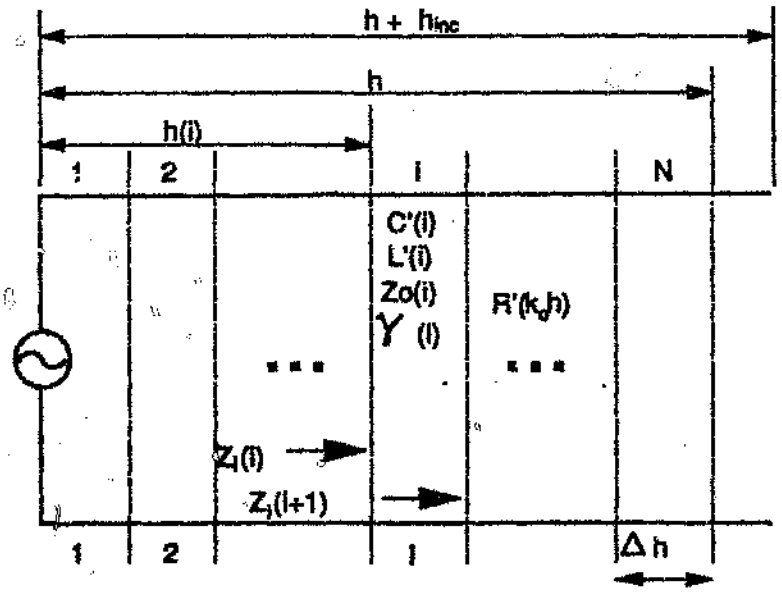


Fig 4.10 The non-uniform lossy transmission line model of a dipole antenna of length l = 2h

This model requires the general lossy transmission line equation to obtain a solution. The equation that must be solved for the general line segment, i, of a line with N segments is:

$$Z_i(i) = Z_o(i)\left[\frac{Z_i(i+1)+Z_o(i)\tanh[\gamma(i)\Delta h]}{Z_o(i)+Z_i(i+1)\tanh[\gamma(i)\Delta h]}\right] \qquad -(4.12)$$

Starting with $Z_i(N+1)$ as an open circuit the equation was solved N times (for i = N .. 1) to yield $Z_i(1)$ - the dipole input impedance.

The line length was adjusted by h_{inc} to take into account the fringing at the dipole end points. The radiation that takes place is taken into account by the series resistance, $R'(k_o h)$ incorporated into this transmission line model. This series resistance was postulated to be constant

with distance from the feed point while being a function of $k_o h = 2\pi h/\lambda$, that is the dipole electrical length. The line series resistance, $R'(k_o h)$, therefore varies with line electrical length and by implication with frequency.

Loads are taking into account by adding them to the intermediate impedance at the segment in which they occur. A load Z_L in segment k will modify $Z_i(k)$ to become:

$$Z_i(k) = Z_i(k) + 2 \cdot Z_L \qquad \text{-(4.13)}$$

The value of the variable characteristic impedance, $Z_o(i)$, is calculated from first principles to be:

$$Z_o(i) = \sqrt{\frac{Z'(i)}{Y'(i)}} \qquad \text{-(4.14)}$$

Similarly the propagation coefficient, $\gamma(i)$, is given by:

$$\gamma(i) = \sqrt{Z'(i)Y'(i)} \qquad \text{-(4.15)}$$

with series impedance per unit length, $Z'(i)$ and parallel admittance per unit length $Y'(i)$, given by:

$$Z'(i) = R'(k_o h) + j\omega L'(i) \qquad \Omega/m$$

$$Y'(i) = j\omega C'(i) \qquad S/m$$

assuming cross conductance G' to be zero.

where:

$$L'(i) = \frac{\mu_o}{\pi} \ln\left[\frac{2h(i)}{a}\right] \qquad H/m$$

$$C'(i) = \mu_o \frac{\epsilon_o}{L'(i)} \qquad F/m$$

Values for $R'(k_o h)$ as well as for h_{inc} are required to use the lossy line theory. These parameters were determined by numerical experiment (Fourie, 1989a) for different thickness dipoles using the reputable King-Harrison (1969) data as bench mark.

The numerical determination was done by iteratively applying the lossy line theory to a specific dipole using an initial guess for both parameters. These starting values were then refined by comparing the result with the King-Harrison result for the same thickness dipole. The process was carried out for all the $k_o h$ values of interest and for different thickness dipoles. The numerical experiment was only performed once and the values stored in a look-up table. Evaluations of loaded dipoles were then performed using these values.

The values which were empirically determined are plotted in figs 4.11 and 4.12.

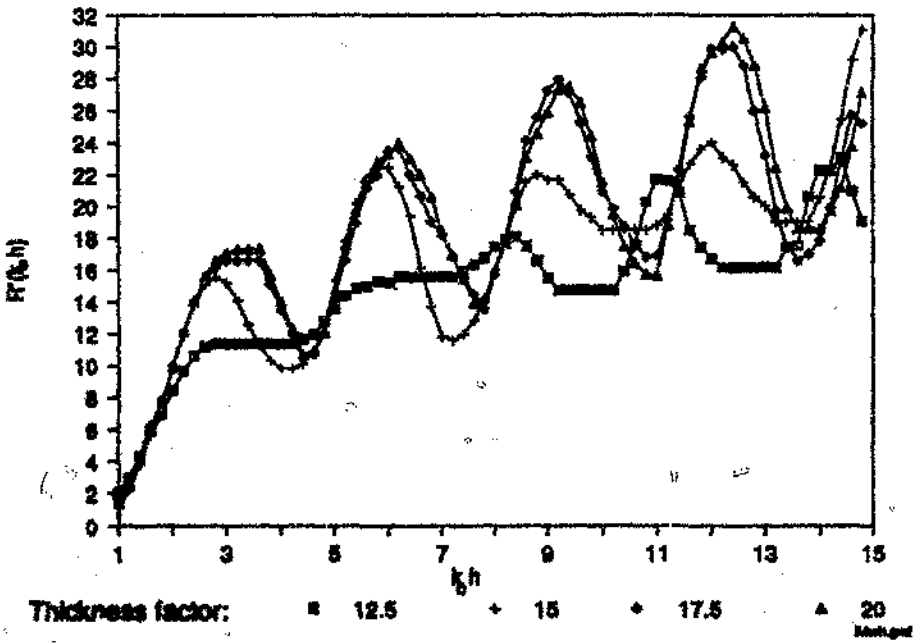


Fig 4.11 The $R'(k_o h)$ values for different thickness dipoles

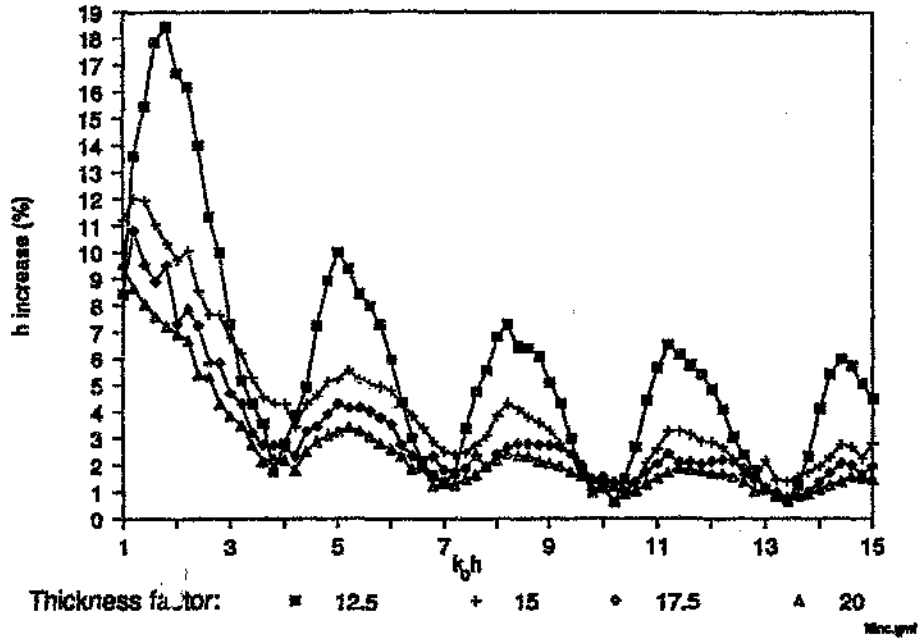


Fig 4.12 The h_{inc} values for different thickness dipoles

The $R'(k_o h)$ results shown are for $h = 23.2$ m and must be modified to the actual dipole half length, h, in order to use it for different length antennas. The equation to do so is:

$$R'(k_o h)_{actual} = R'(koh) \cdot 23.2/h \qquad \text{-(4.16)}$$

The empirically determined parameters are not perfectly smooth. The small fluctuations were due to the fact that the input impedance is not very sensitive to changes in either $R'(k_o h)$ or h_{inc} at specific frequencies. The iterative process hence found an acceptable value while still using large increments. Refining the values to produce a smooth curve will thus have a negligible effect on the accuracy. Smoothing these curves using digital filtering techniques will certainly improve their better appearance without adversely affecting the results.

The current distribution can be calculated on a segment by segment basis once the line parameters are known for a non-uniform line . The current distribution allows for the efficiency to be calculated if all losses are assumed to occur in the lumped loads.

The current at a distance, x, from the generator on a lossy transmission line of length, l, and terminated in a load, Z_L, is given by the equation:

$$I(x) = I(0)\left[\frac{Z_0 \cosh(\gamma(l-x)) + Z_L \sinh(\gamma(l-x))}{Z_0 \cosh(\gamma l) + Z_L \sinh(\gamma l)}\right] \qquad \text{-(4.17)}$$

The current at the feed, I(0), was taken for convenience to be 1 A. The current at any point, i, on the line is found by successively applying the equation to each incremental piece of transmission line with:

$$l = x = \Delta h$$

which yields:

$$I(i+1) = \frac{I(i)Z_0(i)}{Z_0(i)\cosh(\gamma(i)\Delta h) + Z_i(i+1)\sinh(\gamma(i)\Delta h)} \qquad -(4.18)$$

The input impedance, Z_i, is obtained using equation 4.12 as before. The complete current distribution is known after this equation has been applied to all segments 1 to N . The efficiency is then simply obtained by calculating the input power, P_{in}, and the power dissipated in M loads P_L. The variable k corresponds to the segment number where the load occurs and M is the total number of loads.

$$P_{in} = \frac{R_{in}|I(0)|^2}{2} \qquad -(4.19)$$

The power lost in all the loads must be added to yield the total ohmic loss P_L:

$$P_L = \sum_{k=1}^{M} 2 \times R_L(k)|I(k)|^2 \qquad -(4.20)$$

where k is the segment containing a load $Z_L(k) = R_L(k) + jX_L(k)$ in each wire. The efficiency, η , is then given by the equation:

$$\eta = \frac{(P_{in} - P_L)}{P_{in}} \qquad -(4.21)$$

Skin effect losses due to finite conductivity of the dipole elements may also be taken into account by modelling these losses using discrete loads at every segment. The results presented in this thesis assumed perfect conductors however.

4.2.4 Results of Lossy Line method

The ultimate aim of the Lossy Line method presented above is the analysis of loaded dipole antennas. Results are first shown for an unloaded dipole antenna to indicate the match

between results obtained using the lossy line method and the King-Harrison (1969) results. These results serve to validate the empirical method of obtaining the $R'(k_o h)$ and h_{inc} parameters.

The method was ultimately intended for the design and evaluation of loaded dipole antennas and a few examples of these antennas are also evaluated and results compared to measured, published or NEC2 results.

Unloaded dipoles

Impedance values of a dipole with thickness factor, $\Omega = 2 \cdot \ln(2h/a) = 15$ are shown in figs 4.13 and 4.14 below in comparison to the authoritative King-Harrison results to indicate the accuracy of results for unloaded dipoles. Tabulated results are available in Appendix K.

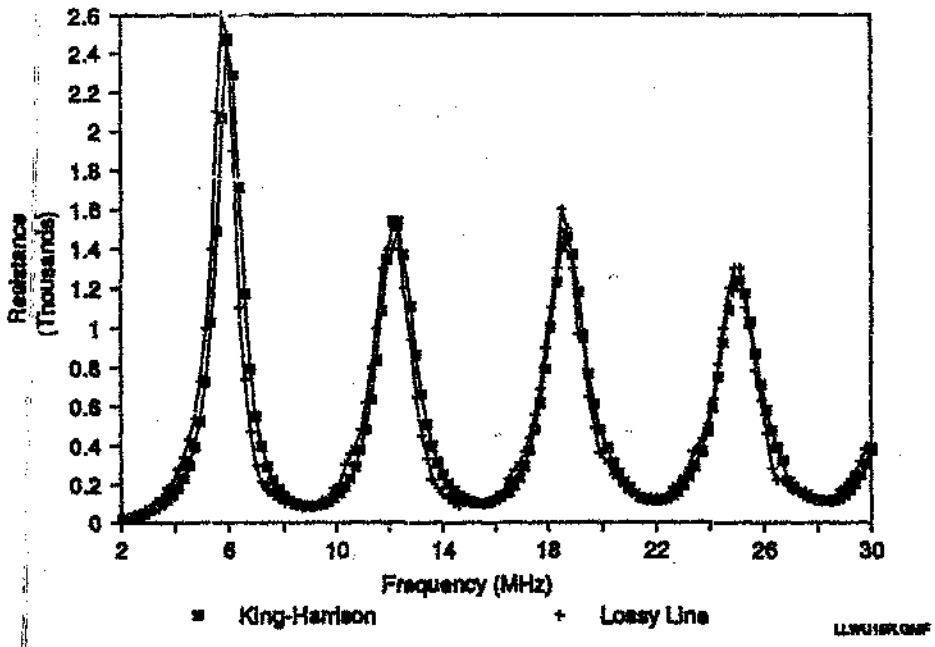


Fig 4.13 The resistance of a dipole with thickness factor of 15 as determined by the Lossy Line method compared to King-Harrison results

Good correlation exists between the lossy line method and the King-Harrison values over a large frequency band. The King-Harrison results were used in the empirical determinations of the parameters for the Lossy Line method. The results above therefore merely indicate the validity of the iterative computational experiment. Results obtained for the loaded dipoles are a suitable test for the technique.

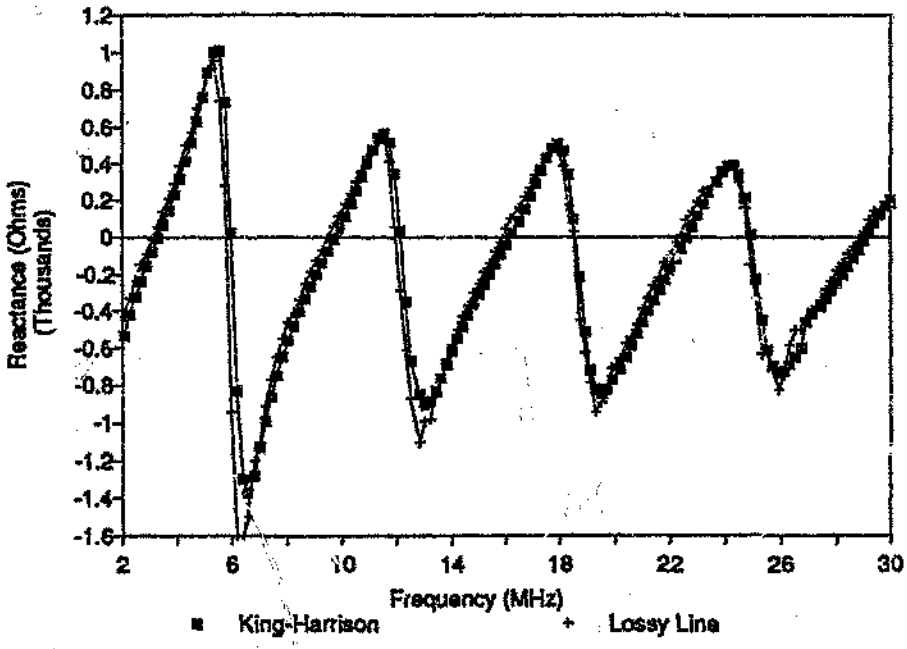


Fig 4.14 The reactance of a dipole with thickness factor of 15 as determined by the Lossy Line method compared to King-Harrison results

The Altshuler dipole

The well known Altshuler (1961) type antenna mentioned before in this thesis was next considered. This antenna was scaled to a total length of 46 m with 330 Ω loads placed 15.5 m from the feed as shown in fig 4.15. The radius was also scaled to ensure that a thickness factor of 12.5 was maintained.

The input impedance and efficiency results for this antenna are shown in figs 4.16, 4.17 and 4.18 with NEC2 results included for comparison. Tabulated results appear in Appendix L.

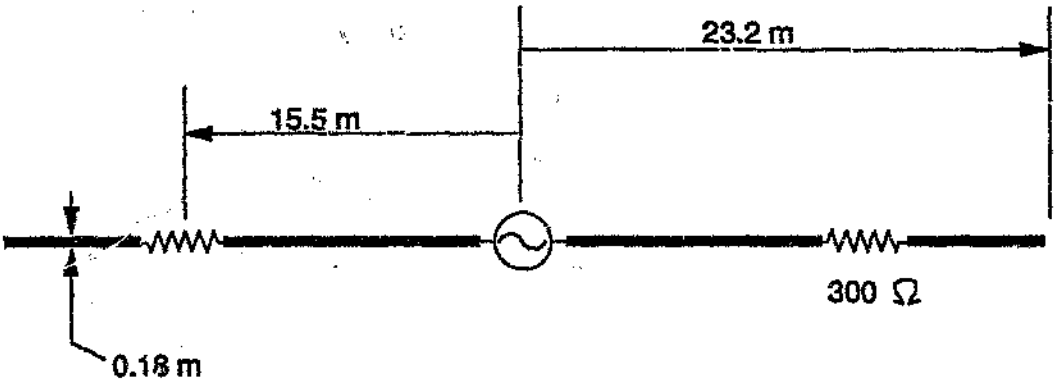


Fig 4.15 Altshuler type antenna used for tests

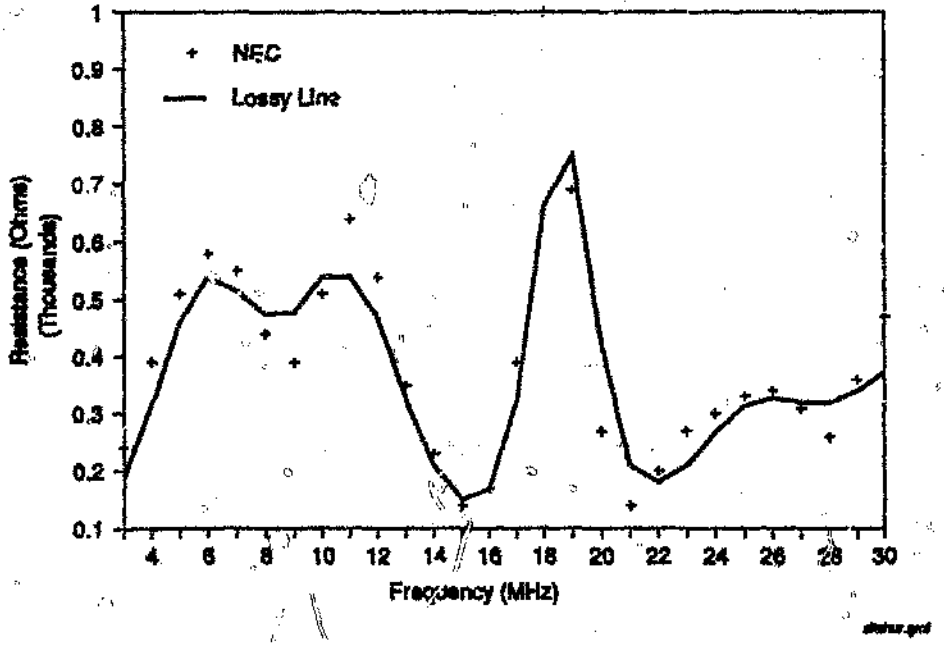


Fig 4.16 Input resistance of the Altshuler type antenna in comparison to NEC2 results

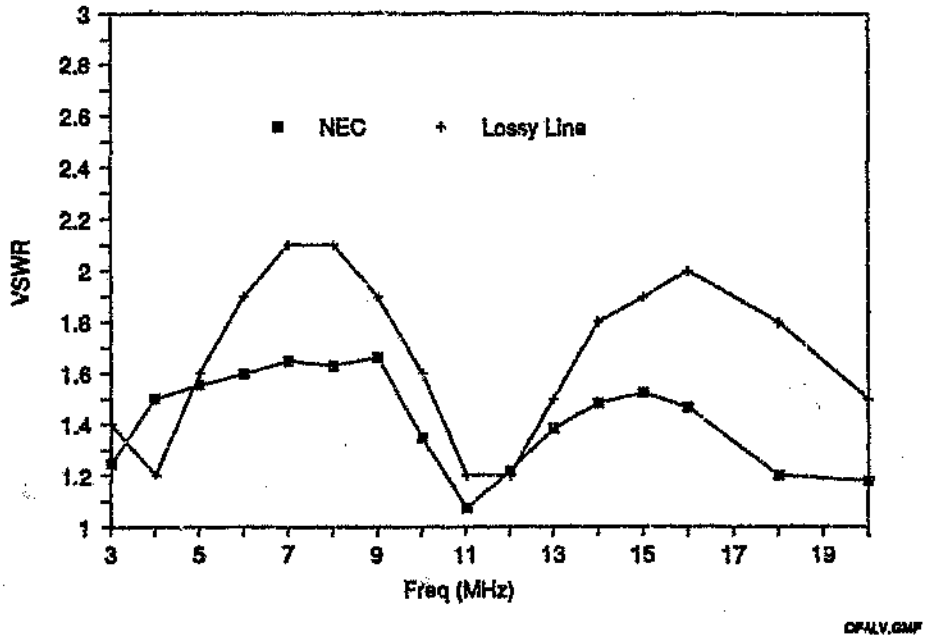


Fig 4.23 The VSWR of the multi-load antenna in comparison to NEC2 results

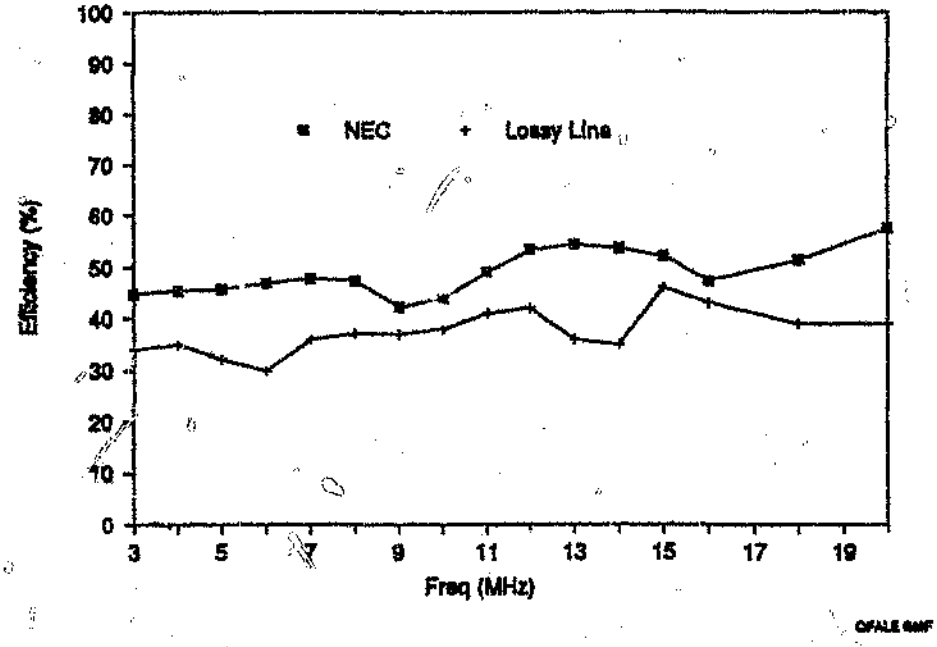


Fig 4.24 The Efficiency of the multi-load antenna in comparison to NEC2 results

The average difference in the VSWR results when compared to the NEC2 results is 0.29. The average difference in the efficiency results is 11% with the NEC2 where the NEC2 results show a overall higher efficiency than that predicted by the lossy line theory. The results indi-

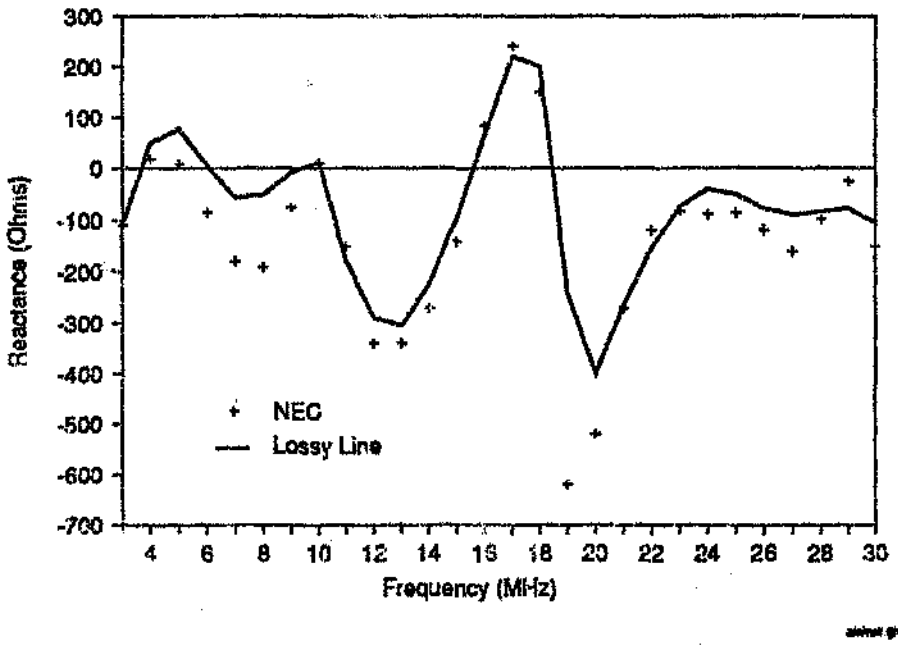


Fig 4.17 Input reactance of the Altshuler type antenna in comparison to NEC2 results

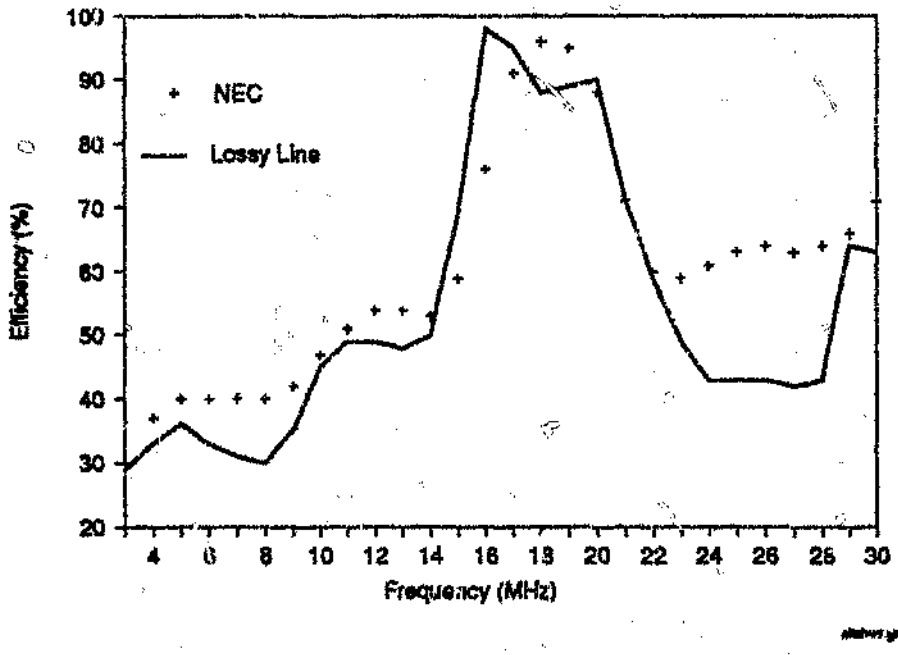


Fig 4.18 Efficiency of the Altshuler type antenna in comparison to NEC2 results

The Lossy Line results are clearly sufficiently accurate for the design of this type of antenna. The average error in the input resistance is 26Ω and in input reactance the average error is 40Ω. It is especially encouraging to note that the efficiency results agree within 7% on average to those obtained using the NEC2 program. This correlation indicate that the Lossy Line method succeeds reasonably well in approximating the current distribution on the wire. The thrust of the research was towards control of current distribution to obtain bandwidth. The Lossy Line method is hence a useful tool to evaluate such attempts.

The Guertler and Collyer antenna

A previous attempt at a lossy line model (Fourie, 1988) produced inaccurate results as soon as reactive loads were included in a structure. The new model should hence be tested using an antenna employing reactive loads. The Guertler and Collyer (1973) dipole employs a parallel inductor and resistor network. This antenna comprises two parallel wires per dipole arm (see Fig 3.6) but may be treated as a single dipole with equivalent radius of:

$$a_e = \sqrt{\left(\frac{2 \cdot 23.2}{0.001}\right)} = 0.09 \quad m$$

The performance of this simplified dipole was evaluated using the Lossy Line method as well as NEC2. The input impedance and efficiency results are compared in figs 4.19, 4.20 and 4.21. These results are also tabulated in Appendix M.

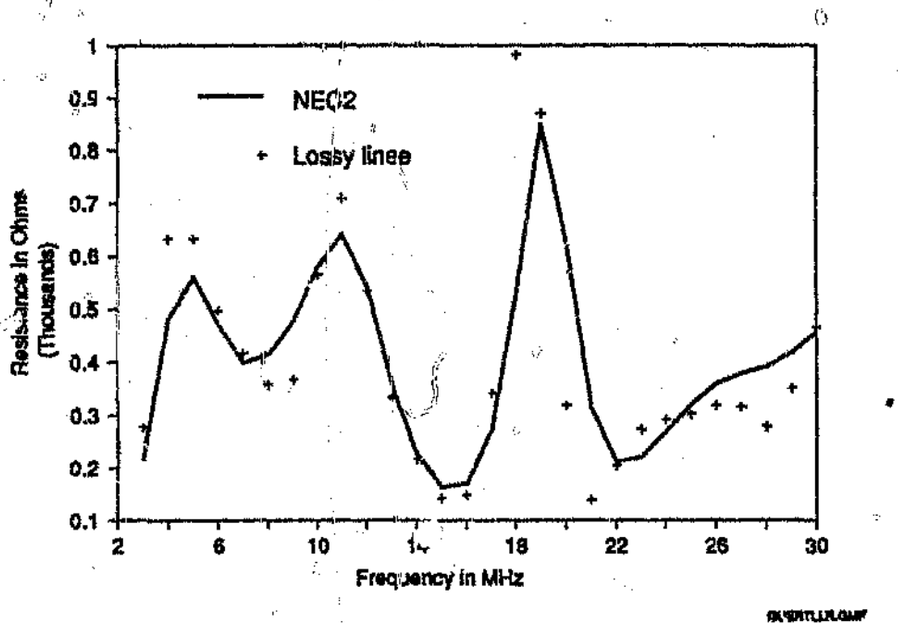


Fig 4.19 Lossy Line and NEC2 input resistance of the Guertler and Collyer antenna

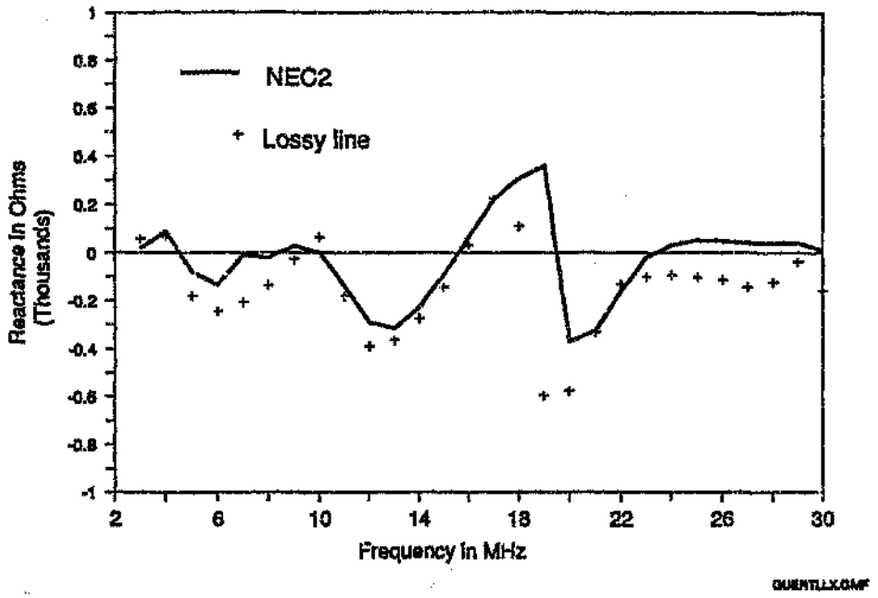


Fig 4.20 Lossy Line and NEC2 input reactance of the Guertler and Collyer antenna

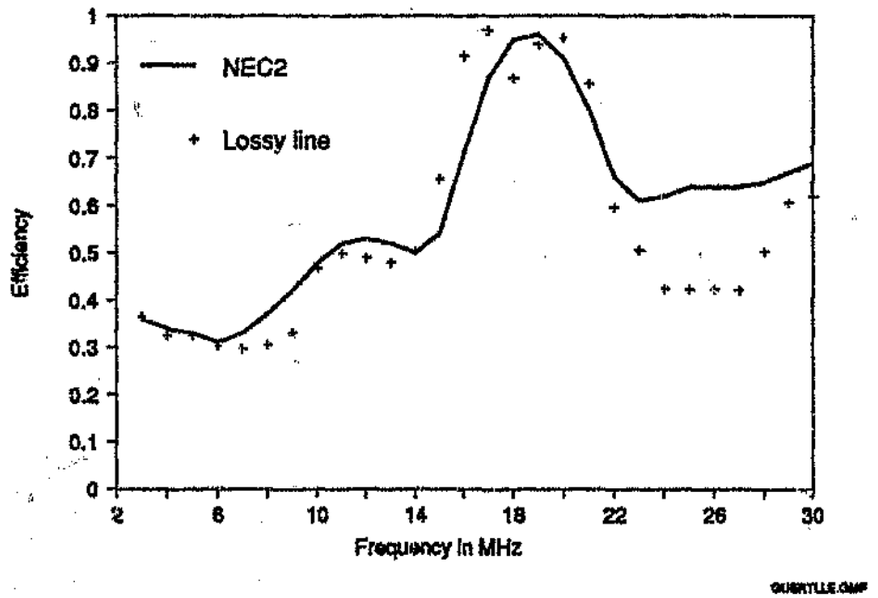


Fig 4.21 Lossy Line and NEC2 efficiency results for the Guertler and Collyer antenna

The average error in the input resistance when compared to NEC2 is 53Ω and the average error in the reactive part is 110Ω. The average error in the reactive part is numerically large but in this case slightly misleading because trends are faithfully reproduced regardless of the

occasional large difference in absolute values. The average difference in the efficiency results when compared to the NEC2 values is 7% which is quite acceptable The results confirm the suitability of the Lossy Line method for design purposes. NEC2 evaluation required approximately 3 hours on an 8 MHz IBM AT computer whereas the Lossy Line results were obtained in approximately two minutes on the same machine.

The multi-load dipole of Clark and Givati

A more complex geometry is the multi-load dipole in Fig 4.22 (Clark and Fourie, 1989). This antenna was designed by Clark and Givati (1987) using a more primitive form of the lossy line theory (Fourie, 1988). The antenna was analyzed as a single thick dipole in accordance with the thick wire emulation theory discussed before. For the wire spacing shown an equivalent radius of 0.13 m is appropriate.

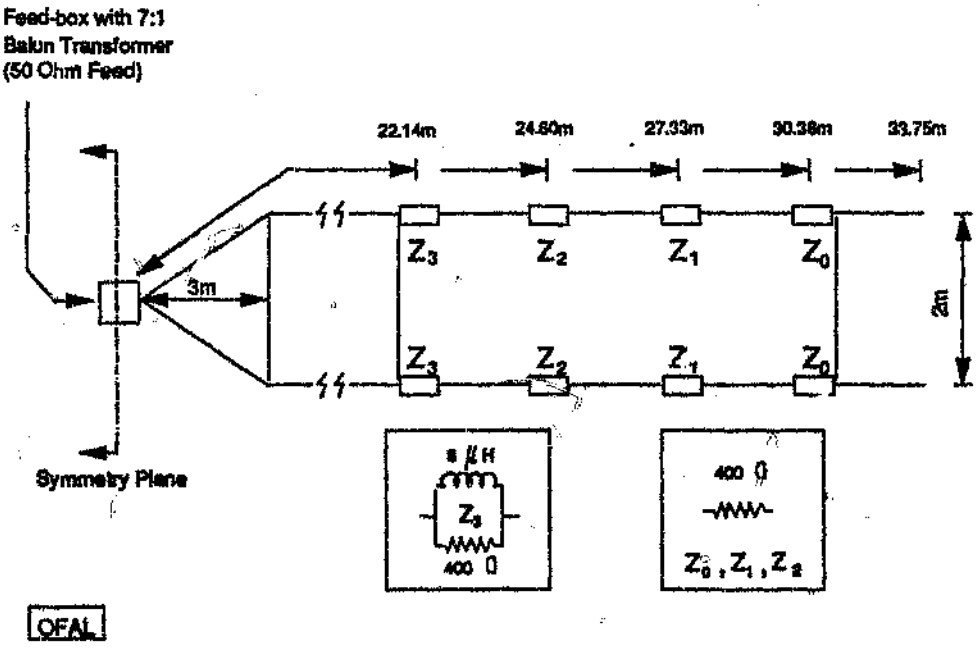


Fig 4.22 A multi-load antenna used to evaluate the Lossy Line method.

VSWR and efficiency results for this antenna is shown in figs 4.23 and 4.24 with tabulated results available in Appendix N.

cate the lossy line model to be successful for initial evaluation and design. Efficiency results give an indication of the accuracy of the current distribution obtained using the Lossy Line method.

4.3 Summary of Performance of Simple HF Broadband Antennas

Chapters 3 and 4 introduced an assortment of HF broadband antennas. Popular geometries were obtained from the literature and evaluated using NEC2 while others were designed during the course of this research. Comparing the performance of the various designs at this stage is useful to provide the reader with an overview of the current state of the art.

The antennas were categorized in terms of structural aspects in order to simplify comparison. The Treharne version was omitted due to its inadequate performance whereas the Harris antenna was similarly ignored since it is more complex than other versions. The Guertler and Collyer dipole is of structurally similar to the SLA and multi-load antenna. The antennas are compared in terms of NEC2 predicted VSWR, efficiency and PRR performance in figs 4.25, 4.26 and 4.27 respectively.

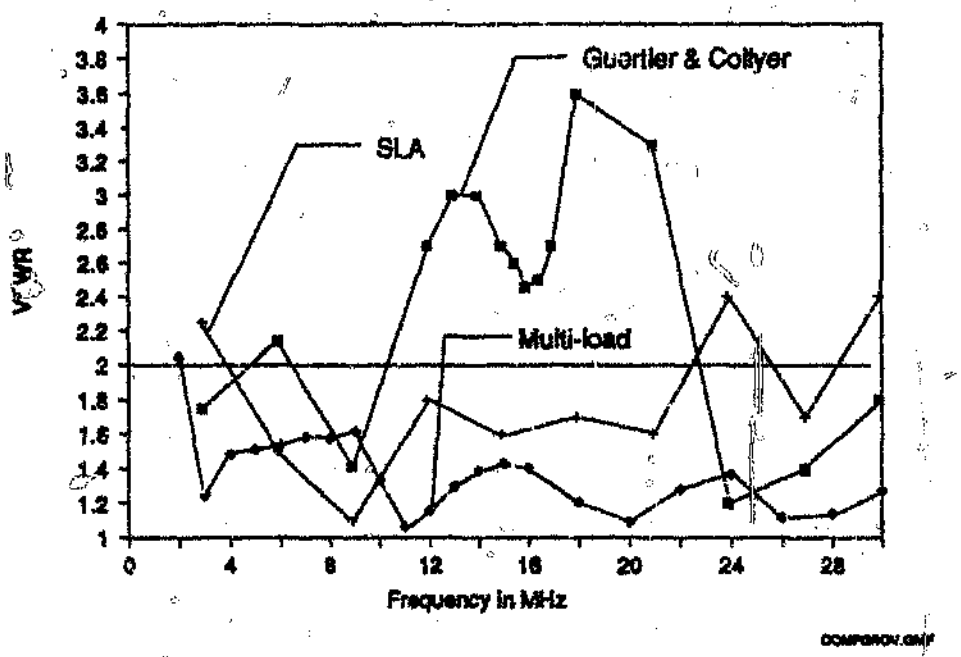


Fig 4.25 VSWR comparison between SLA and Guertler and Collyer designs

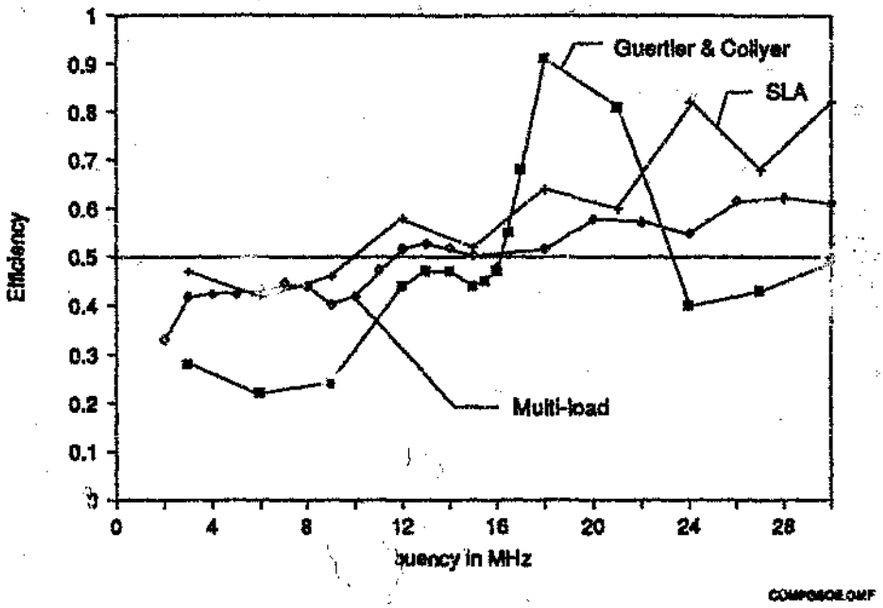


Fig 4.26 Efficiency comparison between SLA, Guertler and Collyer and multi-load designs

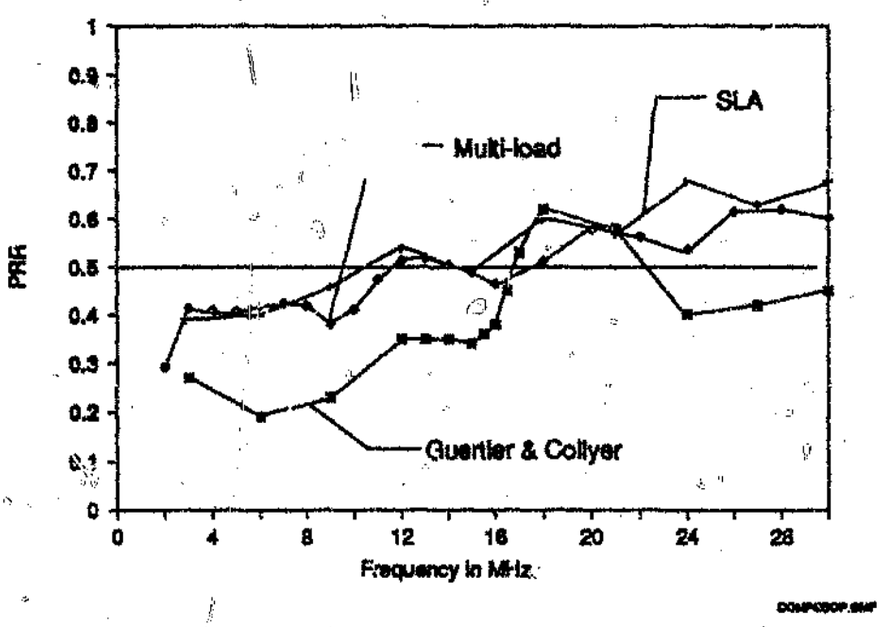


Fig 4.27 PRR comparison between SLA, Guertler and Collyer and multi-load designs

The SLA shows considerable improvement in terms of all parameters when compared to the Guertler and Collyer designs. The VSWR performance of the multi-load antenna which was designed using the Lossy Line method is slightly better than the SLA. The multi-load antenna employs 16 loads and are therefore more complex and expensive. The choice between these two antennas is arguable and the specific application will determine the final preference.

The DTD antenna is structurally very similar to the optimized resistively loaded fan dipole. These two antennas are therefore compared in the graphs below. (Figs 4.28, 4.29 and 4.30)

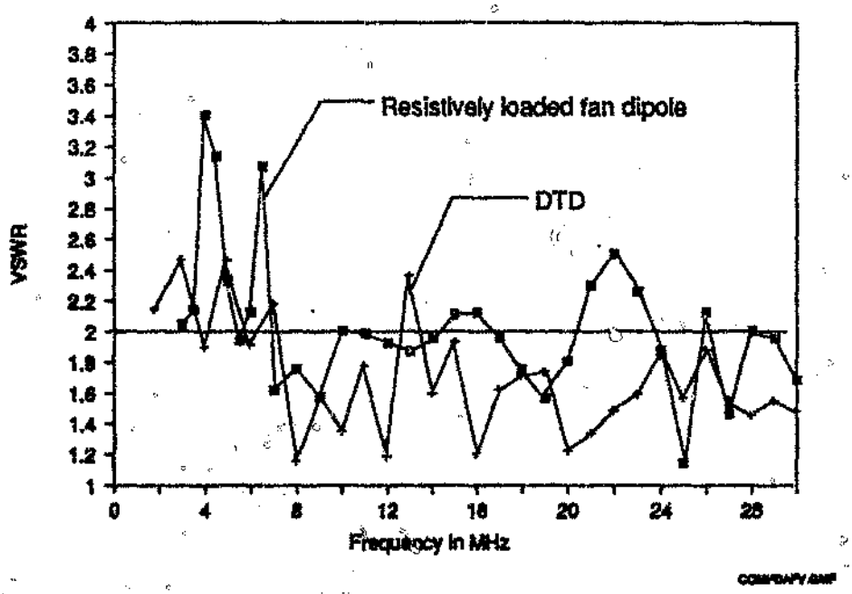


Fig 4.28 Comparison of VSWR performance of DTD and the optimized fan dipole versions

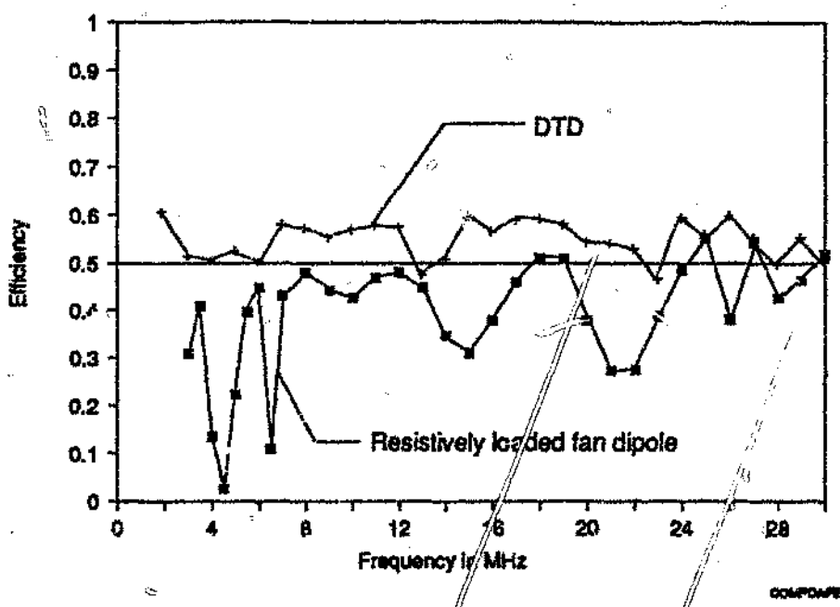


Fig 4.29 Comparison of efficiency performance of DTD and the optimized fan dipole versions

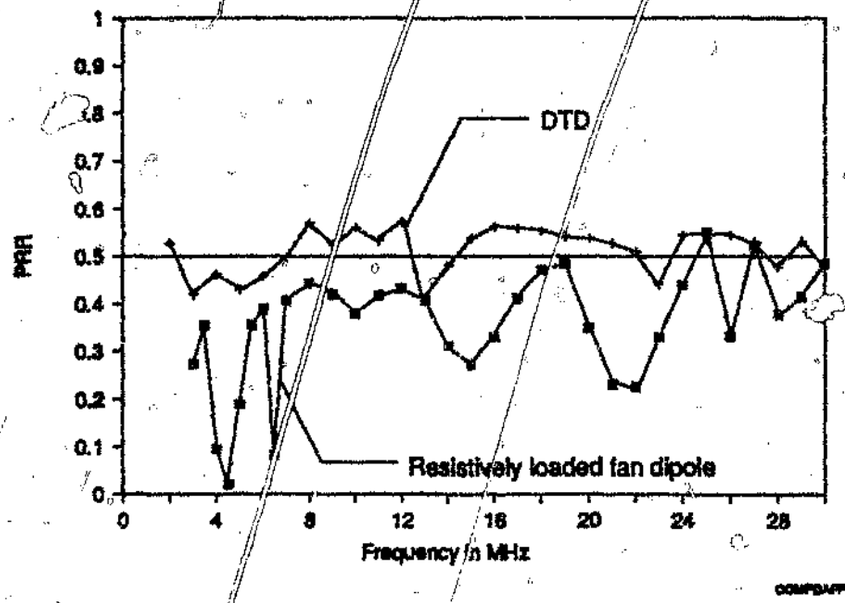


Fig 4.30 Comparison of PRR performance of DTD and the optimized fan dipole versions

The graphs indicate a vastly superior performance by the DTD antenna in comparison to the fan dipole. The DTD performance is remarkable, since it employs only two dipoles as compared to the three of the optimized fan dipole. The feed point circuitry of the DTD is more complex however. The performance of the DTD antenna compares favourably with the more complex SLA and multi-load versions.

4.4 Summary

A generalized novel geometry employing two different length dipoles connected by a transmission line was presented in the first section. Theory to evaluate versions of the DTD antenna was developed. The computation required to evaluate the antenna was greatly simplified by omitting the effect of mutual coupling. The equations were implemented on a IBM personal computer which produced results within seconds. Comparison between the DTD and NEC2 results showed that the mutual coupling between fan dipoles does not affect results markedly.

An exercise was undertaken to optimize a DTD antenna for 2 to 30 MHz operation. The optimized version was evaluated using NEC2 and measurements were also performed on a DTD prototype. The performance of the antenna is noteworthy when considering its structural simplicity. Efficiency performance was better than 45 percent while VSWR never exceeded 2.5:1.

The exploitation of the analogy between transmission lines and dipole antennas resulted in a suitable method for fast analysis of loaded dipole antennas. The computer time required to obtain a solution is proportional to the number of segments the wire is divided into. About 6 segments per wavelength of dipole produced converged results for the most cases. The speed compared favourably with method of moment codes where more segments per wavelength are normally required and the processor time increases exponentially with the number of segments. A NEC2 evaluation of a loaded antenna such as the ones considered here requires 5 hours to evaluate over the HF range whereas the Lossy line method accomplishes the same evaluation in about 1 minute on an IBM PC AT running at 10 MHz. Computer time is clearly significant for design and optimization purposes.

An important point to note regarding the run times stated above is that NEC2 is a general method of moments code. The matrix formed when simulating dipole antennas is Toeplitz and such a matrix enables more rapid analysis. The matrix fill time in this case is proportional to the dipole electrical length. The matrix inversion time is however proportional to the dipole length multiplied by the natural logarithm of the length. The calculation of elements in a method of moments program is considerably more complex than the operations performed

in the lossy line analysis. Such a specialized method of moments code would thus ultimately be slower than the lossy line method for electrically long antennas. The lossy line program has also not been numerically optimized and scope exist to increase the execution speed considerably.

The lossy line method exploits the mechanism of operation of dipole antennas which behave qualitatively like loaded transmission lines. The fact that a transmission line model is successfully employed conveys the important antenna mechanisms to the designer. These mechanisms may then be manipulated to achieve the desired performance as was demonstrated with the design of the multi-load antenna presented above.

A number of broadband geometries were considered in this thesis. An overview of the comparative performance of novel and known designs was hence provided in section 4.3 to gather all the loose ends. The SLA was shown to exhibit superior overall performance when compared to the Guertler and Collyer design. The more complex multi-load antenna of Clark and Givati (1987), developed using the lossy line method, showed slightly improved performance in comparison to the SLA.

The DTD antenna employs novel feed point circuitry. The performance of the DTD was much better than that of the optimized resistively loaded fan dipole. The DTD antenna performance is comparable to that of the multi-load and SLA antennas while these antennas are structurally more complex. It is ironic that the most mundane analytical technique produced the best overall antenna. The power of simple, fast analytical techniques for antenna design was amply demonstrated by the DTD design. The speed of the DTD method literally allowed an exhaustive optimization to be performed on a personal computer. The lossy line method - in itself orders of magnitude faster than the method of moments - was still too slow for this purpose.

The next chapter provides the radiation patterns of these antennas in terms of directive gain. Directive gain does not take the antenna PRR into account and pattern values must be multiplied by the PRR to obtain the full picture. The radiation patterns should hence be evaluated in conjunction with the PRR values in figs 4.27 and 4.20 when assessing the value of a specific antenna.

5 RADIATION PATTERNS OF SIMPLE BROADBAND HF ANTENNAS

The radiation patterns for the antennas analyzed in Chapters 3 and 4 are presented in this chapter. The typical radiation patterns which may be expected from simple dipole and loaded dipole antennas were discussed in Chapter 2. The problems associated with representing three dimensional patterns using different pattern cuts were illustrated. The conclusion was that the elevation plane radiation patterns of resonant and loaded dipoles are generally suitable for short distance communications (0 - 1000 km) while the azimuth patterns will provide omnidirectional coverage for frequencies below 10 MHz. Both the elevation and the azimuth patterns showed larger variations when frequency is increased to 20 and 30 MHz. This led to a decision to concentrate on the antenna input characteristics (impedance, VSWR and efficiency) rather than radiation patterns during the design phase for the following reasons:

- The elevation plane radiation patterns of simple wire antennas were shown to be mainly affected by the mounting height above ground
- The azimuth radiation patterns of simple dipole antennas in an inverted-v configuration were shown to be almost omnidirectional at low frequencies (2 - 10 MHz). At higher frequencies dipole antennas will do not exhibit any specific directional characteristics but variations in azimuth can be observed.
- The simple nature of these antennas in general produce radiation patterns which are a suitable compromise for short distance HF communications. More suitable radiation patterns across the frequency band require an increase in antenna complexity which conflicts with the intended purpose of these antennas.

5.1 Radiation pattern generation, evaluation and presentation

The NEC2 computed patterns obtained from the various antennas considered previously are presented in this chapter. The aim of this chapter is not to perform detailed analysis of the performance of the antennas in an HF environment. The patterns are rather presented and evaluated in a qualitative fashion in terms of their likely performance in an HF communications application. An assessment of their radiation pattern suitability can be made based on the following guide lines:

- The elevation plane patterns should cover take-off angles in the r... 30° to 90° to obtain communication over the intended 0 - 1000 km range (Braun, 1982).
- The azimuth radiation pattern needs to be omnidirectional if full area coverage is to be achieved. Ideally such omnidirectional characteristics need to be maintained in the azimuth plane at all elevation angles.

Compliance to these guide lines is an ideal and exceptions at certain frequencies will generally not render the antennas useless but will reduce the probability of communication under some conditions.

All antennas were evaluated with the feed point 12 m above an average ground ($\sigma = 0.01$ mS ; $\varepsilon_r = 10$) using the NEC2 Fresnel reflection approximation. The validity of this approximation for antenna pattern was confirmed in Chapter 2. Antenna wires sloped down to ground with the wire ends 2 m above the ground plane unless stated otherwise for any particular antenna. Antenna patterns are shown at 5 representative frequencies in the HF band. Three pattern cuts were obtained at each frequency. These were:

- One elevation cut perpendicular to the antenna axis (referred to as : "Perpendicular elevation plane").
- Another elevation cut along the antenna axis (referred to as : "Longitudinal elevation plane")
- An azimuth plane pattern at constant elevation angle, $\Theta = 60°$ (take-off angle of 30°)

The antennas were in all cases oriented with their major axis along the y-axis direction. The perpendicular elevation plane pattern is hence done with constant $\phi = 0°$ whereas the longitudinal elevation plane patterns are performed for $\phi = 90°$.

All radiation patterns are provided in terms of directive gain. The reduction in radiated power due to antenna efficiency is intentionally not reflected in the radiation patterns to allow comparison purely on directive properties of various antennas. The reduction in radiated power due to ohmic loss in the antennas concerned was presented in detail in Chapters 3 and 4.

5.2 Radiation patterns of all the antennas evaluated.

5.2.1 Treharne antenna

The Treharne antenna (see fig 3.2 for antenna dimensions) was evaluated on a 12 m mast with the wires sloping down to 2 m above the ground plane. The three pattern cuts are presented in figs 5.1 to 5.3 for the low frequencies and figs 5.4 to 5.6 for the higher frequencies.

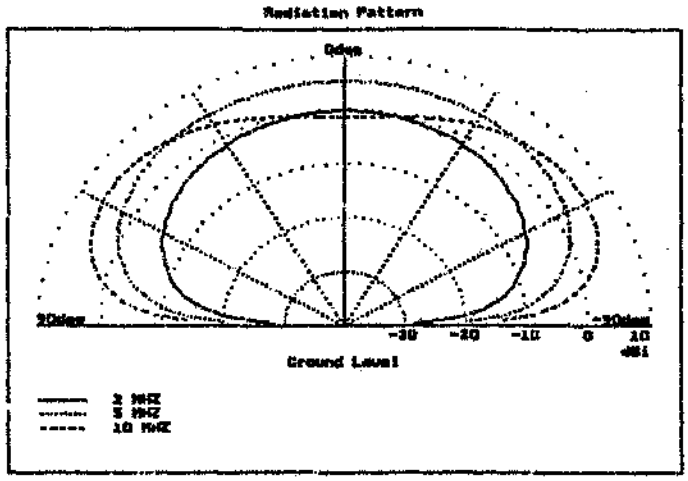


Fig 5.1 Treharne antenna : Elevation plane pattern cut perpendicular to antenna axis. Directive gain for 2 MHz, 5 MHz and 10 MHz.

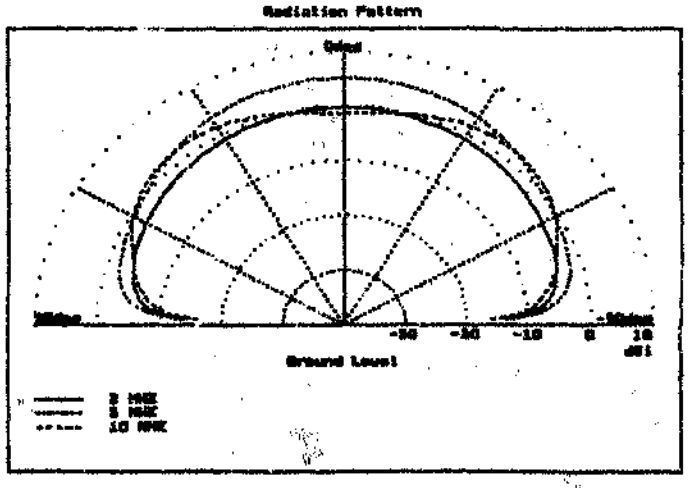


Fig 5.2 Treharne antenna : Elevation plane pattern cut along the antenna axis (longitudinal cut). Directive gain for 2 MHz, 5 MHz and 10 MHz.

Take off angles of 90° down to 30° are typically required for short range communications (0 - 1000 km) as discussed in Chapter 2. The low frequency perpendicular elevation plane patterns (fig 5.1 and 5.2) produce a single main lobe with nulls towards the horizon. The complete elevation angle coverage requirement is not met by all the elevation plane patterns at all frequencies. The elevation plane characteristics are however generally suited to the intended communications range.

The low frequency azimuth plane patterns obtained at a constant take-off angle of 30° (fig 5.3) indicate general omnidirectional azimuth coverage as required.

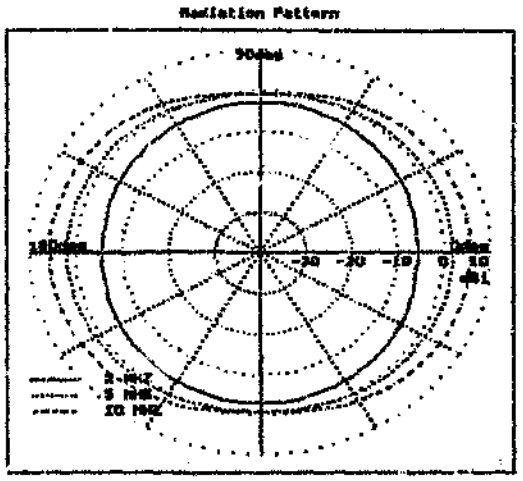


Fig 5.3 Treharne antenna : Azimuth pattern cut for 30 degree take-off angles. Directive gain for 2 MHz, 5 MHz and 10 MHz.

The high frequency elevation plane patterns exhibit more lobes than in the low frequency case for both perpendicular pattern cuts (figs 5.4 and 5.5). This characteristic is unavoidable as shown in Chapter 2 and is due to the interaction between the antenna and the ground plane. Reducing the antenna height will reduce the lobes shown here but antenna impedance bandwidth will suffer as result of the excessive coupling to the ground image. The main beam directions are however still suitable for most short range applications.

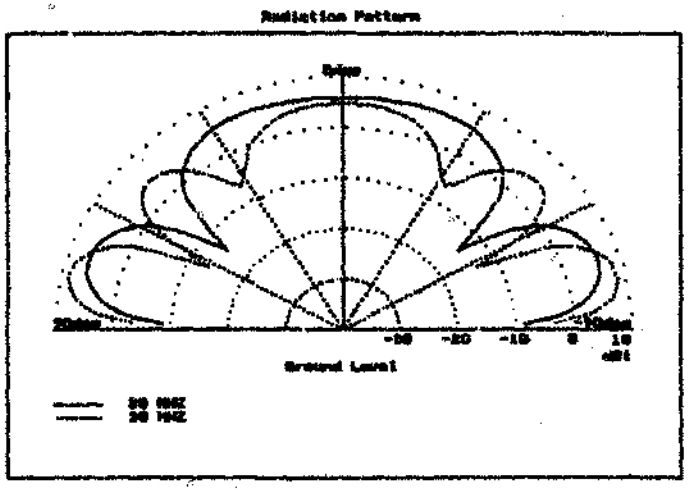


Fig 5.4 Treharne antenna : Elevation plane pattern cut perpendicular to antenna axis. Directive gain for 20 MHz and 30 MHz.

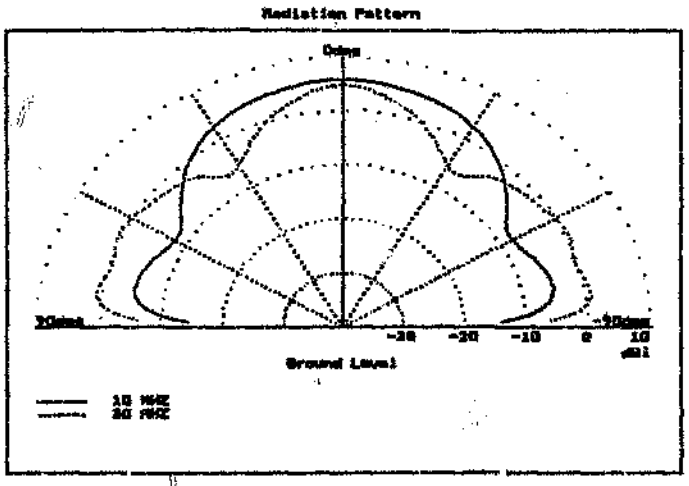


Fig 5.5 Treharne antenna : Elevation plane pattern cut along the antenna axis. Directive gain for 20 MHz and 30 MHz.

The high frequency azimuth plane radiation pattern also indicate more variation (up to 10 dB) as would be expected. These variations differ for azimuth plots at other take-off angles as is suggested by the two perpendicular elevation plane patterns presented. Some azimuth directions will hence be favoured when compared to others at the higher frequencies.

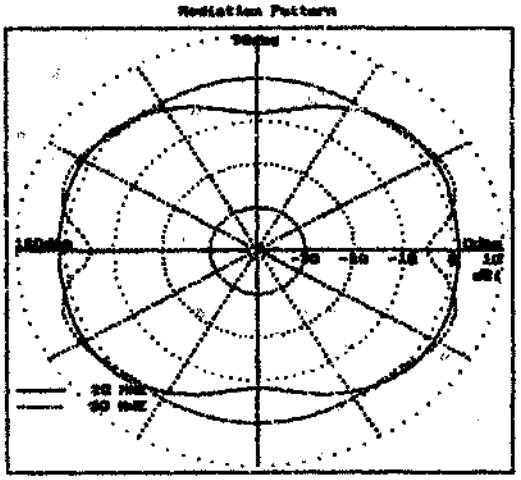


Fig 5.6 Treharne antenna : Azimuth pattern cut for 30 degree take-off angles. Directive gain for 20 MHz and 30 MHz.

In general it is evident that this antenna produce acceptable radiation pattern characteristics at low frequencies (2 - 10 MHz) with more pattern variation at higher frequencies (20 and

30 MHz). The higher frequency range is of less importance in short range HF communications and the range of 2.5 MHz to 15 MHz was shown in Chapter 2 to be sufficient under most conditions.

5.2.2 Guertler and Harris antennas

The Guertler and Harris antennas (see figs 3.6 and 3.10 for dimensions) are similar except for the different wire emulation used in the Harris antenna which does not affect radiation pattern. The antenna was modelled on a 12 m mast with the wires sloping down to 2 m above the ground plane. The three pattern cuts are presented in figs 5.7 to 5.9 for the low frequencies and in figs 5.10 to 5.12 for the higher frequencies.

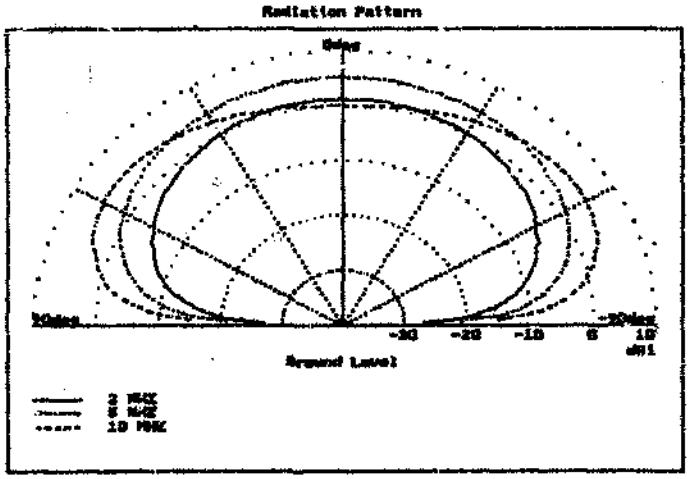


Fig 5.7 Guertler antenna : Elevation plane pattern cut perpendicular to antenna axis. Directive gain for 2 MHz, 5 MHz and 10 MHz.

The low frequency elevation plane patterns (figs 5.7 and 5.8) are once again suitable for short range HF communications since good illumination of take-off angles between 30 ° and 90° is obtained. The low frequency azimuth plane radiation patterns are approximately omnidirectional (fig 5.9).

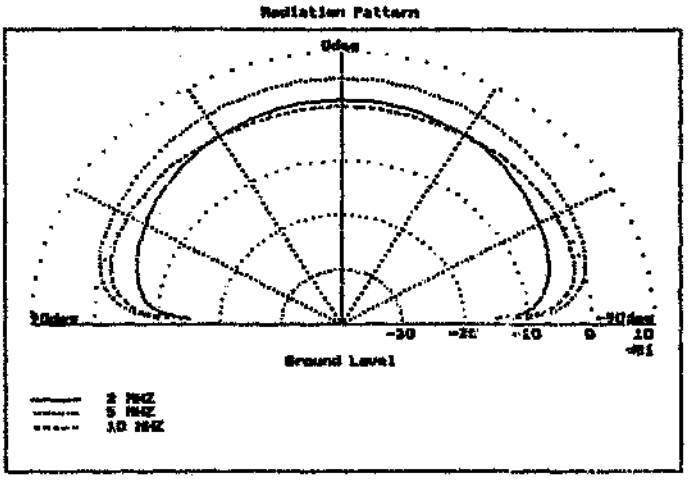


Fig 5.8 Guertler antenna : Elevation plane pattern cut along the antenna axis (longitudinal cut). Directive gain for 2 MHz, 5 MHz and 10 MHz.

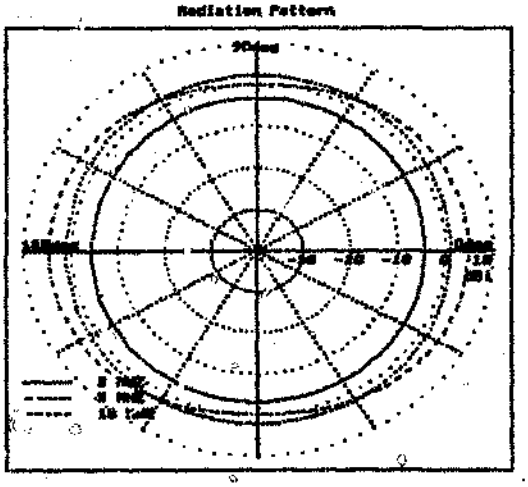


Fig 5.9 Guertler antenna : Azimuth pattern cut for 30 degree take-off angles. Directive gain for 2 MHz, 5 MHz and 10 MHz.

The high frequency elevation plane patterns illuminate almost the entire hemisphere with single nulls in all the patterns (fig 5.10 and 5.11). These nulls are due to interaction between the antenna and the ground plane and can generally not be avoided except by lowering the antenna with other detrimental consequences as discussed before. The high frequency azimuth radiation patterns (fig 5.12) are not directional but show larger variations in radiated power compared to the lower frequency case. All azimuth radiation patterns are displayed at take-off angles of 30° which coincides with a null in the perpendicular elevation plane pattern. This produces quite a sharp null at $\phi = 0°$ and 180° in the high frequency azimuth

pattern. This coincidence exaggerates the variation in the azimuth radiation pattern at some frequencies and once again illustrates the problems associated with representing the patterns of these antennas using selected two dimensional cuts.

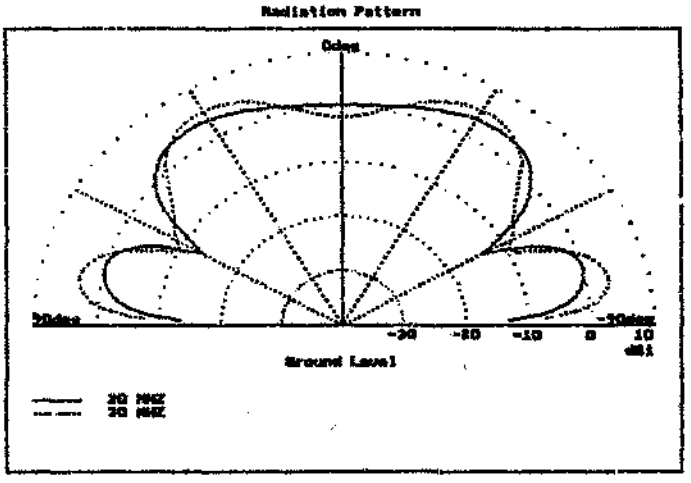


Fig 5.10 Guertler antenna : Elevation plane pattern cut perpendicular to antenna axis. Directive gain for 20 MHz and 30 MHz.

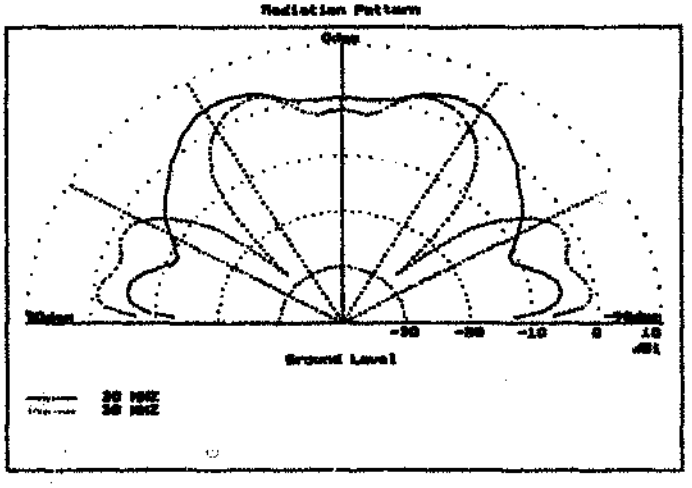


Fig 5.11 Guertler antenna : Elevation plane pattern cut along the antenna axis. Directive gain for 20 MHz and 30 MHz.

The antenna is hence quite suited for tactical short range HF communications at frequencies up to 10 MHz. The behaviour at 20 and 30 MHz is these frequencies are of little importance as was shown before (see 2.2).

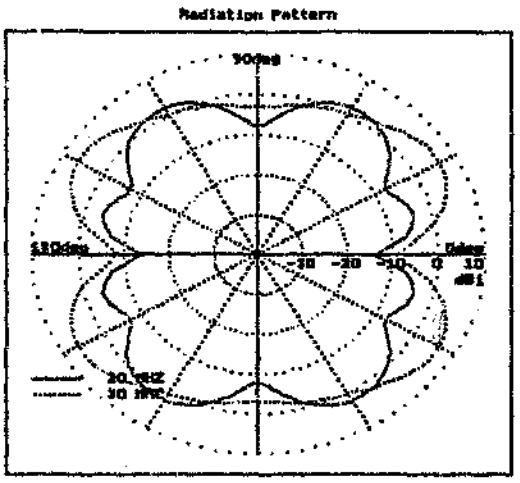


Fig 5.12 Guertler antenna : Azimuth pattern cut for 30 degree take-off angles. Directive gain for 20 MHz and 30 MHz.

5.2.3 Fan dipole antenna

The fan dipole (see fig 3.14 for dimensions) was modelled with all the wire co-planar on a 12 m mast. The wires slope to ground with the wire ends of the two longer dipoles at 2 m height. The shortest dipole slopes to ground with the wire end reaching 5 m height due to practical constraints. The low frequency elevation plane patterns and azimuth plane pattern are shown in figs 5.13 to 5.15. The high frequency patterns are similarly shown in figs 5.16 to 5.18

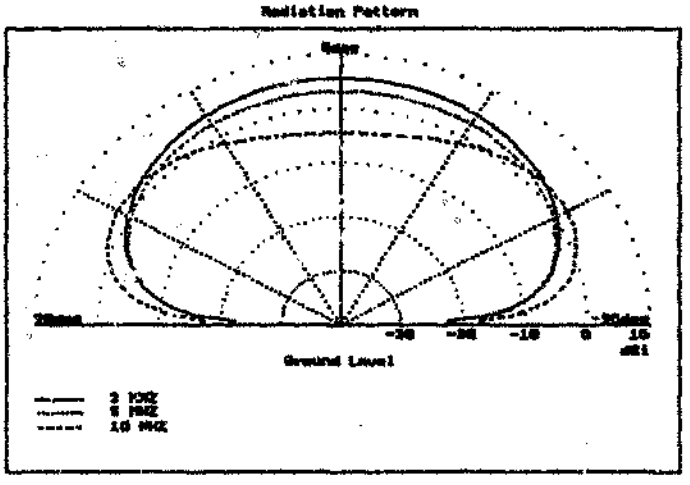


Fig 5.13 Fan dipole : Elevation plane pattern cut perpendicular to antenna axis. Directive gain for 3 MHz, 5 MHz and 10 MHz.

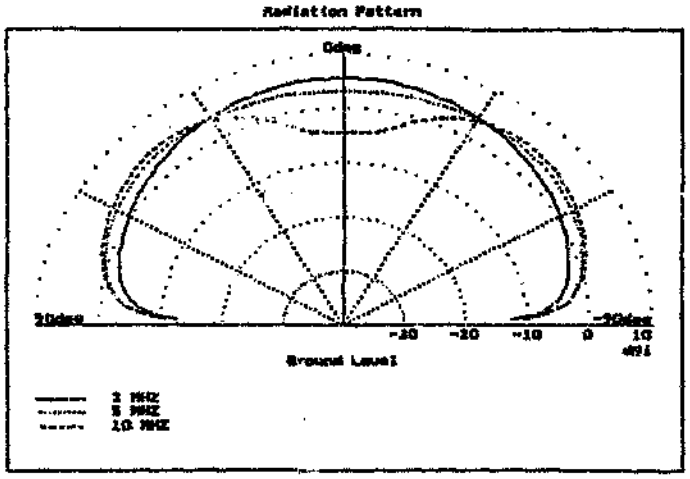


Fig 5.14 Fan dipole : Elevation plane pattern cut along the antenna axis (longitudinal cut). Directive gain for 3 MHz, 5 MHz and 10 MHz.

The low frequency elevation plane patterns (fig 5.13 and 5.14) once again exhibit characteristics suitable for the intended HF communications application. The only possible problem is a reduction in radiated power towards the zenith at 10 MHz which will adversely affect performance for very short ranges. The low frequency azimuth plane performance (fig 5.15) is omnidirectional and ideally suited for communication in all directions as required.

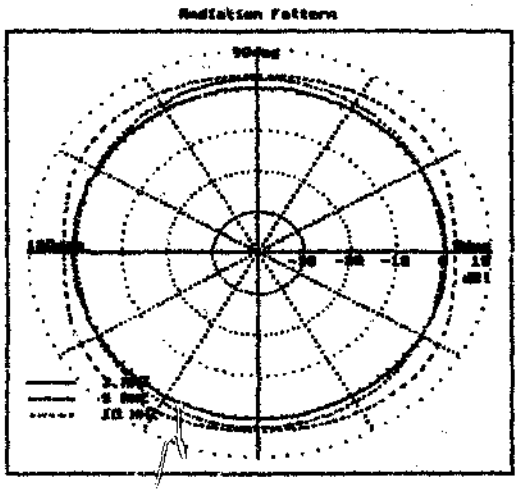


Fig 5.15 Fan dipole : Azimuth pattern cut for 30 degree take-off angles. Directive gain for 2 MHz, 5 MHz and 10 MHz.

The high frequency elevation plane patterns (figs 5.16 and 5.17) show very sharp nulls for take-off angles between 30° and 50 ° which may present problems when the required range

dictates the use of such take of angles. The high frequency azimuth plane pattern (fig 5.18) once again show some variations but the study presented in 2.2 indicated these to be unimportant under m' ospheric conditions.

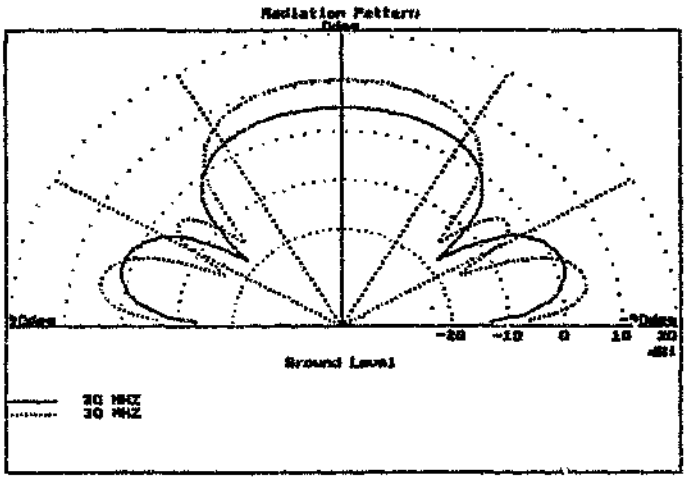


Fig 5.16 Fan dipole : Elevation plane pattern cut perpendicular to antenna axis. Directive gain for 20 MHz and 30 MHz.

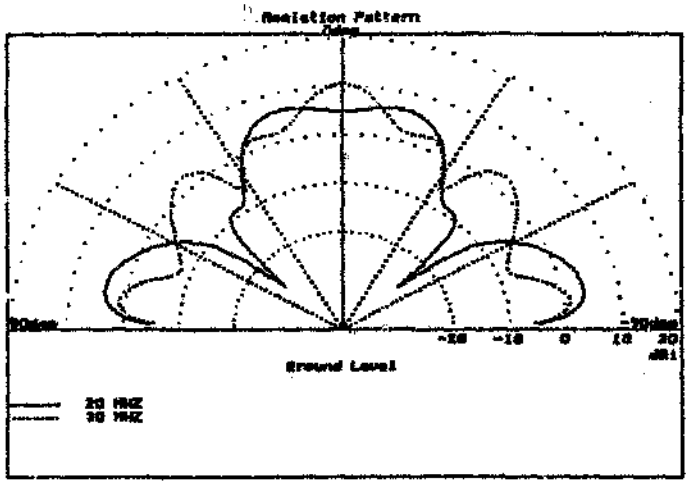


Fig 5.17 Fan dipole : Elevation plane pattern cut along the antenna axis. Directive gain for 20 MHz and 30 MHz.

The relative increase in elevation pattern variation when compared to the travelling wave antennas considered before are due to two factors:

- The antenna consist of resonant dipoles which support standing waves. This generally produce more pattern variations when compared with antennas carrying mainly travelling waves.

- The antenna phase centre depends on which dipole is responsible for most of the radiation at a specific frequency resulting in more uncertainty on the effect of the ground on this antenna's performance.

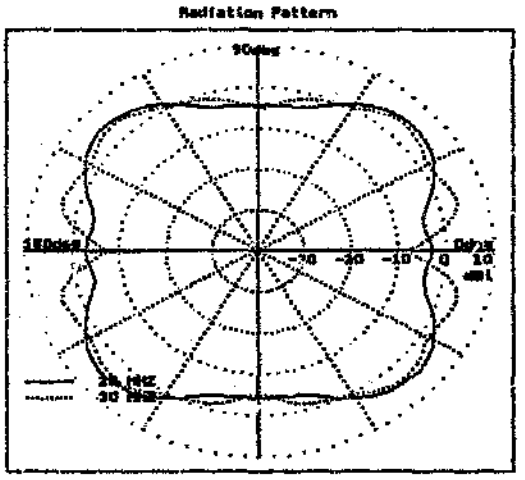


Fig 5.18 Fan dipole : Azimuth pattern cut for 30 degree take-off angles. Directive gain for 20 MHz and 30 MHz.

5.2.4 Staggered load antenna (SLA)

The SLA was modelled with the two wires parallel (see fig 3.20) with the centre point on a 12 m mast and the wires sloping to a final height of 2 m from the ground. The low frequency elevation plane and azimuth plane patterns are shown in figs 5.19 to 5.21 with the high frequency patterns shown in figs 5.22 to 5.24.

The low frequency elevation pattern plots (figs 5.19 and 5.20) indicate that the antenna generally provides suitable illumination for the required application. The only exception is a slight reduction in zenith illumination at 10 MHz in both cases. The low frequency azimuth radiation patterns (fig 5.21) are omnidirectional as expected.

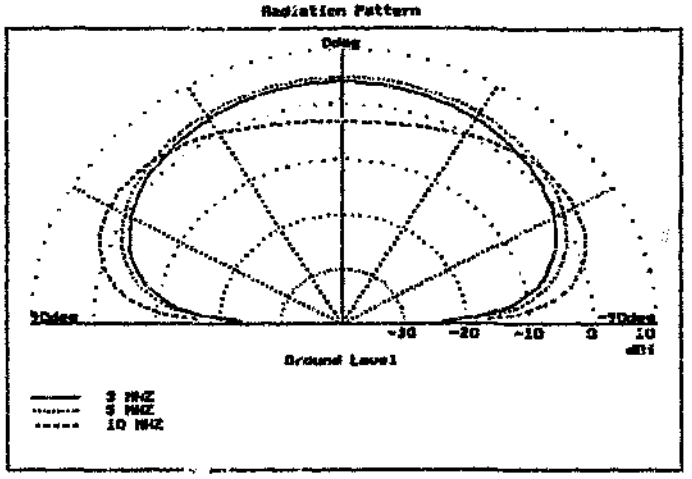


Fig 5.19 Staggered loads antenna (SLA) : Elevation plane pattern cut perpendicular to antenna axis. Directive gain for lowest frequency, 5 MHz and 10 MHz.

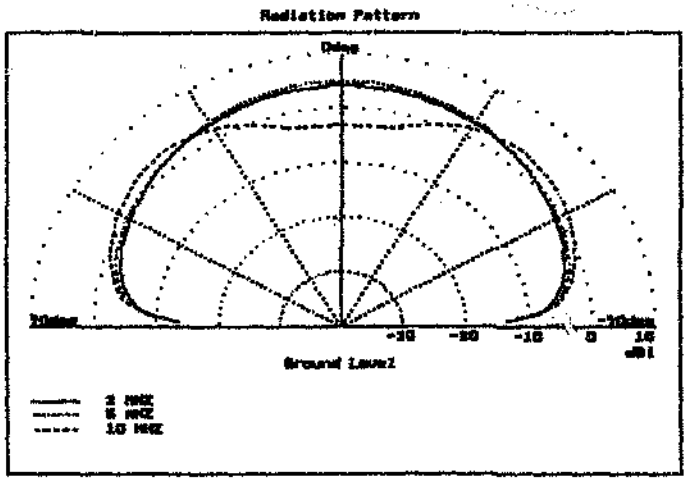


Fig 5.20 Staggered loads antenna (SLA) : Elevation plane pattern cut along the antenna axis (longitudinal cut). Directive gain for lowest frequency, 5 MHz and 10 MHz.

The high frequency perpendicular elevation plane pattern (fig 5.22) is ideally suited for the required ranges at 20 MHz whereas the 30 MHz pattern produces a general reduction in power for lower take-off angles. Operation at frequencies approa[illegible]ng 30 MHz is unlikely for short range communications as shown before (section 2.2).

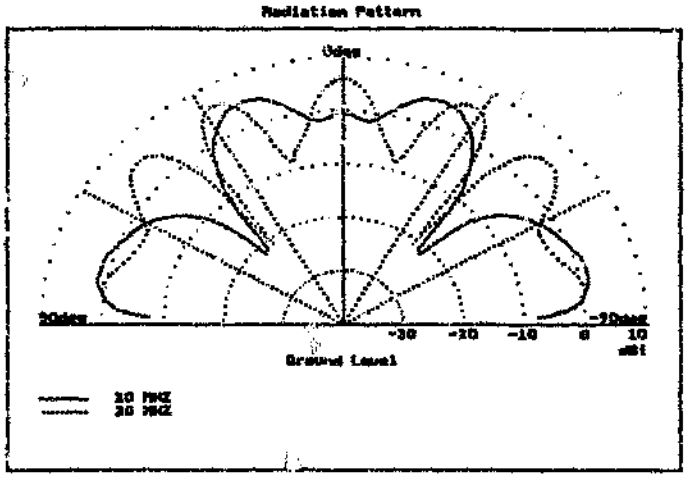


Fig 5.23 Staggered loads antenna (SLA) : Elevation plane pattern cut along the antenna axis. Directive gain for 20 MHz and 30 MHz.

This antenna would be a suitable compromise between structural simplicity and electrical performance for short range tactical HF communications. The pattern variations associated with the high frequency radiation patterns are similar to those of the other antennas studied, but these frequencies are seldom used (see section 2.2). The improved efficiency of this antenna when compared to previous ones examined should be kept in mind, since this is not reflected in the directive gain of the antenna presented here and indicates the overall improvement in performance.

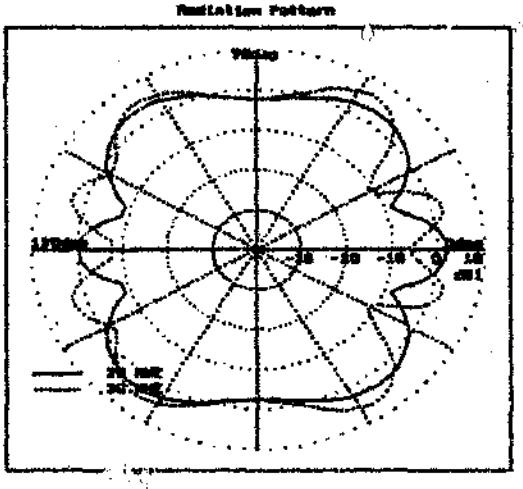


Fig 5.24 Staggered loads antenna (SLA) : Azimuth pattern cut for 30 degree take-off angles. Directive gain for 20 MHz and 30 MHz.

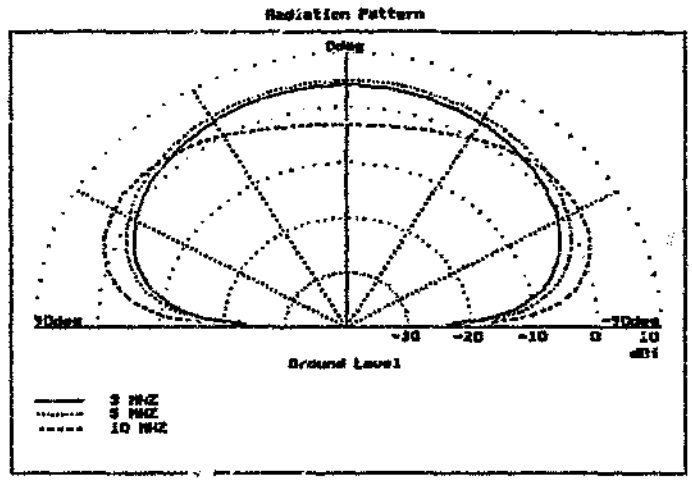


Fig 5.19 Staggered loads antenna (SLA) : Elevation plane pattern cut perpendicular to antenna axis. Directive gain for lowest frequency, 5 MHz and 10 MHz.

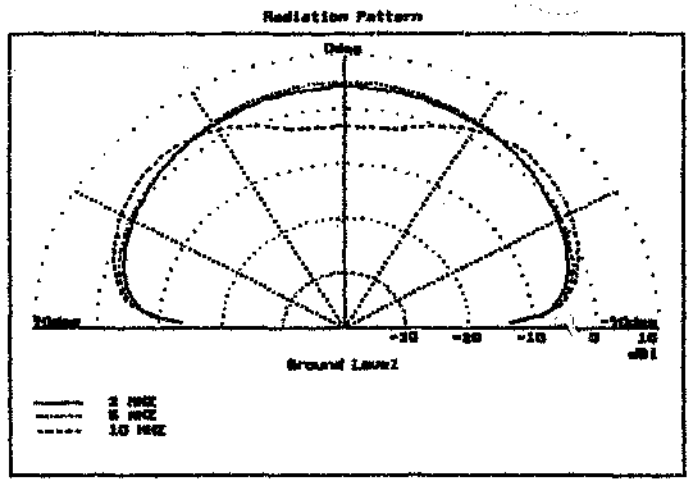


Fig 5.20 Staggered loads antenna (SLA) : Elevation plane pattern cut along the antenna axis (longitudinal cut). Directive gain for lowest frequency, 5 MHz and 10 MHz.

The high frequency perpendicular elevation plane pattern (fig 5.22) is ideally suited for the required ranges at 20 MHz whereas the 30 MHz pattern produces a general reduction in power for lower take-off angles. Operation at frequencies approa[illegible]ng 30 MHz is unlikely for short range communications as shown before (section 2.2).

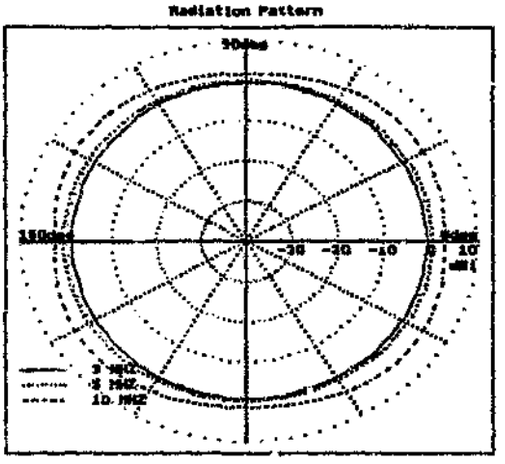


Fig 5.21 Staggered loads antenna (SLA) : Azimuth pattern cut for 30 degree take-off angles. Directive gain for 2 MHz, 5 MHz and 10 MHz.

Note the slight asymmetry in the 30 MHz perpendicular elevation plane pattern shown in fig 5.22 due to the unsymmetrical loading incorporated in the antenna. This anomaly is only evident at the highest frequency and even then is not very significant. The longitudinal elevation plane pattern (fig 5.23) produce strong variations at 20 and 30 MHz. The high frequency azimuth plane patterns (fig 5.24) are omnidirectional with more variations when compared to the lower frequency patterns. The antenna should provide reasonable coverage in most directions even at the relatively unimportant higher frequencies.

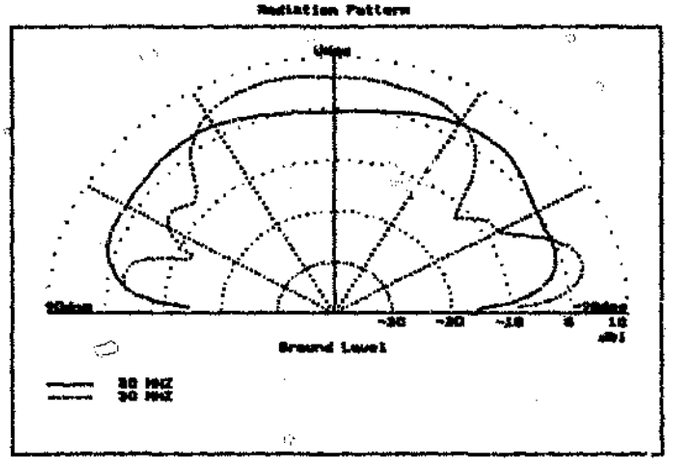


Fig 5.22 Staggered loads antenna (SLA) : Elevation plane pattern cut perpendicular to antenna axis. Directive gain for 20 MHz and 30 MHz.

5.2.5 Multi-load antenna

The dimensions of the multi-load antenna were given in fig 4.22. This antenna was modelled on a 12 m mast with the wires sloping to a final height of 2 m as in the other cases. The low frequency elevation and azimuth plane patterns of this antenna are shown in figs 5.25 to 5.27 while the high frequency patterns are shown in figs 5.28 to 5.30.

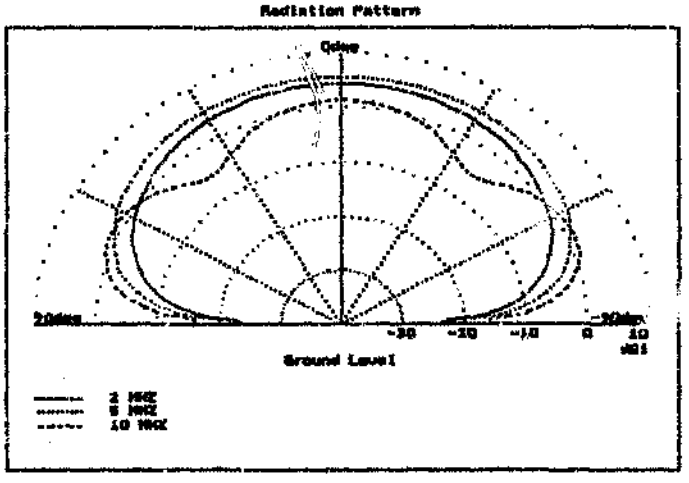


Fig 5.25 Multi-load antenna : Elevation plane pattern cut perpendicular to antenna axis. Directive gain for 2 MHz, 5 MHz and 10 MHz.

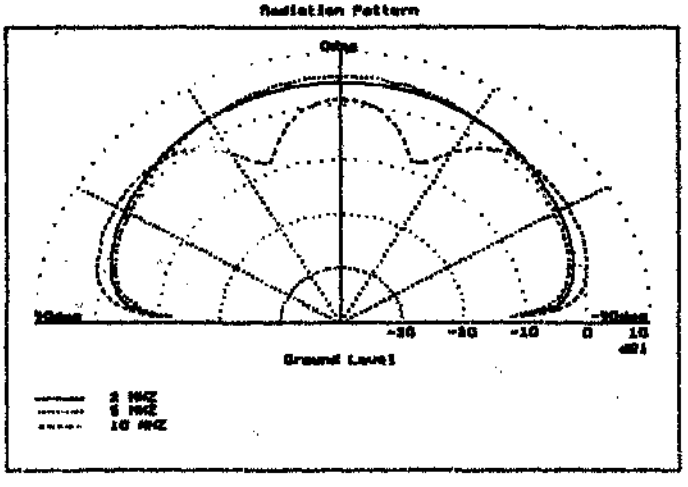


Fig 5.26 Multi-load antenna : Elevation plane pattern cut along the antenna axis (longitudinal cut). Directive gain for 2 MHz, 5 MHz and 10 MHz.

The low frequency elevation plane patterns (figs 5.25 and 5.26) indicate suitable illumination for 2 and 5 MHz with a reduction in power for take-off angles around 60°. This reduction

will affect the performance of the antenna over short ranges in this frequency range when using single F2-layer hop propagation. The low frequency azimuth plane radiation patterns (fig 5.27) are omnidirectional and hence quite suitable.

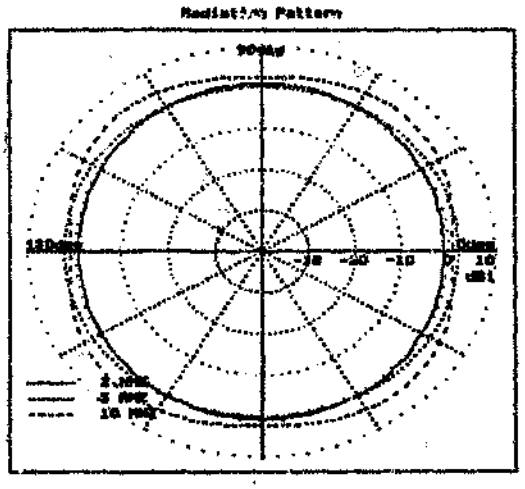


Fig 5.27 Multi-load antenna : Azimuth pattern cut for 30 degree take-off angles. Directive gain for 2 MHz, 5 MHz and 10 MHz.

The high frequency elevation plane patterns (figs 5.28 and 5.29) exhibit large variations, especially at 30 MHz. This undesirable characteristic does not often affect short range communications, since the upper frequencies are almost never required as stated in 2.2. The high frequency azimuth plane patterns (fig 5.30) produce radiation in all directions with some variation - the worsts case being the approximately 12 dB reduction at 20 MHz perpendicular to the antenna axis.

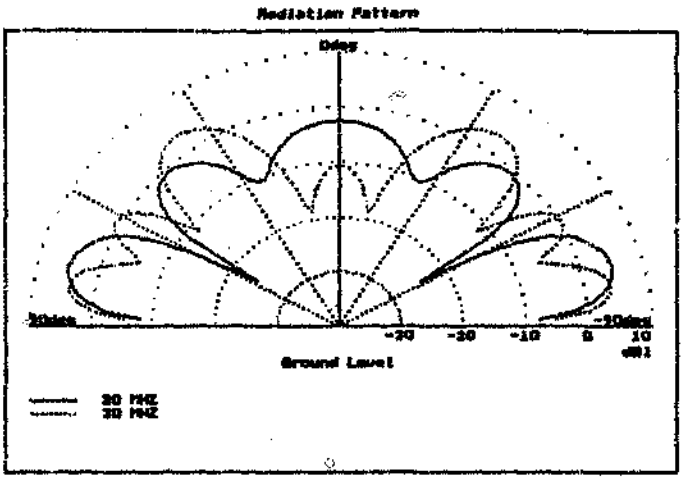


Fig 5.28 Multi-load antenna : Elevation plane pattern cut perpendicular to antenna axis. Directive gain for 20 MHz and 30 MHz.

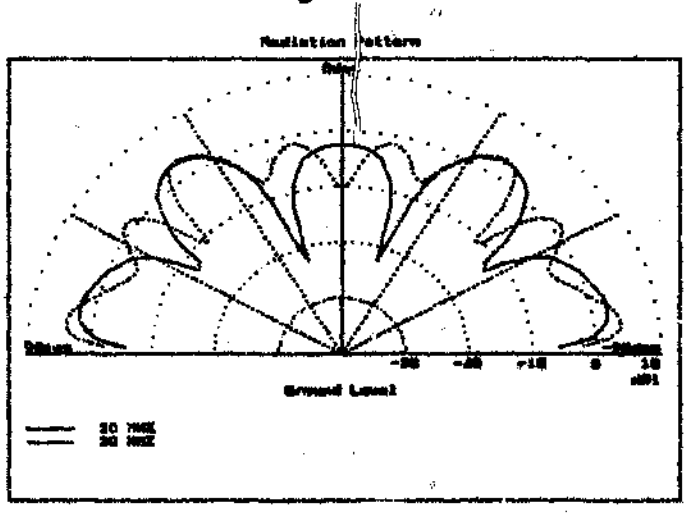


Fig 5.29 Multi-load antenna : Elevation plane pattern cut along the antenna axis. Directive gain for 20 MHz and 30 MHz

The performance of this antenna would again be similar to the ones previously considered in terms of its directive characteristics. The excellent efficiency and VSWR characteristics of this antenna, which are not taken into account in the directivity, should however be born in mind (see Chap 4).

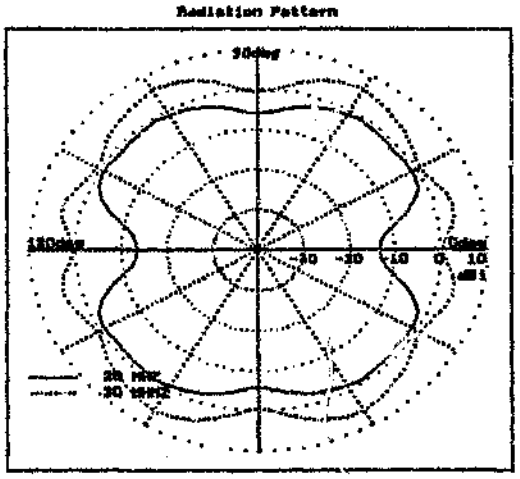


Fig 5.30 Multi-load antenna : Azimuth pattern cut for 30 degree take-off angles. Directive gain for 20 MHz and 30 MHz.

5.2.6 Dipole-Transmission line-Dipole (DTD) antenna.

The DTD antenna (see fig 4.1) was mounted on a 12 m centre mast with the two dipoles perpendicular to each other. The dipoles sloped to a final height of 2 m above ground as in previous cases. The longest dipole was aligned with the y-axis which implies that the perpendicular and longitudinal elevation plane pattern cuts are referenced to the longer dipole. The low frequency radiation patterns of this antenna are shown in figs 5.31 to 5.33, while the high frequency patterns are shown in figs 5.34 to 5.36.

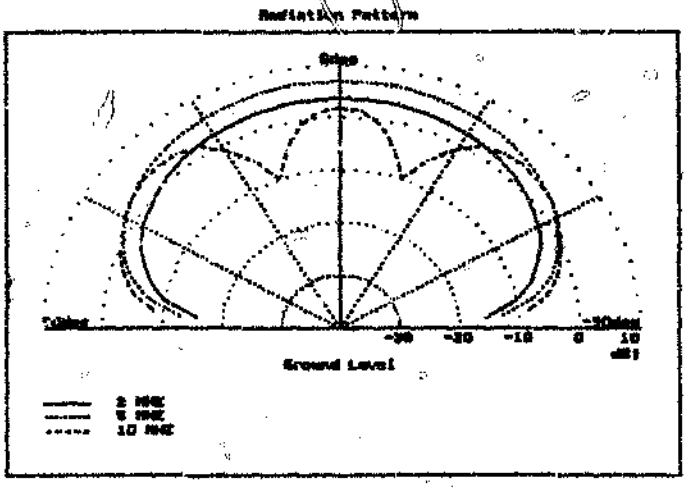


Fig 5.31 DTD antenna : Elevation plane pattern cut perpendicular to longest dipole (74 m) of crossed configuration. Directive gain for 2 MHz, 5 MHz and 10 MHz.

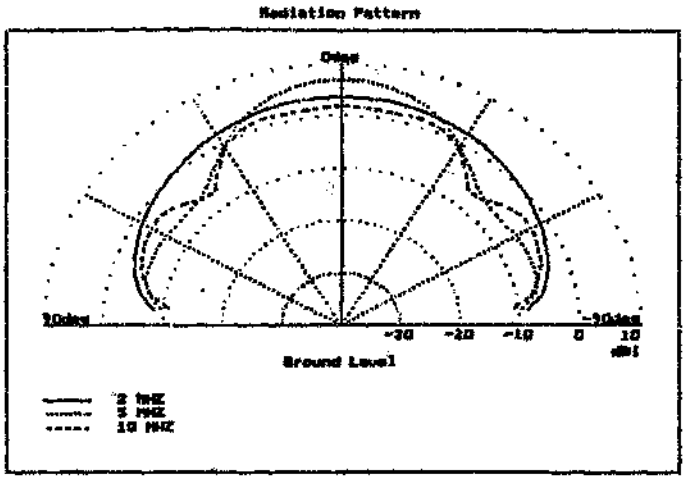


Fig 5.32 DTD antenna : Elevation plane pattern cut along longest dipole (74 m) of crossed configuration (longitudinal cut). Directive gain for 2 MHz, 5 MHz and 10 MHz.

The low frequency elevation plane patterns (figs 5.31 and 5.32) are similar to that of the other antennas considered except for the fairly pronounced lobes in the 10 MHz case. The reduction in power radiated at take-off angles of 70° in directions perpendicular to the antenna (fig 5.31) may degrade communications for ranges where this direction and take-off angle are required. The variations in the longitudinal elevation plane pattern (fig 5.32) are less severe and should not cause major problems. These elevation plane patterns differ from the ones considered previously in that the dipoles themselves are perpendicular to each other and the radiation pattern is influenced by the dominant dipole at any particular frequency.

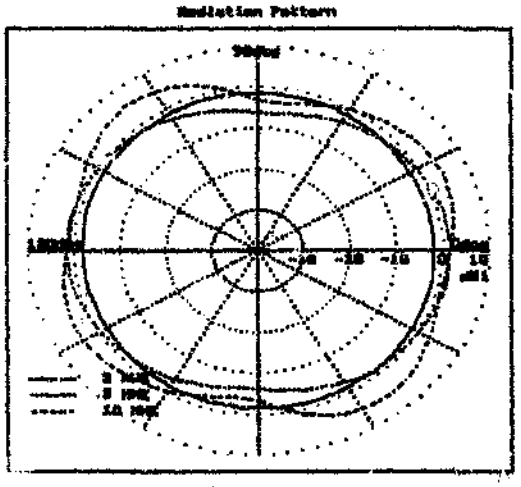


Fig 5.33 DTD antenna : Azimuth pattern cut for 30 degree take-off angles. Directive gain for 2 MHz, 5 MHz and 10 MHz.

The low frequency azimuth plane radiation patterns are reasonably omnidirectional with small variations in power levels. The patterns seem asymmetrical at first glance but are in fact symmetrical about the line $\phi = 135°$ and $\phi = -45°$.

The high frequency elevation plane perpendicular to the longest dipole (fig 5.34) indicate a severe reduction in radiated power for angles close to the zenith at 20 MHz. This is not a major problem, since the rare occasions requiring such high frequencies will call for low take-off angles as discussed in section 2.2. The 30 MHz perpendicular elevation plane pattern is surprisingly omnidirectional with only small variations. The elevation plane patterns along the longest dipole for high frequencies (fig 5.35) produce a good approximation to the required performance. The patterns show very abrupt variations with angle but no deep nulls are produced. The high frequency azimuth plane radiation patterns (fig 5.36) indicate that the radiated power is generally higher perpendicular to the shortest dipole. The overall directivity is however quite suitable for omnidirectional coverage.

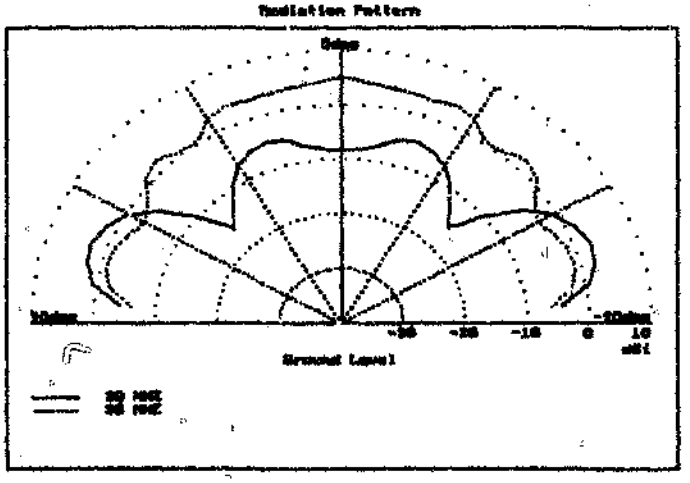


Fig 5.34 DTD antenna : Elevation plane pattern cut perpendicular to longest dipole (74 m) of crossed configuration.

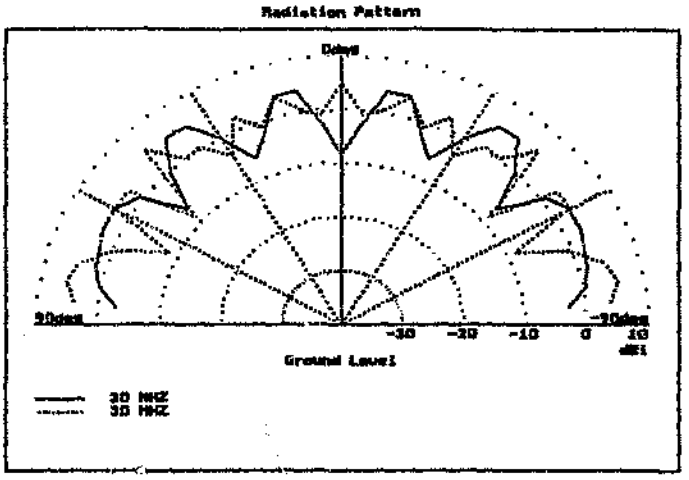


Fig 5.35 DTD antenna : Elevation plane pattern cut along the longest dipole (74 m) of crossed configuration.

The vast improvement in this antenna efficiency and VSWR performance when compared to the physically more complex fan dipole should be borne in mind when assessing the overall value of this antenna (see Chap. 4). The radiation pattern performance of the antenna is quite similar to most of the other antennas evaluated and this antenna presents a very attractive solution when the overall simplicity and PRR performance are taken into account.

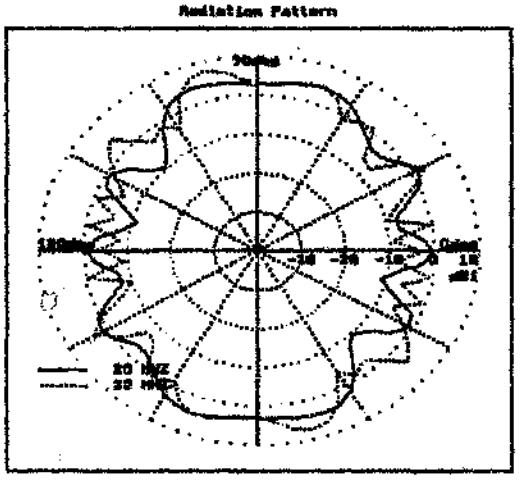


Fig 5.36 DTD antenna : Azimuth pattern cut for 30 degree take-off angles. Directive gain for 20 MHz and 30 MHz.

5.3 Conclusion on radiation pattern performance

The patterns presented in this chapter serve to reinforces the decision to neglect radiation pattern performance during design and optimization of the antennas. The patterns for quite dif-

ferent structures show very similar characteristics and it is clear that problem areas will be difficult to solve without resorting to considerably more complex geometries. The following conclusions can be drawn from the patterns presented:

- The low frequency radiation patterns (lowest frequency to 10 MHz) are overall quite suitable for short distance (0 - 1000 km), omnidirectional, tactical HF communications.
- The elevation plane patterns of most antennas produce some radiated power variation at higher frequencies over the elevation angles of interest. This characteristic is difficult to avoid, since it is mostly due to antenna/ground interaction and cannot be avoided while maintaining the simplicity of the structures. The frequencies where most variations occur are also out of the range of 2.5 to 15 MHz normally required for short distance HF links (see Chapter 2).
- The high frequency azimuth plane radiation pattern also show some variation which will present problems in certain directions and for specific ranges. The patterns are overall not very directive and are suited for omnidirectional communications. The same comment on high frequency performance applies to this conclusion.
- The similar nature of the radiation patterns of the antennas considered indicates that the best approach for improving the overall performance is by maximizing the radiated power (PRR) as indicated earlier.

All antenna types considered in this thesis clearly involve a compromise between physical simplicity and performance to obtain broadband HF performance. The radiation patterns of these antennas are not ideal for the intended application, but present quite a good compromise between performance and structural simplicity. Increasing the radiation efficiency, while maintaining an acceptable VSWR, is clearly an effective method for improving the overall performance of tactical antennas.

6 CONCLUSION

The main theme of this thesis was to show how broadband performance depends on the control of the current distribution on wires. The contention was made that the method of moments often hides the processes governing current distribution and thereby impedes the design process. Methods taking cognisance of the major factors which control the behaviour of specific antennas provide results at the expense of generality and accuracy.

6.1 Summary of Findings and Conclusions

Practical applications for the findings of this study are mostly found in the HF field. Recent developments in HF communications and normal HF related problems were mentioned in the introductory chapter to substantiate this statement. Practical examples of HF antennas were hence of particular interest and the research was primarily undertaken to satisfy needs in this area. The findings, techniques and scaled versions of the antennas are obviously generally applicable.

An assortment of topics related to this study was reviewed in the second chapter. The role of the ionosphere and the antenna radiation pattern were shown to be important, but impractical to manipulate during the design of simple HF antennas. Loaded and unloaded dipole were shown to exhibit suitable radiation patterns in the frequency range of interest. These generally suitable characteristics were assumed to persist for the antennas studied later and a decision was made not to consider radiation patterns during design optimization. The assumed suitability of antenna radiation patterns would rather be evaluated after optimization to substantiate the argument. Salient features of HF broadband antennas, fundamental limitations related to bandwidth, methods of achieving bandwidth and a well known technique for simulating wire antennas were explored. Impedance and radiation efficiency were shown to be important parameters to consider when broadband antennas are evaluated. The Power Radiated Ratio (PRR) was defined to combine the reduction in radiated power due to both impedance and efficiency variations. Various ways to achieve impedance bandwidth were investigated. The conclusion was that it is necessary to incorporate resistive loads in structurally simple broadband antennas. Finally NEC2, a program to analyze wire antennas using the method of moments, was reviewed. Modelling guide lines which are applicable to the antennas of interest were briefly mentioned. Most of the modelling guide lines were identified while simulating simple antennas and this information will hence provide a valuable reference to future designers. The method of moments offered a powerful tool to evaluate antennas but it is slow and mechanisms governing the behaviour of the antennas are not apparent. Simpler and more understandable methods were therefore required for an effective design effort.

The focus in the third chapter was on the ways in which current distribution is controlled to yield wide bandwidth. Techniques were identified by studying traditional designs and their performance. Reasons for unsatisfactory performance were related to inadequate control of the current distribution and the importance of such control was demonstrated. The introduction of a novel staggered loads antenna which employed the mechanisms uncovered in this study confirmed these findings. Measurements and NEC2 results for the SLA showed that significant performance improvement was feasible once the underlying mechanisms were perceived.

Simplified methods applicable to specific geometries were developed and tested in the fourth chapter. The techniques were formulated by identifying the dominant features governing antenna behaviour and neglecting secondary effects.

A method for evaluating multi-wire antennas, with the option of connecting two dipoles by a transmission line, was developed and shown to produce acceptable results. The capability of this method was demonstrated by designing a novel antenna with favourable performance in comparison with others. Measurements on a prototype of this antenna corroborated the predicted performance.

Another method was developed to assess the current distribution on dipoles with one or more complex loads on the dipole arms. The "Lossy Line" method took advantage of the similarities between dipole antenna and transmission line behaviour. A non-uniform, lossy line model was postulated to emulate the current distribution on a dipole antenna. Transmission line parameters were adapted from available theory where possible. The line distributed series resistance and small variations in line length were obtained by computational experimentation. Results of the lossy line method were compared to NEC2 results for a number of examples. The lossy line method achieved sufficient accuracy for design purposes. A multi-load geometry developed by engineers using the lossy line method demonstrated the suitability of this method for antenna design. Measurements and NEC2 results confirmed those obtained using the Lossy Line theory.

Examples of the computer time used by the two methods indicated a speed increase of two or three orders of magnitude in comparison to NEC2. Both of the methods provide insight into antenna operation which was one of the important aspects emphasized at the outset of the document.

The radiation patterns of the antennas studied during chapters 3 and 4 were presented in Chapter 5. These patterns confirmed the suitability of the antennas studied for short range HF communications in terms of directive properties. The decision to place the emphasis on obtaining maximum radiated power during design phases was hence validated.

6.2 Novel Aspects Arising from this Research

At this point the novel aspects presented in this document are highlighted:

- Full performance (input impedance, efficiency and radiation patterns) of published HF broadband antenna designs was determined using the NEC2 code.
- A staggered load HF broadband antenna with improved performance compared to existing antennas was developed and tested.
- A simplified theory to analyze and optimize two dipoles connected by a transmission line was developed and tested.
- A two dipole antenna, with dipoles interconnected by a suitable transmission line, was optimized and proved to be superior to existing antennas.
- A lossy non-uniform transmission line model of unloaded and loaded dipole antennas was developed and it was tested using various examples.

The dominant parameters determining the performance of a specific type of antenna must be manipulated to achieve the design goals. Simple HF broadband antenna performance was shown to by mainly dependant on control of the current distribution. Resistive loading presents a suitable way of manipulating current distribution on simple, low profile HF antennas. The dominant aspects affecting the performance of specific resistively loaded antennas were mathematically modelled while omitting second order influences. Such unsophisticated models in themselves assist in the design by accentuating the elementary principles influencing the behaviour. Convenient tools for rapid evaluation or optimization of broadband geometries were so provided.

The utility of the simple analytical tools was demonstrated by the design of improved HF broadband antennas. Measurements and NEC2 results for the new designs confirmed their superior performance and the validity of the simplified theory. A overview of the performance of the new antennas in comparison to that of known antennas showed an overall improvement in the state of the art.

Appendix A

THEORY OF THE METHOD OF MOMENTS

A 1 Method of moments overview

The method of moments, in general, is described (Thiele, 1973) by considering Fig A1:

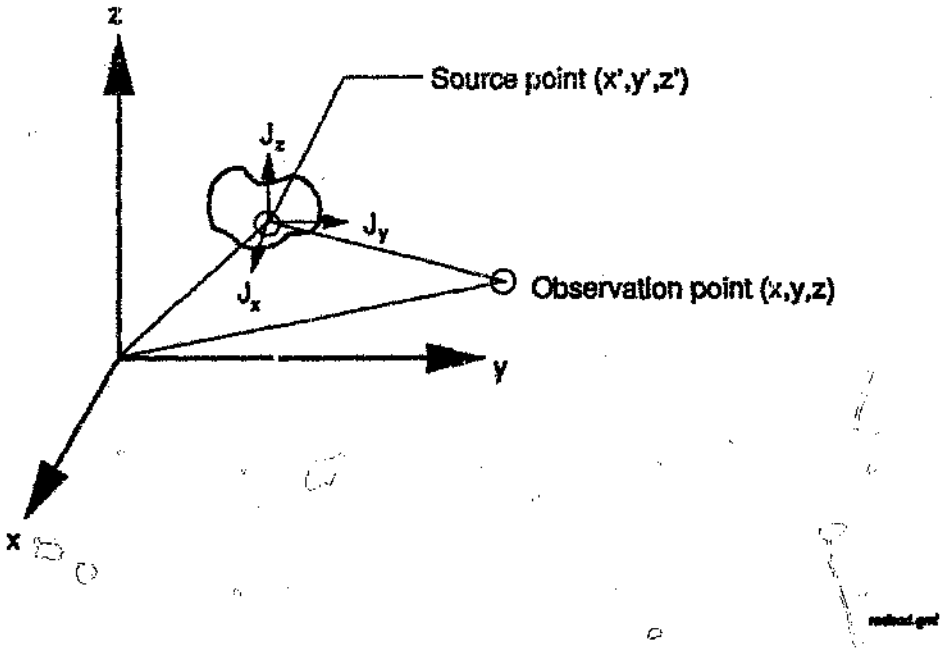


Fig A1 General radiating body

A conducting body with current density, J, has a tangential electric field of zero, by the boundary conditions:

$$0 = E^s_{tan} + E^i_{tan} \qquad \text{A1}$$

where E^s_{tan} is the tangential component of the scattered E - field caused by J. E^i_{tan} is the tangential E-field due to a source located outside the body.

By defining the operator L_{op} and dropping the "tan" notation the following equation is constructed:

$$L_{op}(J) = -E^s = E^i \qquad \text{A2}$$

where E^i is a known excitation function or source.

The required response function, J, is expanded into a series of bases, or expansion functions such that:

$$J = \sum_n I_n \times J_n \qquad \text{A3}$$

Substituting this into A2 leads to:

$$L_{op}\left(\sum_n I_n \times J_n\right) = E^i \qquad \text{A4}$$

And using the linearity of the operators:

$$\sum_n I_n \times L_{op}(J_n) = E^i \qquad \text{A5}$$

The next step is to define a set of weighting, or testing functions W_1 ,W_2, ... over the domain of interest and an inner product is formed. The inner product is the scalar quantity obtained by integrating W and J over the surface under consideration. The notation for this product is $< J, W >$.

Implementing these weighting functions in A5 results in:

$$\sum_n I_n < W_m, L_{op}(J_n) > = < W_m, E^i > \qquad \text{A6}$$

Enforcing this at m = 1 to n results in a set of linear equations which may be expressed in matrix form as follows:

$$\begin{bmatrix} <W_1, L_{op}(J_1)> & <W_1, L_{op}(J_2)> & \cdots \\ <W_2, L_{op}(J_1)> & <W_2, L_{op}(J_2)> & \cdots \\ \cdot & \cdot & \\ \cdot & \cdot & \\ \cdot & \cdot & \\ <W_n, L_{op}(J_1)> & <W_n, L_{op}(J_2)> & \cdots \end{bmatrix} \times \begin{bmatrix} I_1 \\ I_2 \\ \cdot \\ \cdot \\ \cdot \\ I_n \end{bmatrix} = \begin{bmatrix} <W_1, E> \\ <W_2, E> \\ \cdot \\ \cdot \\ \cdot \\ <W_n, E> \end{bmatrix} \qquad \text{A7}$$

This matrix in the compact form is:

$$[Z] \cdot [I] = [V]$$

This is solved by:

$$[I] = [Z]^{-1} \cdot [V]$$

where:

$$J = \sum_n I_n \times J_n$$

In the general method known as Galerkin's method the basis and weighting functions are chosen such that $W_m = J_n$.

The major factors to be considered when using the method of moments are the choice of integral equations for thin wires, expansion and testing functions and feed point models.

A 2 Equations for current distribution on thin wires

Knowledge of the current distribution on thin wires is essential when implementing such a method. A choice of a suitable equation for the current distribution influences the accuracy and capabilities of a given code. To illustrate the merits of a number of equations a short discussion of three such equations are given with symbols as given in Fig A2 (Popovic, 1983).

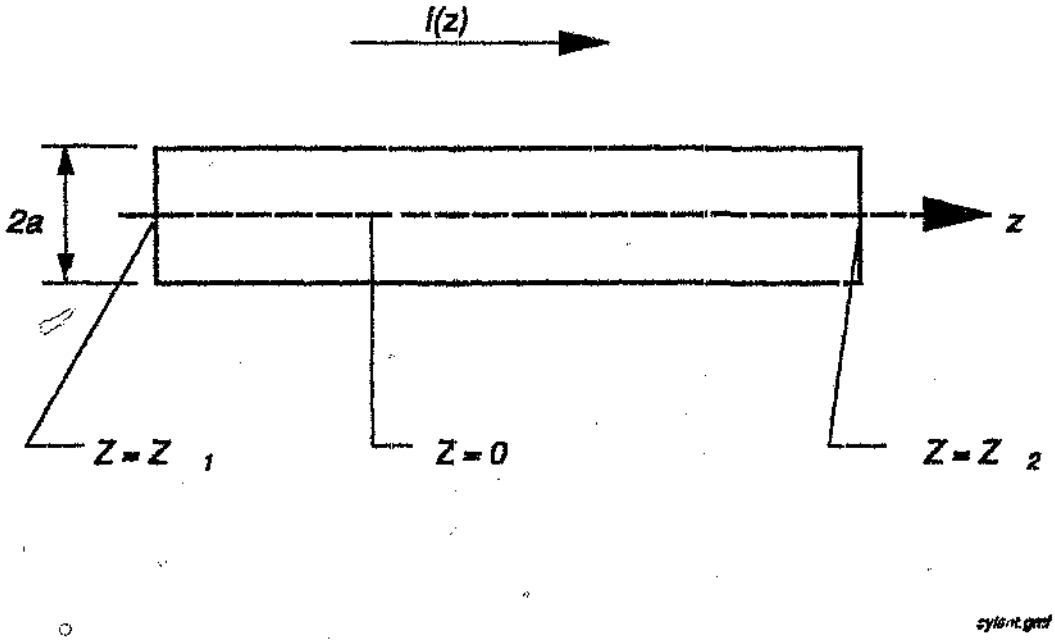


Fig A2 A cylindrical wire antenna

The Hallen equation

This equation has the following form:

$$I(z')g(r)dz' + C_1\cos(kz) + C_2\sin(kz)$$

$$= \frac{k}{j\omega\mu}\int_{z_0}^{z} E_{in}(z')\sin[k(z-z')]dz' \qquad \text{A8}$$

where:

$$g(r) = \exp\frac{-jkr}{4\pi r}$$

$$k = \frac{2\pi}{\lambda}$$

z and z' are the observation and test points respectively

C_1 and C_2 are constants to be determined

E_{iz} is the incident field

r is the distance between test and observation point

The problems associated with this equation is the evaluation of C_1 and C_2, which either makes the integral more complex or requires two additional equations in the matrix system. This equation only allows the use of a delta-gap generator which is not always the most realistic feed model.

Pocklington's equation

Pocklington's equation has the form:

$$\int_{z_1}^{z_2} I(z')\left\{1+\frac{1}{k^2}\frac{d^2}{dz^2}\right\}g(r)dz' = \frac{E_{iz}}{j\omega\mu} \qquad \text{A9}$$

When the indicated differentiation is performed the equation turns out to have terms proportional to $1/r$, $1/r^2$ and $1/r^3$ which are inconvenient from a numerical point of view. Pocklington's equation has the advantage that, unlike Hallen's equation, it does not place constraints on the type of excitation that can be used.

Schelkunoff's equation

This equation has the form:

$$\int_{z_1}^{z_2}\left[I(z')+\frac{1}{k^2}\frac{d^2I(z')}{dz'^2}\right]g(r)dz' - \frac{1}{k^2}\frac{dI(z')}{dz'}g(r)\Big|_{z'=z_1}^{z_2} = \frac{E_{iz}}{j\omega\mu} \qquad \text{A10}$$

The kernel is only dependent on terms in r and $1/r$, which is numerically convenient. However, the current distribution must be differentiable twice, which may be a disadvantage. According to Popovic (1983: 13) this equation has not received the attention it deserves from those working with Method of Moment techniques.

A 3 Testing and expansion functions

Testing and expansion functions are subdivided into sub-domain functions and entire domain functions. Sub-domain functions are piece-wise functions only defined over a small part of the wire. Popular choices are rectangular, delta, triangular and piece-wise sinusoidal functions. Entire domain functions are series-type functions with parameters that allow them to approximate the current distribution in the entire domain. Obvious choices are Fourier series expansions, Maclaurin series, polynomials of sufficient order and power series.

In general it could be said (Thiele, 1973) that sub-domain functions require more segments, but less effort, in the calculation of the impedance matrix. Bases spanning the whole domain can result in rapid convergence for fewer segments, but calculating the impedance matrix is usually not efficient in terms of computer time. A combination of these two methods should result in a interesting compromise.

Such a method was proposed by Turpin (1969). Basis functions stretching over a number of segments are defined and this are used to approximate the current distribution. This results in a N x M matrix for N segments, where M < N/10 usually provides sufficient accuracy.

Popovic (1983: p 26) reported excellent results for antennas longer than a wavelength when using a power series expansion function of the form:

$$I_m(z_m) = \sum_{i=0}^{k_m} I_{mi} z_m^i,\ m=1,..,N$$

where:

k_m is the desired degree of polynomial for the m th segment

N is the total no of segments

A 4 Feedpoint modelling

It is difficult to represent the feedpoint of an antenna mathematically and its formulation severely affects the results esperially when input impedance is of interest. The simplest model for feed point modelling is the so-called delta-gap model shown in Fig A3:

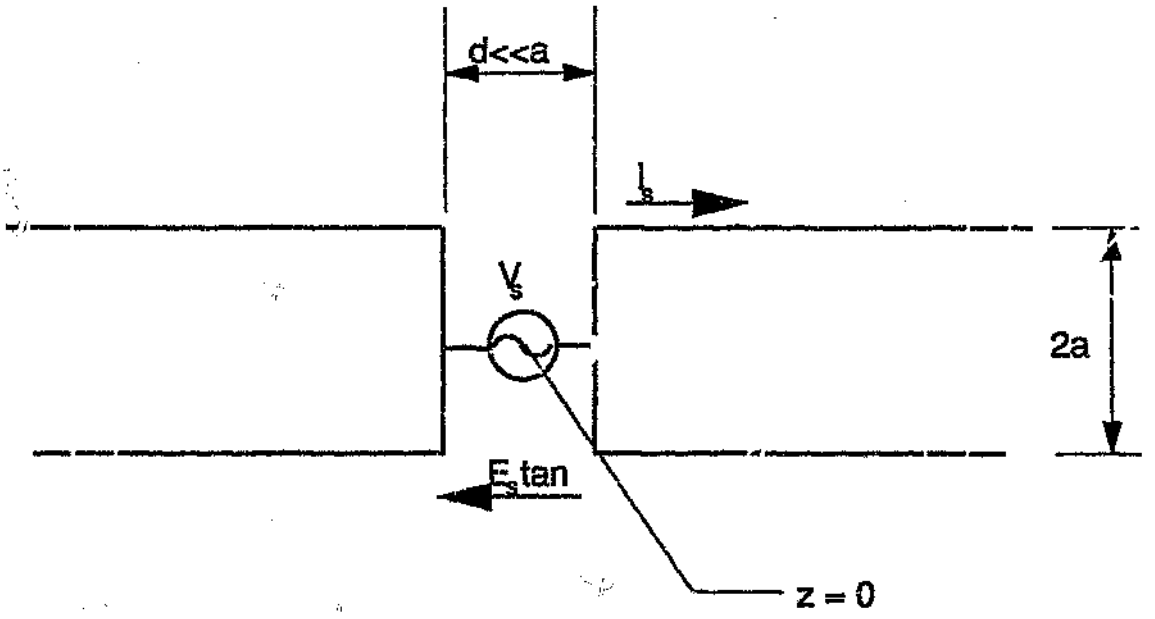


Fig A3 Delta gap generator model

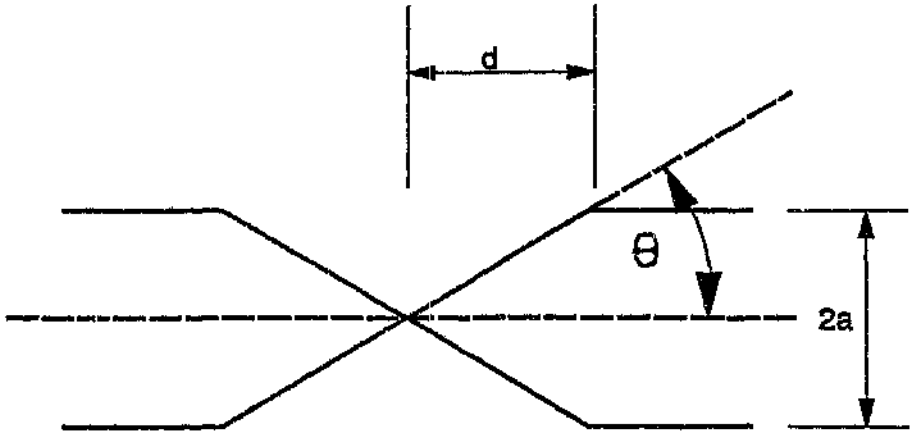
This model is mathematically convenient (Burke and Poggio, 1980), but of a somewhat questionable nature in terms of physical reality. A more realistic source can be modelled as an electric field, E_s , applied over some part of the wire, usually one segment. The applied voltage could then be taken to be:

$V_s = E_s \times$ segment length,

provided that E_s is not appreciably affected by other fields generated by the structure. This model does require that the segment lengths adjacent to the source segment be of length approximately equal to the source segment length.

Burke and Poggio (1980) proposed an alternative source model that is less sensitive to the equality of segment lengths in the source region. For this model, the source is viewed as a biconical transmission line with feed point at the source location, as illustrated in Fig A4.

The voltage $V(s)$ can be found from the transmission line equation:



biconarc.gmf

Fig A4 Biconical transmission line source model

$$V(s) = -jZ_0 \frac{\partial I}{\partial s}$$

Where Z_0 is the average characteristic impedance of the biconical transmission line:

$$Z_0 = 120 \ln\left(\frac{2d}{a} - 1\right)$$

This discontinuity can be introduced by modifying the current expansion on the segment and the model is hence also known as the current discontinuity source model. Other source models are discussed by Popovic (1982), Stutzmann and Thiele (1981) and others, but those above are of significance due to their application in the NEC2 program.

Appendix B

ERROR IN TREHARNE PAPER

Treharne (1983[5]) developed his "periodically truncated pseudo-conical terminated monopole" by considering a simple single wire monopole. The design equation which he developed for the inductor values of this structure was:

$$L_n = 0.9 \cdot l\left(\frac{2}{3}\right)^n \qquad \mu H \qquad \text{B1}$$

Thereafter he defined the "break frequency" of the structure to be that frequency at which the reactance of the parallel inductor of a load equals the resistor value. This equation was simply stated by Treharne but will be derived here to indicate its origin.

$$2\pi f_n L_n = 377 \qquad \Omega$$

that is:

$$f_n = \frac{377}{2\pi L_n} \qquad MHz \qquad \text{B2}$$

replacing L_n with (B1) results in

$$f_n = \frac{67(3/2)^n}{l} \quad \text{as in Treharne's paper} \qquad \text{B3}$$

Treharne subsequently extended these equations to the pseudo-conical case and mentioned that the loads could now be considered to be in parallel (i.e. the resistor and inductor values should be doubled). This is confirmed by the example given in his article where the ultimate inductor value is stated to be 60 μH. The value obtained by using equation B1 is 30 μH, hence the factor of 2 given in the equation in 3.1.1. The value of the parallel resistor stated in the same example is 400 Ω i.e. the same value as was used in the single wire case. (The resistor value of 400 Ω instead of 377 Ω was presumably used in this example for simplicity). Thus B3 cannot be used to determine the break frequencies for the pseudo-conical two wire structure and B2 should rather be used. The other possibility is to double the resistor values to 800 Ω to be consistent with the parallel loads principle in which case the B3 would clearly still be valid.

Appendix C

EXPERIMENTAL METHODS

All the experiments were done with the antennas arms drooping from the centre mast in the "drooping dipole" configuration. The mast height given was hence for the centre support and wires sloped to within 1 m of the ground. The experimental method for the various antennas is given below.

C 1 Treharne antenna

Instrument: Hewlett-Packard HP 4815 A vector impedance meter.

Transmission line: 13.5 m of 300 Ω twin wire line. Measured Z_0 of 335 Ω and velocity factor of 0.81.

Environment: Open field with natural grass.

Mast: 6 m fibreglass.

Comments: Converted input impedance values to feed antenna feedpoint using the transmission line equation. Measurements were taken twice and repeatability was typically better than 5 percent. The measurements were done at the antenna terminals without using an impedance transformer.

C 2 Staggered loads antenna (SLA)

Instrument: Hewlett-Packard HP 4815 A vector impedance meter.

Transmission line: 8.6 m of 300 Ω twin wire line. Measured Z_0 of 335 Ω and velocity factor of 0.81.

Environment: Open field with natural grass.

Mast: 8 m fibreglass mast.

Comments: Measurements with antenna arms 5 and 90 degrees apart. Input impedance values measured at the end of the transmission line were converted to the antenna feedpoint using the transmission line equation. Measurements were taken twice and repeatability was typically better than 5 percent. Measurements were taken at antenna terminals without using any impedance transformer.

C 3 Dipole-transmission line-dipole (DTD)

Instrument: Hewlett-Packard HP 4815 A vector impedance meter.

Transmission line: 12.0 m of RG-58 Ω coaxial cable. Measured Z_0 of 56 Ω and velocity factor of 0.66.

Environment: Open field with natural grass.

Mast: 10 m metal pole.

Comments: Input impedance were converted to VSWR values and correction was made for the cable loss. Measurements were taken twice and repeatability was typically better than 5 percent. The antenna was equipped with impedance transformer for measurement.

C 4 Multi-load antenna

Instrument: Hewlett-Packard HP 4195 network analyzer.

Transmission line: 12.0 m of RG-58 50 Ω coaxial cable. Measured Z_0 of 56 Ω and velocity factor of 0.66.

Environment: Open field with natural grass.

Mast: 10 m metal lattice mast.

Comments: Instrument was calibrated to cable feed point to read antenna terminal impedance values. A continuous measurement sweep showed the results to be stable. Antenna was equipped with the required 7:1 impedance transformer for measurement.

Appendix D

TABULATED RESULTS OF TREHARNE ANTENNA

NEC2 Results - Treharne Antenna

Note: VSWR calculated with respect to 400 Ohms.

Freq. in MHz	Z mag. (Ω)	Zphase (degrees)	VSWR	Eff.(%)	PRR (%)
3	530	36	2.1	2	2
4	971	10	2.5	4	3
5	888	-21	2.5	5	4
6	621	2	2.45	6	5
7	437	-293	1.7	7	7
8	348	-15	1.3	8	8
9	343	5	1.2	11	11
10.5	485	15	1.4	18	18
12	533	4	1.35	24	24
13.5	441	3	1.1	27	27
15	397	20	1.4	31	30
16.5	539	34	2.0	42	37
18	783	23	2.2	57	49
19.5	690	0	1.7	59	55
21	480	7	1.25	48	47
22.5	540	30	1.9	40	36
24	787	28	2.4	57	47
25.5	888	12	2.3	62	52
27	803	1	2.0	57	51
28.5	709	-2	1.8	50	46
30	700	3	1.75	47	43

Measured Results - Treharne Antenna

Freq. (MHz)	Z mag. (Ω)	Z phase	VSWR
3	616	26	1.9
4	1077	1	2.7
5	876	-14	2.3
6	640	-23	1.9
7.5	331	-21	1.5
9	237	-5	1.7
10.5	340	5	1.2
12	466	-4	1.2
13.5	513	0	1.3
15	490	16	1.4
16.5	445	32	1.8
18	430	26	1.6
19.5	454	13	1.3
21	470	3	1.2
22.5	512	7	1.3
24	602	17	1.7
25.5	654	32	2.2
27	638	26	2.0
28.5	605	18	2.0
30	484	18	1.45

Appendix E

TABULATED RESULTS FOR THE GUERTLER DIPOLE

NEC2 Results

Note: VSWR calculated with respect to 300 Ohms

Freq. in MHz	Z mag. (Ω)	Z phase (degrees)	VSWR	Eff. (%)	PRR (%)
3	176	-7	1.75	28	27
6	602	-16	2.14	22	19
9	426	3	1.42	24	23
12	800	-10	2.7	44	35
13	737	-32	3.0	47	35
14	540	-46	3.0	47	35
15	326	-50	2.7	44	34
15.5	241	-47	2.6	45	36
16	160	-34	2.46	47	38
16.5	120	3	2.5	55	45
17	168	41	2.7	68	53
18	410	57	3.6	91	62
21	825	-30	3.3	81	58
24	264	-8	1.2	40	40
27	375	13	1.4	43	42
30	465	22	1.8	49	45

Appendix F

TABULATED RESULTS FOR THE HARRIS ANTENNA

NEC2 Results

Note: VSWR with respect to 300 Ohms

Freq.	Z mag. (Ω	Z phase (degrees)	VSWR	Eff.(%)	PRR (%)
3	196	-10	1.6	32	30
6	430	-15	1.6	31	29
9	417	4	1.4	40	38
12	595	-16	2.1	53	46
15	271	-42	2.3	50	44
18	272	49	2.7	80	64
21	720	-10	2.5	93	77
24	216	-23	1.7	62	60
27	284	23	1.5	58	57
30	100	24	1.7	65	62

Appendix G

TABULATED RESULTS FOR THE RESISTIVELY LOADED FAN DIPOLE

NEC2 results

Freq. in MHz	Z real (Ω	Z imag. (Ω)	VSWR	Efficiency	PRR
3	196.44	28.03	2.05	0.31	0.27
3.5	473.11	331.48	2.14	0.41	0.35
4	532.91	586.70	3.40	0.13	0.09
4.5	162.35	195.52	3.14	0.03	0.02
5	172.42	19.30	2.33	0.22	0.19
5.5	291.40	203.17	1.94	0.40	0.36
6	821.52	136.73	2.13	0.45	0.39
6.5	223.10	-305.71	3.07	0.11	0.08
7	248.95	-26.06	1.62	0.43	0.41
8	454.13	236.86	1.76	0.48	0.44
9	256.18	26.51	1.57	0.44	0.42
10	425.28	291.55	2.00	0.43	0.38
11	719.87	198.12	1.99	0.47	0.42
12	721.45	-158.09	1.93	0.48	0.43
13	408.38	-257.78	1.87	0.45	0.41
14	218.18	-87.94	1.96	0.35	0.31
15	211.70	118.14	2.11	0.31	0.27
16	341.02	278.81	2.12	0.38	0.33
17	577.40	277.52	1.96	0.46	0.41
18	701.81	6.37	1.75	0.51	0.47
19	445.02	-185.25	1.57	0.51	0.48

Freq. in MHz	Z real (Ω	Z imag. (Ω)	VSWR	Efficiency	PRR
20	224.47	-38.97	1.81	0.38	0.35
21	213.57	167.14	2.30	0.27	0.23
22	283.01	297.86	2.51	0.28	0.22
23	491.[illegible]	360.13	2.26	0.39	0.33
24	677.83	184.35	1.88	0.49	0.44
25	419.07	-51.65	1.14	0.55	0.55
26	345.04	281.35	2.12	0.38	0.33
27	568.80	67.09	1.46	0.54	0.52
28	418.98	289.41	2.00	0.43	0.38
29	612.02	263.85	1.96	0.46	0.42
30	655.05	84.61	1.68	0.52	0.49

Appendix H

TABULATED RESULTS FOR THE STAGGERED LOADS ANTENNA

NEC2 Results

Note: - VSWR with respect to 500 Ohms

Freq. in MHz	Z mag.	Z phase	VSWR	Eff.(%)	PRR (%)
3	222	1	2.3	47	40
6	643	18	1.5	42	40
9	505	6	1.1	46	46
12	773	-20	1.8	58	54
15	382	-20	1.6	52	49
18	702	23	1.7	64	60
21	520	-25	1.6	60	57
24	746	40	2.4	82	68
27	512	-30	1.7	68	63
30	475	45	2.4	82	68

Measured Results with the included angle, $\phi = 5°$

Note: - VSWR calculated with respect to 500 Ohms

Freq. in MHz	Z mag. (Ω	Z phase in degrees	VSWR
3.5	247.00	35.00	2.30
4.6	660.00	23.00	1.90
7.0	482.00	-18.00	1.45
8.0	395.00	-7.00	1.15
9.0	394.00	8.00	1.15
10.5	494.00	8.00	1.15
12	500.00	-15.00	1.40
13.5	390.00	-32.00	1.80
16.5	231.00	25.00	2.05
18	493.00	18.00	1.45
19.5	700.00	-16.00	1.90
22.5	250.00	32.00	2.20
25	550.00	34.00	2.00
27	353.00	-48.00	2.60
30	364.00	39.00	2.10

Measured Results with the included angle, $\phi = 90°$

Note: - VSWR calculated with respect to 400 Ohms

Freq. in MHz	Z mag. (Ω)	Z phase in degrees	VSWR
3	219.00	19.00	2.45
4	650.00	42.00	2.35
7.5	660.00	-18.00	1.50
9	580.00	11.00	1.30
10.5	690.00	16.00	1.39
12	670.00	-4.00	1.35
13.5	505.00	-26.00	1.60
16.5	310.00	21.00	1.85
18	732.00	19.00	1.70
19.5	900.00	-20.00	2.00
22.5	455.00	38.00	2.05
24	980.00	30.00	2.45
25.5	1070.00	-2.00	2.10
27	533.00	-31.00	1.75
30	448.00	35.00	1.95

Appendix I

DESCRIPTION AND USER MANUAL FOR THE PROGRAM SIMULATION AND ANALYSIS OF LOADED DIPOLE ANTENNAS (SALDA)

The program Simulation and Analysis of Linear and Dipole Antennas, SALDA, was written as a research tool to aid the design of various antenna types. The program contains novel theory developed as part of the Ph. D. programme. As such the package should be viewed as a research tool for an engineer rather than a well rounded software product.

SALDA is reasonably user friendly in that the program is totally menu driven and has considerable error checking on user input. It does not however have any help facility except for standard user prompts. Most of the theory embedded in this program is described in chapter 4 and it is useful to study these before the program is seriously used. The program output is available in graphical, tabular, printer and data file formats.

The program is compiled for the IBM compatible machines with system memory of 640 kB. The source code for the program was written in Turbo Pascal 4 and contains some 12 000 lines of code. The program requires a standard Colour Graphics Adapter (CGA), but may be recompiled to run with Hercules, ATT and EGA monitors.

I1 Features

- Analysis of multi-wire dipole antennas connected to each other by a transmission line
- Optimization of dipole-transmission line-dipole (DTD) antennas over user specified ranges of parameters
- Inclusion of perfect earth into analysis of DTD and drooping DTD antennas. (This feature increases the run time considerably and was hence not discussed in the main document)
- Analysis of dipoles with distributed loads
- Evaluation of antenna impedance versus frequency when serial and parallel resistors are added
- Calculation of antenna impedance, VSWR, efficiency and PRR over frequency ranges of interest
- Output of above parameters in tabular, graphical, printer and data file formats
- Graphical tools to superimpose the characteristics of various antennas and hence compare performance

- Ability for user to enter antenna characteristics obtained elsewhere for comparison to program generated output or other antennas

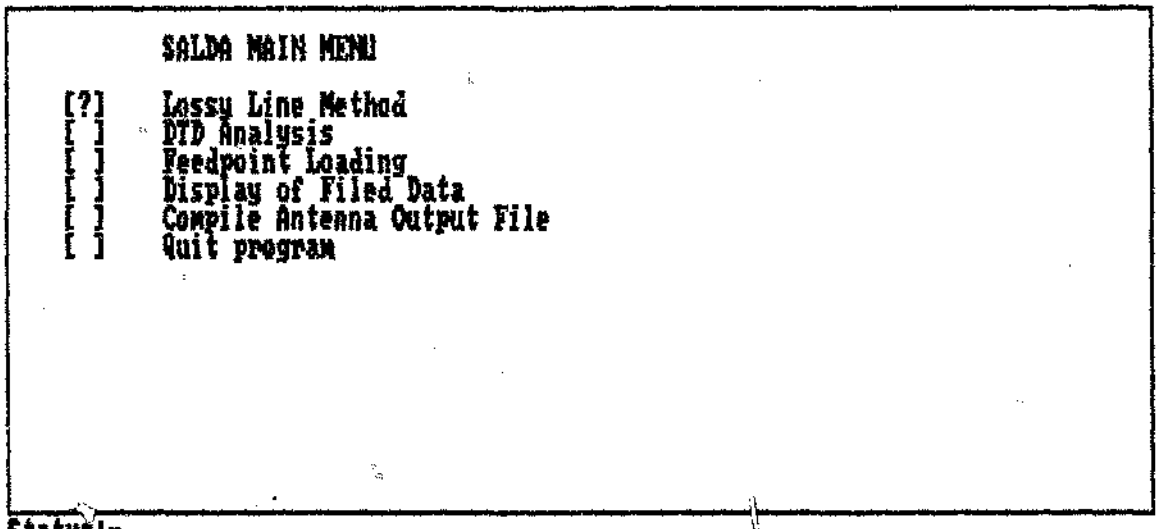
I2 Getting Started

The files necessary to run the program appear on the first diskette. The second diskette contains source code as standard Turbo Pascal units.

If a hard disk is available then create a sub-directory by typing MKDIR SALDA from the root directory

Type CD SALDA to change to the new directory. Insert the first diskette into the A drive of the machine and issue the command COPY A:*.* at the command line. The executable and necessary data files will now be transferred to the hard disk

To start the program type SDA_2 on the command line and the main menu should appear:



This is the general format of menu screens and the ? may be moved to the required position using the cursor keys. The status, prompt and warning screens provide the user with some additional information during sessions.

I3 Menu by Menu explanation

The first menu to appear upon initiating the program is the main menu shown below:

```
          SALDA MAIN MENU

   [?]    Lossy Line Method
   [ ]    DTD Analysis
   [ ]    Feedpoint Loading
   [ ]    Display of Filed Data
   [ ]    Compile Antenna Output File
   [ ]    Quit program
```

Status:-

Prompt:- Use arrow keys and <-| to select option ?

Warning:-

This menu allows the various options provided by this program to be accessed. Say the cursor is positioned on the first item and the enter key pushed the control menu for the lossy line feature will appear:

```
        LOSSY LINE METHOD INPUT :

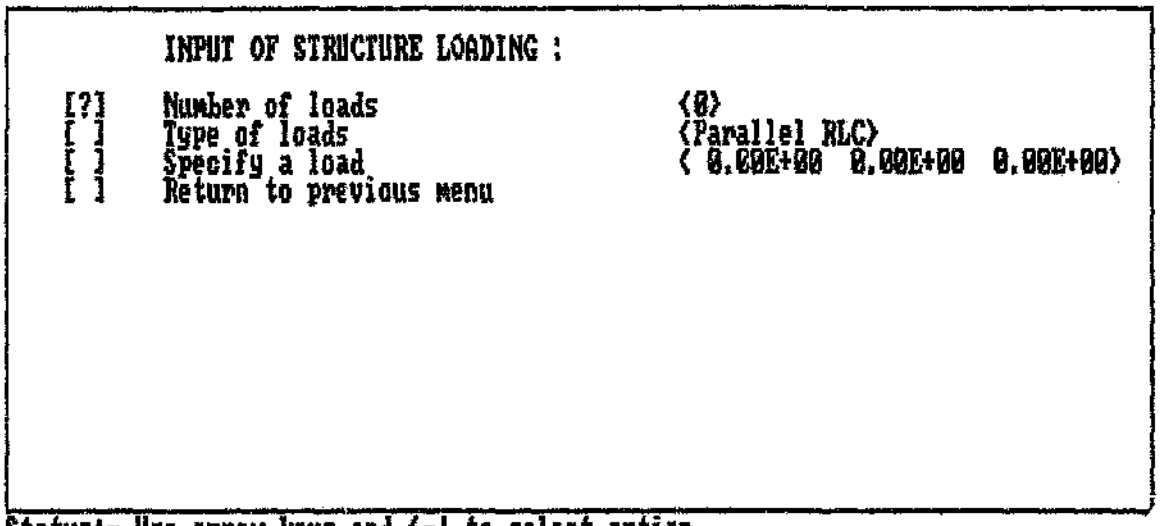
[ ]   Dipole halflength                  ( 2.320E+01)
[?]   Radius                             ( 1.000E-01)
[ ]   Frequency range                    ( 0.00E+00  0.00E+00  0.00E+00)
[ ]   Loading                            (0)
[ ]   Run Problem
[ ]   Supervisor input
[ ]   Determining parameters
[ ]   Exit to previous menu
```

Status:- Use arrow keys and <-! to select option

Prompt:-

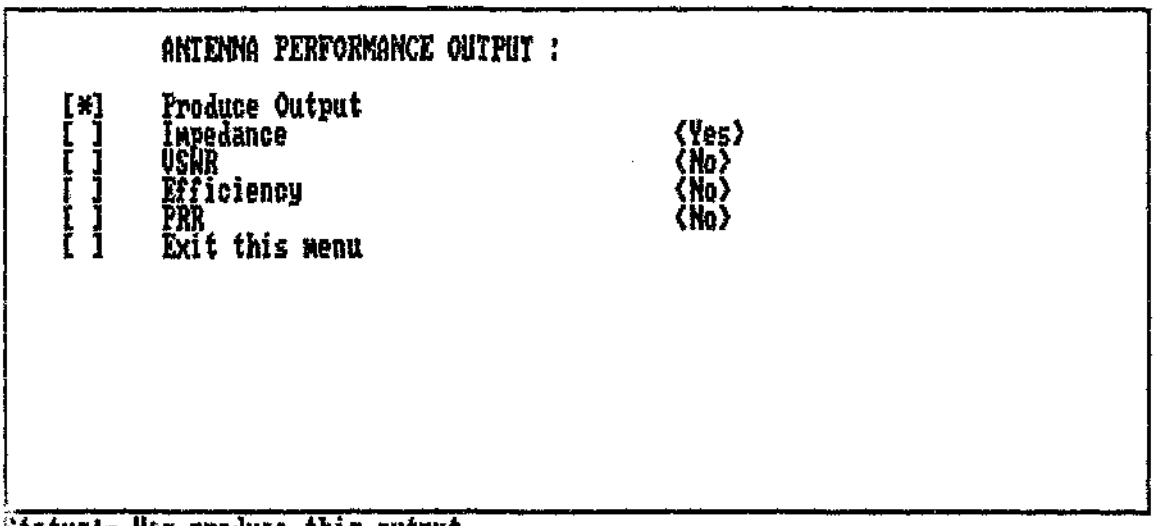
Warning:-

This menu allows for the input of the relevant numerical values while showing their default values on the right hand side of the screen. The two options *supervisor input* and *determining parameters* are not for general use but was included for purpose of research into more efficient methods of performing Lossy Line Analysis. If the antenna is to be impedance loaded this may be specified by choosing that option and the following menu will appear:



The two types of loads that may be used are series RLC and parallel RLC. These configurations allow a rich variety of realistic loads, which will then be transformed into the appropriate complex impedance depending on the frequency of operation. Once loads are being specified the user is prompted for values of components and distance of load from feed point. Up to 10 loads may currently be incorporated into a structure. The loads are also assumed to be symmetrical therefore only one load at every distance needs to be defined. When load specification has been performed the user may return to the Lossy Line Control Menu and choose the RUN PROBLEM option.

The prompt screen will indicate the progress by displaying each frequency and after the full range has been evaluated a output menu will appear:



Status:- Yes produce this output

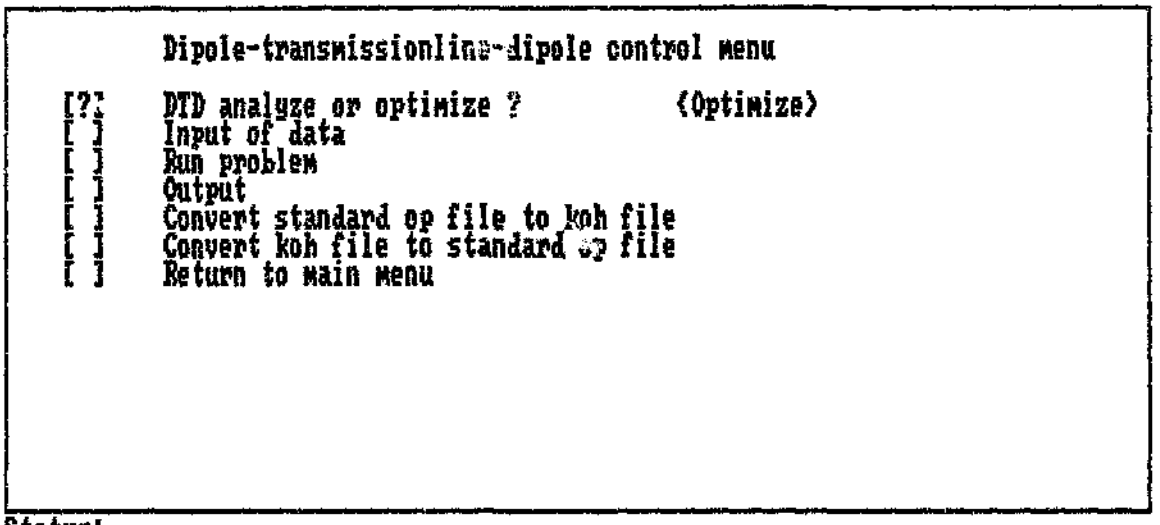
Prompt:- Push function key for desired output ?

Warning:-

1)SCRNPRINT 2)SCRNPLOT 3)FILE O/P 4)EXIT

The cursor may be moved around in this menu and the parameters of interest selected. When the user is satisfied with the selection the PRODUCE OUTPUT item should be selected and the menu at the bottom of the screen will appear. This menu is activated by pushing the function key corresponding to the number in front of each choice. Using this feature the output parameters may be graphically displayed in the form of tables on the screen or the data may be stored as a normal ASCII file for later use. By pushing the EXIT option (F4) the main menu may again be accessed to change the selection or to return to the Lossy Line Control Menu.

On return to the main menu the next item of interest is the DTD analysis option. When this is chosen the menu below will be displayed:



Status:-

Prompt:- Use arrow keys and <-i to select option ?

Warning:-

The first option on this menu determines whether the user wants to optimize a specific antenna or just analyze it. The optimization procedure involves a brute force evaluation of all possible combinations within a user specified range of parameters. In that case only average VSWR and maximum VSWR is calculated and stored in a file for each configuration. If the analyze option is selected then only one configuration is evaluated, but full results over the specified frequency range may be obtained.

The next three options allows for input, running of the program and production of output. The last two options allow for file conversion between normal ASCII files and files for use with the DTD analysis.

In the DTD theory it is always assumed that the free space input impedance of the interconnected dipoles are known. These are stored in the so called "koh files" and read by the program when required. Four standard koh files are supplied with the program. These are:

- WU125X.DAT for dipoles of thickness factor 12.5
- WU-15.DAT for dipoles of thickness factor 15
- WU175X.DAT for dipoles of thickness factor 17.5
- WU-20.DAT for dipoles of thickness factor 20

where thickness factor, Ω is:

$$\Omega = 2\log\left(\frac{length}{radius}\right)$$

These files were extracted from impedance tables for different thickness factor dipoles. The interesting aspect about this file conversion feature is that other antennas (perhaps loaded dipoles analyzed using the Lossy Line Method) may be connected via transmission line to each other with possible beneficial resuits. This has not yet been attempted but is an interesting possibility.

Say the user select the OPTIMIZE option and then INPUT the following menu is displayed

```
          Dipole Transmission Line Dipole Optimization Input

   [ ]    Feed antenna optimization range     ( 4.00E+01  8.00E+01  1.00E+01)
   [ ]    Far antenna optimization range      ( 4.00E+01  8.00E+01  1.00E+01)
   [ ]    Optional 2nd feed antenna range     (-1.69E-23  8.85E+37 -0.00E+00)
   [ ]    Transmission line length range      ( 1.10E+01  2.00E+01  1.00E+00)
   [ ]    Z0 range                            ( 1.00E+02  5.00E+02  1.00E+02)
   [ ]    Frequency range                     ( 2.00E+0   3.00E+07  1.00E+06)
   [ ]    Feed antenna koh datafile           (wu-20.da )
   [ ]    Far antenna koh datafile            (wu-20.dat)
   [ ]    Optional Feed antenna koh datafile  (wu-20.dat)
   [ ]    USNR threshold for output recording ( 3.00E+00)
   [ ]    Output datafile name                (test.out)
   [ ]    Monitor progress on screen          (FALSE)
   [ ]    Three or two antennas?              (two wires)
   [ ]    Series or parallel?                 (T1 and feed ant. in parallel)
   [?]    Quit this menu
Status:-

Prompt:- Use arrow keys and (-! to select option ?

Warning:-
```

This menu allows the user to specify the range of values over which the optimization is to be performed. In this example for instance the user has specified that the first dipole lengths should be varied from 40 m to 80 m in 10 m increments. Normally only two dipoles are used but a third dipole that will be connected in parallel with the feed point dipole may be specified. The user is also prompted for three file names containing the free space impedance data for the various antennas. The program defaults to the WU-20.DAT files for all three dipoles since thin wire structures are usually of interest and these have typical thickness factor of about 20.

The VSWR THRESHOLD prompt defines a upper limit on average VSWR above which results will not be written to the output file specified by the OUTPUT DATAFILE NAME option. The progress of the optimization process may be monitored on the screen using that option and the last option allows the user to put the feedpoint dipole in series or in parallel with the transmission line.

A sample of the output file from this optimization routine is shown below:

This is output of a optimization run on a parallel combination of
two antennas. Antenna 1 are in parallel with a transmission
line connecting it to antenna 2.
The antennas have impedances as provided in files:
wu-20.dat wu-20.dat

A number of parameters were varied as given below: <start, end, inc.>

Dipole 1 length: 4.30E+01 5.30E+01 5.00E+00
Dipole 2 length: 6.90E+01 7.90E+01 5.00E+00
Trans. line length: 7.00E+00 1.30E+01 1.00E+00
Z0 range: 5.00E+02 5.00E+02 1.00E+00
Each possibility has been evaluated over a freq. range of:
2.00E+06 1.60E+07 1.00E+06
All average VSWR values below 1.00E+01 were recorded

RESULTS
=======
ant.1 length, ant.2 length, line length, Z0
average VSWR, best matching impedance

4.30E+01 6.90E+01 7.00E+00 5.00E+02
6.794387254.E+00 1.9483149969E+02 2.6991361792E+01

4.30E+01 6.90E+01 8.00E+00 5.00E+02
7.1021793121E+00 2.4274765657E+02 3.2120676711E+01

4.30E+01 6.90E+01 9.00E+00 5.00E+02
7.4452245577E+00 2.7739846029E+02 3.5118077024E+01

4.30E+01 6.90E+01 1.00E+01 5.00E+02
7.1984402171E+00 2.3194839268E+02 2.9652900258E+01

Appendix K

TABULATED RESULTS FOR UNLOADED DIPOLE WITH THICKNESS FACTOR OF 15

Freq. in MHz	King and Harrison (1969) impedances		Lossy line impedances	
	Real	Imaginary	Real	Imaginary
2.05	18	-532	29	-430
2.26	17	-420	30	-330
2.47	26	-325	48	-240
2.67	37	-239	51	-150
2.88	47	-159	75	-93
3.08	60	-82	80	-13
3.29	75	6	110	55
3.5	93	69	130	140
3.7	116	146	180	210
3.91	144	228	200	290
4.11	181	315	280	390
4.32	230	410	340	500
4.52	297	515	430	570
4.73	390	631	540	700
4.94	525	759	730	780
5.14	728	891	1000	910
5.35	1030	1000	1400	960
5.55	1490	1010	2100	740
5.76	2070	734	2600	280
5.96	2470	21	2500	-940
6.17	2290	-831	1900	-1600
6.38	1710	-1300	1100	-1600
6.58	1170	-1370	740	-1500
6.79	793	-1280	470	-1200
6.99	551	-1130	300	-1100
7.2	394	-992	210	-910
7.4	291	-864	170	-770
7.61	221	-750	140	-650
7.82	173	-650	120	-550
8.02	139	-561	100	-460
8.23	115	-480	95	-410
8.43	99	-405	89	-340
8.64	89	-336	85	-250
8.84	84	-270	84	-190
9.05	84	-206	92	-130
9.25	87	-143	95	-74
9.46	96	-81	120	-5.6
9.67	108	-18	130	54

(continued)

4.30E+01 6.90E+01 1.10E+01 5.00E+02
7.4742414716E+00 2.5633006154E+02 3.1846447143E+01

4.30E+01 6.90E+01 1.20E+01 5.00E+02
7.8236922552E+00 2.8458201277E+02 3.4032096595E+01

If the user selected the analyze option the menu displayed will be:

```
        Dipole Transmission Line Dipole Analyze Input

  [?]   Geometry Input
  [ ]   Frequency range                    ( 2.00E+06  3.00E+07  1.00E+06)
  [ ]   Ground plane present ?             (False)
  [ ]   Interwire coupling (for angle betwee(False)
  [ ]   Average interwire spacing (for coupl( 3.0000000000E+01)
  [ ]   Avarage antenna height (if ground pl( 1.2000000000E+01)
  [ ]   Quit this menu
```

Status:-

Prompt:- Use arrow keys and <-| to select option ?

Warning:-

This menu allows the input of control information as indicated by the prompts. It is also during analysis that the coupling between adjacent dipoles may be taken into account (Fourie, 1989b) and a perfect earth plane may be specified (Fourie, 1989c). When these options are specified the program runs 10 to 100 times slower than using the very simple analysis neglecting these aspects.

To enter the geometry select the appropriate option and the following menu will be displayed:

```
        Dipole Transmission line Dipole Geometry Input

[ ]    Feedpoint (1st) dipole length       ( 4.80E+01)
[ ]    Far Dipole (2nd) length             ( 7.40E+01)
[ ]    Optional feed dipole (3rd) length   ( 5.03E-15)
[ ]    Transmission line length            ( 1.10E+01)
[ ]    Z0 of tranmission line              ( 5.00E+02)
[ ]    1st antenna koh datafile            (wu-20.dat)
[ ]    2nd antenna koh datafile            (wu-20.dat)
[ ]    3rd (optional) antenna koh datafile (wu-20.dat)
[ ]    Three or two dipoles ?              (two wires)
[ ]    Series or parallel connection?      (T1 and feed ant. in parallel)
[?]    Quit this menu
```

Status:-

Prompt:- Use arrow keys and <-| to select option ?

Warning:-

The options in this menu is clearly similar to that displayed under the optimize option and the user can refer to that for explanation of the various prompts.

If a problem has been run the user can return to the DTD Control menu and display the output in the same way to that employed in the Lossy Line Output Menu. This menu is shown below:

```
        ANTENNA PERFORMANCE OUTPUT :

  [*]   Produce Output
  [ ]   Impedance                          (No)
  [ ]   VSWR                               (Yes)
  [ ]   Efficiency                         (No)
  [ ]   PRR                                (No)
  [ ]   Exit this menu
```

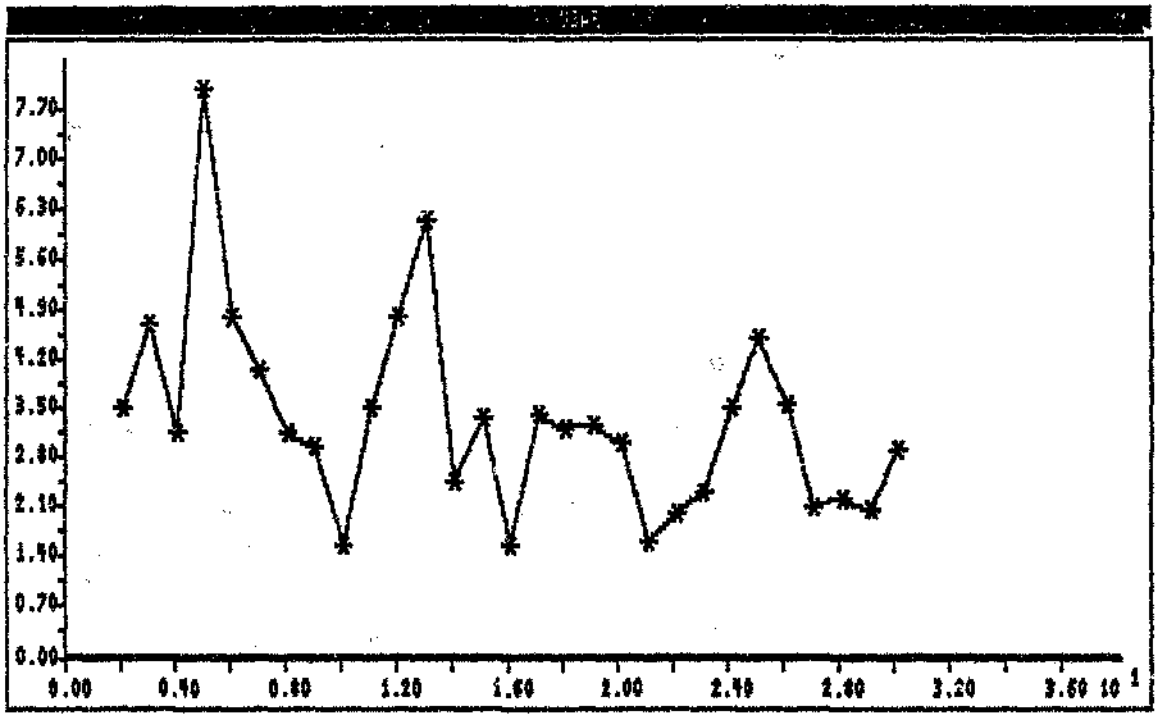
Status:- No suppress this output

Prompt:- Push function key for desired output ?

Warning:-

1)SCRNPRINT 2)SCRNPLOT 3)FILE O/P 4)EXIT

An example of the VSWR performance of an unloaded DTD antenna with feed point dipole of 48 m, transmission line of 11 m and characteristic impedance of 500 Ohm and far dipole of 74 m is shown below:



Returning to the main menu the next interesting option is FEEDPOINT LOADING. Selecting this introduces the following menu:

```
          INPUT FOR FEEDPOINT LOADING OF ANTENNAS

   [ ]    Unloaded Impedance File          (test.out)                  )
   [ ]    Series resistance                ( 4.000E+01)
   [?]    Parallel resistance              ( 1.20E+03)
   [ ]    Run problem
   [ ]    Exit to main menu
```

Status:- Use arrow keys and <-| to select option

Prompt:-

Warning:-

The file name of a previously generate ASCII file should be specified and both series and parallel resistor values may then be defined. By choosing the run option the program will solve the circuit equations involved and calculate the resultant impedance, VSWR, efficiency and PRR of the antenna. By iteratively changing the series and parallel resistor values the user can manually optimize these parameters for the desired VSWR and efficiency performance.

The next option on the main menu is the DISPLAY OF FILED DATA. This option invokes the following menu:

```
        FILE DISPLAY OPTIONS

[ ]   file name 1                          <wu125x.out>
[ ]   file name 2                          <wu175x.out>
[ ]   file name 3                          <NONE>
[*]   Produce output
[ ]   Return to main menu
```

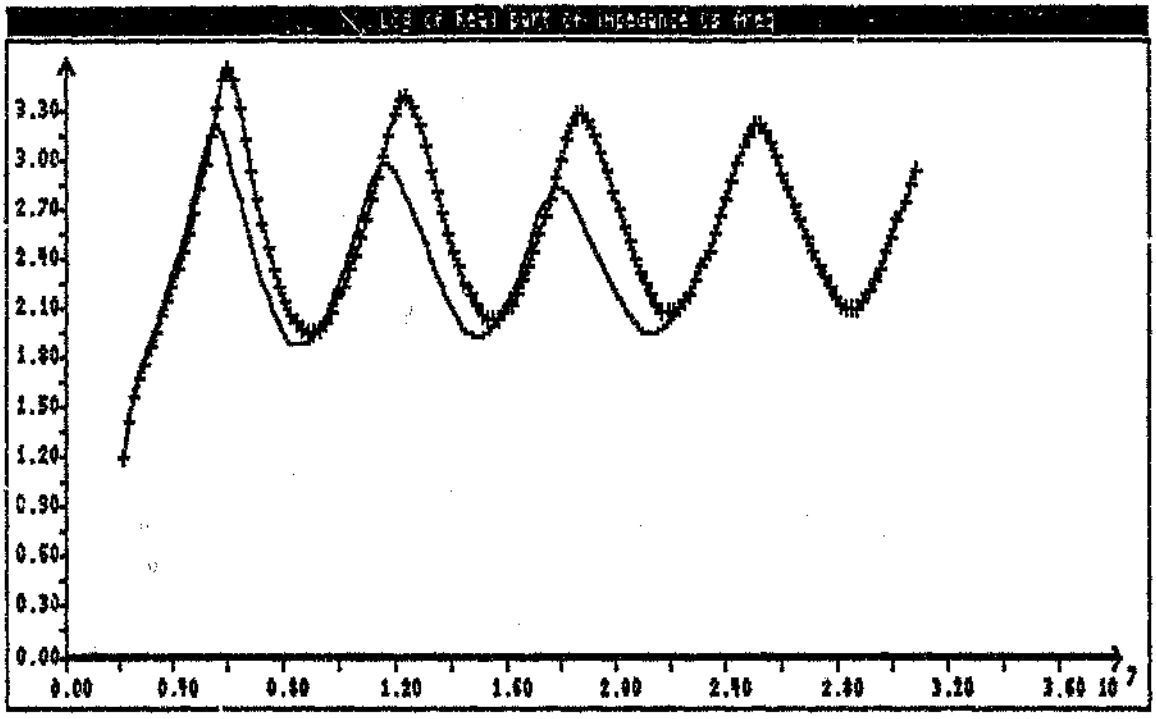
```
Status:-

Prompt:- Use function keys to select option ?

Warning:-

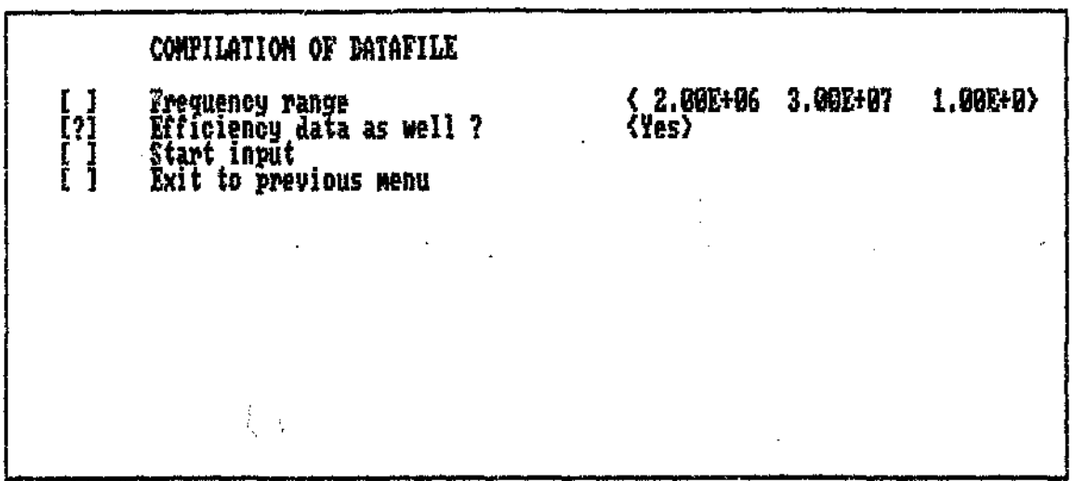
1>Zplt 2>Zlog 3>Vplt 4>Cplt 5>Pplt 6>Scrn 7>Prntr 8>Exit
```

The user may specify three previously generated ASCII file names to be displayed. When satisfied with his selection the PRODUCE OUTPUT option is selected and the function keys menu will appear at the bottom allowing the user to plot impedance on linear or logarithmic vertical axis, plot VSWR, efficiency or PRR as well as display numerical results on the screen or printer. An example of the real part of impedance of two different thickness factor dipoles are shown below:



These superimposed performance displays is very useful in comparing relative antenna performance

The last option on the main menu, COMPILE ANTENNA OUTPUT FILE, invokes this menu:



This allows the user to construct an ASCII data file in a suitable form for SALDA from data obtained elsewhere. This is very useful in the case where data from another program such as NEC2 is to be [illegible]ed to SALDA output.

I4 Software bugs and limitations

Although every attempt has been made to ensure that no software bugs are present in the program these invariably occur and the best approach is to list these such that the user is aware of them:

- The backspace key does not work when entering file names
- When exiting from the output menu under the FEEDPOINT LOADING menu this menu is not regenerated. The program will still work if the user remembers which position correspond to which option
- Input checking ensures that real numbers are entered when required etc. but does not protect against obviously wrong numbers or uninitialized options. Such actions may cause a run time error.
- If plot output of the feedpoint loading menu is activated the program abor[illegible]

- No checking is done to ensure that the relevant koh file in the DTD theory extends to the lowest and highest frequencies of interest. These files extend from koh values of 1.0 to 16.0 and antennas outside of these limits will produce meaningless results or run time errors.
- When the third wire option in the DTD theory is specified coupling to this wire is not calculated. Coupling between wires therefore only operates for the 2 wire DTD antenna.

15 Limitations

- Only 100 frequency points or segments may be specified
- Only 10 loads
- CGA screens are required

Appendix J

TABULATED RESULTS FOR DTD

Note: VSWR with respect to 300 Ohm.

NEC 2 Results

Freq. in MHz	Z real (Ω)	Z imaginary (Ω)	VSWR	Efficiency
2	253.40	210.40	2.15	0.53
3	139.80	-104.00	2.47	0.42
4	569.30	0.79	1.90	0.46
5	142.70	-111.00	2.46	0.43
6	573.90	-10.90	1.91	0.46
7	186.00	-150.00	2.18	0.50
8	299.50	-43.30	1.16	0.57
9	223.00	-91.20	1.58	0.53
10	404.10	11.88	1.35	0.56
11	228.80	135.20	1.78	0.54
12	312.50	49.70	1.18	0.57
13	628.40	-200.00	2.36	0.40
14	199.00	-56.10	1.60	0.48
15	249.80	-176.00	1.93	0.54
16	278.10	49.17	1.20	0.56
17	297.60	145.70	1.62	0.56
18	310.30	165.70	1.71	0.56
19	380.20	-171.00	1.74	0.54
20	248.00	-16.40	1.22	0.54
21	235.40	42.31	1.34	0.53
22	217.00	57.91	1.48	0.51
23	189.00	8.77	1.59	0.44
24	321.90	191.60	1.84	0.55
25	441.60	84.08	1.57	0.54
26	283.20	-187.00	1.88	0.55
27	461.00	-38.40	1.56	0.53
28	206.20	-8.07	1.46	0.48
29	460.90	32.96	1.55	0.53
30	206.90	29.01	1.48	0.48

Measured results

Freq. in MHz	VSWR
2	1.30
2.5	1.10
3	1.80
3.5	1.40
4	1.20
5	1.30
6	1.60
7	1.40
8	1.50
9	2.00
10	1.10
11	1.40
12	1.70
13	1.80
14	1.60
15	2.00
16	2.00
17	1.70
18	1.80
19	1.50
20	1.60
21	1.80
22	1.60
23	1.50
24	2.10
25	1.80
26	1.80
27	2.00
28	1.90
29	2.30
30	1.70

Freq. in MHz	King and Harrison (1969) impedances		Lossy line impedances	
	Real	Imaginary	Real	Imaginary
9.87	126	45	180	110
10.1	151	111	200	180
10.3	185	180	300	230
10.5	230	252	350	300
10.7	291	328	390	360
10.9	374	404	480	440
11.1	486	479	620	470
11.3	639	539	800	520
11.5	842	565	1000	540
11.7	1090	518	1300	410
11.9	1350	347	1400	59
12.1	1540	33	1400	-290
12.3	1540	-350	1500	-610
12.5	1370	-669	1200	-870
12.8	1110	-848	940	-1100
13	865	-903	650	-990
13.2	6[illegible]	-885	450	-980
13.4	[illegible]9	-830	330	-840
13.6	39[illegible]	-762	220	-770
13.8	31[illegible]	-690	180	-660
14	248	-619	150	-580
14.2	201	-551	130	-500
14.4	167	-487	99	-430
14.6	141	-425	89	-370
14.8	122	-367	110	-300
15	110	-310	190	-250
15.2	102	-254	100	-190
15.4	99	-200	99	-140
15.6	101	-146	110	-79
15.8	107	-91	120	-30
16	118	-45	140	49
16.2	134	18	150	100
16.5	158	83	230	160
16.7	190	151	270	220
16.9	234	221	310	270
17.1	293	293	370	340
17.3	372	365	440	380
17.5	477	432	[illegible]0	440
17.7	616	485	69[illegible]	470
17.9	795	507	90[illegible]	470
18.1	1000	470	1100	390
18.3	1230	338	1300	170
18.5	1410	97	1600	30
18.7	1460	-215	1500	-450

(continued)

Freq. in MHz	King and Harrison (1969) impedances		Lossy line impedances	
	Real	Imaginary	Real	Imaginary
18.9	1370	-512	1300	-620
19.1	1180	-718	970	-780
19.3	965	-821	930	-940
19.5	769	-845	650	-890
19.7	607	-822	490	-810
19.9	481	-773	360	-710
20.2	384	-714	310	-660
20.4	309	-650	250	-570
20.6	256	-586	230	-540
20.8	209	-524	190	-470
21	175	-463	160	-390
21.2	150	-403	150	-330
21.4	132	-346	130	-260
21.6	121	-289	130	-220
21.8	114	-233	130	-140
22	112	-177	130	-100
22.2	115	-121	130	-34
22.4	124	-63	140	11
22.6	139	-6	180	89
22.8	161	54	200	140
23	193	116	240	190
23.2	239	179	280	250
23.4	293	241	370	260
23.7	370	301	440	310
23.9	470	353	510	350
24.1	596	388	640	370
24.3	751	390	820	400
24.5	926	336	1000	300
24.7	1090	211	1200	160
24.9	1210	12	1300	-150
[illegible]	1240	-225	1300	-330
25.3	1170	-446	1100	-630
25.5	1030	-607	1000	-620
25.7	868	-696	730	-710
25.9	714	-728	630	-820
26.1	582	-721	460	-740
26.3	474	-691	280	-580
26.5	387	-648	220	-500
26.7	318	-599	220	-500
26.9	215	-45[illegible]	190	-440
27.1	183	-415	170	-390
27.4	159	-373	150	-340
27.6	140	-330	130	-280

(continued)

Freq. in MHz	King and Harrison (1969) impedances		Lossy line impedances	
	Real	Imaginary	Real	Imaginary
27.8	126	-288	130	-240
28	117	-245	120	-180
28.2	112	-202	120	-140
28.4	112	-158	120	-92
28.6	117	-113	130	-54
28.8	126	-67	170	-5.3
29	143	-20	190	34
29.2	166	27	230	96
29.4	199	75	260	140
29.6	244	122	320	150
29.8	303	165	380	180
30	378	200	410	160

Appendix L

TABULATED RESULTS FOR ALTSHULER DIPOLE

Note: VSWR calculated with respect to 400 Ohm.

NEC2 Results

Freq. in MHz	Resistance	Reactance	VSWR	Efficiency	PRR (%)
3	240	-110	1.8	0.29	29
4	390	18	1.1	0.33	33
5	510	9.1	1.3	0.36	36
6	580	-85	1.5	0.33	33
7	550	-180	1.7	0.31	31
8	440	-190	1.6	0.3	30
9	390	-76	1.2	0.35	35
10	510	10	1.3	0.45	45
11	640	-150	1.8	0.49	49
12	540	-340	2.2	0.49	49
13	350	-340	2.5	0.48	48
14	230	-270	2.7	0.5	50
15	1[illegible]0	-140	3.2	0.69	69
16	[illegible]70	83	2.5	0.98	98
17	390	240	1.8	0.95	95
18	1000	150	2.6	0.88	88
19	690	-620	3.5	0.89	89
20	270	-520	4.5	0.9	90
21	140	-270	4.3	0.71	71
22	200	-120	2.2	0.59	59
23	270	-83	1.6	0.49	49
24	300	-89	1.4	0.43	43
25	330	-86	1.3	0.43	43
26	3[illegible]0	-120	1.4	0.43	43
27	310	-160	1.7	0.42	42
28	260	-98	1.7	0.43	43
29	360	-25	1.1	0.64	64
30	470	-150	1.5	0.63	63

Lossy Line results

Freq. in MHz	Resistance	Reactance	Efficiency(%)
2	116	-393	19
3	190	-108	30
4	313	47	37
5	460	78	40
6	540	5	40
7	515	-56	40
8	474	-50	40
9	477	-8	42
10	540	11	47
11	540	-180	51
12	470	-290	54
13	325	-305	54
14	210	-225	53
15	150	-95	59
16	170	63	76
17	320	220	91
18	660	200	96
19	750	-240	95
20	420	-400	88
21	210	-264	71
22	180	-155	60
23	210	-74	59
24	267	-40	61
25	313	-51	63
26	327	-78	64
27	320	-90	63
28	320	-82	64
29	340	-78	66
30	372	-105	71

Appendix M

TABULATED RESULTS FOR GUERTLER AND COLLYER ANTENNA

Note: VSWR calculated with respect to 350 Ohm.

Lossy line results

Freq. in MHz	Resistance	Reactance	VSWR	Efficiency	PRR
3	278	58.2	1.50	0.366	0.351
4	632	66	1.60	0.325	0.307
5	632	-178	1.77	0.325	0.300
6	497	-245	1.78	0.303	0.279
7	417	-205	1.64	0.298	0.281
8	357	-136	1.46	0.305	0.295
9	367	-27.3	1.12	0.330	0.329
10	565	65.5	1.44	0.468	0.453
11	709	-177	1.92	0.499	0.450
12	534	-388	2.35	0.490	0.410
13	333	-361	2.63	0.480	0.383
14	217	-272	2.89	0.504	0.385
15	141	-143	3.26	0.657	0.473
16	147	30	2.75	0.916	0.717
17	341	224	1.85	0.969	0.882
18	982	110	2.48	0.868	0.712
19	870	-594	3.33	0.940	0.668
20	319	-575	4.40	0.953	0.575
21	138	-330	5.02	0.856	0.474
22	203	-130	2.25	0.596	0.507
23	273	-101	1.64	0.506	0.477
24	291	-92.9	1.53	0.425	0.406
25	302	-102	1.50	0.422	0.405
26	318	-113	1.48	0.422	0.406
27	316	-143	1.59	0.421	0.399
28	280	-121	1.66	0.504	0.473
29	352	-37.9	1.18	0.605	0.601
30	467	-159	1.48	0.620	0.597

Lossy line results

Freq. in MHz	Resistance	Reactance	VSWR	Efficiency
3	215	19	1.401924	0.36
4	480	90	1.689282	0.34
5	560	-80	1.919509	0.33
6	471	-134	1.770622	0.31
7	400	-8	1.334550	0.33
8	414	-20	1.386745	0.37
9	477	26	1.600844	0.42
10	580	0	1.933333	0.48
11	640	-140	2.262099	0.52
12	543	-292	2.487194	0.53
13	360	-314	2.554846	0.52
14	226	-226	2.4[illegible]057	0.5
15	163	-91	2.067728	0.54
16	170	64	1.879681	0.71
17	272	222	2.148037	0.87
18	530	309	2.541968	0.95
19	850	360	3.400429	0.96
20	628	-370	2.959828	0.91
21	313	-323	2.751340	0.8
22	210	-162	2.059615	0.66
23	220	-20	1.376606	0.61
24	268	31	1.167442	0.62
25	320	54	1.203925	0.64
26	360	50	1.267571	0.64
27	379	41	1.303212	0.64
28	392	41	1.339996	0.65
29	420	40	1.423452	0.67
30	458	12	1.529619	0.69

Appendix N

TABULATED RESULTS FOR MULTI-LOAD ANTENNA

Note: VSWR calculated with respect to 350 Ohm.

NEC2 Results

Freq in MHz	Resistanc	Reactance	VSWR	Efficiency	PRR
2	191.90	-104.90	2.05	0.33	0.29
3	360.23	78.21	1.25	0.42	0.41
4	517.35	18.61	1.48	0.43	0.41
5	519.86	-53.58	1.51	0.42	0.41
6	511.95	-85.75	1.54	0.44	0.42
7	489.05	-133.45	1.59	0.45	0.42
8	419.87	-162.15	1.58	0.44	0.42
9	303.66	-151.54	1.62	0.40	0.38
10	289.61	-71.35	1.34	0.42	0.41
11	335.81	-16.12	1.06	0.47	0.47
12	398.31	-26.86	1.16	0.52	0.51
13	412.97	-79.68	1.31	0.53	0.52
14	382.14	-117.33	1.39	0.52	0.51
15	336.26	-122.92	1.43	0.50	0.49
16	300.10	-98.90	1.41	0.48	0.46
18	295.10	-24.41	1.21	0.52	0.51
20	354.92	-30.25	1.09	0.58	0.58
22	328.42	-82.16	1.28	0.57	0.56
24	259.76	-31.23	1.37	0.55	0.54
26	313.31	0.06	1.12	0.62	0.61
28	311.85	-20.47	1.14	0.62	0.62
30	281.16	-32.46	1.27	0.61	0.60

Measured VSWR

Freq. in MHz	VSWR
2	1.90
3	1.53
4	1.08
5	1.25
6	1.27
7	1.50
8	1.70
9	1.76
10	1.77
11	1.52
12	1.19
13	1.19
14	1.39
15	1.54
16	1.48
18	1.44
20	1.19
22	1.11
24	1.29
26	1.13
28	1.00
30	1.19

Lossy Line results

Freq. in MHz	Resistance	Reactance	VSWR	Efficiency
3	290	-87	1.4	34
4	400	32	1.2	35
5	540	31	1.6	32
6	630	-130	1.9	30
7	480	-290	2.1	36
8	340	-260	2.1	37
9	270	-180	1.9	37
10	260	-100	1.6	38
11	310	-49	1.2	41
12	380	-51	1.2	42
13	430	-120	1.5	36
14	370	-210	1.8	35
15	290	-200	1.9	46
16	230	-160	2.0	43
17	220	-100	1.8	39
18	250	-51	1.5	39
19	310	-54	1.2	48
20	350	-120	1.4	50

REFERENCES

Altshuler, EE (1961) The travelling-wave linear antenna. *IRE Transactions on Antennas and Propagation*, Vol. No. 4, July 1961, pp 324 - 329.

Austin, BA. (1986). Wire Antennas for Tactical HF communications. *Elektron (Publication of the SAIEE)*, Vol 3, No 6, June 1986, pp 17 - 21.

Austin, BA (1985). Ionospheric and geographical effects on the choice of tactical and point-to-point HF antenna systems. *Electronics Letters*, Vol. 21, No. 22, 7 November 1985, pp 1107 - 1108.

Austin, BA and Fourie, APC (1986a) The JASCO broadband antenna. *SALBU (Pty.) Ltd. contract report no. 4*, Department of Electrical Engineering, University of the Witwatersrand, P O WITS, 2050, R.S.A. November 1986.

Austin, BA and Fourie, APC (1986b) The ZS Electroniques Fan Dipole. *SALBU (Pty) Ltd contract report no. 3*, Department of Electrical Engineering, University of the Witwatersrand, P O WITS, 2050, R.S.A. October 1986.

Austin, BA and Fourie, APC (1988). Numerical modelling and design of loaded broadband wire antennas. *Proceedings of the IEE Fourth International Conference on HF Radio Systems and Techniques*. Conference Publication Number 284, London, April 1988, pp 125 - 129.

Balanis, CA (1982). Antenna Theory. (1st edition) *Harper and Row*, 1982.

Braun, G (1982). Planning and Engineering of Shortwave Links. *Siemens Aktiengesellschaft, Heyden & Son Ltd*, 1982.

Burke, GJ and Poggio, AJ. (1980) Numerical Electromagnetics Code (NEC) - Method of Moments, Parts I, II and III. *NOSC TD 116*, Naval Ocean Syst. Center, San Diego, CA, July 19, 1977 (NEC-1); revised Jan. 2, 1980 (NEC-2).

Clark, AR and Fourie, APC (1989) Problems with thin wire emulations of thicker wires using NEC2. *Proceedings of the 5th annual review of progress in Applied Computational Electromagnetics*, Monterey, California, March 1989, pp 584-593.

Clark, AR and Givati, O (1987). Computer aided design of an HF broadband antenna. *Final year design report*, Department of Electrical Engineering, University of the Witwatersrand, Johannesburg, November 1987.

Dawson, J and Darnell, M. (1985) An HF system design with embedded channel evaluation. *Proceedings of the 3rd International Conference on HF Communication Systems and Techniques*, Conf. Publ. No. 245, Feb. 1985, pp 1 - 7.

Fitzgerrel, RG Radiation Efficiencies of Half-wave Dipole Antennas. *IEEE Transactions on Antennas and Propagation*, Vol. AP-13, No. 2, March 1965, pp 326-327.

Fourie, APC (1988). Simple technique for analyzing and optimizing loaded broadband antennas. *Proceedings of the SAIEE Second Joint Symposium on Antennas & Propagation and Microwave Theory & Techniques*, Pretoria, August 1988, pp 21.1 - 21.10.

Fourie, APC (1989a) Simple method to compute the current distribution, input impedance and efficiency of thick unloaded and loaded dipole antennas. *Proceedings of the 5th Annual review of progress in Applied Computational Electromagnetics*, Monterey, California, March 1989, pp 621 - 635.

Fourie, APC (1989b). DTD Theory. *SALBU Contract report no. 1*, Department of Electrical Engineering, University of the Witwatersrand, Johannesburg, 2050, February 1989.

Fourie, APC (1989c). Techniques of analysis of drooping dipoles. *SALBU Contract report no. 3*, Department of Electrical Engineering, University of the Witwatersrand, Johannesburg, 2050, February 1989

Fourie, APC and Austin, BA (1987) Improved HF broadband wire antenna. *Electronic Letters*, Vol. 23, No. 6, 12th March 1987, pp 276 - 278.

Gnabs, VK. (1966) Breitbandige rundstrahlantennen fur kurzwellen. *Telefunken-Zeitung*, Vol. 39, No. 2, Feb. 1966, pp 186 - 193.

Guertler, RJF and Collyer, GE. (1973) Improvement in travelling wave dipoles. *Proceedings of the IREE Convention*, Melbourne, Aug. 1973, pp 70 - 71.

Hall, CJ and Maclean, TSM (1971) Simple method of antenna analysis leading to the mode-theory results. *Proceedings of the IEE*, Vol. 118, No. 3/4, March/April, 1971, pp 511 - 514.

Hansen, PM. (1972) The radiation efficiency of a dipole antenna located above an imperfectly conducting ground. *IEEE Transactions in Antennas and Propagation*, Vol. AP-20, No. 6, November 1972, pp 766 - 770.

Hansen, RC. (1981) Fundamental limitations in antennas. *IEE Second International conference on Antennas & Propagation*, Conf. Publ. No. 195, April 1981, pp 333 - 337.

Harrington, RF. (1968) Field computation by Moment Methods. *Macmillan*, New York, 1968.

Harris, DW. (1982) The Australian broadband dipole. *Amateur Radio (Aust.)*, Vol. 50, No. 4, April 1982, pp 9 - 11.

Isbell, DE (1960) Log periodic dipole arrays. *IRE Transactions on Antennas and Propagation*, Vol. AP-8, No. 3, May 1960, pp 260 - 267.

King, RWP and Harrison, CW. (1969). Antennas and waves - A modern approach. *The MIT Press*, Mass. Appendix 4, Tables of Impedance and Admittance of electrically long antennas, 1969.

Kubina, SJ (1983) Numerical modelling methods for predicting antenna performance on aircraft. *AGARD lecture series no. 131*, Sept 1983, pp 9-1 to 9-38.

Maclean, TSM (1973) Signal/Noise ratio of travelling-wave dipole. *The Radio & Electronic Engineer*, Vol. 43, No. 9, Sept 1973, pp 534 - 537.

Maslin, NM (1987) HF Communications : a systems approach. *Pitman Publishing*.

Mason, HP. (1963) Some factors influencing the design of broad-band HF monopole aerials. *Proceedings of the IEE*, Vol 110, No. 9, September 1963, pp 1543 - 1553.

McGregor, DN, Wieselthier, JE, Baker, DJ, Ephremides, A and Hauser, JP (1985) Networking concepts for HF naval applications. *Proceedings of IEE 3rd International Conference on HF Communications Systems and Techniques*, Conf. Publ. No 245, 26 - 28 February 1985, pp 13 - 17.

Noonan, CR (1981) HF communications in defence. *Communications and Broadcasting*, Vol. 8, June 1981, pp 15 - 20.

Nyquist, DP and Chen, KM (1968) The travelling-wave linear antenna with nondissapative loading. *IEEE Transactions on Antennas and Propagation*, Vol. AP-16, No. 1, January 1968, pp 21 - 31.

Peixeiro, C. (1988) Design of log-periodic dipole antennas. *IEE Proceedings*, Vol 135, Pt. H, No. 2, April 1988, pp 98 - 102.

Poggio, AJ and Mayes, PE (1971) Bandwidth extension for dipole antennas by conjugate reactance loading. *IEEE Transactions on Antennas and Propagation*, Vol. AP-19, No. 4, July 1971, pp 544 - 547.

Popovic, BD, Dragovic, MB and Djodjevic, AR. (1983) Analysis and synthesis of wire antennas. *Research Studies Press.*

Popovic, BD. (1984) Generalisation of the Concept of equivalent radius of thin cylindrical Antennas. *IEE Proceedings*, Vol. 131, No. 3, June 1984, pp 153 -158.

Raggett, RJ (ed.), (1983) Jane's Military Communications, 4th edition. *London: Jane's Publishing Company Ltd*, 1983.

Ramsdale, PA. (1978) Wire Antennas in Advances in Electronics and Electron Physics. *Academic Press*, 1978, pp. 123 - 196.

Rogers, DC and Turner, BJ (1985) Connectivity improvement through path and frequency diversity. *Proceedings of the IEE 3rd International Conference on HF Communication Systems and Techniques*, Conf. Publ. No. 245. Feb. 1985, pp 8 - 12.

Royce, RK (1985) HF broadband antennas and RF distribution. *Proceedings of the IEE 3rd International Conference on HF Communications Systems and Techniques*, Conf. Publ. No 245, 26 - 28 February 1985, pp 131 -135.

Schelkunoff, SA. (1941) Theory of antennas of arbitrary size and shape. *Proceedings of the IRE*, Vol. 29, Sept. 1941, pp 493 - 521. Reprinted in the *Proceedings of the IEEE*, Vol. 72, No. 9, Sept. 1984, pp 1165 -1190.

Schelkunoff, SA. (1943) Electromagnetic Waves. Ninth printing, *D. van Nostrand Company*, 1943, chaps. 7 and 11.

Schelkunoff, SA. (1952) Advanced Antenna Theory. *John Wiley and Sons*, 1952, Chaps. 2 and 5.

Sevick, J (1976) Broadband matching transformers can handle many kilowatts. *Electronics*, Nov 25, 1976, pp 123 - 128.

Smith, GS (1977) An analysis of the Wheeler Method for measuring the radiation efficiency of antennas, *IEEE Trans. on Antennas and Propagation*, Vol. AP-25, No. 4, July 1977, pp 552-566.

Stutzman, WL and Thiele, GA. (1981) Antenna Theory and Design. *John Wiley & Sons*, Inc, 1981.

Theron, JC (1983) Tactical antennas and their application in the military environment. *Proceedings SAIEE Symposium on Antennas and Propagation*, 16-18 May, pp. V.1 - V.9.

Thiele, GA (1973). Wire Antennas from the book Computer Techniques for Electromagnetics, ed. R Mittra, *Pergamon Press*, 1973, pp 7 -73.

Townsend, DH (1985) Broadband HF system design for naval ships. *IEE 3rd International Conference on HF Communications Systems and Techniques*, Conf. Publ. No 245, 26 - 28 February 1985, pp 112 - 116.

Treharne, RF. (1983a) Natural wave logarithmically truncated Beverage antenna. *Journal of Electrical and Electronics Engineering*, IE Aust & IREE Aust., Vol. 3, No. 3, Sept 1983, pp 223 - 227.

Treharne, RF. (1983b) Multi-purpose whole-band HF antenna architecture. *Journal of Electrical and Electronics Engineering*, IE Aust & IREE Aust., Vol. 3, No. 2, June 1983, pp 141 - 152.

Turpin, RH (1969) Basis transformation, least square and characteristic mode techniques for thin wire scattering analysis. *Ph. D dissertation*, The Ohio State University, Columbus, Ohio, 1969.

Watterson, CC (1979) Methods of improving the performance of HF digital radio systems. *NTIA Report 79 - 29*, U.S. Dept. of Commerce, October, 1979.

Williams, HP (1966) Antenna theory and design. (Second Edition), *Sir Isaac Pitman & Sons Ltd*, 1966.

Wilson, QC (1985). Portable and mobile antennas for frequency agile HF systems. *IEE 3rd International Conference on HF Communications Systems and Techniques*, Conf. Publ. No 245, 26 - 28 February 1985, pp 107 - 111.

Woolf, EA. (1988) Antenna Analysis. *Artech House*, 1st edition, 1988.



Author: Fourie Andries Petrus Cronje.
Name of thesis: Analysis And Design Of Simple Antenna Geometries For Broadband High Frequency Communications.

PUBLISHER:
University of the Witwatersrand, Johannesburg
©2015

LEGALNOTICES:

Copyright Notice: All materials on the University of the Witwatersrand, Johannesburg Library website are protected by South African copyright law and may not be distributed, transmitted, displayed or otherwise published in any format, without the prior written permission of the copyright owner.

Disclaimer and Terms of Use: Provided that you maintain all copyright and other notices contained therein, you may download material (one machine readable copy and one print copy per page)for your personal and/or educational non-commercial use only.

The University of the Witwatersrand, Johannesburg, is not responsible for any errors or omissions and excludes any and all liability for any errors in or omissions from the information on the Library website.